Modelling the influence of widespread afforestation on UK hydrology

Marcus Buechel

Christ Church

University of Oxford

Supervised by

Prof. Simon Dadson, University of Oxford

Dr Louise Slater, University of Oxford

A thesis submitted for the degree Doctor of Philosophy

Oxford, July 2023

“I rather believe that time is a companion who goes with us on the journey and reminds us to cherish every moment, because it will never come again. What we leave behind is not as important as how we've lived.”

Acknowledgements

First and foremost, I would like to express my gratitude and thanks to my supervisors, Simon Dadson and Louise Slater. Without their time, insightful thoughts, and most importantly their enthusiasm there is no doubt this work would not have been possible. I will be forever grateful for the lessons, in all their shapes and guises, they taught me on this journey.

Secondly, as I note later in this work, it often takes a 'village' to run a model and that is certainly true when attempting to use JULES! I thank both Emma Robinson and Toby Marthews for tirelessly dealing with all my initial queries as I fumbled around trying to initially run JULES. Undoubtedly this work would not have been possible without the infrastructure and help of the JASMIN and CEDA teams. Along the entire process they have adeptly answered and helped resolve any of my problems. I also give my thanks to Ségolène Berthou and the rest of the Met Office team who really helped develop and improve the final piece of work. At the start of this journey, I would never have dreamt of attempting such a complex study and I owe it to them all for making it possible.

Importantly, I am thankful for all my friends and family who supported me along the way. It has been a joy to know such an incredible group of individuals in the NERC DTP and I will always look back in fondness on the memories we have made. It has been an honour to be a part of, and run, the Oxford Hydrology Group and I am glad it was a forum to enable people to gather when times have been difficult. There are many friends in the Geography department and the Water Lab who have made this experience enjoyable and exciting. Katrin Wilhelm particularly has driven me to achieve more, and I will take that forward with me. I am grateful to all the students who have pushed my understanding but also dealt with many a geographical rant! Finally, there are the people closest to home who have always been there for me in the good and the bad times. Thank you to my family for helping me when times got tough and for making the load lighter.

Sarah Thursby-Pelham I write my thanks to you separately to emphasise that you have been, and are, the true power behind all of this. You have been my guiding light throughout and made this an adventure of a lifetime. Here's to whatever comes next.

Abstract

With increasing atmospheric CO_2, the hydrological system is moving towards more frequent and intense hydroclimatic extremes. With the greater risk this poses to society, we need solutions that reduce atmospheric CO_2 and mitigate water-related hazards. Afforestation, mooted to reduce atmospheric CO_2 and mitigate flood risk, is being proposed internationally at greater temporal and spatial scales than ever witnessed before. Previous work has assessed the hydrological consequences of woodland planting at relatively small scales (< 10 km^2) or at global scales with low process and spatial resolution. There is a clear need for evidence at countrywide scales on whether afforestation will achieve its intended goals.

The work here seeks to determine the influence of widespread afforestation on UK hydrology. The UK plans to annually plant 30 000 hectares of trees to reach its Net Zero goals. This work uses land surface modelling at a higher complexity than is often undertaken when understanding woodland hydrology. Land surface models include a relevant set of Earth system processes, which is critical when drawing conclusions about woodland hydrology. The final research piece uniquely couples a land surface model and convection-permitting atmospheric model to simulate the hydrometeorological consequences of UK widespread afforestation.

In this thesis, afforestation location has a minimal impact on terrestrial hydrology compared to afforestation extent. However, in a land-atmosphere model configuration, woodland along Great Britain's west coastline increases surface roughness, producing heavier rainfall. Median streamflow reduces by 2.8% ± 1.0 (1 s.d.) for a ten-percentage point increase in catchment broadleaf woodland but there is no consistent reduction of extreme floods. Afforestation minimally impacts hydrological processes compared to changes in precipitation, temperature, and CO_2. More arid catchments show greater streamflow sensitivity to woodland expansion potentially increasing the likelihood of drought formation with afforestation.

Work here provides a critical step forward in our understanding of afforestation impact on hydrology and the utility of land surface models in answering policy-relevant questions.

Abbreviations

ANOVA – Analysis of Variance
CEH – Centre for Ecology and Hydrology
CHESS – Climate, Hydrological and Ecological research Support System
CMIP – Coupled Model Intercomparison Project
CPM – Convection Permitting Model
ESM – Earth System Model
FDC – Flow Duration Curve
GB – Great Britain
GCM – Global Climate Model
IHDTM – Integrated Hydrological Digital Terrain Model
JULES – Joint UK Land Environment Simulator
KGE – Kling-Gupta Efficiency
KW – Kruskal Wallis
LAI – Leaf Area Index
LSM – Land Surface Model
LULC – Land Use & Land Cover
MAE – Mean Absolute Error
MSE – Median Streamflow Elasticity
NBS – Nature Based Solutions
NFM – Natural Flood Management
NSE – Nash-Sutcliffe Efficiency
PDM – Probability-Distributed Model
PFT – Plant Functional Type
PPI – Percentage Point Increase
PPoA – Percentage Points of Afforestation
PTF – Pedotransfer Function
RCM – Regional Climate Model
RCP – Representative Concentration Pathway
RFM – River Flow Model
RMSE – Root Mean Squared Error
RR – Runoff Ratio

SSP – Shared Socioeconomic Pathway

SUMMA – Structure for Unifying Multiple Modeling Alternatives

TWI – Topographic Wetness Index

UK – United Kingdom

Table of Figures

Table of Tables

Table of Supplementary Figures

Table of Supplementary Tables

Table of Contents

1. Introduction

The work herein investigates the hydrological consequences of widespread afforestation using numerical modelling. It is geographically centred over the United Kingdom and uses the Joint UK Land Environment Simulator (JULES) land surface model, both independently and coupled with a convection-permitting model, to explore this research need. In this way, several important conclusions are derived about woodland, and modelling, hydrology.

Firstly, this work provides another line of evidence into the potential hydrological consequences of afforestation at countrywide scales. Relative to climate, increases in woodland have a minimal impact in altering water resources and are unlikely to substantially reduce the greatest flood peak magnitudes. Dependant on the model setup, woodland in certain locations across Great Britain could increase or decrease water supply.

Secondly, using one of the most complex land surface models at our disposal enables exploration of critical biophysical factors that could influence the response of the UK's hydrology to widespread afforestation in ways we may not currently be aware of. This not only advances modelling studies focusing on afforestation but also evaluates the plausibility of land surface model responses to drastic perturbations.

Overall, this work provides both answers and further avenues for research to answer the question about the potential hydrological consequences of widespread afforestation.

1.1. Background and Motivation

Land cover is the surface occupying an area of land on Earth. This ranges from bare ground, grass, and trees to anthropogenic features such as cities and roads. Land cover properties, such as its roughness, mediate the response of catchments to water fluxes. We must therefore understand the effects of land cover change on future societal water resources. Developing our knowledge of how land cover alters hydrological pathways aids comprehension of the role land cover enacts in hydrological extremes: droughts and floods.

Afforestation, whereby new trees are planted, is currently being proposed internationally over large areas in a relatively short period of time. This would make it one of the most significant land cover changes across Earth, alongside urban areas. Policymakers, scientists, and the public are all interested in afforestation for many reasons. One still debated impact is its hydrological effects.

Woodland impacts water, carbon, nutrient and energy fluxes and as all these systems interact dependently, none cannot be accurately predicted independently. This makes it incredibly difficult to fully comprehend and isolate how widespread afforestation could impact the terrestrial water cycle. Observational studies of relatively small catchments (< 10 km^2) exist exploring the impact of woodland on water resources, but it is not possible to extrapolate these results over large regions due to the complexity of interacting processes. Currently, no observational experiments exist with clear evidence of what the proposed large increase in woodland could do to water resources in temperate regions.

If we are to predict water resource change with afforestation, we must turn to models that include all relevant Earth systems and not just hydrology. Models communicate the relationship and connection of processes, systems and ideas whilst allowing for the extrapolation of phenomena across time and space. We use them to explore what has been and what is and might be.

As our understanding of the world has become more multifarious, so too have the models that we use to explain and predict our environment. Land surface models (LSMs) have rapidly evolved over the past few decades. They began as the lower boundary conditions for models predicting atmospheric processes, predominantly energy and water fluxes, but have now evolved to include a plethora of systems. These include the carbon cycle, urban processes, and agricultural practices. Land surface models are therefore ideal to tackle questions of the 21st century which require more interdisciplinary approaches. Additionally, it is in the development and testing of these models that not only do we improve them but also our understanding of the world around us.

With the most advanced models of the Earth system, we can begin to model and learn the influence of widespread afforestation on UK hydrology.

1.2. Thesis Outline

Three main chapters provide the central thrust of this thesis which deal with understanding the potential consequences of widespread afforestation using LSMs, both uncoupled and coupled with the atmosphere. There are then two additional chapters, the Literature Review and the Conclusion which buttress the work.

Chapter 2, the Literature Review, lays the foundation. Initially it discusses the field of hydrology, its scope, and the need to explore the hydrological consequences of our actions, such as land cover change and flood risk. Within these concepts, woodland hydrology and hydrology within land surface models are delved into. This chapter also briefly touches upon nonstationarity in the hydrological system and why a bottom-up full process-based understanding of the system is required and not just a top-down lens that treats catchments as abstract concepts. A short summary is then provided which succinctly ties the Literature Review together and emphasises the literature gap this work aims to fill.

The three main chapters are focused around three central questions.

How does the location of afforestation across Great Britain influence the terrestrial streamflow response? (Chapter 3) This chapter uses a large ensemble of afforestation scenarios based on catchment structure and existing land cover to determine the response of twelve diverse catchments across the UK to afforestation. Not only is the sensitivity of the hydrological system to tree planting investigated but also the ramifications across the whole streamflow spectrum. Terrestrial modelling studies have not previously been undertaken at this scale when exploring afforestation streamflow impact.

How could potential afforestation compare to climate changes when considering their impact on terrestrial hydrological processes within JULES? (Chapter 4) In the fourth chapter a plausible countrywide afforestation scenario for Great Britain is run with JULES for both a present and future climate scenario to understand whether climatological differences would lead to significant differences in the terrestrial water stores and fluxes. A simple factorial sensitivity analysis detects the effects of land cover change on hydrological processes within the model when compared to climate forcing.

How can afforestation influence hydrometeorological processes in the future when coupling a land surface model with a convection-permitting climate model? (Chapter 5) In the final chapter of research, JULES is coupled with a convection-permitting atmospheric model for a future climate scenario and extreme afforestation scenario. This aids elucidation into potential land-atmosphere feedbacks. Furthermore, it provides answers on whether significantly different model responses to a coupled land and atmosphere exist compared to an uncoupled LSM model setup. The research is unique for undertaking such an analysis at such a high spatial and temporal resolution with this model type.

Those three pieces of work provide the research necessary to address questions of how widespread afforestation could influence UK hydrology if implemented, whilst also testing whether our most complex models are adequate to the task.

The concluding chapter summarises the previous chapters and provides some initial thoughts and further research to both advance LSMs and our understanding of the potential implications of widespread afforestation on global water resources. Subsequently there are appendices that provide additional data to the three research chapters and a summary of how LSMs can be used to understand hydrology.

2. Literature Review

This chapter provides a backdrop to the following work by summarising our existing knowledge of the hydrological system, the hydrological consequences of afforestation and modelling.

2.1. Hydrology

2.1.1. Background and Concepts

The water system is continually evolving, along with our understanding of it. Water is the lifeblood of society; civilisations live or die on it. Our study of all things related to water is known as hydrology. Since the time of the ancient Greek philosophers, humanity has realised the importance and need to comprehend hydrology (Koutsoyiannis and Mamassis, 2021). Even after millennia of attempting to comprehend the entire water cycle, there is still much we do not understand.

In 1977, Luna Leopold discussed the philosophy of water management in response to the severe Californian droughts (Leopold, 1977). In his keynote speech, Leopold noted how humanity often seeks to bend rivers to its needs despite being a 'living and breathing' system (evoking William Davis's concepts from the 19th Century). The idea of water resources being something we must work with, not force to our needs, perfectly articulates the need for hydrology if we are to live within our water planetary boundary (Gleeson *et al.*, 2020) [Figure 2.1]. In the 21st Century, with the acknowledgment that we live within a global common, it is increasingly important we look at the hydrological system more holistically, and integrated, way than ever before to illuminate humanity's intended and unintended interactions with it and the resulting consequences.

Over time, our understanding of the hydrological system has become increasingly interdisciplinary due to the large number of Earth system components with which it overlaps (Rahman *et al.*, 2022). Initial perceptual hydrological models treated water resources in isolation from other Earth system components [Figure 2.1]. A perceptual model being any idea

of the whole, or fragment, of a system, subjective to the views and opinion of an individual. When constructing our understanding of the hydrological system, we first must build a perceptual model of the system using both new observations and prior knowledge (Beven and Chappell, 2021; Wagener *et al.*, 2021; Beven and Lane, 2022; Kirchner *et al.*, 2023). One can imagine original perceptions of a 'water cycle' in which it rains, the water flows through the catchment and evaporates back into the atmosphere. However, it is now acknowledged that this view is rather too simplistic as humans are integrated within the hydrological system and its high dependency and interconnection with other Earth systems.

As the hunt for the fundamental governing laws of hydrology continues, it is critical we search for relationships and interactions both within and outside our current knowledge of hydrology (Dooge, 1986). Crucially, a hydrological system can be seen as a mixture of both deterministic and stochastic components (Milly *et al.*, 2015) and this stochastic element leads some to believe it is impossible to truly know how a catchment hydrologically functions. This is particularly acute when identifying a catchment's response to forcing (e.g., water extraction and land surface alteration). By adopting an Earth systems-based approach to hydrology, it becomes possible to identify and isolate potential mechanisms within the scope of inquiry and minimise uncertainty due to the unknown.

In this work, the hydrological system of a region or catchment is treated as essentially the division between structural and storage features and processes that encapsulate the fluxes within the water system (Bracken and Croke, 2007; McMillan, 2022). This paradigm of the terrestrial water cycle allows investigations to delve into the many interactions and connections of hydrology within different parts of the Earth system. Fundamentally, it allows the use of numerical models (discussed later) to represent the hydrological environment to question our understanding of our world.

Approximately 773 000 km^2 of the Earth's surface is covered by rivers and streams (Allen and Pavelsky, 2018) which constantly change their extent and location according to a range of factors (e.g. van Meerveld *et al* 2019). Streamflow, or the runoff within rivers and streams, is a signal that contains all the information of all hydrological processes upstream of the recording point (Blöschl *et al.*, 2007; Pattison and Lane, 2012). That makes it an important variable to explore when determining catchment disturbance influence downstream. However, to note, it is important to look at all system interactions within a catchment, and not just the culmination

of a multitude of catchment attributes. Changes in climate, catchment structural characteristics and land cover can all be detected by using streamflow. Looking at river flow is also essential as it provides water for settlements and it can have serious ramifications on adjacent populations (e.g., flooding).

As we head deeper into the Anthropocene (the potential geological epoch that defines humanity's influence on the planet (Crutzen, 2002)), we must further consider the role of humans in the hydrological cycle (Gleeson *et al.*, 2020). It is more important than ever to determine the process-based response of the hydrosphere to anthropogenic perturbations and directly attribute relevant changes. In this way, informed decisions can be made to ensure humanity survives within its means.

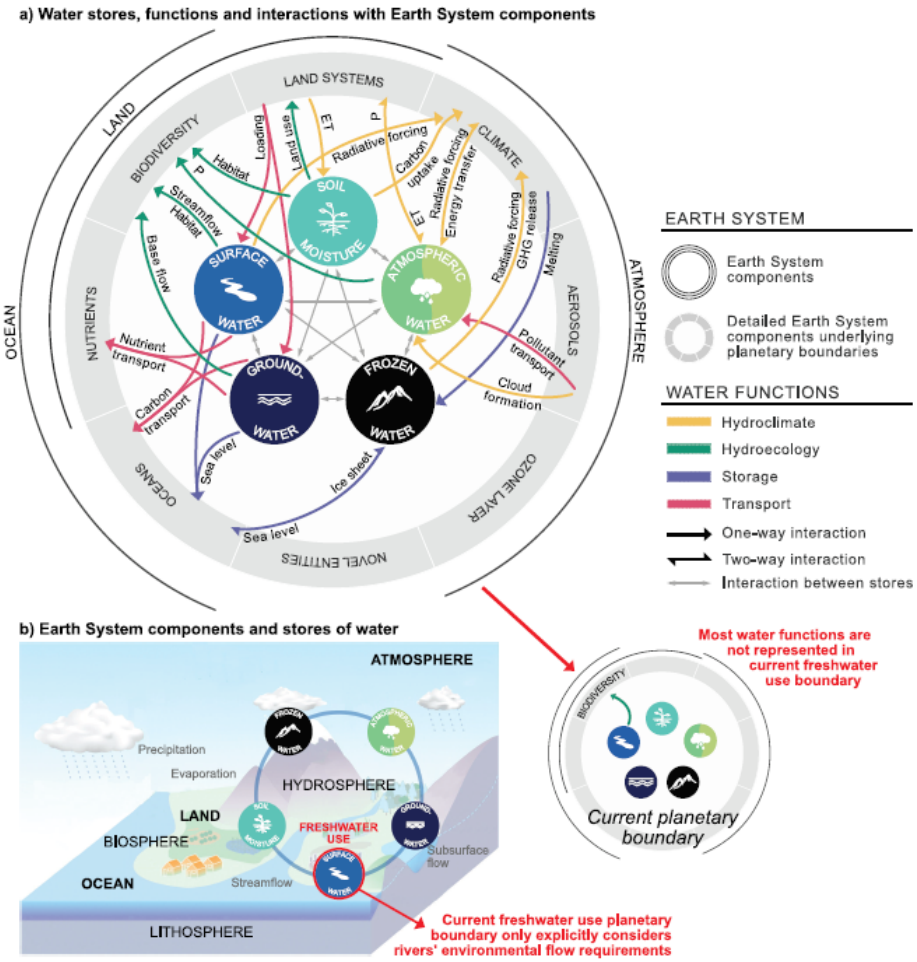

Figure 2.1: Figure from Gleeson et al. (2020) demonstrating the role and interaction of the hydrosphere within the Earth System boundary.

2.1.2. Hydrology: A Changing System

The hydrological system is complex. By its fundamental underlying principles, it is continually in flux. There is an incredible amount of dependent interacting processes which can make disentangling the influence of individual factors on hydrology difficult (Slater and Wilby, 2017). In the quest to find the underlying hydrological laws covering both space and time over multiple scales, we must use both global-scale and small catchment hydrological studies to find knowledge parsimony across scales (Eagleson, 1986). Even trying to answer simple questions on how land cover, climate and hydraulic structures influence high streamflow in catchments, the answer is always 'it depends' (Blöschl, 2022). As humans have an increasing impact on processes and we reach potential tipping points within systems (Lenton *et al.*, 2008), it becomes increasingly important for us to understand the full mechanistic processes of an entire Earth system and not just a singular output.

Unequivocally humans have increased the amount of atmospheric greenhouse gases (IPPC, 2019). Consequently, this is altering the entire water cycle leading to fewer catchments functioning hydrologically similarly to their past environment (Jaramillo *et al.*, 2022). Both precipitation and evaporation have, and will, generate significantly different hydrological conditions for catchments in the future. The Clausius-Clapeyron relationship indicates that the atmosphere can potentially hold 7 % more water for every 1 °C of warming (Trenberth, 2011; Allan *et al.*, 2020). This is important to acknowledge as increasing greenhouse gases could lead to more water being stored in the atmosphere with a greater energy potential. Increasingly, evidence is being found that heavy rainfall events could be shorter and more intense both globally and across the UK (Westra *et al.*, 2014; Fowler *et al.*, 2021; Wasko, Nathan, *et al.*, 2021). In the last decade alone, an estimated quarter of rainfall records were attributable to climate change (Robinson *et al.*, 2021). However, current increases in temperature do not translate into increased flooding globally (Wasko, 2021). Global land evapotranspiration has also been predicted to have increased by approximately 10% between 2003-2019 mainly due to changes in temperature (Pascolini-Campbell *et al.*, 2021). These temperature increases are leading to the evolution of greater distances forming between evaporation sources and precipitation sinks (Gimeno *et al.*, 2021). In that sense any change to the land surface, and evaporation sources, would not only impact local terrestrial hydrology, but also water resources further afield than previously. This reinforces the need to fully comprehend the entire

hydrological system if we are to understand the consequences of climate change on the hydrosphere. Significant changes in one part of the system may not convert into a detectable change in another.

Determining the impact of climate on terrestrial hydrology is important as it has a significant role in our ability to predict catchment function (Addor *et al.*, 2017; Tyralis *et al.*, 2021). Even without climate change the present climate can produce the record breaking hydrological events seen in previous years without climate change (Thompson *et al.*, 2017). There is a 34% chance of somewhere in England and Wales breaking the regional rainfall record each winter (Thompson *et al.*, 2017). This means we are likely to observe 'unprecedented' rainfall in the future and need to be prepared regardless of a changing climate.

In the UK, precipitation patterns have both been observed, and projected, to be changing significantly across all seasons. Observations of precipitation in winter have shown a consistent monotonic increase (Burt *et al.*, 2016; M. Kendon *et al.*, 2023). In model projections, summer precipitation decreases overall, although future heavy rainfall events are expected to be shorter and more intense (Kendon *et al.*, 2014; Gadian *et al.*, 2018; Fowler *et al.*, 2021). There also appears to be an increase in the number of convective rainfall events in winter and autumn which may make weather extremes, and resulting terrestrial hydrological consequences more severe (Cotterill *et al.*, 2021; E. J. Kendon *et al.*, 2023). Future projections using Weather@home show small precipitation increases in winter but large decreases in summer (Guillod *et al.*, 2018) leading to drought and high-precipitation events potentially increasing in magnitude and frequency across the UK. However, to note, there is incredible uncertainty in how precipitation will change in upland regions with current projections (T. R. Murphy *et al.*, 2019). Overall, in the UK it can be assumed catchment water inputs are expected to alter in future; how this may play out with terrestrial processes is not fully understood.

Use of models (discussed later) can only replicate global hydrology patterns if human impacts are included and not just natural radiative forcing (Gudmundsson *et al.*, 2017, 2021). This emphasises the need to acknowledge our anthropogenic climate driving hydrology towards a new trajectory, which could cause negative consequences upon society. Although the climate is often attributed to be the main issue for climate-related disasters it should be implicit that human elements (such as mismanaged risk mitigation) often increase the risk of the hazard (Raju *et al.*, 2022), particularly as populations increasingly become more exposed to

hydrological extremes (Tellman *et al.*, 2021). Therefore, as discussed earlier, with changing climate and terrestrial conditions, we need to understand all the hydrological components in conjunction with one another and not just in isolation if we are to predict and work with water resources.

Within catchments, many factors alter their hydrological functioning. Some of these factors include the topography, soil and geology, and land use and cover. Land cover is continually changing due to human modification of the Earth's surface. To understand the true impact of land cover on terrestrial hydrology requires an interdisciplinary approach as the factors influencing both the cover and use crosses multiple fields (Rogger *et al.*, 2017). This then has impacts on how floods, and runoff, propagate and manifest themselves within a catchment [Figure 2.2]. For example, agricultural practices would require a knowledge of biology, economics, and social practices to determine water flow pathways which could increase flood risk.

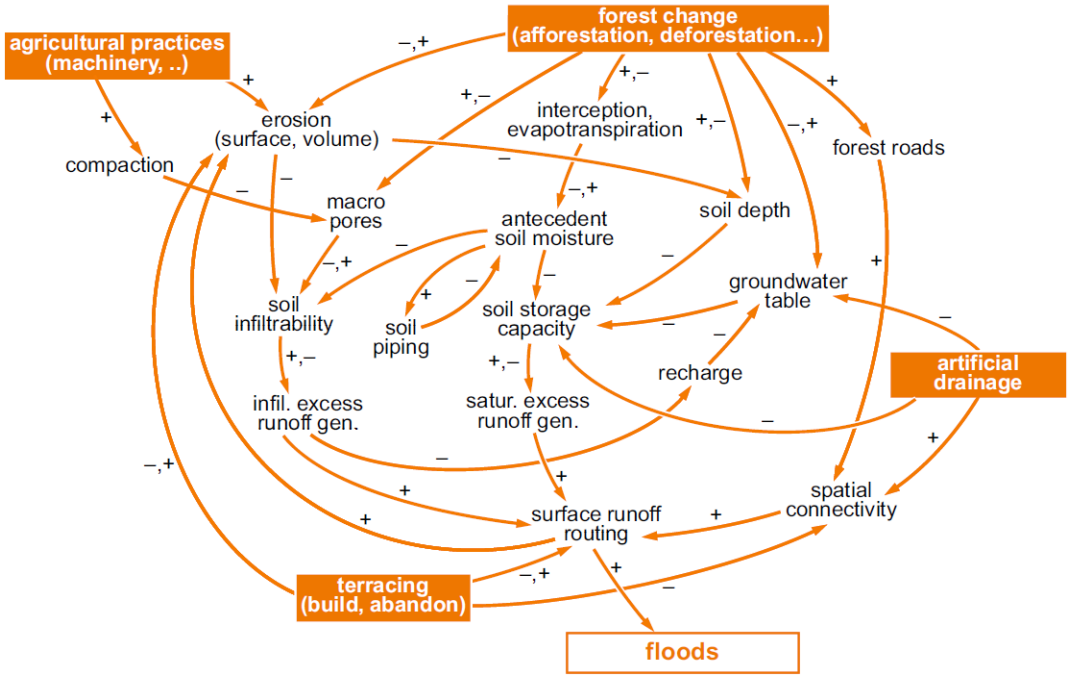

Figure 2.2: Interactions of land use changes and how they affect floods within catchments (Rogger et al. 2017).

The plus and minus signs indicate positive and negative feedbacks between the individual components.

The dissipative nature of hydrological systems means there are often significant changes in regime near land cover changes and intervention, but these become less detectable the further away from the change (Blöschl *et al.*, 2007) [Figure 2.3]. Land cover and use impacts merge and either compound and negate other catchment alterations which can make detection and attribution of land cover changes on hydrology difficult at larger spatial and temporal scales.

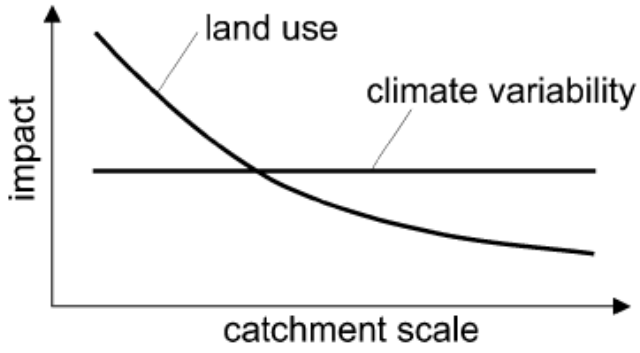

Figure 2.3: Blöschl et al. (2007)'s hypothesised impact of land use and climate on the hydrological response of a catchment.
On the y axis the hydrological impact increases upwards and on the x axis the spatial extent of the hydrological response to land use and climate variability across a catchment.

Both climatic and terrestrial processes influence the water cycle. If we are to understand hydrological extremes, an explicit understanding of their drivers is required. One location where flooding is a contemporary issue is the United Kingdom.

2.1.3. Flooding in the UK

Changes in the hydrological system can generate negative consequences for humanity. The most common and costly hazard is flooding. Over the past few decades floods have significantly increased and are now the most common type of natural hazard (Razavi *et al.*, 2020). Flood risk is distributed unevenly across the world but it is clear that global warming, and the intensification of the hydrological cycle is likely to lead to more flooding (Lorenzo *et al.*, 2016) and without any action on reducing flood risk, the absolute cost of flooding is expected to substantially increase both globally and in the UK (Winsemius *et al.*, 2016; Bates *et al.*, 2023).

It is important to put the current floods into context and understand that they are not a constant phenomenon. Flooding phases can often be described as flood rich and flood poor (Wilby and Quinn, 2013). Paleo-records have improved our understanding of both the frequency and magnitude of flood-rich and poor periods over hundreds of years. A 1500-year paleo-flood record from sediments at Brotherswater show nine multi-decadal periods of more frequent flooding (Schillereff et al., 2019), in addition, similar records from Bassenthwaite Lake find floods from 1990 onwards are unprecedented in its 558-year palaeoflood record (Chiverrell et al., 2019). Compiling datasets from across Europe, Blöschl *et al.* (2020) find the last three decades are amongst the most flood-rich periods of the last 500 years in Europe. The reduced floods beforehand may have made the current flooding more surprising to water managers and hence disasters, so we must fully comprehend these events if we are to prepare for the future (Merz *et al.*, 2021). In fact, Kjeldsen & Prosdocimi (2018) created a new test to determine whether a flood event can be considered surprising or not. The greatest spatial extent of surprising events in the UK came from more recent events and the most 'surprising' events were those that were unexpectedly large across multiple different catchments. All this evidence suggests that the current period of flooding is unprecedented and requires urgent attention to reduce the risks they pose to society.

The flood generation mechanisms of catchments across the UK are broadly similar. Many UK floods are caused by rainfall occurring over long time periods, generating high antecedent soil moisture conditions (Berghuijs, Harrigan, *et al.*, 2019). This means that it is not always the most extreme rainfall events that generate floods with only 34% of annual maxima daily flood events matched by an equivalent daily rainfall maxima (Ledingham *et al.*, 2019). The dominance of this flood-generating mechanism has not changed substantially since the 1960s. Notably in the British Isles, flood synchronicity has increased where adjacent catchments flood simultaneously, predominantly due to antecedent soil moisture (Berghuijs, Allen, *et al.*, 2019). This poses a challenge for hazard preparedness and resilience due to the spatial scale of flooding. Most recent research has shown that a current shift in flood generation processes are leading to the increased flooding observed with a 5% increase in the frequency of flood-rich periods due to a shift from rain on dry soil to wet soil (Tarasova *et al.*, 2023). It is therefore important to understand the mechanisms that will influence antecedent soil moisture in the UK if we are to try and reduce flood risk.

Multiple observational studies using river gauge data in the UK find a trend in changes in river flow. Across the UKBN2 network Harrigan *et al.*, (2018) find a median trend magnitude of +14.3% for winter flows across the network with in an increase in high flow indices for 70% of the network (apart from during the March-April-May period where they decreased). Using areal models Prosdocimi *et al.,* (2019) find peak flow magnitudes have been increasing across Great Britain as well, with an acceleration in the trend seen in peak flows since the 1980s. The strongest signal of this trend is seen in northern England, parts of Scotland and Wales with weaker signals in southern and central England. When considering the scale of floods, flood frequency curves are beginning to 'flatten' with the largest floods (e.g. 1 in 100 year) not necessarily becoming larger, but the more frequent floods (e.g. 1 in 5 year) becoming greater in magnitude (Griffin *et al.*, 2019). Faulkner *et al.,* (2019) illustrate that non-stationary flood-frequency analysis leads to flow estimates 55% higher than stationary estimates in the north-west England with an upward trend in flows for a quarter of river flow gauges across Great Britain. Considering more modern streamflow datasets, flood magnitude and frequency is increasing across the UK, and this requires attention to resolve the challenges it poses to the public.

We need not only develop an accurate understanding of catchment function, but also develop infrastructure to guide a river to our needs if we are to mitigate the currently growing flood risk. There are two current philosophies behind flood mitigation infrastructure. One is 'hard engineering' in which structures, such as revetments and walls are constructed, that change the course of flood waters away from vulnerable areas. The second is 'soft engineering' which attempts to work with catchment processes to alter the pathway of flood waters more passively. This includes nature-based solutions (discussed in the following section), but it requires a clear understanding of natural processes. Of note, is the mooted ability of tree planting to reduce downstream flood magnitude.

2.2. Woodland Hydrology

2.2.1. Recent Afforestation Attention

Afforestation has received ever-growing attention in the last decade. This is due to a number of its proposed benefits which include but not limited to: increased biogenic carbon storage, reduced soil erosion, increased biodiversity, resources (such as food and wood), reduced air and water pollution, flood reduction, temperature reduction (shade) and societal wellbeing. Woodland is therefore planted to achieve one, or a number, of these goals. The spatial extent of additional tree cover being proposed, in a relatively short time in comparison to natural afforestation, means that this is one of the most radical LULC changes of the 21st Century.

Arguably the primary reason for afforestation at present is its proposed ability to reduce atmospheric carbon dioxide. As society tries to reach Net Zero carbon emissions by 2050, approaches are required that not only reduce the amount of CO_2 emissions, but also ways to absorb and 'sink' CO_2 out of the atmosphere. Via the process of photosynthesis, trees can drawdown CO_2 and store the carbon as biogenic material and release oxygen. This makes them particularly attractive as an approach to reach Net Zero. However, incredibly large amounts of woodland are required to reach to match the challenge. Modelling shows that forest-based climate mitigation is more efficient than biomass energy with carbon capture and storage (Harper *et al.*, 2018). Furthermore, even making afforestation a commercial prospect, and not just an environmental regeneration exercise, would be effective in reaching Net Zero (Forster *et al.*, 2021). However, woodland needs to be planted in the right areas, or it might have unintended consequences (discussed later).

A large number of nations are proposing to use afforestation to reach their Net Zero goals; 42% of Nationally Determined Contribution plans include afforestation plans (Seddon *et al.*, 2020). There are international agreements such as the *Bonn Challenge* (https://www.bonnchallenge.org/), *Afr100* (https://afr100.org/) and the *Reducing Emissions from Deforestation and Forest Degradation* (https://redd.unfccc.int/). Major companies such as *Apple* (https://www.apple.com/uk/newsroom/2021/04/apple-and-partners-launch-first-ever-200-million-restore-fund/) and *Microsoft* (https://blogs.microsoft.com/blog/2020/01/16/microsoft-will-be-carbon-negative-by-2030/)

have also promised to plant large areas of woodland to reduce their CO_2 impact. A larger set of international afforestation examples can be found in Seddon *et al.,* (2020). If nature based solutions (NBS) to our challenges, including afforestation, are implemented quickly it could be possible to reduce global warming (Girardin *et al.*, 2021). This ideology is therefore leading to a rapid implementation of afforestation, even if we may not necessarily be precisely correct in our assertions.

To ensure forests achieve their intended goals, there is a need for science to make sure targets are achievable and broadly result in their intended goals. At present, there is concern that afforestation is being treated as a 'silver bullet' without fully considering its ability to generate the intended outcomes (Seddon *et al.*, 2021). Other tree-based avenues for climate mitigation also need to be considered such as regenerating existing forest, which may lead to a different suite of environmental impacts (Cook-Patton *et al.*, 2020). Therefore, research is required to enable afforestation to have the maximal positive benefits with minimal negative drawbacks and ensure it is a valid and appropriate approach to reach Net Zero.

Woodland planting location is particularly important to note when attempting to use afforestation as a carbon mitigation tool because without consideration it could lead to unintended consequences. As two examples, Warner *et al.* (2021) illustrate how reforestation could lead to carbon loss with tree planting in the Scottish Highlands, and use of an integrated assessment model suggests afforestation could drive food prices up and increase world hunger as trees cover areas of plant growing potential (Doelman *et al.*, 2018). The existing terrestrial water resources available for woodland are important to acknowledge as well as it governs the amount of carbon trees can capture (Humphrey *et al.*, 2021; Wang *et al.*, 2022). If woodland is planted in particularly arid areas, this may cause challenges for existing water resources for settlements, whilst also not reducing atmospheric carbon to a significant degree. Other potential negative consequences of proposed afforestation include destruction of protected habitats and fragile grasslands, displacement of farming, increased deforestation and reduced water quality with increased quantity used. It is therefore critical that we determine where we can best plant woodland to achieve maximal benefits.

In this work, the main question being asked is, what are the potential hydrological consequences of widespread afforestation in the UK?

2.2.2. Woodland in the UK

The areal extent and composition of UK woodland has substantially changed since the start of the Flandrian Transgression and the Holocene approximately 12,000 years ago. It started from predominantly being birch (*Betula*) and pine (*Pinus*) for the first two millennia before reaching a climax community of elm (*Ulmus Procera*), oak (*Quercus Robur*) and lime (*Tilia x Europaea)* across England and Wales and pine in highland Scotland (Godwin, 1975). The balance between broadleaf woodland in the south and coniferous in the north of the UK continues to the present day.

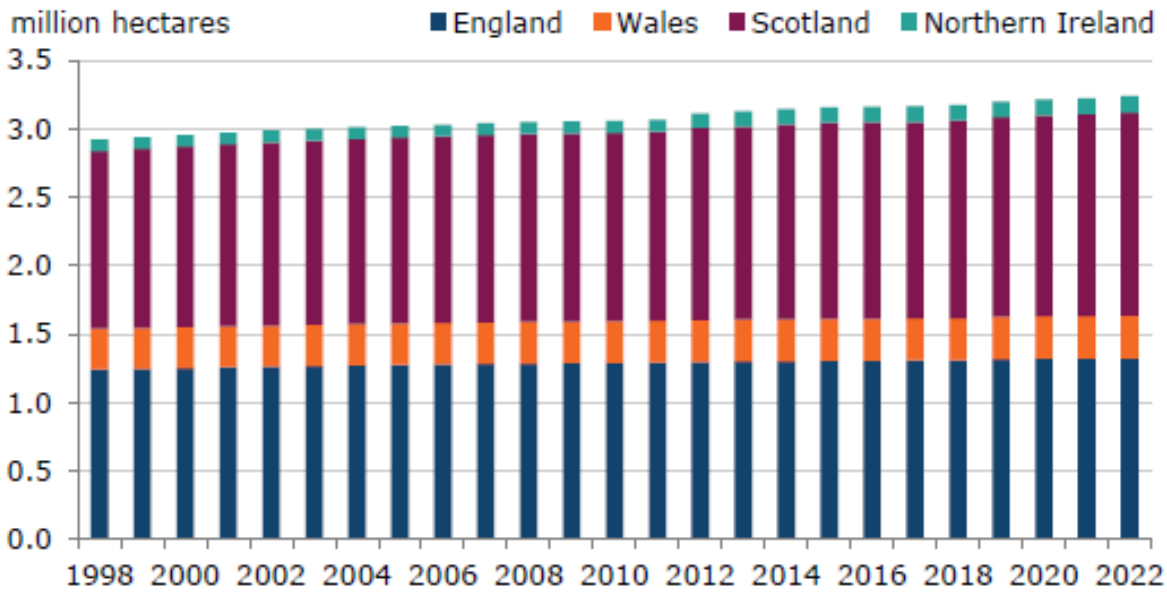

Figure 2.4: Area of UK woodland between 1998 to 2002 as separated by UK region (Forestry Commission, 2022).

The area of UK land currently occupied by woodland is the lowest in Europe and other developed nations after continual clearance and use. At the start of the 20th century only approximately 5% of land was woodland but with the establishment of the Forestry Commission, the amount of woodland across the UK has substantially increased (Ares *et al.*, 2021). Between 1976 and 1989 annual planting rates averaged around 25,000 hectares before falling to about 19,000 between 2000 and 2001 (Ares *et al.*, 2021). At present there are roughly 3.24 million hectares of woodland (c.13 % of the UK's land cover) with c.14 000 more hectares planted between 2021 and 2022, the majority in Scotland [Figure 2.4]. At present the largest amounts of land cover change across the UK is rotation forestry and replanting conifers (Cole

et al., 2018). The state of UK woodlands is debated with some arguing they are neglected as standard practice (Dandy, 2016). This of course raises questions about the environmental implications of additional woodland across the UK and whether our existing knowledge of UK afforestation impacts is sufficient if we plan to grow more trees.

To reach Net Zero, the UK Government, on the recommendation of the Committee on Climate Change, is trying to plant up to 30 000 hectares of trees a year by 2030 (Committee on Climate Change, 2018). The Welsh Government itself wishes to plant at least 2000 hectares a year up to 2030 (Welsh Government 2018). Deciding where these trees can be planted is difficult as the high rates of afforestation in the 20th century mean the majority of locations best suited to afforestation have already been taken (Thomson *et al.*, 2018). This is creating a situation where woodland planting area is far below Government ambition (Environmental Audit Committee, 2023).

The global tree restoration potential dataset predicts an extra 4.2 million hectares of additional woodland available in the UK (Bastin *et al.*, 2019), but despite its criticisms of plausibility (Friedlingstein *et al.*, 2019), it would lead to losing 30-50% of protected habitats in the UK and thus is not a realistic scenario (Wilkes *et al.*, 2020). Different afforestation scenarios have been proposed for the UK and its individual nations (Bradfer-Lawrence *et al.*, 2014; Manzoor *et al.*, 2019; Sing and Aitkenhead, 2020), however there is no guaranteed strategy on how and where trees will be planted across the country. As previously acknowledged it is important to understand the multiple potential benefits of afforestation which interlinks with where trees might be planted. Determining the hydrological consequences of afforestation and whether there are ideal locations to mitigate floods is essential to enable planting the right trees in the right place.

2.2.3. The Hydrological Consequences of Afforestation

Observing and determining afforestation impact on hydrology is not a modern endeavour. Pliny the Elder, in the first century AD, first wrote of the connection between forests and the hydrological cycle. Throughout European history, the influence of forests on water resources has continually been documented with the debate of forests and flooding going back to at least the 19th century (Andréassian, 2004).

Forestry impact on water resources is governed by several factors. Firstly, the spatial extent of woodland planted, where it is planted and the position of planting relative to the surrounding landscape (Vertessy *et al.*, 2003). Importantly, as the proportion of land afforested increases, the hydrological signal of afforestation increases (Blöschl *et al.*, 2007; Marapara *et al.*, 2021). Secondly, the influence the water usage of trees which is governed by the climate, water availability and tree biophysical properties (Morris and Benyon, 2005). Despite woodland detectably impacting hydrology, when attributing overall land cover impact on streamflow, forestation only has a small impact on predicting flow (Oudin *et al.*, 2008). Do *et al.*, (2017) found the inclusion of forests did not significantly impact their ability to predict maximum annual streamflow globally. Other attempts to attribute woodland streamflow impact have similarly struggled to detect a significant signal (Anderson *et al.*, 2022). The relatively small influence of woodland on the hydrological cycle when monitoring catchment outputs can make determining the exact impact of afforestation challenging. It is often easier to attribute a reduction in streamflow with afforestation at scales less than 10 km^2 but at larger scales (> 100 km^2) it becomes increasingly difficult (Nisbet and Thomas, 2021). In contrast to these results, clustering of the hydrological signatures of North American catchments actually found forest fraction, and aridity, as the best explainers of determining the cluster classifications (Jehn *et al.*, 2020). Furthermore, observations from across the United States and Australia, a streamflow attribution analysis found deforestation and wetter climates produced larger annual discharges and, afforestation and drier climates decreased annual discharge (Booij *et al.*, 2019). However other research has attributed increasing global annual runoff with deforestation, but not detected a decrease with afforestation (Zhang *et al.*, 2017). These indicates the complicated and mixed picture surrounding the exact hydrological consequences of afforestation and why this occurs.

To understand afforestation hydrology, paired catchment studies are often utilised. Here, two catchments with similar hydrological behaviour, which are geographically close, and have stationary processes, are used to run an experiment whereby one catchment element, in this case woodland cover, is changed and the resulting impact is monitored in comparison to the catchment where there is no change [Figure 2.5]. In designing these experiments it is essential that only the dependent variable (e.g., land cover) changes, but it is difficult to control so many factors (Bosch and Hewlett, 1982). Furthermore, it can only often be done with relatively small

catchment sizes (< 5 km^2) to minimise uncertainty in control variables. However, paired catchment studies have been invaluable in our understanding of hydrological processes such as developing the variable source area concept - fundamental for our models such as TOPMODEL (Beven *et al.*, 2021). An early example paired catchment work was undertaken by Professor Engler in Switzerland at the start of the 20th century to understand flooding, changes in bedload and landslides in catchments with deforestation (Engler, 1919; McCulloch and Robinson, 1993). The Wagon Wheel Gap in Colorado is another study which clearly defined the role of forest cover on changes in water yield with forest cover (Andréassian, 2004).

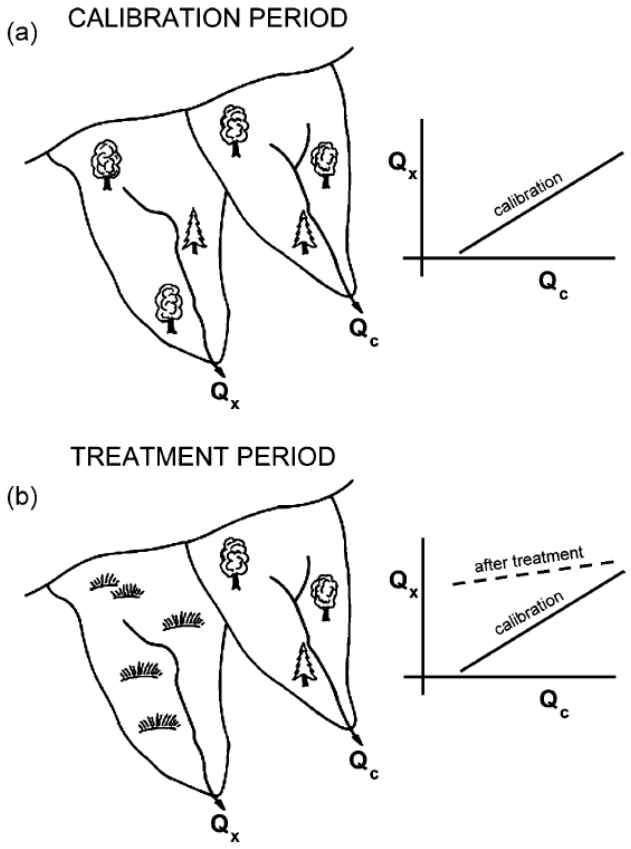

Figure 2.5: Diagram explaining how paired catchment studies are used (Hewlett, 1982).
In the calibration period (a) the streamflow of both catchments (Q_c and Q_x) is compared and recorded. In the treatment period (b), one catchment is altered, and the response is compared to the calibration period. With woodland hydrology, often the one catchment attribute changed is the spatial extent of trees.

In the UK, one of the most famous experimental catchments is the Plynlimon catchment in Wales at the head of the Severn river which has produced over 40 years of observations and by 2012, over 500 papers (Robinson *et al.*, 2013). In the 1950s, Law argued that planting trees in

headwaters could substantially reduce downstream water resources (Law, 1956). This led to the infamous debate in hydrology and afforestation: water supply versus demand (Ellison *et al.*, 2012). In response, the Plynlimon catchment experiment was set up to provide answers. The demand-side of the water yield debate following afforestation often relies on evidence from smaller catchments that show reduced overall water yield downstream. However, the supply-side of the debate argues woodland, when considering larger spatial scales (even beyond catchment boundaries), can intensify the hydrological cycle and increase overall water downstream. This was noted by Calder & Newson back in 1979 (Calder and Newson, 1979). In water-limited catchments therefore, which may be particularly arid, afforestation could make water resource issues worse as trees utilise all available water to grow (Calder, 2007). In contrast, in an energy-limited catchment, afforestation could reduce flood risk. In the early stages of forest growth at Plynlimon, evaporation rates in wooded areas far exceeded surrounding grasslands (Hudson *et al.*, 1997; Marc and Robinson, 2007). Therefore, it was thought evaporation from the catchment could reduce flooding. However, there was no significant reduction in the largest flows (Kirby *et al.*, 1991). Over time the level of evaporation diminished and was less after felling. Similar effects have been observed in other paired-catchment studies around the world (Bathurst *et al.*, 2018, 2020). There are therefore continual questions being added to the debate on the controls woodland has on catchment hydrology and arguably we are not much closer to fully resolving the initial question.

Plynlimon is not the only catchment that has helped inform our understanding of how woodland can alter catchment streamflow. What follows is a set of examples, that although not comprehensive, gives an indication of the broad evidence of woodland effect on streamflow. The Coalburn catchment (northern England) had a similar setup to Plynlimon and complete woodland cover, compared to grassland, reduced annual runoff by 24% (Bathurst *et al.*, 2018). Bathurst *et al.* (2020) looked at similarly sized catchments (0.34 - 3.1 km^2 in size) from around the world and found forest cover could reduce peak streamflow by up to 50% compared to grassland catchments. Looking beyond paired catchment studies, a number of global studies have also investigated the influence of woodland on terrestrial hydrology. One early study looked into 26 catchments datasets and found annual runoff reduced by approximately 44% when grasslands were replaced with woodland, with greater proportional reductions in more arid areas (Farley *et al.*, 2005). Of note, there were greater increases in evapotranspiration than there were decreases in runoff as it was hypothesised that the trees reached deeper water

sources to supply the increased transpiration. One of the more widely cited pieces of research is that of Bradshaw *et al.*, (2007) who found a 10% decrease in woodland cover increased flood frequency between 4-28% in 56 developing countries (Bradshaw *et al.*, 2007). However further work reanalysed this data and showed 83% of the variation in flood reporting could be explained by population density compared to 10% with deforestation, suggesting that the assumption that forests protect us from floods led to the wrong conclusion (van Dijk *et al.*, 2009). A meta-analysis of studies from around the world learnt forestation reduces annual river flow by 23% after 5 years which increases to 38% after 25 years (Bentley and Coomes, 2020). In areas of higher precipitation, greater increases in forest area and conversion from agricultural land generated the largest flow reductions. A global review of 312 global watersheds observed a statistically significant influence of forest cover on annual runoff but not to afforestation when considering scales from less than 1000 km^2 and more (Zhang *et al.*, 2017). This study, similarly to earlier studies, also found that annual runoff is more sensitive in water-limited watersheds compared to energy-limited ones. It is therefore important when considering both the location and the spatial scale of the inquiry when investigating afforestation influence on water resources. All of these studies above clearly illustrate that catchments which are completely wooded are likely to have on average a lower water yield and overall runoff. This does not fully answer the question on whether we can use it as a form of nature-based solution for water management. To emphasise, a systematic review of forest restoration on water yield revealed that most studies, as above, report decreases in water yields following intervention but in South America, you normally see an increase, which could be the influence of the greater scales of forestation involved (Filoso *et al.*, 2017). One of the main challenges that arise from these studies is the difficulty of determining the effect of woodland on large catchment scales. Many of the aforementioned studies have investigated afforestation impact on small catchments and when larger catchments have been investigated, similar original conclusions are not found. Further work is therefore required to bridge the gap to understand the consequences of afforestation at countrywide scales.

One approach to meet this challenge is to use modelling. Attempts to model the impact of afforestation on the hydrological system can be found all the way back to the start of the 21st century (e.g., Gush *et al.*, 2002). Numerical modelling work often shows woodland reducing overall runoff and below is a set of examples. Modelling afforestation using oak and conifers in the Lake District, Aberdeenshire and the Southern Uplands of Scotland, led to similar reductions in mean annual surface runoff, but riparian woodland minimally impacted surface

runoff comparing between the different catchments (Smith *et al.*, 2018). After generating 7000 landscapes of varying afforestation fragmentation in the Conwy catchment, Wales, it was modelled that regardless of planting location, additional woodland would reduce overall runoff (Thomas et al., 2020). A study using TOPMODEL and investigating land management strategies in two UK upland catchments found 80% woodland cover produced the greatest reduction in the discharge peak (Bond *et al.*, 2022). Iacob *et al.*, (2017) researched whether increasing afforestation in the Tarland catchment, Scotland, could mitigate climate change using a model. They found it would reduce increased flow from climate change but large-scale woodland expansion of more than 75 % of catchment area would be needed to maintain peak flows at present levels. A similar analysis which conducted a cost benefit analysis study found afforestation would only be beneficial for hydrological services with climate change in certain scenarios, such as those where this is more frequent flooding (Dittrich *et al.*, 2019). These results illustrate that the changing nature of the hydrological system needs to be acknowledged in conjunction with changes in woodland cover on the Earth's surface if attempting to quantify potential streamflow. However, use of these models can be limited as they do not account for the full complexity of modelling afforestation where there needs to be recognition of the biophysical and the hydrological factors (M. Cooper *et al.*, 2021). There is a need therefore for numerical models that account for all the relevant Earth systems such as the carbon and nutrient cycles as well as including more temporally dynamic water storage features (e.g., the canopy).

There is a strong debate on planting trees in the right place to achieve maximal benefits and further research is required to reduce the homogenisation of the hydrological cycle, with minimal benefits for all (Levia *et al.*, 2020). Studies, often modelling, have investigated the impact of woodland location on streamflow, as it is difficult to undertake experimental catchments that can be set up to answer this question. Modelling projected that planting coniferous trees in lowland farming areas, compared to other regions in a catchment, would have the greatest impact on reducing the highest flows (Iacob *et al.*, 2017). Early modelling using the Topog model by Vertessy *et al.* (2003) suggested that planting trees in the lower 30% of a catchment would reduce annual runoff more than the upper 30%. Although a different climate to the temperate regime of the UK, modelling in the tropical Andes also alludes to the idea that forest location is more influential than fragmentation when trying to reduce overland and storm flows (Hurtado-Pidal *et al.*, 2022). All these pieces of work indicate that afforestation location is critical in altering the hydrological response of a catchment to woodland planting,

whether this is realistic (as discussed later) is up for debate as much of the evidence is based on models that may not be fully representative of the needed Earth systems to answer the question.

There are many smaller scale observational studies that have investigated in greater process granularity the influence of woodland on hydrological fluxes. Woodland has been shown to increase soil conductivity and overall soil moisture. Examples of soil conductivity increases stretch from the forested headwaters of North Carolina (Scaife *et al.*, 2020) to the moors of Dartmoor (Murphy *et al.*, 2021). This is also true across tree species where Scots pine (*Pinus Sylvestris*) and sycamore (*Acer Pseudoplatanus*), in both grazed and ungrazed conditions, had greater soil hydraulic conductivity than adjacent pastures (Chandler *et al.*, 2018). When looking at the water table below forest strips it can be seen that the depth is lower than adjacent grasslands with forest drying being deeper and longer into autumn (Peskett *et al.*, 2020). This is important to note as the height of the water table has a significant control on vegetation growth and tree root depths (Roebroek *et al.*, 2020), although these will continue to develop and evolve during the Anthropocene (Hauser *et al.*, 2022). The attributes of woodland to both decrease the soil moisture store and increase the speed in which rainfall can penetrate the soil, has led to the belief that woodland should be able to 'slow the flow' of storm runoff.

Research has also shown that evaporation rates from woodland can be higher than shorter vegetation, particularly in upland regions. Using published meteorological data, Page *et al.* (2020) calculate wet-canopy evaporation losses in mountainous regions in the UK range from 1.5 to 39.4 mm day^{-1} (or 2 to 38% gross rainfall) on rainfall events of over 100 mm day^{-1}. This provides strong evidence again of woodland, particularly in upland regions, could reduce the amount of rainfall contributing to stormflow. However, the amount of evaporation depends on tree species with higher rainfall interception rates of 25-45% for conifers compared to 10-25% for broadleaves (Nisbet, 2005). Furthermore, the age of the woodland can also play a role where evapotranspiration rates can vary as the trees become more mature (Marc and Robinson, 2007; Thomas and Nisbet, 2007; Neill *et al.*, 2021). These studies therefore illustrate the complex relationship which woodland play on determining the fate of rainfall within a catchment.

Due to observed characteristics, it has been extensively hypothesised that woodland could act as a form of Natural Flood Management (NFM) by reducing peak streamflow (Dadson *et al.*,

2017; Lane, 2017; Ellis *et al.*, 2021). This involves intercepting and evaporating water from the canopy, creating hydraulic roughness for overland flow, enhancing infiltration and generating soil macropores, and increasing soil moisture capacity by using water for growth. There is a risk of research bias with opinions being swayed by wishful thinking, however. As noted by Carrick *et al.* (2019), although across seven studies and 156 papers, there was a slight reduction in channel discharge with afforestation it was suggested that there might be publication bias. The review by Stratford *et al.* (2017) of 71 studies of similar Köppen climate classification to the UK indicates that the majority of statements support the belief that increased tree cover decreases peak flow, and decreased cover increased peak flow when considering both modelling and observational studies. When looking at just the observational studies, there are a notable number that suggest the opposite is true or there is no effect. An increasing amount of modelling using similar models may reinforce perceptions found in the existing modelling studies (Stratford *et al.*, 2017; Carrick *et al.*, 2019). When considering small floods, there is consensus that flood peaks reduce with more tree cover, but no influence is detectable on the largest floods with the addition or removal of trees. Unfortunately much of the catchment-based evidence for woodland influence on streamflow for NFM has a high UK bias and thus further work is required to find more studies that go beyond these temperate regions (Connelly *et al.*, 2020). Further studies are therefore required to build upon our current research and find new approaches, methodological and conceptual, to determine whether afforestation can provide positive water resource management. There is also a need to bring both public and scientific perceptions of woodland influence on hydrology together given its complex nature (Calder, 2002).

It has been frequently noted woodland can reduce low to moderate streamflow events but has increasing irrelevance at higher flows (Lane *et al.*, 2005; Rogger *et al.*, 2017; Bathurst *et al.*, 2020). For example, Soulsby *et al.* (2017) concluded that in the River Dee catchment, Scotland, the biggest floods were unlikely to be affected by forest cover due to high antecedent soil moisture conditions. Another study in Belgium notes woodland did not reduce high flows but made runoff less flashy (Brogna *et al.*, 2017). However, it has been repeatedly documented that forestry practices make the determination of afforestation impacts difficult (Beschta *et al.*, 2000; Bathurst *et al.*, 2018) which is not helped by the issue that deforestation effects are not the same as afforestation (Robinson *et al.*, 1991). Forestry practice impacts can include soil compaction, road construction and artificial drainage which may lead to opposite or different

magnitudes of effects to natural woodland. The complexity of factors influencing the impact of woodland would suggest that we need to move beyond simple comparisons of forested compared to non-forested catchments (Neill *et al.*, 2021). This is particularly acute as research has indicated that catchment runoff is sensitive when woodland with low ecosystem complexity is subjected to external disturbances (Yu *et al.*, 2022). It is therefore essential when trying to determine the impact of afforestation on the hydrological system that we understand everything that may be generating the phenomena we observe. A particularly difficult challenge when using observational data in which we may not have all the necessary information.

Woodland can have a significant influence upon hydrological fluxes and stores within small catchment spatial scales. However, as briefly alluded to, once we begin to explore its influence over large spatial scales (> 1000 km^2), it can have considerable ramifications further afield. If woodland both 'slows the flow' and evaporates a significant portion of water from the catchment following transpiration and rainfall interception, where does that water go?

2.2.4. The Broadscale Hydrological Impacts of Afforestation

It is increasingly recognised afforestation not only has intra-catchment effects, but also inter-catchment influences. This is predominantly due to its influence on atmospheric water fluxes: precipitation and evaporation. Transpiration generates a signification proportion of precipitation over land (Trenberth *et al.*, 2007), thus illustrating that, depending on hydrological controls and climate, woodland can have a significant role on the hydrological cycle, particularly as it makes up to a third of the Earth's surface (Bonan, 2008). At scales of 1000 km^2 and more forests can have a substantial effect on the hydrological cycle as air passing over forested areas can produce twice as much rainfall as short vegetation (Spracklen *et al.*, 2012). It is quite a quick turnover as globally 70% of plant transpiration comes from precipitation in the current month compared to only 18% in the deeper unsaturated soils annually (Miguez-Macho and Fan, 2021). This adds to the complexity of why streamflow response to afforestation may get washed out as increased precipitation offsets potential terrestrial water resource reduction.

Many studies have investigated and attempted to quantify the large-scale hydrological impacts of afforestation on hydrometeorology. Via a range of methods, it was predicted that if all available land was converted to forest, actual evapotranspiration would increase and runoff would decrease (Trabucco *et al.*, 2008). Recent work by van Dijke & Teuling (2022) with a 1 km^2 Budyko-model suggests that using the global tree restoration potential created by Bastin *et al.*, (2019) would increase evaporation, due to deeper roots, higher leaf area and lower albedo. As a consequence, this would increase downwind precipitation with enhanced moisture recycling with an approximate increase of global precipitation of about 0.7% per year. Further work focusing on Europe, using observation-based continental-scale statistical models, also indicate that changing rain-fed agricultural land would significantly change precipitation patterns, with a particular increase in downwind precipitation in summer (Meier *et al.*, 2021). Modelling changes in streamflow and evapotranspiration found a combination of land cover changes, including afforestation/reforestation and urbanisation, enhanced evapotranspiration by between 5-15% comparing the decades of 1955-1965 and 2005-2015 (Teuling *et al.*, 2019). These pieces of work all indicate that when looking at a continental landmass, woodland is likely to have a significant impact on precipitation by increasing the amount of evaporation and consequently the amount of atmospheric water.

Forests can also have more significant global impacts on the hydrosphere in relation to hydroclimatic extremes. Insua-Costa *et al.*, (2022) estimate that North American forests could have transported more than 463 billion litres to Europe for the 2021 European floods, which is more than the contribution of water from surrounding seas. This is a strong illustration of how exchanging more terrestrial water stores to the atmosphere can have severe consequences with afforestation. Furthermore, it has been suggested that CO_2 fertilisation and land use changes have led to an overall increase in leaf area across the planet, leading to an overall increase in the global precipitation over land by 1.2% (Cui *et al.*, 2022). On the opposite side of the equation, deforestation can lead to a reduction in precipitation. As an example, when considering the Amazon, deforestation reduces regional rainfall with a strong feedback between soil moisture and drought propagation (Staal *et al.*, 2020). Therefore, if we are looking at how to use widespread afforestation as a form of NBS, we must look at spatial extents far greater than the local planting location.

The influence of forests on evaporation, and thus precipitation, rates is far from certain (Bonan, 2008). This is predominantly due to the uncertainty in partitioning sensible and latent heat

fluxes as a consequence of the lower woodland albedo. Teuling *et al.*, (2017) detected enhanced cloud formation over large forest regions in western Europe and suggested the lower albedo and rougher surface enables more efficient exchange of heat, moisture and momentum. Xu *et al.*, (2022) use of satellite observations also shows a larger sensible heat driver with smaller cloud enhancement in forests with lower sensible heat. Satellite and atmospheric boundary-layer models illustrate the impact of cloud cooling of afforestation in the midlatitudes which could reverse the partitioning in heat fluxes observed (Cerasoli *et al.*, 2021). This raises a further impact of afforestation on atmospheric conditions which is the canopy height and resulting influence on the atmospheric boundary layer. It adds further roughness, and this has been shown to have an influence on reducing cyclone intensity due to additional friction (Belušić *et al.*, 2019). Breil *et al.*, (2020) utilised a land surface model and learned afforestation amplified the diurnal temperature cycle due to greater surface roughness increasing the atmospheric sensible heat transport. Part of the challenge in determining the balance in sensible and latent heat fluxes is the time-varying nature of water stores. Using observations from flux towers from across Europe it was shown surface heating was initially twice as high in forested regions than grasslands due to the increased evaporation but as the soil moisture store became depleted, it became warmer than the forested areas over the long term (Teuling *et al.*, 2010). It is therefore critical that models, and our understanding, acknowledge the role of woodland on energy fluxes as it has impacts that propagate beyond the Earth's surface.

Part of the challenge in calculating evaporative rates is due to models showing divergent responses in the partitioning of sensible and latent heat fluxes. Work done by Lejeune *et al.*, (2017) illustrates disagreement between the CMIP5 models with latent heat flux production in summer which would aid evaporative cooling and alter cloud formation. When exploring forestation in the Land Use and Climate Across Scales project, there was a similar decrease in albedo, but again divergence in the partitioning of sensible and latent heat fluxes (Davin *et al.*, 2020). Reasons for differences between models could be unrealistic root distributions, photosynthetic parameters and water uptake formulations within some of these models as seen in the work of Meier *et al.*, (2018) with the Community Land Model. However, despite the challenges in which land surface and Earth system models (discussed later) find themselves with, they offer the most comprehensive and advanced representation of hydrological processes on Earth. Despite their hydrological representation often being discussed as rudimentary, it is their strength to combine the breadth of interconnected Earth system processes to represent the

Earth's surface more faithfully. In this way, the provide an adequate basis from which to investigate the role afforestation could have on the hydrological system.

To summarise, afforestation can have a significant impact on global water resources and energy balances, but our understanding is still limited. This has led to models of all varieties representing woodland in opposing manners, which indicates a need for more research into both our base understanding of woodlands and how to implement this into models. There is research at small catchment scales and large global model studies, but further research is required to develop a full process-based understanding of the impact of woodland on countrywide terrestrial water cycles.

2.3. Models

2.3.1. The Modelling Paradigm

Models allow us to make sense of data. We use them to not only learn about the world around us, but also to predict how it does, and will, change. A range of models exist, ranging from perceptual, empirical, conceptual, all the way to physical. Each one of these model types vary in their complexity from those that contain a small number of ideas to those which are a combination of a large, interlinked array of processes and feedbacks between elements. By using observations, we can start by making a perceptual model of a system before moving on to formulate more comprehensive models.

One paradigm often used to describe modelling for understanding the world is the data-driven versus physics-based approaches. In the data-driven approach, often a method is applied that derives relationships between variables. Data-driven methods range from regression and correlations to the more frequently and recently discussed machine learning methods (Kratzert *et al.*, 2019; Berghuijs *et al.*, 2021; Nearing *et al.*, 2021). The philosophy of these models is that minimal bias is imparted on the system, only in the decision of variables to explore. However, this can lead to difficulties in deriving actual processes as it is fundamentally a 'black box' with no physics-based understanding and can also make it difficult to find new measurements that improve our understanding of a system. Any physics-based understanding is imparted by the modeller and thus introduces bias by their own views that was intended to have been removed using these methods. We therefore use physics-based models, that include our data-derived world representations, to investigate if these are accurate enough to produce our observations.

Physics-, or process-based, models are seen from the perspective of being either top-down or bottom-up. Top-down models offer simple empirical relationships of reality, as if viewing the system as a whole, whereas bottom-up attempt to represent physical processes and apply them upwards to larger scales (Peel and McMahon, 2020). To some extent all models lie on a continuum between these two states and so one cannot be viewed as explicit from the other (Hrachowitz and Clark, 2017) [Figure 2.6]. It is important to have both top- and bottom-process representation if we are to truly know a singular system from multiple perspectives.

The statistician George Box is attributed to suggesting the idea that all models are wrong, but some are useful and this is important to consider when thinking about modelling (Box, 1976a). Importantly he emphasises the need for a scientist to know what is 'importantly wrong' such that a model is an appropriate representation of reality. Process-based numerical models go through a life cycle in their formulation. We start by creating the perceptual model, then a quantitative model, the governing equations are solved, model parameters are determined, predictions evaluated and these steps are repeated to refine our model (Beven and Freer, 2001). In this way we can think of a model as a learning process of the world around us where its creation not only aids prediction of the world but as a form of falsification of our hypotheses (Beven, 2007; McMillan *et al.*, 2022). In this sense, the question should not be 'how good is a model' but rather what the model is useful for (Clark, Vogel, *et al.*, 2021).

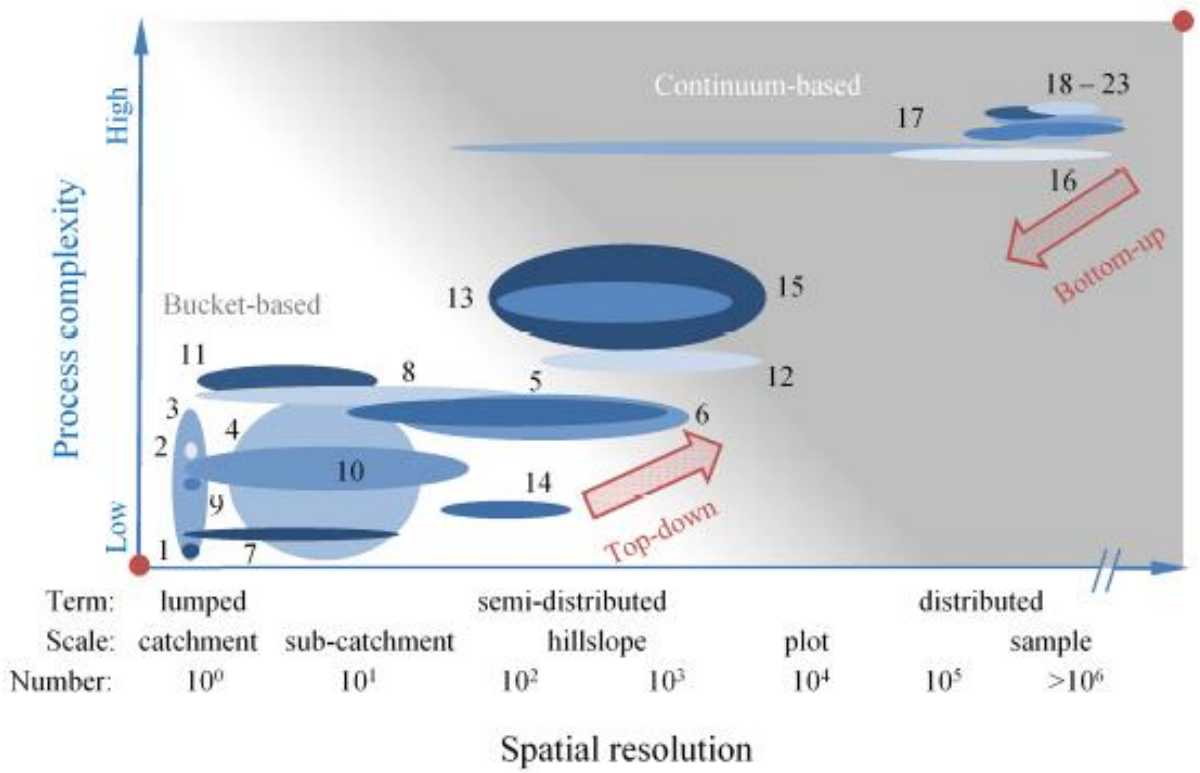

Figure 2.6: Simple diagram from Hrachowitz & Clark (2017) presenting the continuum of models across spatial and process resolution.

A list of the model numbers being represented can be found in the original article. Of note, 1 represents a unit hydrograph, 12 TOPMODEL (Beven and Kirkby, 1979) and 18 PARFLOW (Maxwell et al., 2015).

Over time, models have become more complex as we collect more data on Earth system processes and computational resources enable more sophisticated interlinkages between processes. This has led to not only a plethora of models being created, but also a quest to find all the relevant processes. At its core, this targets the principle of parsimony, or as George Box calls it an 'economical description of natural phenomena' (Box, 1976, p.792) where a model should be as complex enough to capture all relevant information related to the system in question, but simple enough as to reduce the uncertainty in our assessment (Wainwright and Mulligan, 2013). We have therefore reached a point where we are hunting models that generate the right result for the right reason (Kirchner, 2006). This leads to the dichotomy of model *accuracy* and *fidelity* where it can be difficult for a model to achieve both. Model *fidelity* in essence is the model being faithful to the physical processes in which Martyn Clark and others (2015, p.2538) note needs a 'sagacious choice of both process parameterisation and model parameters'. The challenge begins on where to find the balance between what needs to have explicit parametrisations and what needs to be parameterised (Bierkens *et al.*, 2015). However, due to epistemological uncertainty within system processes our implementation of said processes are often flawed and the reductionist approach may leave relevant processes unincluded. For example, the influence of the carbon cycle on soil moisture. Machine learning is a perfect example of illustrating an accurate model that is potentially unlikely to be *fidelious*[1], whereas the most start-of-the-art Earth Systems Models are seeking to achieve fidelity but are comparatively inaccurate. One idea to help improve the fidelity of models is to develop 'laugh tests' or Turing tests in which the realism of the produced model is evaluated (Clark, Zolfaghari, *et al.*, 2021; Beven and Lane, 2022; Beven *et al.*, 2022). This is particularly important as effective parameters have become too easy to implement and costly to not fully understand (Beven *et al.*, 2022).

With this continual model development comes a need to understand the uncertainty augmented within them. Machine learning overcomes uncertainty related to observational data by including effective parameters which account for potential errors within the data, whereas a physics-based model is limited by the fundamental laws of physics and the data it uses (for example water cannot be created or destroyed to match the data) (Beven, 2020; Nearing *et al.*, 2021). The physics-based modeller will therefore forever hunt the 'holy grail' of hydrological

[1]Martyn Clark advocates the use of an Olde English adjective *fidelious* to the language surrounding hydrological modelling to explain a model's fidelity (https://uofs-comphyd.github.io/blog/fidelious).

modelling, closing the water balance, in vain until the uncertainty and error in the observational data is reduced (Beven, 2006).

Another form of uncertainty to consider is aleatory uncertainty from the random nature of the system. This is often defined as a probability distribution in which there are more and less likely outcomes, but this leads to a large range in the potential deterministic model outputs. Engineers often embrace the aleatory uncertainty but ignore the epistemic uncertainty when creating predictions (Wasko, Westra, *et al.*, 2021). This of course raises significant issues in which engineered infrastructure may be blind to dangers that pose critical weaknesses to its ability to perform correctly.

When parameterisations and governing equations are implemented, there is also a need to embrace the potential errors associated with the numerical implementation of the model which has led for a call to try and separate the numerical implementation from the governing equations (Clark and Kavetski, 2010; Clark, Zolfaghari, *et al.*, 2021). Colloquially errors caused by the numerical implementation have been called 'numerical daemons' which are often summoned by extreme events pushing the calculations to their upper limits (La Follette *et al.*, 2021). The numerical implementation can often refer to the time-stepping procedure in numerical physical-based models such as forward and backward Euler methods. There can also be hard-coded constants in models which lead to unrealistic and inaccurate results (Cuntz *et al.*, 2016). When using these numerical models, we must therefore be aware that it can be difficult to separate the science from the practicality of applying our understanding within a model. Any output from these models must be understood through this guise.

There is a form of social practice that accompanies the use of a model as well. When making a model, one must consider the fidelity, complexity, practically and data availability of the model and associated resources (Clark, Nijssen, Lundquist, Kavetski, Rupp, Woods, Freer, Gutmann, Wood, Brekke, *et al.*, 2015). This has led to the models becoming social constructs rather than objective tools suggesting that it 'takes a village' to run a model (Melsen, 2022). This produces situations where a model is used more on the ease of application and legacy, rather than being appropriate and able to represent the relevant processes (Addor and Melsen, 2019). Often when setting up a model it is remarked that the majority of the time is consumed setting up the model compared to answering the scientific question (Arheimer *et al.*, 2020; Knoben *et al.*, 2022). By increasing the spatial resolution by a factor of 10 you increase the calculation and storage

requirements by a factor of 100 (Bierkens *et al.*, 2015). As such there are many model structures, parameterisations and numerical implementations that have developed both dependently and independently of the wider modelling community.

Sometimes calibration can produce compensatory parameters to get the 'right' answer for the wrong reason (Kirchner, 2006). Arguably the reason there are so many models is due to an insufficient understanding of the world around us. We must therefore use models as multiple working hypotheses if we are to learn more about the world around us and to improve our predictions (Buytaert and Beven, 2011; M. P. Clark *et al.*, 2011). An alternative suggested in the hydrological community is to create a community model (Weiler and Beven, 2015), but this is unlikely at present with the number of current models. The key paradigm continuing the pursuit in the hydrological sciences, and others, is the want of a 'model of everywhere' (Beven, 2007; Blair *et al.*, 2019). The idea that it is possible to create a model, that given the appropriate driving data and information, can accurately simulate processes anywhere. The hunt for a model of everywhere relies on invalidating models on our inductive quest to ensure that models that perform at a particular space and time can across all scales. However, models are only as good as the data and information that drives them (Beven and Lane, 2022).

All these ideas and concepts must be noted when considering the challenges facing prediction of floods and droughts with modelling and process understanding being key challenges (along with data and human-water interactions) to our ability to accurately predict hydroclimatic extremes (Brunner *et al.*, 2021).

2.3.2. Numerical Hydrological Modelling

Essentially, the hydrological system can be rudimentarily represented as a series of stores and fluxes (McMillan, 2022). Perceptually considering hydrology in this manner enables us to create models to represent it. Each hydrological model is unique to the modeller, being a representative system that incorporates, and even exaggerates, the functional parts of certain parts of the hydrological system at the expense of information that is deemed irrelevant (Box, 1976b; Foster *et al.*, 1986; Beven and Chappell, 2021). There is no one agreed model structure for creating a catchment hydrological model. At its most basic the model is comprised of inputs, states and outputs (Liu and Gupta, 2007). The most basic model would encode this information

as precipitation (input), catchment water storage (state), and evaporation and runoff (outputs). However, even with these most simple models, many ways exist to parameterise these fluxes and stores. For example, streamflow can be separated into both fast and slow flow components. Model parameters and architecture therefore lead to nonlinear and linear process representation that generates varying sensitivities and flux responses that vary in both time and space (Mai *et al.*, 2020; Bittner *et al.*, 2021; Van Kempen *et al.*, 2021)

It has been argued rainfall-runoff catchment modelling does not require a high degree of complexity. Beven (1989) suggests three to five parameters should be more than sufficient to predict runoff while Kirchner demonstrates the Plynlimon catchment can be represented with a single equation as well as models with more parameters (Kirchner, 2009). However, the uniqueness of place and the continuum of processes, both in time and space, means a large number of models exist that attempt to capture all the processes needed to predict hydrology anywhere (Beven, 2020; Horton *et al.*, 2022). This of course is at odds to the idea that there should be a unifying model of everywhere. Current hydrological models range from those that only require a few parameters to calibrate for individual regions (e.g. GR4J (Perrin *et al.*, 2003)) to more complex process-based models that are used at countrywide and continental scales. These have been implemented in ways in which they can be used and applied easily with a basic understanding of programming making them accessible and testable within the hydrological community (Slater *et al.*, 2019; Astagneau *et al.*, 2021).

Due to a potential lack of knowledge on how to implement hydrological lessons from the catchment to the global scale, models developed for certain locations are now extrapolated beyond their intended spatial scales (M. P. Clark *et al.*, 2011; Blöschl *et al.*, 2019). For example, TOPMODEL was developed according to the variable source area concept and in-depth testing of a few locations, such as the Mendips, UK, however it is now used ubiquitously around the world (Beven and Kirkby, 1979; Beven *et al.*, 2021). This is despite several of its known deficiencies such as representing the water table as parallel to the surface. In the search for the most representative and relevant hydrological system representations there has been a rise in model intercomparison projects that look into the structural representation of catchments such as FUSE (Clark *et al.*, 2008), MARRMoT (Knoben, Freer, Fowler, *et al.*, 2019) and DECIPHeR (Coxon *et al.*, 2019). These are now enabling us to find the most appropriate parameterisations that represent the diversity of known processes.

The structure of physically based spatially distributed hydrological models often takes one of two forms: distributed integral models whereby fluxes are in a one-dimensional column connected by a network (e.g. river) or distributed differential models whereby lateral fluxes are explicitly represented (Beven and Kirkby, 1979). This central decision is essential for determining the resultant numerical implementation of the model and it can become difficult to shift the central tenant once it has been decided. At their core, physically based hydrological models still follow the blueprint articulated by Freeze & Harlan (1969) and pursue the same purposes of understanding past and future events to improve our knowledge (Freeze and Harlan, 1969; Simmons *et al.*, 2020). One of the earliest models was the Stanford Watershed Model in the 1960s when computational constraints reduced (Crawford and Burges, 2004; Beven, 2013). Similarly, although hydrological models have evolved, they still have the same fundamental underlying concepts and parameterisation decisions of this original model. This suggests that in the current scientific community the founding tenets of the 1960s hold despite an exponential increase in our knowledge of the world. Whether this is correct must be continually challenged and discussed.

A major task facing process-based bottom-up hydrological models is the issue of scale implementation of processes. These models extrapolate processes studied at small scales in laboratories to spatial extents many orders of magnitude greater than studied (Blöschl and Sivapalan, 1995; Seyfried and Wilcox, 1995). Interestingly, due to the complexity of systems, the nuances of complexity are smoothed out at larger spatial scales due to the nature of hydrology. For example, distributed precipitation across a model only improved the results of a distributed hydrological models in a few occasions (e.g. convective rainfall) (Loritz *et al.*, 2020). However, this does not necessarily mean that we are getting the right answers for the right reasons. The origin of ideas for our numerical models must be acknowledged if we are to analyse their outputs.

Distributed physically based hydrological models are an important way in which we undertake impact assessments of hydrological phenomena. Increasing computational power and hydrological understanding has generated many complex hydrological models. Fundamentally, they fulfil the water balance ‘holy grail’ criteria (Beven, 2006) whilst continuing to follow the fundamental modelling blueprint (Freeze and Harlan, 1969). A few examples include: SHETRAN (Ewen *et al.*, 2000), WaterGAP (Döll *et al.*, 2003), ParFlow (Maxwell *et al.*, 2015), LISFLOOD (van der Knijff *et al.*, 2010), HBV (Bergström and Rapporter, 1976), VIC (Liang

et al., 1994), and MIKE SHE (Refsgaard *et al.*, 1995). Over time these models have evolved by adding or refining existing processes to generate more accurate results. Some have common ancestry such as SHETRAN and MIKE SHE, which started from the Système Hydrologique Européen but have subsequently branched off into separate Danish and UK endeavours (Abbott *et al.*, 1986; Beven, 2013). Distributed physically based hydrological models are important as they provide time-evolving solutions to partial differential equations (e.g., water flow in a soil column). This makes them invaluable for exploring hydrological system responses over time, such as during flood or drought conditions in relation to a catchment's water stores and fluxes. At catchment scales they have been useful in understanding forest hydrology (e.g., Birkinshaw *et al.*, 2014), land use (e.g., Schilling *et al.*, 2014; Gao *et al.*, 2018) and land management practice changes (e.g., Hankin *et al.*, 2017). Physically based hydrological models are therefore relevant in understanding impact change assessments and further developing our understanding of hydrology. Their singular focus on more accurately representing the hydrological system is now leading to model developers incorporating and exploring adjacent relevant systems for their improvement (Beven, 2013).

Current hydrological models are currently behind in our understanding of the hydrosphere. For example, they do not sufficiently represent groundwater processes (Gleeson *et al.*, 2021; Berghuijs *et al.*, 2022), the movement of streams (van Meerveld *et al.*, 2019), the permanence of flow over time (Messager *et al.*, 2021) or account for the two water worlds hypothesis (McDonnell, 2014). This fundamentally touches upon our insufficient knowledge of water fluxes due to our inability to fully observe and comprehend the system. This has serious consequences for predicting how subsurface flows will evolve and thus influence groundwater stores (Condon *et al.*, 2020). If we do not accurately predict these flows, then inaccurate predictions may emerge. Therefore, again this must be considered when analysing model outputs and developing existing models for the future.

Hydrological modelling can lead to the idea of the hammer and nail syndrome – if all you have is a hammer (model) than everything looks like a nail (hydrological question) (Horton *et al.*, 2022). By 2010 over 75% of hydrological scientific publications were model studies which arguably led to reinforcement of our perceptual environment despite the need for further discovery (Burt and McDonnell, 2015), however since then, there has been a decrease in the number of modelling studies (Rahman *et al.*, 2022). This is a combination of finding observations to feed our understanding and the need to find governing laws beyond those

represented already in models. Caution should therefore be applied before using a model to ensure it is appropriate to the scientific query.

With our uncomprehensive understanding of hydrological processes, a range of models have developed which incorporate all the factors in which the modeller believes to be relevant (M. P. Clark *et al.*, 2011). Considering the future, this means that there is large divergence in hydrological projections as a result of model architecture (Melsen *et al.*, 2018). In areas in which our understanding is minimal, this therefore leads to large uncertainty. A good example of this is the southeast of the UK where many models do not converge on a precise direction and magnitude in flow regime (Chan *et al.*, 2022; Lane *et al.*, 2022). This would suggest that our current models are unfit for these hydrological processes and thus as a community there is a need to find out why and how this can be improved. In the future it will be important to embrace largescale hydrology and data-driven machine learning approaches as we seek to find the universal laws required to accurately and faithfully model the hydrology of everywhere (Addor *et al.*, 2020; Nearing *et al.*, 2021). By taking this approach we can incorporate our hydrological models with models that account for additional processes, such as land surface models.

2.3.3. Land Surface Models

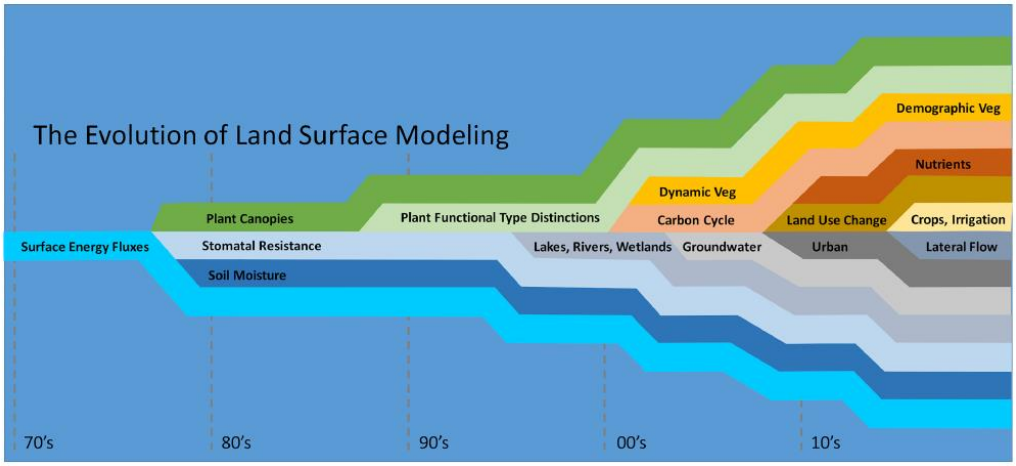

Figure 2.7: Evolution of Land Surface Models from the 1970s to the present day (Fisher & Koven, 2020).

Land Surface Models (LSMs) utilise large amounts of data, computing power, and systems understanding to comprehend, and project, the world around us. At their core, LSMs are

essentially numerical models solving fluxes of water, energy and carbon between the atmosphere and land surface (Fisher and Koven, 2020). Initially they were just used as the lower boundary conditions for atmospheric models but now there is an understanding that greater process granularity is required to accurately simulate fluxes between the land and atmosphere (Blyth *et al.*, 2021). For example, soil moisture is not just treated as a parameter to 'soak' up errors in the energy balance anymore which it initially was treated as (Blyth, 2002).

Importantly it has been recognised that an accurate energy balance at the surface requires an accurate implementation of hydrology. LSMs have evolved from just surface energy fluxes in the 1970s to include dynamic plant functional types, nutrient and carbon cycles, lateral flows, anthropogenic land use and separation of terrestrial land surface hydrology (Fisher and Koven, 2020) [Figure 2.7]. They have become increasingly interdisciplinary and provided a focus to explore complex issues requiring understanding in multiple different fields. However, arguably this has made them incredibly unwieldy and difficult to understand (Clark, Zolfaghari, *et al.*, 2021). As additional Earth systems have been added on, the number of interlinkages and dependencies between them has steadily increased which can potentially lead to emergent responses not necessarily envisioned. Despite the challenges in fully comprehending all the system interactions within LSMs, their major findings include the biophysical response of climate to increasing CO_2 (Sellers *et al.*, 1996; Betts *et al.*, 2007) and how coupling the carbon cycle to the atmosphere could strengthen the global warming rate (Cox *et al.*, 2000).

A wide range of choices exist in the creation of LSMs. These include the thermodynamics (canopy radiation and turbulence, atmospheric stability, soil profiles), hydrology (horizontal and vertical distribution, infiltration, surface and subsurface runoff, groundwater, evapotranspiration, interception) and biology (phenology, competition, limiting factors, nutrient cycling). At present new ideas and concepts are being implemented such as nutrient cycles and human activities which will require further appropriate judgments in their implementation. All these decisions result in high epistemic uncertainty within LSMs and the high number of free parameters can potentially lead to overfitting or challenges in producing fidelity in the model (Bierkens *et al.*, 2015). Even with the most state-of-the-art models we are unable to represent all processes, despite our continual quest to include all that are known (Hrachowitz and Clark, 2017).

The construction of LSMs can be considered haphazard whereby processes have been bolted on over time to represent processes relevant and understandable to the implementer, but not to the rest of the community. There is therefore a need to make LSMs more modular so that processes can be added and removed accordingly and this is openly being developed (Clark, Nijssen, Lundquist, Kavetski, Rupp, Woods, Freer, Gutmann, Wood, Gochis, *et al.*, 2015; Hallouin *et al.*, 2022). This would also enable the introduction of deep learning process representation that could both improve the accuracy of modern LSMs and boost our understanding of machine learning (Bennett and Nijssen, 2021).

There has been a continual development of the hydrological processes within LSMs, as well as other processes [Figure 2.8]. Appendix 1 contains a short summary of how land surface models can be used to tackle hydrological queries. The first explicit representation of global hydrology within a model can be accredited to Manabe in 1969 which was a simple bucket model in which soil moisture was treated as a single store with inputs and outputs (Manabe, 1969). The next major evolutionary step in LSM hydrology could be argued to be the addition of the 1-D Richards equation modelling the distribution of water through the soil column (Cox *et al.*, 1999). This allowed for a more realistic representation of soil moisture and its effect on near-surface sensible and latent heat fluxes. Following the Project for Intercomparison of Land Surface Parameterisation Schemes (Henderson-Sellers *et al.*, 1995) there was acknowledgement of the importance of lateral and subsurface flows that were subsequently added (Bierkens *et al.*, 2015). At present, we are beginning to include a 3-D representation of saturated flow through soil and plant dynamics as well as including groundwater in LSMs (Bisht and Riley, 2019; Batelis *et al.*, 2020). However, the current hydrology in LSMs is incredibly rudimentary with major limitations considered to be saturated overland flow mechanisms and the sub grid representation (Bierkens *et al.*, 2015; Blyth *et al.*, 2021). The Protocol for the Analysis of Land Surface Models (PALS) Land Surface Model Benchmarking Evaluation Project (PLUMBER) revealed the partitioning of sensible and latent heat fluxes are dependent on hydrological processes that are outperformed by simple statistical models (Best *et al.*, 2015). This raises the question of whether the information provided to LSMs is being used correctly, or if errors in the data are being accounted for within the statistical fitting procedures (Haughton *et al.*, 2016). This reveals that there are still challenges to overcome if we are to create LSMs with high accuracy *and* fidelity.

Figure 2.8: LSM system development from before 2000 and potential future directions (Blyth et al., 2021).

Most of the state of the art models continue to have simple water fluxes and pedotransfer functions (PTFs) (Samaniego *et al.*, 2017). PTFs interpolate the hydraulic properties of soils depending on their composition (e.g., soil, silt and clay percentage) and as such have a strong influence on the modelled soil moisture. The most commonly used PTFs, van Genuchten (1980), Brooks and Corey (1964) and Clapp and Hornberger (1978), perform well in temperate areas but less well in soils with deeply weathered clays (Fan *et al.*, 2019). Furthermore, organic, carbon-rich soils are often poorly-represented by PTFs (Vereecken *et al.*, 2022) and the data underpinning the soil composition in areas of high organic matter often have a huge deviation on their predicted levels due to differences in the methodology used to derive them (Feeney *et al.*, 2022). The choice of PTF can have a significant impact on both the water and energy fluxes as they alter water migration rates through the soil column. Many LSMs also use look-up tables as a way to parameterise PTFs, but this negates the acknowledgement of there being a continuum of hydraulic and soil properties (Samaniego *et al.*, 2017). It also makes it more difficult to truly compare, analyse and improve our LSMs. Attempts have also been made for data assimilation pedotransfer parameters with observational data but this can lead to situations where parameters can become physically implausible (E. Cooper *et al.*, 2021). Challenges

facing the development of PTFs are the measurement of soil hydraulics, comprehensive databases, the addition of relevant predictors and developing time-dependent PTFs (Vereecken *et al.*, 2010). There is hope for improving soil moisture prediction with current PTFs, as by using the most recent soil maps, that include soil vertical heterogeneity, hydraulic properties calculated by PTFs outperformed the classic look-up tables often used (Xu *et al.*, 2023). PTFs, although steadily improving, illustrate the challenges facing the implementation of global hydrology within LSMs.

Another set of processes to consider within LSMs are the evaporative processes. Alteration of the parameterisations related to evaporation will consequently influence further water stores and thus fluxes. Simply changing the evaporative resistance of an LSM generates significantly divergent terrestrial hydrological simulated responses (Laguë *et al.*, 2019). The modification of soil parameterisations also noticeably changes predicted evaporation rates (Teuling *et al.*, 2009; Maina *et al.*, 2022). The transpiration component of evaporation is influenced by vegetation root representation, stomatal conductance, and the leaf area index. All these components are influenced by adjacent Earth systems such as nutrient cycles, energy and of course hydrology.

Vegetation in LSMs is also crudely represented with the hydraulics and root representation being in critical need to evolve. Many LSMs represent vegetation roots as a 1-D singular big root model which is not representative of root dynamics at finer scales (Vanderborght *et al.*, 2021). When roots are implemented in this manner, if roots are too shallow in a model, there can be a situation where there is premature reduction in evaporation in dry periods where the topsoil becomes too dry (Teuling *et al.*, 2009; Blyth *et al.*, 2019). This has downstream consequences on other systems within the LSM that rely on an accurate calculation of soil moisture (e.g., runoff and plant phenology). Furthermore, not utilising plant hydraulics creates situations where there is inaccurate plant water uptake and sensitivity to soil moisture stress (Meier *et al.*, 2018; Liu *et al.*, 2020). This can lead to vegetation in LSMs being overly sensitive to the water level in the upper soil layer during drought conditions (Harper *et al.*, 2021; Zhao *et al.*, 2022). Of note with the current avenues to improve LSM hydrology, lateral water flows within a LSM improved ecosystem resilience within the models suggesting this may be a key epistemic uncertainty to resolve to improve vegetation representation and response to hydrology (Chang *et al.*, 2018a). The way in which land cover is characterised produces different realisations of the sensitivity to land cover with some finding it significant (Pitman *et*

al., 2009; De Noblet-Ducoudré *et al.*, 2012; Zhou *et al.*, 2023) and others finding it relatively insignificant (Gedney *et al.*, 2006). It is therefore important that we acknowledge and comprehend all the parameterisations that are responsible for replicating vegetation processes within models.

Global hydrology made a push into LSM representation to create 'models of everywhere' (Beven, 2007; Blair *et al.*, 2019). As we have pushed to finer spatial and temporal scales, a number of challenges have arisen which were muted at coarser resolutions (Wood *et al.*, 2011; Beven and Cloke, 2012). For example, the issue of topography and heterogeneity in moisture and energy fluxes within a landscape (Bisht and Riley, 2019; Fan *et al.*, 2019). Eric Wood and colleagues identified six main challenges facing LSMs to achieve hyper-resolution (1 km): improve surface and subsurface interactions, improve land-atmosphere dynamics, include water biogeochemical cycles, represent human processes, utilise computer advancements, and develop remote sensing datasets (Wood *et al.*, 2011). To overcome these challenges requires increased access to parallel computing, infrastructure able to support data requirements and programmatic support which has only more recently been realised. In addition, there is a need to create more observations from which to validate, calibrate and investigate to further improve our models (Beven *et al.*, 2019). Recent examples of trying to create the first generation of these 'models of everywhere' include the initial work of Maxwell *et al.*, (2015) who simulated surface and subsurface flows over continental North America and Hoch *et al.* (2023) who ran PCR-GLOBWB over Europe. However, these authors acknowledge that this is a step in the journey and most certainly not the destination for meeting the grand challenge of hyper resolution LSMs. It is with using LSMs at the finest spatial resolutions feasibly possible that we can test the veracity of outputs with our observations and thus refine the models accordingly.

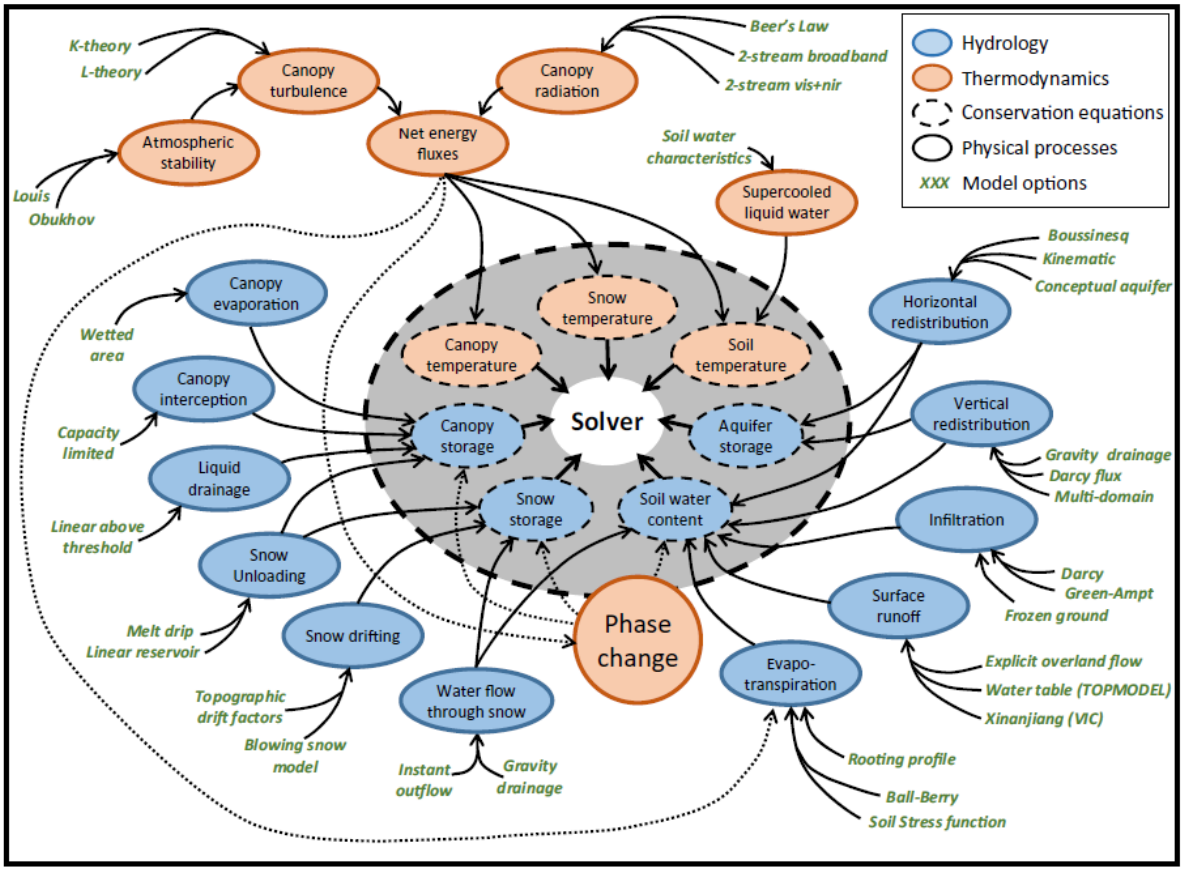

Figure 2.9: Simplistic diagram of the modelling decisions that can be made with SUMMA (Clark, Nijssen, Lundquist, Kavetski, Rupp, Woods, Freer, Gutmann, Wood, Gochis, et al., 2015).

This illustrates not only the complexity of the number of decisions a modeller must make when creating a land surface model, but also how they have downstream consequences on the overall calculations.

One avenue of research recently investigated further is the numerical implementation of LSMs. As system states change through time, a numerical solver is needed to calculate the evolution of flux and stores. Depending on the numerical solver, one may obtain different results despite the same underlying physics (Clark and Kavetski, 2010; Clark, Zolfaghari, *et al.*, 2021). In addition, the architecture and structure of the model within grid cells can alter the results. This has led to the development of projects, such as SUMMA, where the differing model choices for a LSM can be explored (Clark, Nijssen, Lundquist, Kavetski, Rupp, Woods, Freer, Gutmann, Wood, Brekke, *et al.*, 2015) [Figure 2.9]. The underlying architecture of LSMs has also been challenged. The Hydro-Blocks framework for representing hydrological response units, similar to TOPMODEL, suggests that the spatial granularity should not be gridded

arbitrarily but rather to hydrologically similar areas (Chaney *et al.*, 2016). This is a unique and interesting idea with recent research suggesting that 100 tiles is enough to represent a fully distributed LSM (Noah-MP) whilst running at 1% of the computational cost (Torres-Rojas *et al.*, 2022). New ideas are continually being developed to find new and more appropriate ways to create a community modelling framework (Hallouin *et al.*, 2022). We need to make sure computational work is reproducible and transferable to enable further exploration of the best LSM configuration and design (Hutton *et al.*, 2016; Bandaragoda *et al.*, 2019; Knoben *et al.*, 2022). It is through using LSMs in different scenarios that one can build a picture of consequences of our actions when developing these more complex models.

There are a number of significant LSMs used globally. These include Noah-MP (Niu *et al.*, 2011), ORCHIDEE (Krinner *et al.*, 2005), HTESSEL (Balsamo *et al.*, 2009) and JULES (Best *et al.*, 2011). A comprehensive list of LSMs can be found in Blyth *et al.* (2021) and Bierkens *et al.* (2015). A further description of the JULES (Joint UK Land Environment Simulator) LSM can be found in Chapters 3, 4 and 5 along with equations explaining its hydrological parameterisations.

JULES as an LSM has evolved greatly over time. The original model began as the original UK Met Office model used in its numerical weather prediction system and evolved into MOSES (Met Office Surface Exchange Scheme) (Essery *et al.*, 2001). Over time it became more what can be considered an LSM by including heterogeneous grid cells, dynamic vegetation and more realistic water fluxes and stores. At its core, JULES calculates changes in water, energy and carbon fluxes and can be run either independently or coupled with a global circulation model (GCM) [Figure 2.10]. It can be considered a distributed integral model in which computations take place in each grid cell. This means that the computations of one cell have no bearing on adjacent cells when JULES is run in uncoupled mode. Only the advective river routing schemes in JULES connect the river flow via a flow direction grid. There are a number of meteorological variables required to drive JULES when it is uncoupled: short- and longwave radiation, precipitation, U and V components of wind, temperature, specific humidity and surface pressure. Each grid cell is disaggregated into tiles which represent the various surfaces within the model. Vegetation can either be dynamic with plant physiology and phenology as explicitly parameterised within JULES or the dynamic global vegetation model TRIFFID (Top-down Representation of Interactive Foliage and Flora Including Dynamics) can be used (Cox, 2001). JULES requires ancillary data on both soil properties and land cover regardless of coupling.

Each surface type, and vegetation type, requires parameters to calibrate how it interacts with the different fluxes and stores. For the PTFs, JULES uses a look-up table to interpret the hydraulic properties of the soil ancillaries. A full breakdown of the parameters and options found in JULES can be found at: https://jules-lsm.github.io/latest/index.html. Written in the Fortran 90 language, the different modules in which the model is compiled from are described in 'namelists'. A description of the base namelists for running JULES in the configurations found in Chapters 3 and 4 can be found in Appendix 5.

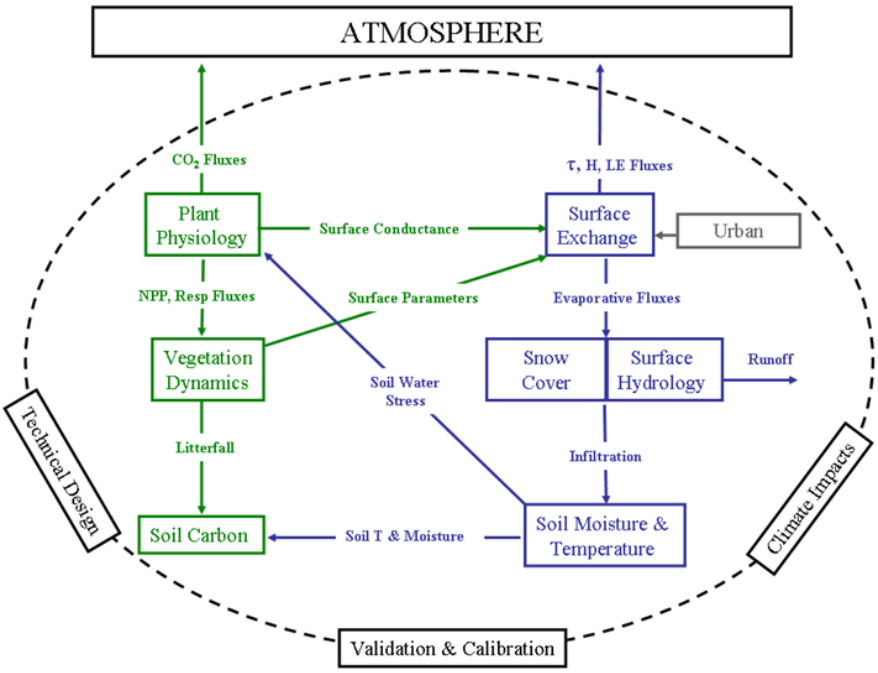

Figure 2.10: Initial model structure of JULES from Best et al., (2011).

This diagram illustrates the physics modules found within JULES. Lines show process connections between modules. The outer dashed circle represents the work surrounding JULES.

The development of LSMs is an attempt to reduce the epistemic uncertainty of the world around us. However, the land surface is strongly coupled with the atmosphere and so it becomes necessary with certain scientific queries to couple LSMs with atmospheric models. Due to the nature of woodland on energy and water fluxes if we are to understand the full impact of afforestation on the water cycle, this can be an appropriate modelling setup.

2.3.4. Coupling LSMs and Atmospheres

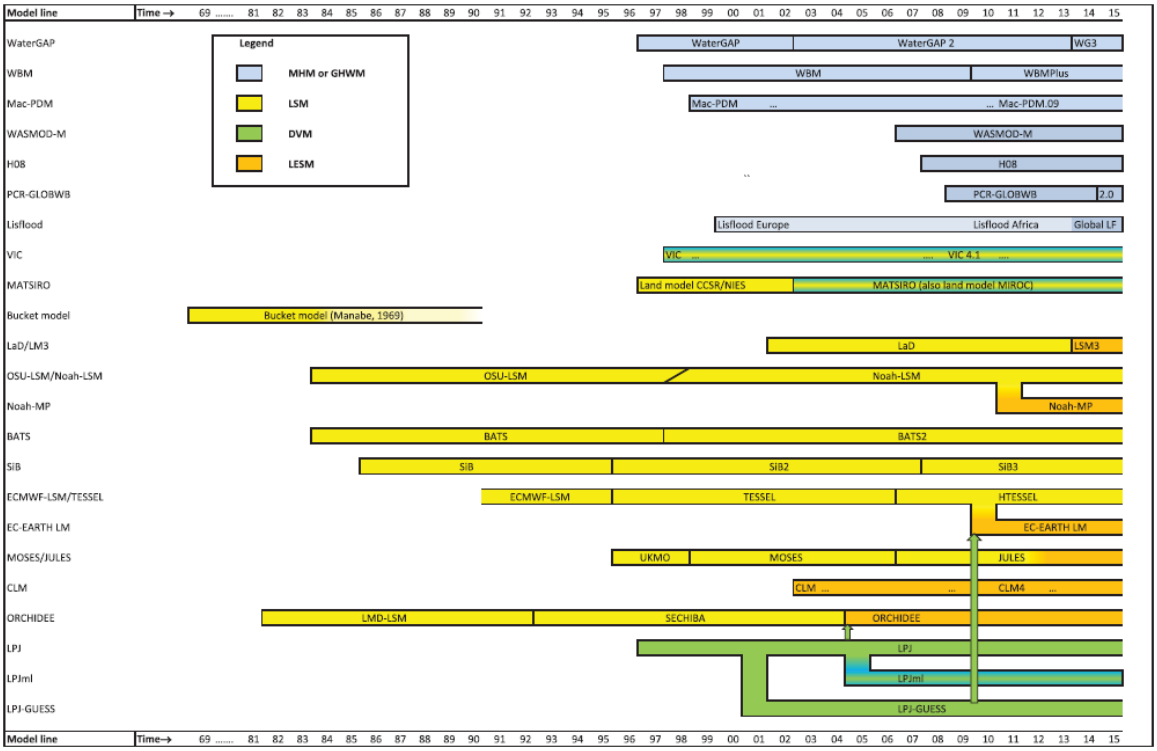

Figure 2.11: Evolution of global hydrological models from 1969 until 2015 (Bierkens et al., 2015).

MHM: Macroscale hydrological model; GHWM: global hydrology and water resources model; LSM: land surface model; DVM: dynamic vegetation model; LESM: LSMs used in Earth System Models.

As LSMs have developed over time they have slowly evolved to be used as the land component of Earth system models where the atmosphere and the land surface are more explicitly linked (Bierkens *et al.*, 2015) [Figure 2.11]. In the mantra proposed by Beven in 2007, there is an acknowledgment that if we are to predict and understand the most extreme hydrological events, we must include as much of the Earth system as possible (Beven, 2007). An example response to this community challenge was by Lewis and Dadson (2021) who coupled JULES with ocean and atmospheric models to recreate the 2013/14 winter floods. This found broadly correct, but not necessarily accurate, results. As stated previously, LSMs are now moving beyond being simple lower boundary conditions for atmospheric models and are becoming essential for obtaining the rights answers for the right reasons. They are moving to increase their *fidelity*. It has become increasingly clear the importance of coupling the land surface with the atmosphere

when considering large-scale processes. For example, without coupling the land surface with the atmosphere you can get soil dryness rapidly following land cover changes such as widespread afforestation in China (Li *et al.*, 2018). This is also revealed in studies simply investigating the feedback between wet soils and the formation of rain above (Hohenegger *et al.*, 2009; Cioni and Hohenegger, 2017). If we are to understand the impact of largescale environmental changes on hydrology it is therefore important to look beyond the Earth's surface and include relevant atmospheric processes.

As we have approached models of everywhere, there has been a need to re-evaluate the representation of precipitation within coupled systems. In the largest models, GCMs, there is an issue of 'drizzle' across a gridbox meaning that more extreme precipitation events are 'washed out' (Dolman and Gregory, 1992; Blyth *et al.*, 2021). However, now we are able to explicitly simulate convective precipitation rather than apply a scaling factor of the grid which has significantly improved our representation of heavy rainfall events (Kendon *et al.*, 2014; Prein *et al.*, 2015). These are known as Convection Permitting Models (CPMs). The CPMs show a better representation of precipitation cycles (Berthou *et al.*, 2020) and predict much higher and short duration rainfall magnitudes in future with climate change (Kendon *et al.*, 2020; E. J. Kendon *et al.*, 2023). However, it should be noted that by coupling CPMs with a land surface model you can get substantially different hydrological responses to the land surface such as overfilling of the canopy due to the higher intensity of precipitation (Folwell *et al.*, 2022). Therefore, simply coupling LSMs with the atmosphere needs a recognition of all the parameterisations within both models as there can be unintended consequences if there is not a thorough understanding of their interactions.

More comprehensive models which seek to include all processes relevant to the distribution and transfer of water, energy and carbon on Earth, are known simply as Earth System Models (ESMs). This means coupling the atmosphere, oceans and land and their associated processes. With the isolation of the development of the different models, now is a great renaissance in ESM development to strive for results of high accuracy and fidelity. As alluded to in the prior section on LSMs, this is driving major scientific advances to improve hydrological, and associated systems, within LSMs, thus ensuring errors are not due to the individual processes. ESMs are even beginning to be emulated by deep learning approaches to study the influence of climate and land cover scenarios to reduce computational cost, and aid our understanding of the numerical implementation of ESMs (e.g. TIMBER v0.1) (Nath *et al.*, 2022).

One of the essential systems included within ESMs is vegetation dynamics which is constantly improving (McDowell *et al.*, 2020). This has allowed them to be used in many studies to understand the impacts of vegetation, and afforestation, on the Earth's water and energy fluxes. Below are a few examples in which they have been utilised in this manner. Use of the Community Earth System Model 2 recently illustrated the impact of forestation globally altering the strength of the Hadley Cell, slowing the Atlantic Meridional Overturning Circulation, and increasing global precipitation by 0.8% (Portmann *et al.*, 2022). Interestingly, CESM2 has shown high precipitation accuracy with spatial resolution, but temperature is more dependent on land use (Devanand *et al.*, 2020). In a comparison of ESMs, De Hertog *et al.* (2022) explored land use and cover changes between afforestation and crop expansion and found broad consistency in the local effects of surface temperature with deforestation but found little consistency with energy balance component changes between them. Similarly, several studies looking at afforestation impacts using the Coupled Model Intercomparison Project have shown divergence on energy fluxes represented with additional woodland (Lejeune *et al.*, 2017; Davin *et al.*, 2020). This is important as sensible heat fluxes are shown to be the main driver of present global-mean precipitation since preindustrial time (Myhre *et al.*, 2018), and it is critical get the balance right for calculating evaporation rates. Calculations of evapotranspiration in many of these models is often underestimated, particularly in drier regions, which is likely due to inaccurate representations of soil structure and parameterisations (Zhao *et al.*, 2022). ESMs also suggest that vegetation-based climate mitigation could reduce global temperatures due to plant sequestration, but this declines relative to the amount of warming (Alkama *et al.*, 2022). Similar results were found using the Canadian Earth System Model back in 2011 when replacing croplands with forests (Arora and Montenegro, 2011). ESMs, and not just LSMs, provide valuable insights into the potential consequences of future vegetation cover changes, but there are still many model representation challenges to overcome.

2.4. Summary

This chapter has travelled from the underlying hydrological concepts and themes before exploring how hydrology as a system is evolving and the risks it poses to society. It demonstrates not only a lack of complete knowledge on how floods develop as a function of

catchment and climate attributes, but also how we can best mitigate their negative consequences. One potential source of flood management is to use nature-based solutions, or natural flood management. This includes planting woodlands as a strategy to 'slow the flow' but despite the wealth of literature on the topic of woodland hydrology there are three fundamental issues. Firstly, for the scale of afforestation proposed in the UK, predominantly to reach Net Zero targets, there are no studies that can provide answers on the countrywide effect of planting this amount of woodland on countrywide water resources. Secondly, it is undetermined how woodland hydrology may compare to changes in climate. Finally, woodland hydrology is so multifaceted that further research and hypothesis generation is required to build a better understanding of woodland impact on the terrestrial water cycle.

To answer these hypothetical unknowns, we can turn to numerical hydrological models. However, reviews on the effects of woodland hydrology on streamflow indicate that there is a split in predictions when comparing observations with model outputs. A potential reason for this is the large epistemological uncertainty of relatively simple hydrological models previously utilised to predict afforestation influence on the hydrological system. They do not necessarily include all the mandatory Earth systems to represent woodland impact more accurately and faithfully on water fluxes. Land surface models, and similar modelling frameworks, incorporate a significant proportion of the relevant processes. Despite also not being completely accurate as the simpler hydrological models, they present the most start-of-the-art tool in which to ask, how could potential widespread afforestation influence hydrology at countrywide scales?

The following three pieces of research attempt to fulfil the literature and knowledge gap by the novel approach of utilising LSMs, coupled and uncoupled to the atmosphere, at the edge of what is technically possible to currently achieve.

2.5. Model and Methods Summary

2.5.1. Model Description for Chapters: 3, 4, 5

The land surface model JULES is used in this thesis. A summary of the representation of water fluxes within JULES for Chapters 3, 4 and 5 follows. Chapters 3 and 4 use exactly the same model configuration, whereas Chapter 5 uses a separate model configuration. The similarities and differences between these two model configurations of JULES is explained.

In Chapters 3 and 4, JULES runs uncoupled from an atmospheric model and the calculations of each grid cell are independent of each other. The model version is 5.6 with further details and the relevant user guide found at https://jules-lsm.github.io/vn5.6/. The base namelist for the model configuration is in Appendix 5. It is based on the configurations developed in three previous studies (Robinson, Blyth, Clark, Finch, *et al.*, 2017; Blyth *et al.*, 2019; Martínez-De La Torre *et al.*, 2019). In Chapter 5, JULES is predominantly in its regional land atmospheric science configuration in which the decisions and setup validation can be found in Bush *et al.* (2020, 2023).

A detailed description of water fluxes within JULES can be found in Best *et al.* (2011) and Blyth *et al.* (2019) and Chapter 3.5.2 (including relevant equations).

JULES represents a unit area (or grid cell) into tiles divided between plant and non-plant surfaces. Where there is no plant, precipitation reaches the surface unimpeded. When there is vegetation, precipitation interacts with the canopy such that it can fill the canopy store or bypass it as throughfall if the rate of precipitation is high enough. The rate of throughfall is dependent on the size of the canopy storage (related to the Leaf Area Index), the precipitation rate and existing water in the canopy. The surface energy balance determines the rate of evapotranspiration in conjunction with the amount of water stored in the canopy.

Surface runoff in JULES can be one of two processes: infiltration or saturation excess overland flow. Infiltration excess runoff occurs when the precipitation rate is greater than the infiltration rate of the underlying soil. The infiltration rate of the soil is calculated using pedotransfer functions and soil properties as designated by the ancillary soil data. In the case of vegetation,

there is also an enhancement factor (designated in the model namelist) added to the initially predicted soil infiltration rate to account for the macropores developed by root systems. To generate saturation excess overland flow, the proportion of the grid cell saturated is determined. In Chapters 3 and 4 the Probability Distributed Model is used to calculate the fraction of grid cell saturation (Moore, 2007; Clark and Gedney, 2008). In this setup, a topography-derived parameterisation for the parameters of this model are used such that in steep areas, it takes little additional rainfall to generate saturation excess overland flow (Martínez-De La Torre *et al.*, 2019). In Chapter 5, the rainfall-runoff model TOPMODEL is used instead of the Probability Distributed Model to calculate surface runoff and grid cell fraction of saturation (Clark and Gedney, 2008). Any remaining water from precipitation that has not been converted into runoff or intercepted by the vegetation is then routed into the soil column.

The Darcy-Richards equation calculates the vertical water flux in the soil column within JULES. To do this, it requires hydraulic suction and conductivity soil properties calculated with pedotransfer functions and static lookup tables within JULES. In Chapters 3 and 4, the van Genuchten pedotransfer function is used compared to the Brooks & Corey one in Chapter 5 (Brooks and Corey, 1964; van Genuchten, 1980). Vegetation accesses water in the soil column layers depending on the root density function and transpires at a rate conditional on the volumetric soil moisture critical and wilting points. As the soil layers become saturated, excess water flows to lower soil column layers and added to the subsurface runoff.

In Chapters 3 and 4, the River Flow Model uses the surface and subsurface runoff to route the flow according to a flow direction grid and calculates streamflow (Bell *et al.*, 2007; Dadson *et al.*, 2011). In Chapter 5, there is no kinematic wave approximation of river flow and as such there is no streamflow analysis.

The spatial domains and boundary conditions of JULES in Chapters 3 and 4 are different to that of 5. In the first, JULES runs at a spatial resolution of 1 km, based on the British National Grid, and a 30-minute timestep. In the second configuration, where JULES is coupled with a Convection Permitting Model, it is a 2.2 km grid with a 30 second timestep to enable more accurate simulation of convective systems. In the uncoupled configuration the meteorological data drives the model, and land surface outputs such as evaporation have no further ramifications to the evolution of the system, but in the coupled configuration the atmospheric

model drives the land surface model and the outputs it generates feedback into the atmospheric model.

The basic premise of the experiments in the following chapters is to run simulations with the original land cover and then compare this to scenarios of afforestation. In Chapter 3, the hydrological differences are between base land cover and the approximately 300 different woodland afforestation scenarios. In Chapter 4, the differences are between the original land cover and the two afforestation scenarios (50% and 100%). Chapter 5 is more complex in that there are two time periods and two model ensemble members from the UKCP18 model ensemble. This means calculated hydrometeorological differences are between original land cover and the one afforestation scenario developed using the appropriate period and ensemble member [Table 2.1].

Table 2.1: Simulation suites created for Chapter 5.

Suite codes (e.g., mi-bb991) represent the different model runs used in the study of Chapter 5. Simulations for the periods of 2040-2060 and 2060-2080 have two separate ensemble members from the UKCP18 model ensemble. Horizontal shading of the rows indicate model runs from the same ensemble member. To elaborate, mi-bb991 and mi-bb189 are the same model ensemble and their corresponding afforestation scenarios are mi-bd601 and mi-bd602 which altogether could be taken as the period 2040-2080. The full time periods could not be simulated due to computing and time resources.

Time Period	Ensemble Member	Base Land Cover Scenario	Afforestation Scenario
2040-2060	1	mi-bb991	mi-bd601
	2	mi-bc000	mi-bd603
2060-2080	1	mi-bb189	mi-bd602
	2	mi-bb216	mi-bd604

2.5.2. Validation of JULES

As a land surface model JULES has undergone continuous development, which has led to many investigations into the validity of its output. What follows is a summary of some key validation studies that emphasise the appropriateness of the application of this model for understanding

the consequences of widespread afforestation on UK hydrology, as well as things to consider when evaluating its output. To finalise, some of the validation work undertaken at the start of the thesis is shown, and Appendices 3 & 4 contain the metrics that quantify model output accuracy.

Plant hydrology was initially implemented within JULES by Alton *et al.* (2009) that showed runoff and evapotranspiration at a global and seasonal timescales was broadly correct. However, that study also illustrated evapotranspiration is overestimated early in the growing season. JULES generally overestimates evapotranspiration, particularly more in temperate forests, which is likely due to it overestimating albedo (Van den Hoof *et al.*, 2013; Blyth *et al.*, 2019; Wiltshire *et al.*, 2020). As demonstrated by Best *et al.* (2015), JULES, along with other LSMs, outperform the simulated latent heat fluxes of simpler physically-based models, but they all perform worse than a simple three-variable nonlinear regression (humidity, temperature and shortwave radiation). This suggests JULES and other LSMs are missing essential mechanisms for accurately predicting evaporation. Runoff therefore can be underpredicted in JULES due to the overestimation of evaporation (Blyth *et al.*, 2011).

It is important that the biomechanics of JULES, plant functional type parameters, and their interaction in low soil moisture conditions, are all accurate and these have been improved and validated (Harper *et al.*, 2016, 2021). The additional plant functional types added by Harper *et al.* (2016), such as evergreen and deciduous trees, improved both Gross and Net Primary Productivity of plant functional types, but Net Primary Productivity could be overestimated at times in temperate mixed forests by up to 30% (Ritchie *et al.*, 2019).

The rainfall-runoff models within JULES were initially implemented by Clark and Gedney (2008). Chapters 3 and 4 utilise the Probability Distributed Model (Moore, 2007) tuned according to topography (Martínez-De La Torre *et al.*, 2019). Using JULES with this rainfall-runoff model configuration generated Nash-Sutcliffe Efficiency Scores of over 0.8 for the River Thames. However, in the study of Martínez-De La Torre *et al.* (2019) it was noted infiltration into the soil column was not sufficient.

Considering hydrological extremes, there is also strong agreement with the structure and timing of events using JULES, but there is no precise accuracy in their formation and decay (Prudhomme *et al.*, 2011; Harding *et al.*, 2014; Lewis and Dadson, 2021). Miller *et al.* (2011)

show that the original versions of JULES had difficulty in producing flood frequencies, and Prudhomme *et al.* (2011) note that the model produced large areas of high and low flow which could be due to the dominance of slow-responding subsurface flows (coupled with large water storage areas).

On several occasions, the runoff produced by JULES has been shown to be more inaccurate when compared to physically-based hydrological models such as HBV and WaterGAP that use regionally calibrated parameters (Prudhomme *et al.*, 2011; Beck *et al.*, 2016; Telteu *et al.*, 2021).

Studies consistently show JULES is not good at representing streamflow in areas where the geology is highly permeable (Le Vine *et al.*, 2016; Martínez-De La Torre *et al.*, 2019). The success of hydrological processes in JULES is strongly coupled with the underlying geology (Weedon *et al.*, 2023) and recent attempts, although not included in this thesis, have attempted to improve the representation of groundwater in JULES which greatly improved soil moisture dynamics (Batelis *et al.*, 2020).

Input data to JULES can seriously impact the derived conclusions. Cooper *et al.* (2022) demonstrated that the soil ancillary data significantly altered the calculated evaporative fraction. By optimising the soil ancillary, JULES was able to hold soil moisture for longer and thus reduce the evaporative fraction in summer months. Biases in precipitation and temperature datasets strongly influenced global runoff in LSM simulations that included JULES (Papadimitriou *et al.*, 2017).

The mechanism in which water is distributed through the soil column in JULES means the topsoil is very reactive to precipitation events which can lead generate flashy runoff responses dependent on the topsoil volume water content, or very low soil moisture variability in lower layers (Williams *et al.*, 2019; Lewis and Dadson, 2021).

JULES demonstrates strong sensitivity to CO_2 regarding plant hydrology due to the implemented physiological forcing (Betts *et al.*, 2007). This is often higher than other comparable LSMs and its influence on processes is debatable (Prudhomme *et al.*, 2014; Sellar *et al.*, 2019). CO_2 fertilisation likely needs to be better constrained (Ritchie *et al.*, 2019).

Some initial validation experiments were conducted before Chapter 3. To understand the response of altering the primary distribution parameter of the PDM (explained in 3.5.2.). In these base experiments, the JULES configuration found in Chapters 3 and 4 was run with the original (unaltered) land cover, but the primary distribution parameter was adjusted between 0.5 and 2.5. The Tamar catchment (Station ID: 47001 - https://nrfa.ceh.ac.uk/data/station/info/47001) was selected as a representative catchment in which a number of simulations could quickly be run for a ten year period. Figure 2.12. shows a simulation run between 2000 and 2010 for distribution parameter 0.5, Figure 2.13. shows distribution parameter 2.5, and Figure 2.14. represents when the distribution parameter adjusted according to topography (as in the configuration of Chapters 3 and 4).

When considering the output from JULES with streamflow, regardless of the parameterisation of the PDM, the model broadly simulates the correct hydrology over long periods. There is no consistent bias, but some flow events are overestimated whereas others are underestimated. For instance, JULES creates a large flow event during 2003, not as large as in the observational dataset, but none of the parameterisation can generate the scale of flood event in Autumn 2000. This could be due to model deficiencies not generating high flow events accurately (such that the antecedent soil moisture is incorrect). Furthermore, due to the numerical timestep of the model and the daily output of streamflow there are instances where the high flow event can be a day out from the observations.

The main impact of changing the PDM parameter is on the flow variability and flow recession speeds, as the parameter increases the flow variability grows with higher and lower flow events generated by the model. When JULES is parameterised by topography (as in Chapters 3 and 4), it better recreates high and low flows as seen in Figure 2.14. This would suggest that this model configuration is generating saturated excess overland flow events more successfully than when compared to when the distribution parameter of the PDM is static.

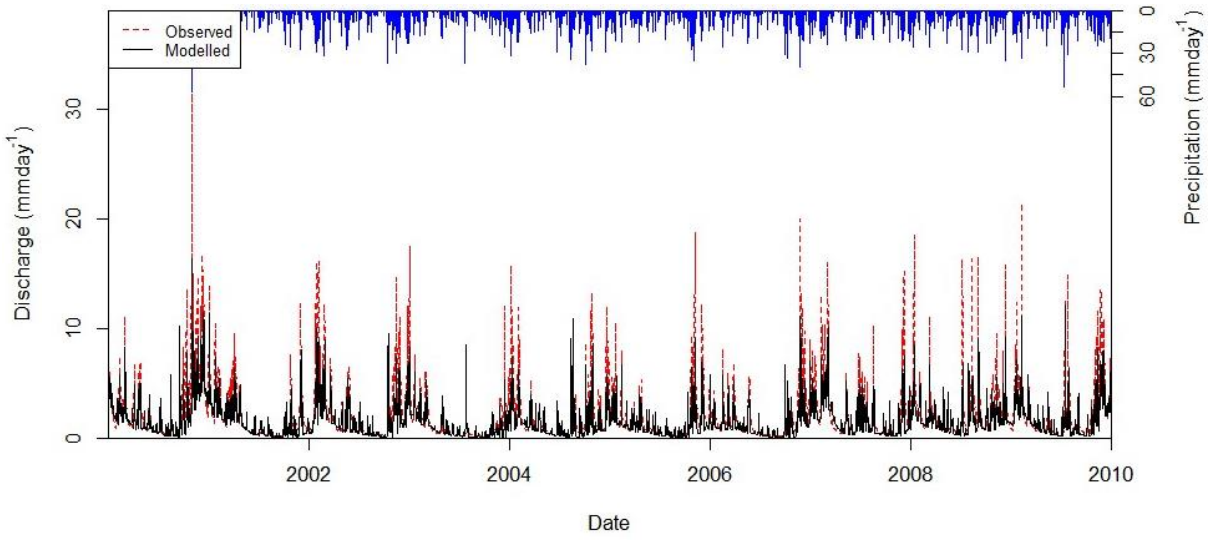

Figure 2.12: Observed discharge compared to modelled for the period 2000 to 2010 when JULES' PDM distribution parameter is 0.5.

This is for the River Tamar catchment. Precipitation is included to show the reaction of the catchment, simulated and observed, to water input.

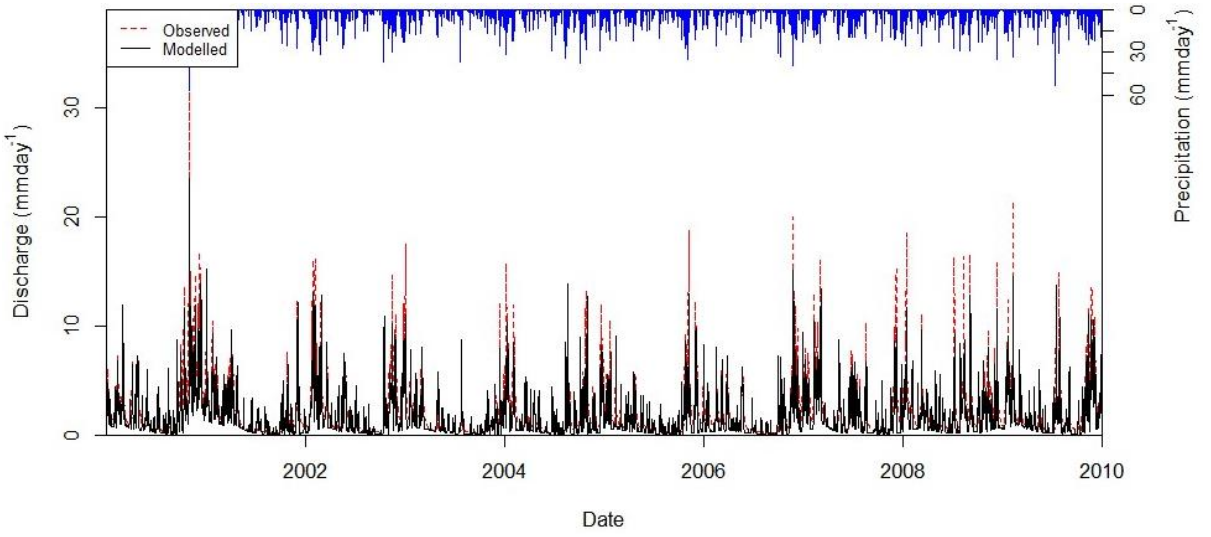

Figure 2.13: Observed discharge compared to modelled for the period 2000 to 2010 when JULES PDM distribution parameter is 2.5.

This is for the River Tamar catchment. Precipitation is included to show the reaction of the catchment, simulated and observed, to water input.

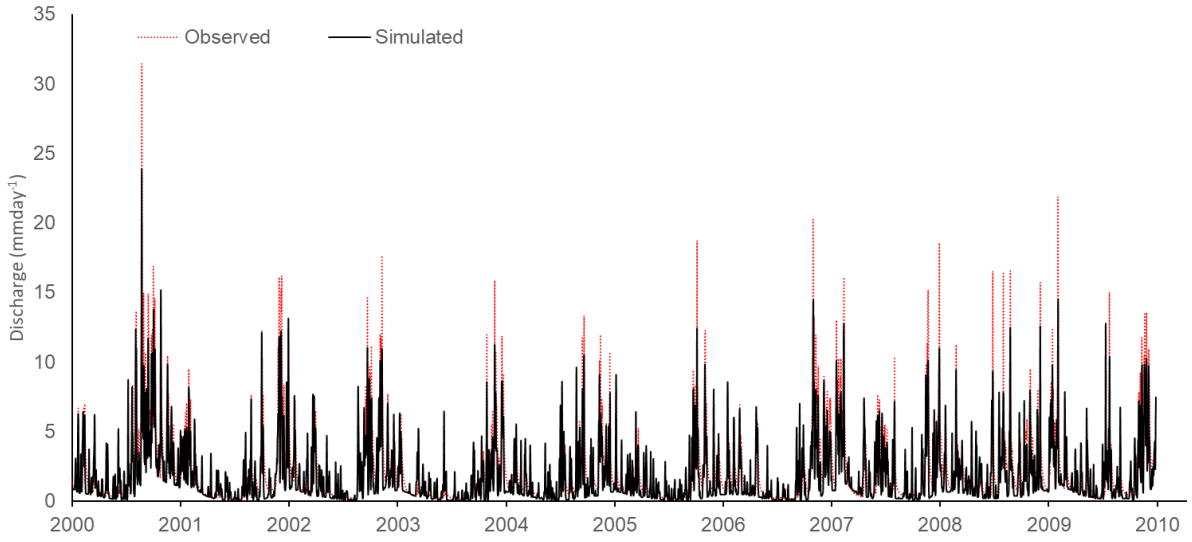

Figure 2.14: Observed discharge compared to modelled for the period 2000 to 2010 with JULES when PDM is parameterised by topography.

This is for the River Tamar catchment.

Unfortunately, there is not a consistent and long enough data record from which to compare the water flux outputs of JULES to systematically. However, using the COSMOS-UK network (further described in 3.5.2.) it is possible to determine the accuracy of JULES (H. M. Cooper *et al.*, 2021). Comparing the potential evapotranspiration in JULES for Alice Wood (a broadleaf woodland), the consistent overestimation noted in earlier validation studies is apparent (particularly in summer months) [Figure 2.15]. This is likely due to the albedo being too low and thus leading to a high amount of evaporation with high net radiation. A similar effect can be seen at the grassland site, Chimney Meadows, although this is not consistent across all sites [Figure 2.16]. Considering topsoil moisture (first 0.1 m and top layer in the JULES configuration), changes are broadly correct, but it is also overestimated for the period in both the temperate woodland and grassland COSMOS sites shown below [Figures 2.17 & 2.18]. Furthermore, soil moisture is highly responsive to recharging events (precipitation). The exact location of these COSMOS-UK sites can be found in Supplementary Figure S3.8.

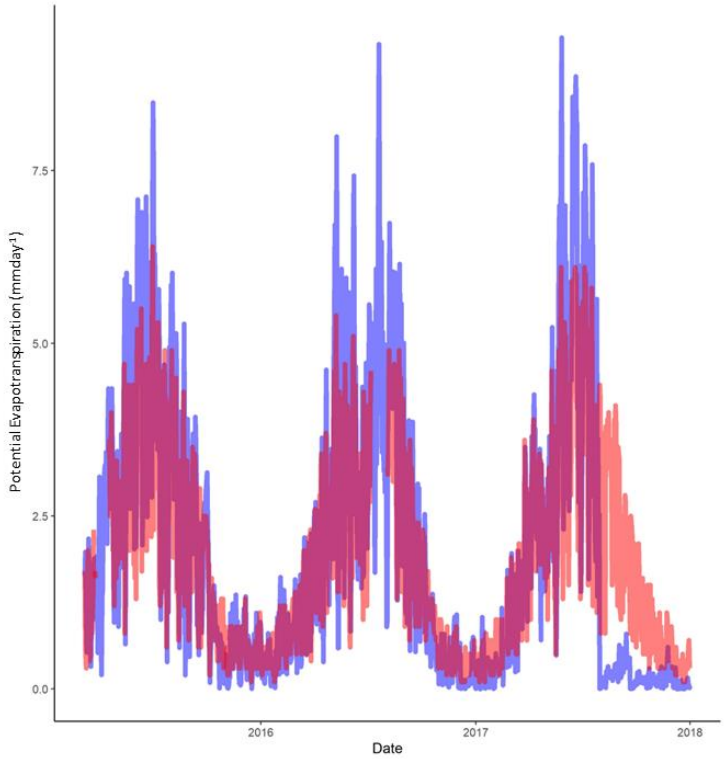

Figure 2.15: Comparison of potential evapotranspiration at the Alice Wood COSMOS-UK site as calculated using the Penman-Monteith equation.

Red represents the observations and blue the simulated output from JULES. An error in the diagnostic potential evapotranspiration calculation occurs in the latter half of 2017.

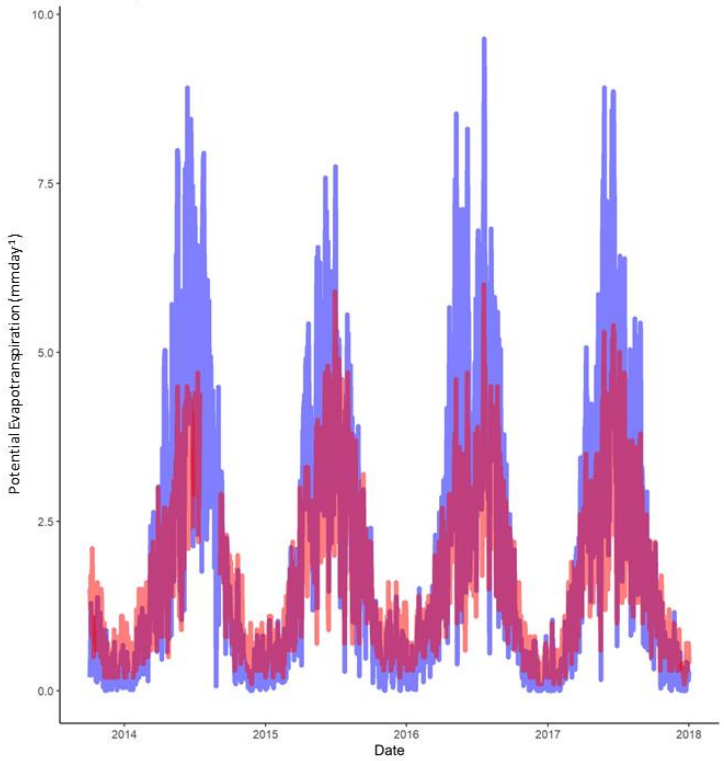

Figure 2.16: Comparison of potential evapotranspiration at the Chimney Meadows COSMOS-UK site as calculated using the Penman-Monteith equation.

Red represents the observations and blue the simulated output from JULES.

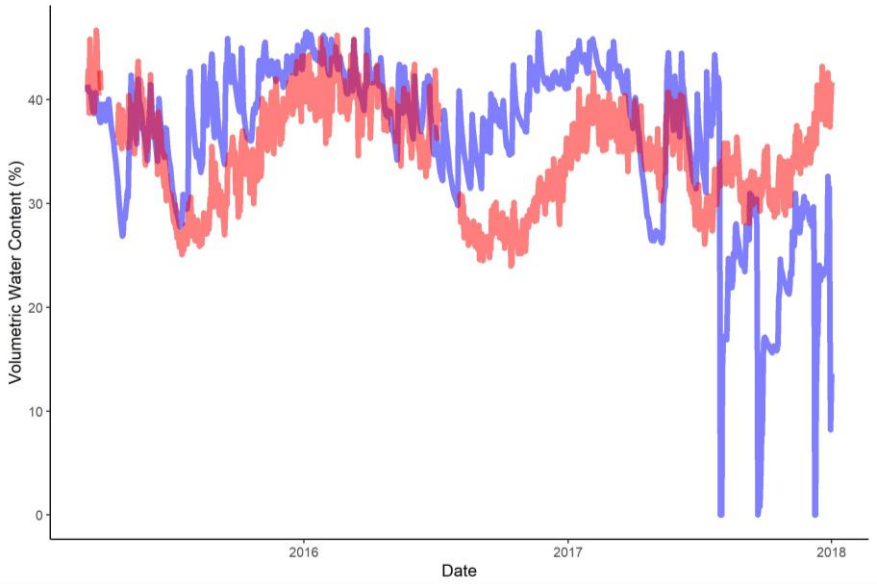

Figure 2.17: Comparison of topsoil moisture at the Alice Holt COSMOS-UK site.

Red represents the observations and blue the simulated output from JULES. An error in the diagnostic topsoil moisture occurs in the latter half of 2017.

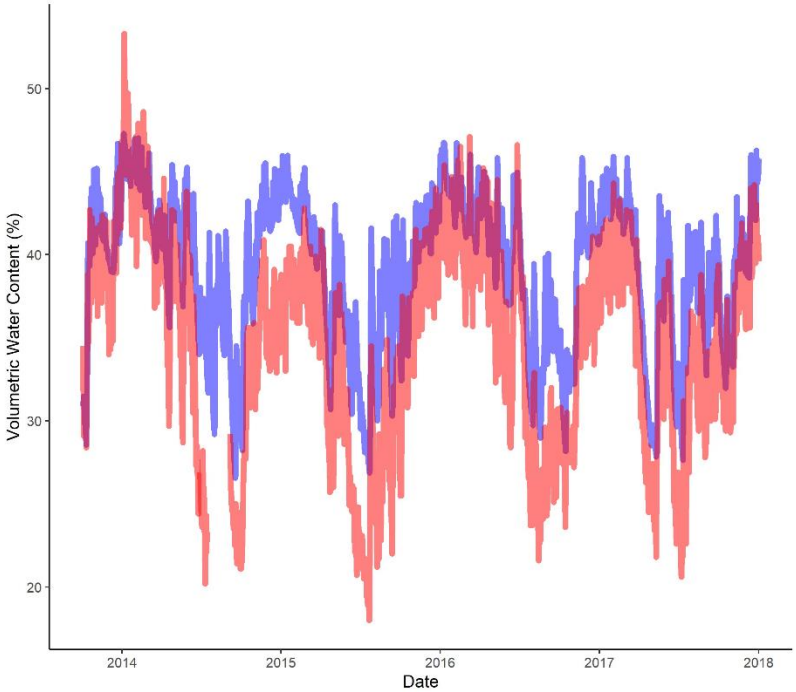

Figure 2.18: Comparison of topsoil moisture at the Chimney Meadows COSMOS-UK site.

Red represents the observations and blue the simulated output from JULES.

3. Hydrological impact of widespread afforestation in Great Britain using a large ensemble of modelled scenarios

---

This chapter has been published as a research article in Nature Communications Earth and Environment. Marcus Buechel ran the simulations, analysed the results and created the figures. All co-authors contributed to editing the manuscript. We acknowledge Adriaan J. Teuling, David Scott and an anonymous reviewer for providing review comments that improved this chapter.

Citation: Buechel, M., Slater, L. & Dadson, S. Hydrological impact of widespread afforestation in Great Britain using a large ensemble of modelled scenarios. Communication Earth & Environment 3, 6 (2022). https://doi.org/10.1038/s43247-021-00334-0

3.1. Abstract

Ambitious afforestation proposals in the last decade target potential flood mitigation and carbon storage benefits but without a systematic, large-scale (> 1000 km^2) quantitative evaluation of their impacts on streamflow. Here, we assess the impact of afforestation on streamflow across twelve diverse catchments (c.500-10,000 km^2) using a high-resolution land-surface model with a large ensemble of afforestation scenarios. Afforestation consistently decreases median and low streamflow. Median modelled flow is reduced by 2.8% ± 1.0 (1 s.d.), or 10 mm yr^{-1} ± 2.1 (1 s.d.), for a ten-percentage point increase in catchment broadleaf woodland. We find no nationally-consistent reduction of extreme floods. In larger catchments, planting extent is a stronger control on streamflow than location. Our results suggest that despite its potential environmental and societal benefits, widespread afforestation may inadvertently reduce water availability, particularly in drier areas, whilst only providing a modest reduction in extreme flood flows.

3.2. Introduction

Much debate exists about the possible large-scale land cover change impacts on catchment hydrology across temporal and spatial scales (Blöschl *et al.*, 2007; Lane, 2017). Afforestation is suggested to have many co-benefits such as improving biodiversity, air and water quality, providing timber, enhancing human well-being and reducing flood risk (Burton *et al.*, 2018; Seddon *et al.*, 2020). Widespread afforestation is often suggested as a solution for achieving Net Zero (balancing carbon emissions with removal) by numerous groups including the UK government (Committee on Climate Change, 2019a, 2020). However, there is a limited understanding about how effective woodland is for Natural Flood Management in modifying water fluxes and stores over large catchments (Dadson *et al.*, 2017; Lane, 2017). Impacts of land cover on hydrology are particularly important to understand due to changing streamflow regimes both in the UK and globally (Griffin *et al.*, 2019; Gudmundsson *et al.*, 2019; Hannaford *et al.*, 2021; Slater, Villarini, *et al.*, 2021).

Land cover exerts strong localised controls on the water balance and streamflow timings within a catchment that can be difficult to detect over larger scales (Blöschl *et al.*, 2007; Rogger *et al.*, 2017). Numerous studies have investigated the influence of afforestation on hydrology, including plot-scale studies to understand infiltration rates and ground water levels, and small catchment studies evaluating the impact of land-cover change on streamflow and water quality (Marc and Robinson, 2007; Bathurst *et al.*, 2018; Murphy *et al.*, 2021). However, these studies are often smaller than 1000 km^2 in size, and it is unknown whether the impacts of afforestation may scale up over larger catchments, given its complex influence on streamflow (Vertessy *et al.*, 2003; Stratford *et al.*, 2017; Carrick *et al.*, 2019). Furthermore, few systematic evaluations exist of how afforestation location and extent may influence catchment hydrology across a wide range of climatic and physiographic conditions (Bathurst *et al.*, 2020; Slater, Anderson, *et al.*, 2021).

This study is a theoretical assessment of the extent to which afforestation extent and location in catchments predominantly over 1000 km^2 in size may increase or decrease streamflow across temperate catchments in the British Isles. We hypothesize that: (i) increasing afforestation extent should proportionally reduce streamflow at all exceedances (Stratford *et al.*, 2017; Zhang *et al.*, 2017); (ii) catchments may be more hydrologically responsive to certain

afforestation locations such as upland compared to lowland regions (Blöschl *et al.*, 2007; Lane, 2017); (iii) catchment properties such as climate and soil types may differentiate a catchment's hydrological response to afforestation (Zhou *et al.*, 2015). Our work is the first, to our knowledge, to employ a high-resolution 1 km^2 physics-based land surface model to quantify the impact of afforestation on streamflow across multiple catchments using a large ensemble of land cover scenarios. This approach allows us to isolate drivers influencing catchment sensitivity, determine individual hydrological processes altered by widespread afforestation, elucidate the uncertainty generated by afforestation location and most importantly find the impact of afforestation over large spatial extents on streamflow. Beyond the British Isles, our results describe the influence of afforestation on temperate catchment hydrology.

We focus on twelve diverse catchments (areas covering 511 to 9931 km^2) which capture multiple hydrological regimes, drainage patterns, soil, and land cover types to understand catchment properties influencing streamflow response to afforestation [Figure 3.1] [Supplementary Table S3.1]. Using the Joint UK Land Environment Simulator (JULES) run at a 30 minute time step, we simulate the hydrological implications of a large ensemble of broadleaf afforestation scenarios (Best *et al.*, 2011; D. B. Clark *et al.*, 2011) [Methods]. JULES simulates carbon, water and energy fluxes at the land surface when driven with a time series of meteorological data. Further details about the model setup can be found in the Methods.

Systematic criteria were used to generate up to 288 broadleaf afforestation scenarios per catchment for planting within grasslands [Methods], in line with afforestation scenarios that show improved pastures and rough grasslands will be the most likely initial afforestation locations in the UK (Thomson *et al.*, 2018). However, we note this approach does not consider other factors such as the socio-economic implications of afforestation location. Initially we identify separate planting locations in each catchment using either stream order (Strahler, 1957; Shreve, 1966) (relative size of stream in a catchment) or propensity for saturation (Beven and Kirkby, 1979) (how likely a location is to be wet after rainfall) [Methods]. Stream order varies from one to seven (small to large stream) and propensity for saturation from one to five (low to high saturation level). We create watersheds (catchment boundaries) that are both within, and outside, each of the defined catchment planting locations [Supplementary Figure S3.1]. Broadleaf woodland planting was then either random, with approximately 25 and 50% randomly distributed within the chosen locations, or around existing land cover at 25 and 50 m buffers. Discussion exists over where to plant woodland in relation to existing land cover. To

investigate these planting locations, we systematically add woodland around watercourses (Thomas and Nisbet, 2007; de Sosa *et al.*, 2018), urban areas (Fuller *et al.*, 2016; Gunnell *et al.*, 2019) and existing broadleaf woodland (Woodland Expansion Advisory Group, 2012; Burton *et al.*, 2018). Afforestation according to these planting criteria generated between 234 and 288 scenarios and between 0 and c. 40 percentage point increase in broadleaf woodland per catchment [Supplementary Figure S3.2]. However, owing to the available space and catchment area the same extent of maximum afforestation could not be achieved in all catchments; nor do we account for the possible effect of forest stand age on catchment hydrology (Marc and Robinson, 2007). A large ensemble of scenarios provides evidence to ascertain whether hydrological change in catchments is primarily driven by planting location or extent, and to quantify the variability, or uncertainty, induced by afforestation across catchments.

To characterise afforestation influence on streamflow we use eight hydrologic metrics (Olden and Poff, 2003; Addor *et al.*, 2017). For analysing extreme and average streamflow, we calculate the top 1 % (very high flow), 5 % (high flow), 50 % (median flow), 90 % (low flow) and 95 % (very low flow) quantiles of daily flows for the period 2000 to 2010. This period allows us to observe the impact of land cover change in a flood rich period (Wilby and Quinn, 2013; Blöschl *et al.*, 2020) and avoid uncertainty in catchment hydrology when comparing scenarios to original land cover that would substantially change over longer periods. We compute the slope of the flow duration curve, to quantify flow variability (Yadav *et al.*, 2007; Brown *et al.*, 2013); median streamflow elasticity, to measure catchment streamflow response to yearly changes in precipitation (Sankarasubramanian *et al.*, 2001; Sawicz *et al.*, 2011); and runoff ratio to calculate water balance changes related to streamflow and evaporation (Milly, 1994). To determine catchment hydrological responsiveness to afforestation, we calculate the median regression slope of changes in streamflow metrics for every percentage point increase in afforestation over the study period, for each catchment and watershed afforestation area (Koenker and Bassett, 1978). This regression slope is a proxy for catchment responsiveness to afforestation and is used to infer the median change in a hydrologic metric due to afforestation in a catchment. For each catchment, Spearman's rank correlation is calculated between the quantified catchment sensitivity to afforestation and catchment attributes (Coxon *et al.*, 2020). To establish the impact and significance of different planting locations on hydrologic metrics according to catchment and land cover location we undertake a one-way analysis of variance (ANOVA) test.

3.3. Results and Discussion

3.3.1. Afforestation extent influence on streamflow

Afforestation on average reduces streamflow linearly at all streamflow quantiles within JULES [Figure 3.1]. At the highest flows we find a small reduction of streamflow with increases in broadleaf woodland (median reduction of 1.3 % ± 0.6 (one standard deviation) and 1.4 % ± 0.6 for the top 1 % and 5 % flows respectively, per ten percentage point increase in woodland) [refer to Supplementary Table S3.2 for percentage and absolute values]. These percentage changes in the high flows are relatively small compared to flood peak magnitudes, meaning a substantial area of the catchment would need to be afforested before an appreciable reduction in flow is observed. The correlation strength is moderate ($\rho = -0.46 \pm 0.17$ across individual catchments [Supplementary Table S3.3]) suggesting afforestation location and other factors can affect streamflow reduction at the highest flows [Figure 3.1a-c]. There appears to be a weaker correlation between afforestation extent and high flow reductions in small catchments compared to the largest (e.g., Tamar, $\rho = -0.35$; Severn-HB, $\rho = -0.77$ [Supplementary Table S3.3]). This finding suggests the impact of afforestation location is important in smaller catchments but in the larger catchments, the locational impact is diluted, making it more difficult to disentangle afforestation location (Rinaldo *et al.*, 1991; Rinaldo and Rodriguez-Iturbe, 1996). Targeted afforestation for flood management may therefore be detectable in smaller catchments, but become less impactful as broadleaf woodland extent is scaled up over larger catchments (Dadson *et al.*, 2017; Lane, 2017). Greater uncertainty exists in how afforestation extent and location will impact streamflow in smaller catchments, with a wide range of possible responses. However, there is a more predictable hydrological response to land cover change in the largest catchments, regardless of the location changed.

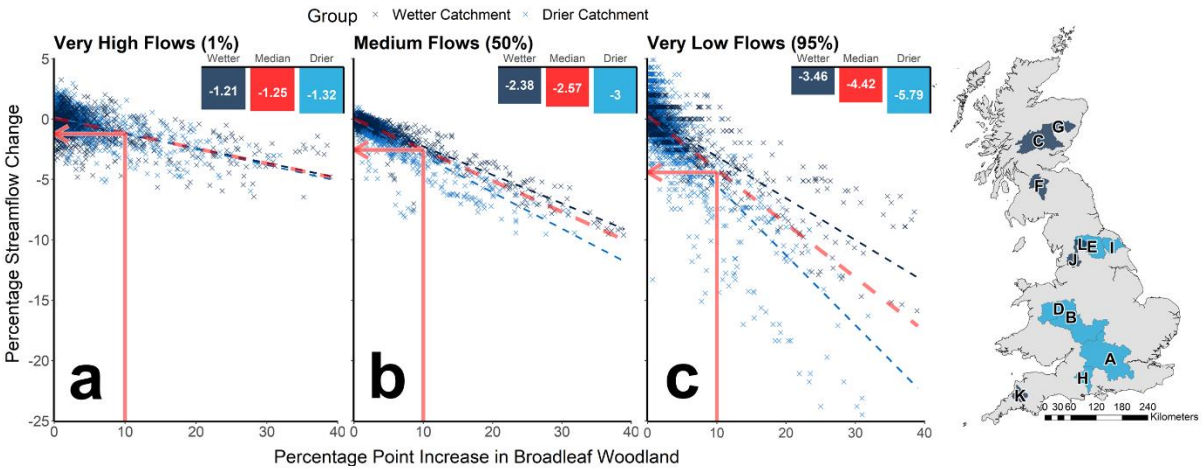

Figure 3.1: Effect of afforestation on high, median, and low flows across Great Britain. *Three scatter graphs illustrating the percentage reduction in flow quantile levels for each percentage point of woodland planted in the different catchments. Reduction in a) the top 1 % of flows, b) the median flows and c) the 95% quantile of daily flows. Each data point represents an afforestation scenario in a single catchment. Dashed red lines represent the median reductions in the different flow quantiles for all catchments. Dark blue represents the six wetter catchments (mean precipitation 3.11 – 4.16 mm day^{-1}) and lighter blue, the six drier catchments (1.99 – 2.55 mm day^{-1}). Bars show the reduction in each flow level per ten percentage point increase in broadleaf woodland for the different groups as well as the median reduction for all catchments in red. Catchment locations are shown on the right and the lettering code can be found in Supplementary Table S3.1.*

Afforestation impact on catchment hydrology varies seasonally, with large decreases in runoff in the winter, spring, and autumn months and no decrease or minor increases in summer months within JULES [Supplementary Figure S3.3]. An increase in high flows for some catchments coincides with the timing of the highest flows during summer months. Our simulations suggest that this increase in high flows is due to an increase in topsoil moisture leading to greater levels of saturation excess overland flow following periods of high intensity rainfall. In all periods, there is increased evaporation from intercepted water stored in the canopy, but this increase in topsoil moisture is primarily driven by a decrease in soil evaporation [Supplementary Figure S3.4]. Particularly in the winter and spring periods, an increase in soil evaporation results from loss of leaves from the broadleaf woodland, followed by regrowth. In the model, reduced canopy cover increases exposure of the soil surface to incoming shortwave radiation and reduces aerodynamic resistance, leading to an increase in potential evaporation. With broadleaf planting on grasslands there is increased soil infiltration, soil and canopy evaporation and

transpiration rates, and so we therefore find a commensurate reduction in both the surface and subsurface runoff. In contrast, in the summer months a decrease in modelled soil evaporation increases topsoil moisture (because the increase in canopy foliage reduces soil exposure to shortwave radiation and surface windspeed). As broadleaf woodland can achieve a higher leaf area index than the grasslands, the increase in topsoil moisture enhances saturation levels at rainfall interception (at the soil) and thus surface runoff. It should also be noted the increase in topsoil moisture may be due to differences in the root structures of broadleaf woodland and grasslands represented in JULES. While broadleaf woodland is modelled to have a root depth of 3 m, grasslands have root depths of 0.5 m, resulting in a potential over-drying of the topsoil.

Afforestation extent reduces simulated median and low flows the most, with −2.8% ± 1.0 and −4.3% ± 3.1 respectively per ten percentage points of afforestation [Supplementary Table S3.2]. Strong correlations between median and low flow reduction and afforestation suggest extent has a stronger influence on reducing streamflow than location, and this finding is supported by previous studies ($\rho = -0.83 \pm 0.12$, $\rho = -0.75 \pm 0.15$ [Supplementary Table S3.3]) (Brown *et al.*, 2013; Birkinshaw *et al.*, 2014; Rogger *et al.*, 2017; Afzal and Ragab, 2019; Bentley and Coomes, 2020). Each percentage point of afforestation in a catchment reduces the median flow by 1.0 mm yr^{-1} ± 0.21. Reduction of the median and low flows is primarily due to modelled increases in evaporation [Supplementary Figure S3.4], which is either from the woodland canopy or the soil surface when deciduous trees shed their leaves. Small increases in woodland area increase the lowest flows on average the most for the smallest catchments, due to the increased summer topsoil moisture, which is not balanced by the increased evaporation in subsequent months. As woodland area increases, there is a greater reduction in overall flows and more water leaves the catchment model domain by evaporation, reducing the lowest flow quantiles. Downstream of small afforestation locations there would not be any major disturbances to streamflow, and it may provide slight buffering against drought conditions.

Catchment response to afforestation extent is also clear using the flow regime metrics (runoff ratio, slope of the flow duration curve and catchment elasticity). We find a reduced contribution of rainfall in streamflow with a decrease in the runoff ratio (−1.9 % ± 0.6 per ten percentage points of afforestation) as reported in previous studies (Iacob *et al.*, 2017; Bathurst *et al.*, 2018). Modelled flow regimes become more variable with strong decreases in low and lesser decreases in high flow quantiles, increasing the slope of the flow duration curve (1.1 % ± 0.7 per ten

percentage points of afforestation). Greater variance between flow regime variability and afforestation suggests planting location more strongly controls streamflow regimes than extent ($\rho = -0.46 \pm 0.23$ [Supplementary Table S3.3]). Catchment discharge response to yearly changes in rainfall also decreases with broadleaf afforestation by modulating rainfall input to a catchment (median reduction in catchment elasticity of $-3.5\,\% \pm 1.2$ per ten percentage points of afforestation). Changes in a catchment's rainfall regime would therefore be less detectable in streamflow observations. These findings highlight the fact that simulations of future streamflow using physics-based models depend not only on climatic changes but also land cover changes. Without the inclusion of land cover changes considerable uncertainty will be introduced into projections of future flooding, drought and water management (Wasko, Westra, *et al.*, 2021)

3.3.2. Afforestation location influence on streamflow

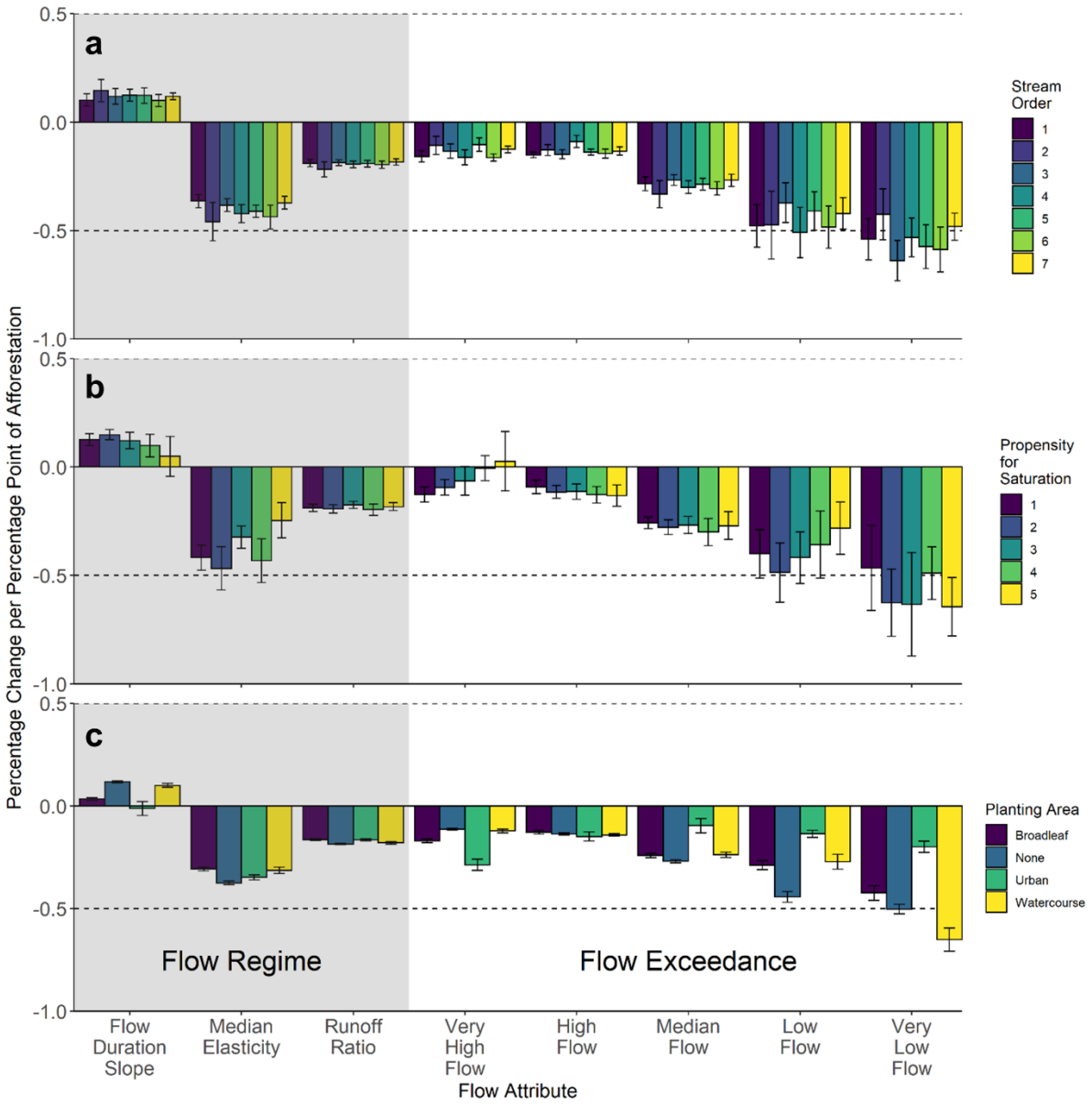

Figure 3.2: Percentage streamflow change for each percentage point of afforestation. *Sensitivity of catchment hydrology to afforestation in relation to a) stream order, b) propensity for saturation, c) planting area. "None" in planting area indicates absence of preferential planting location, i.e. planting randomly at 25 and 50 % within a catchment area. Left three metrics (grey shading) reflect flow regimes, whereas those on the right represent five flow quantiles. The vertical axis indicates the median quantile regression slope for the percentage change in the hydrologic indicator per percentage point increase in broadleaf woodland. For example, a quantile coefficient of -1 would represent a median 1% decrease for each percentage point increase in woodland. Each bar represents the mean quantile coefficient for all catchments and the error bars represent the standard error.*

ANOVA reveals highly significant differences ($p < 0.01$) in simulated flow reductions for all flow quantile levels when planting across the different stream orders, apart from the very highest flows [$F(1,670) = 5.3$, $p = 0.022$] [Figure 3.2a]. This highly significant difference in streamflow reduction across stream orders for the hydrologic metrics is due to differences in the largest and smaller streams, suggesting woodland acreage matters more than planting location. To emphasise, when the same area of broadleaf is planted for each stream order there is no highly significant difference between orders ($p > 0.01$). Runoff reduction according to stream order is also highly significant as seen in the runoff ratio and catchment elasticity [$F(1,670) = 17.93$, $p < 0.01$; $F(1,670) = 14.01$, $p < 0.01$]. Again, these differences are due to planting between the largest and the smaller streams. Flow regime variability differences by stream order location were not as significantly different [$F(1,670) = 5.11$, $p = 0.0241$] suggesting catchment planting area does not consistently lead to differences in flow regime variability.

Planting according to different saturation areas led to significantly distinct reductions in streamflow for both the median and low flows in JULES when planting extent is not constant [$F(1,478) = 4.89$, $p < 0.01$; $F(1,478) = 11.11$, $p < 0.01$] [Figure 3.2b]. However, the difference between saturation areas is less significant for all other flow quantiles and when planting extent becomes fixed in each area, the differences between streamflow reductions are not significant ($p > 0.01$). This means selecting afforestation sites within areas that are more or less likely to become saturated may not necessarily lead to different hydrological responses downstream, if planting the same acreage. However, afforestation effects differ the most between the least and most likely areas of saturation when planting acreage is not fixed ($p = 0.011$), with greater reductions in the modelled runoff ratio in the least saturated areas. Benefits observed at small afforestation plot scales may not size up to larger catchments and could have a negligible impact on reducing the highest flows.

Planting location, around urban, broadleaf, watercourses, or randomly, leads to different simulated streamflow dynamics [Figure 3.2c] even when area planted is constant. Not planting according to existing land cover greatly reduces streamflow at all flow quantiles compared with planting around the three existing land cover types. The difference in planting area location is greatest for low flow quantiles (ANOVA $p < 0.001$) compared with high flow quantiles ($p < 0.01$). Overall, no single best planting location could be identified around existing land covers if trying to provide Natural Flood Management benefits (Short *et al.*, 2019). We find consistent,

minimal differences in streamflow when planting around urban and watercourses, across all flow quantiles. Planting location also significantly reduces catchment runoff ($p < 0.001$) for both runoff ratio and catchment elasticity; the largest differences occur when planting is not according to existing land cover but when it was random. However, location effect on flow regime variability is more nuanced, with notable differences between planting around urban, watercourse locations, and randomly.

The difference in streamflow reduction is not significantly different when planting woodland inside and outside of the various drainage basin locations [Supplementary Figure S3.5]. Often it is debated whether interventions to reduce maximum flows are more effective in the headwaters or the valley floor downstream (Lane, 2017). This modelling study finds no compelling difference in streamflow, including extreme flood flow changes, when similar acreage is planted in the headwaters or the valley floor. However, in our study only one tree type is planted, so location may matter more for other tree types. In addition, our model does not simulate the effects of forest management techniques such as ditching and coppicing that might also have an influence on streamflow (Robinson and Dupeyrat, 2005; Birkinshaw *et al.*, 2014).

3.3.3. Catchment properties altering streamflow sensitivity to afforestation

Catchment climate exerts a strong influence on the hydrological response to afforestation in different types of catchments when comparing model results to their attributes. There are strong associations between climate properties and median flow reduction [Table 3.1]. As a catchment's average rainfall (and runoff ratio) increase, afforestation has a smaller effect on streamflow reduction in JULES [Figure 3.1a-c]. We find planting broadleaves has less of an impact on low flow conditions and droughts in wetter locations, and a greater response in drier areas. Drier catchments are more likely to show decreases in runoff from afforestation, due to increased rates of potential evapotranspiration and water usage, as seen in other studies (Birkinshaw *et al.*, 2014; Iacob *et al.*, 2017; Zhang *et al.*, 2017) [Figure 3.1]. A negative association with catchment aridity emphasises this point. In situations of high rainfall, and thus high runoff events, the same runoff generation processes will be present in a catchment with and without afforestation. In these situations, land cover will only have a minimal impact on flow reduction. Here, the strong correlation with catchment elevation is likely influenced by

differences in average rainfall ($\rho = 0.8$, $p = 0.0032$). Few of the catchment properties shown in Table 3.1 exhibit significant correlations with catchment response to afforestation at the high and low flows. This could be due to differences in planting location with catchment attributes not capturing the temporal and spatial elements of runoff generation mechanisms influenced by afforestation or the greater variability in extremes. Catchment area has a strong negative association between high flow reduction and afforestation potentially due to the greater relative reduction in the specific discharge of larger compared to smaller catchments.

Table 3.1: Sensitivity to afforestation with catchment properties.

*Spearman correlation between catchment attributes and percentage change in hydrologic metric with afforestation extent. Asterisks indicate significance: *, p < 0.05; **, p < 0.005; ***, p < 0.0005. The aridity index is characterised as the ratio between catchment mean precipitation and mean potential evapotranspiration. A larger correlation table can be found in Supplementary Figure S3.6.*

	Mean Precipitation (mm day $^{-1}$)	**Aridity Index**	**Baseflow Index**	**Soil Porosity**	**Soil Hydrological Conductivity (cm day^{-1})**	**Soil Depth to Bedrock (m)**	**Area (km^2)**	**Mean Elevation (m.a.s.l)**
Flow Duration Slope	*-0.25*	*0.34*	*-0.33*	*0.09*	*-0.08*	*0.67* *	*-0.12*	*-0.27*
Median Elasticity	*0.71* *	*-0.77* **	*-0.57*	*-0.14*	*0.41*	*-0.71* *	*-0.38*	*0.73* *
Runoff Ratio	*0.9* ***	*-0.8* ***	*-0.55*	*-0.01*	*0.33*	*-0.76* *	*-0.47*	*0.7* *
Very Low Flow	*0.56*	*-0.5*	*-0.19*	*0.1*	*0.04*	*-0.62* *	*-0.13*	*0.31*
Low Flow	*0.31*	*-0.42*	*-0.24*	*-0.59* *	*0.15*	*0.13*	*0.52*	*0.61* *
Median Flow	*0.77* *	*-0.82* **	*-0.44*	*-0.41*	*0.41*	*-0.54*	*-0.08*	*0.81* **
High Flow	*0.43*	*-0.42*	*-0.43*	*0.33*	*0.25*	*-0.46*	*-0.85* **	*0.24*
Very High Flow	*0.38*	*-0.39*	*-0.28*	*-0.22*	*0.6* *	*-0.24*	*-0.48*	*0.4*

There are not many significant associations between simulated catchment hydrology changes and catchment soil attributes [Table 3.1]. This suggests that catchment soil properties may have a minimal role altering catchment hydrology response to afforestation, at least in the JULES model. However, the slight significant negative association between soil depth to bedrock and changes in streamflow regimes with afforestation suggests afforestation may alter longer term hydrological fluxes. In catchments with deeper soils, where subsurface flow dominates, afforestation is likely to reduce the subsurface component of streamflow, decreasing runoff ratio and catchment elasticity whilst increasing flow regime variability. A similar effect can

also be seen in the low flows, albeit slight. This effect may be overemphasised in JULES owing to its uniform soil depth and so could be due to runoff generation mechanisms using topographic slope.

3.4. Conclusions

This study has quantified potential afforestation impacts on temperate catchment hydrology in Great Britain using a high-resolution land surface model. We find afforestation reduces streamflow at all flow quantiles with a clearer impact observed at median and low flows than high flows in twelve catchments over 500 km^2. When attributing changes in streamflow, afforestation location in the catchment can influence the highest and lowest streamflow extremes, particularly in smaller catchments. We find the extent of afforestation is more important than its location, particularly for the median flows. Simulated catchments with low rainfall and deep soils are more hydrologically responsive to afforestation than others in our chosen catchments. We show the effects of widespread afforestation on streamflow over multiple spatial scales within catchments can be significant and thus are important to include when establishing projections of hydrological change. These results provide quantitative insight into key water management decisions regarding the extent and location of afforestation in temperate regions and suggest caution is required when advocating widespread tree planting to mitigate future hydro-climatic change or to attempt to control flooding in large catchments.

3.5. Methods

3.5.1. Catchment Locations and Input Data

To determine the impact of afforestation on catchment hydrology we select twelve varied catchments from across the British Isles [Figure 3.1]. These catchments capture a range of hydrological regimes, drainage patterns and catchment soil and land cover properties to determine how such factors may influence catchment response to afforestation. Being predominantly > 1000 km^2 in area (ranging from 511 to 9931 km^2 in size), they are adequately represented in a hydrological model to integrate processes at a 1 km^2 spatial resolution (Crooks *et al.*, 2014; Martínez-De La Torre *et al.*, 2019). Two catchments are nested within larger ones,

the Ure within the Ouse, and the Severn at Bewdley (Severn-B) within the Severn at Haw Bridge (Severn-HB) [Figure 3.1].

The period 2000-2010, a flood-rich period for the British Isles (Wilby and Quinn, 2013; Blöschl *et al.*, 2020), is chosen to assess afforestation influence on streamflow as it allows us to avoid uncertainty that would be associated with land cover changes over a longer period when comparing to baseline results. This length of simulation period also reduces the computational demand with large ensemble of land cover scenarios. Accordingly, the CEH land cover map for the year 2000 (Fuller *et al.*, 2002), in the form of the CHESS-land dataset (Martínez-de la Torre *et al.*, 2018), is used to provide configurational datasets specifying soil hydraulic and thermal properties, vegetation characteristics, and orography, for the model at a 1 km^2 spatial resolution for the unaltered land cover scenarios. This dataset has successfully been used in other studies (Blyth *et al.*, 2019; Martínez-De La Torre *et al.*, 2019). The 25 m rasterised land cover map is reclassified into eight different land cover types [Supplementary Tables S3.4 & S3.5] and used to derive afforestation scenarios related to land cover before being converted to a percentage land cover fraction at a 1 km^2 spatial resolution. To provide the required meteorological driving data we use the CHESS-met dataset (Robinson, Blyth, Clark, Comyn-Platt, *et al.*, 2017) which includes long-wave and short-wave radiation, air temperature, specific humidity and pressure. The 50 m CEH Integrated Hydrological Digital Terrain Model elevation data is used to derive topographical and catchment attributes as well as catchment boundaries and river networks (Morris and Flavin, 1990). Soil hydraulic information comes from the Harmonized World Soil Database and was made uniform across each grid cell (Wieder *et al.*, 2014).

3.5.2. The Model

The Joint UK Land Environment Simulator (JULES) is a physically-based land-surface model that simulates the fluxes of carbon, water and energy at the land surface when driven by a time series of atmospheric data (Best *et al.*, 2011; D. B. Clark *et al.*, 2011). Multiple studies have used JULES before including investigation into evapotranspiration drivers across Great Britain (Robinson, Blyth, Clark, Finch, *et al.*, 2017; Blyth *et al.*, 2019), atmospheric river formation over Europe (Paltan *et al.*, 2017), the impact of solar dimming and carbon dioxide on runoff (Gedney *et al.*, 2014) and developing river routing algorithms with a Regional Climate Model

(Dadson *et al.*, 2011). JULES is routinely used at the Met Office, where it is coupled with several other models to understand future changes globally and across the UK, by bridging the atmosphere, land surface and ocean (H. Lewis *et al.*, 2019). This study is predominantly a theoretical, scenario-based modelling study designed to draw out general principles and to quantify the relation between afforestation and hydrological response, and as such the results are not intended to provide detailed guidance for specific practical actions.

The use of a process-based model enables us to investigate physical explanations for the hydrological impacts of changes in land cover and the explicit representation of vegetation that will influence fluxes, partitioning and storages within the realm of epistemic uncertainty for other conceptual and hydrological models where vegetation is not included. JULES models both plant phenology and canopy storages (Best *et al.*, 2011; D. B. Clark *et al.*, 2011). When changing the plant functional type in JULES, both the properties of the above-ground vegetation (such as canopy height and leaf area index) and the soil infiltration factor and the root depth are altered (Best *et al.*, 2011). However, there are several caveats that must be considered with this approach. First, the model configuration used in the present study is uncoupled from the atmosphere and so large-scale land cover changes cannot alter nearby weather (Meier *et al.*, 2021). Second, each grid cell is hydrologically separated from adjacent cells, with streamflow and runoff hydrologically uncoupled from the rest of the system. Soil water also does not flow between grid cells. Third, soil thermal and hydraulic properties are uniform across a grid cell. This reduces the impact of hydrological pathways within a cell and the interaction of vegetation with these varying soil types that could have ramifications at multiple temporal and spatial scales. For example, within the cell there may be vegetation that is water-stressed (e.g. valley sides) compared with vegetation where water is not limited (e.g. floodplain) which would change how much transpiration is possible and thus runoff (Fan *et al.*, 2019).

Precipitation in the model is partitioned by vegetation and when it reaches the soil surface it is portioned into either infiltration excess overland flow, at a rate controlled by the hydraulic conductivity of the soil, or saturation-excess overland flow as determined by the Probability Distributed Model (PDM) (Moore, 2007; Clark and Gedney, 2008). Throughfall (T_F) through the canopy is dependent on the rainfall and the existing water in the canopy:

$$T_F = P\left(1 - \frac{C}{C_m}\right)\exp\left(-\frac{\varepsilon_r C_m}{P\Delta t}\right) + P\frac{C}{C_m} \quad (1)$$

where P is the rainfall rate (kg m^{-2} s^{-1}), C is the amount of water in the canopy (mm), C_m is the maximum water storage of the canopy (mm) and ε_r is the fraction of the grid cell occupied by convective precipitation. The maximum amount of canopy water storage is a function of the leaf area index (L):

$$C_m = A_m + B_m L \tag{2}$$

where A_m is the ponding of water on the soil surface and interception by leafless vegetation (mm) and B_m is the rate of change of water holding capacity with leaf area index. At each timestep (n) the canopy storage is updated thus:

$$C^{(n+1)} = C^{(n)} + (P - T_F)\Delta t \tag{3}$$

Based on the surface energy balance, the fraction of the proportion of water stored in the canopy compared with the maximum canopy capacity of that plant type is used to calculate the effective surface resistance to determine tile evapotranspiration.

Surface runoff is generated by two processes in JULES: infiltration excess, where the water flux at the surface is greater than the infiltration rate of the soil, and saturated excess overland flow where the water flux at the surface is converted to runoff when the soil is completely saturated. To calculate the saturation excess overland flow, the PDM (Clark and Gedney, 2008) is used to determine the fraction of the model grid cell that will be saturated (f_{sat}) which is the used as a multiplier to convert any excess water reaching the surface to runoff:

$$f_{sat} = 1 - \left[\frac{max(0, S - S_0)}{S_{max} - S_0}\right]^{\frac{b}{b-1}} \tag{4}$$

where S is the fraction of the grid cell soil water storage, S_0 is the minimum storage at and below which there is no surface saturation (mm), S_{max} is the maximum grid cell storage (mm) and b is the Clapp and Hornberger (Clapp and Hornberger, 1978) soil exponent. We use the topography-derived parameterisation for the b and S_0/S_{max} parameters to reduce individual calibration with the following relationship (Martínez-De La Torre *et al.*, 2019):

$$\begin{cases} b = 2.0 \\ S_0/S_{max} = max\left(1 - \frac{s}{s_{max}}, 0.0\right) \end{cases} \tag{5}$$

where s is the grid cell slope (°) and s_{max} is the maximum grid cell storage (mm). Once interception and surface runoff have been calculated, the remaining water enters the soil. This water is allocated to the different soil layers within the soil column by using the Darcy-Richards equation:

$$W = k\left(\frac{d\varphi}{dz} + 1\right) \tag{6}$$

where W is the vertical flux of water through the soil (kg $m^{-2}s^{-1}$), k is soil conductivity (kg $m^{-2}s^{-1}$), φ is suction (m) and z is the vertical flux of water through the soil (m). To calculate suction and soil conductivity we use the van Genuchten (van Genuchten, 1980) scheme:

$$\left(\frac{\theta}{\theta_s}\right) = \frac{1}{\left[1 + (\alpha\varphi)^{\left(\frac{1}{1-m}\right)}\right]^m} \tag{7}$$

where θ is the average volumetric soil moisture (m^3 m^{-3}), θ_s is the soil moisture at saturation (m^3 m^{-3}), α and m are van Genuchten parameters dependent on soil type. The hydraulic conductivity is calculated thus:

$$K_h = K_{hs}S^{\varepsilon}\left[1 - \left(1 - S^{\frac{1}{m}}\right)^m\right]^2 \tag{8}$$

where K_h is the hydraulic conductivity (m s^{-1}) and K_{hs} is the hydraulic conductivity for saturated soil (m s^{-1}). ε is an empirical value set at 0.5 in JULES and S is found by:

$$S = \frac{(\theta - \theta_r)}{(\theta_s - \theta_r)} \tag{9}$$

where θ_r is the residual soil moisture (m^3 m^{-3}). Vegetation can access water from each level in the soil column as a function of the root density where the fraction of roots (r) in each soil layer (l) from depth z_{l-1} to z_l is:

$$r_l = \frac{e^{-\frac{2z_{l-1}}{d_r}} - e^{-\frac{2z_l}{d_r}}}{1 - e^{-\frac{2z_t}{d_r}}} \tag{10}$$

where z_l is the depth of the l-th soil layer, d_r is the root depth (m) and z_t is the total depth of the soil column (m). The water flux extracted from a soil layer is e_lE where E is transpiration (kg $m^{-2}s^{-1}$) and e_l can be found by:

$$e_l = \frac{r_l\beta_l}{\sum_l r_l\beta_l} \tag{11}$$

and β_l is defined by:

$$\beta_l = \begin{cases} 1 & \theta_l \geq \theta_c \\ (\theta_l - \theta_w)/(\theta_c - \theta_w) & \theta_w < \theta_l < \theta_c \\ 0 & \theta_l \leq \theta_w \end{cases} \tag{12}$$

where θ_c and θ_w are the volumetric soil moisture critical and wilting points respectively (m^3 m^{-3}) and θ_l is the unfrozen soil moisture at that soil layer (m^3 m^{-3}). In this configuration of JULES, when a soil layer becomes saturated, the excess water is routed to lower layers. When the bottom layer becomes fully saturated any excess water is added to the subsurface runoff. Both

the surface and subsurface runoff are then passed to the River Flow Model (Bell *et al.*, 2007; Dadson *et al.*, 2011) which routes the flows according to a flow direction grid (Davies and Bell, 2009).

This study uses a combination of calibrated model parameters from the previous work of Robinson et al. (2017) and Martinez-de la Torre et al. (2019) (Rose suites u-bi090 and u-au394 respectively, which can be found using the Rose/Cylc suite control system: https://metomi.github.io/rose/doc/html/index.html). We compare observed streamflow from the NRFA database (Vitolo *et al.*, 2016) with model output for the years 2000-2010 using the base land and CHESS-met datasets. The model is spun-up for the years 1990-2000 to ensure soil moisture content has been equilibrised. To quantify the accuracy of the model we use a range of standard error metrics. These include the Nash-Sutcliffe Efficiency (Nash and Sutcliffe, 1970) measure:

$$NSE = 1 - \frac{\sum_{i=1}^{n}(Q_{sim} - Q_{obs})^2}{\sum_{i=1}^{n}(Q_{obs} - \bar{Q}_{obs})^2} \quad (13)$$

Kling-Gupta Efficiency (Gupta *et al.*, 2009):

$$KGE = 1 - \sqrt{(r-1)^2 + \left(\frac{\sigma_{sim}}{\sigma_{obs}} - 1\right)^2 + \left(\frac{\mu_{sim}}{\mu_{obs}} - 1\right)^2} \quad (14)$$

Root Mean Squared Error:

$$RMSE = \sqrt{\sum_{i=1}^{n}(Q_{sim} - Q_{obs})^2} \quad (15)$$

Mean Absolute Error:

$$MAE = \frac{\sum_{i=1}^{n}|Q_{sim} - Q_{obs}|}{n} \quad (16)$$

where Q_{sim} is the simulated discharge, Q_{obs} is the observed discharge, r is the linear correlation between observation and simulations, $\sigma_{sim|obs}$ is the standard deviation of discharge, $\mu_{sim|obs}$ is the mean of discharge and n is the number of observations. We also use NSE(log(Q)) and KGE(1/Q) to understand how well the model can reproduce low flows. Using these measures, we find that JULES performs satisfactorily apart from the Avon Catchment which may be due to fast subsurface flows generated by its geology (Martínez-De La Torre *et al.*, 2019) [Supplementary Table S3.7]. With process-based models it is difficult to both accurately reproduce physical processes and make the output faithful to reality due to epistemic uncertainties (Beven *et al.*, 2011). Even though model performance is not the same as achieved

with calibrated conceptual or empirical models it allows us to determine the effects of vegetation changes on the hydrological cycle.

JULES' ability to faithfully represent hydrological land surface processes in Great Britain has been evaluated in several studies (Blyth *et al.*, 2019; E. Cooper *et al.*, 2021; Pinnington *et al.*, 2021) and the plant functional type parameters it uses at global scales (Slevin *et al.*, 2015; Harper *et al.*, 2016). To validate the ability of our configuration of JULES to represent soil moisture and potential evapotranspiration rates we compare the model output with observations from twelve COSMOS-UK sites within our catchments covering grasslands, croplands, coniferous and broadleaf woodland (H. M. Cooper *et al.*, 2021) [Supplementary Figure S3.8]. We evaluate model performance from the start of the COSMOS-UK station records until the 1st January 2018 so that we use the same forcing data as our experiments. Station start dates vary from October 2013 to August 2017. We compare COSMOS-UK observed soil moisture to the first 0.1 m of the soil column in JULES and evaporation to the sum of the soil evaporation and plant transpiration. We find a median KGE score of 0.44 for the topsoil moisture and 0.53 for potential evaporation [Supplementary Tables S3.9 & S3.10]. Low error metrics observed for topsoil moisture are due to systematic undercalculation by JULES (E. Cooper *et al.*, 2021). At our broadleaf sites, Alice Holt and Wytham Woods, we find both systematic over and underprediction of the topsoil moisture respectively. In line with other studies, we find that there is a slight overestimation of evaporation in JULES (Van den Hoof *et al.*, 2013; Blyth *et al.*, 2019). As illustrated by the median coefficients of determination between the COSMOS-UK and JULES data of 0.62 and 0.60 for the topsoil moisture and evaporation respectively, JULES broadly represents changes in these variables over time.

3.5.3. Land Cover Scenarios

Modelling the influence of afforestation on catchment hydrology has been attempted before but usually only at the scale of a single catchment for a limited range of scenarios. In this study we focus on the theoretical effect of widespread planting of broadleaf trees to examine whether planting location is a stronger control on hydrological response than afforestation extent by using a large ensemble of up to 288 land cover change scenarios. We choose to focus just on broadleaf woodland for several reasons. First, we are trying to replicate a landscape that could be considered a natural climatic climax community that might occur if it had not been for

human intervention during the Holocene. Second, broadleaf woodland has the potential to absorb and store carbon in soils for longer time periods. Finally, to reduce computational cost and the issue of potentially expanding the errors induced by potentially spurious parameters of needleleaf woodland in this version of JULES (Broadmeadow *et al.*, 2018). Although potential woodland planting locations have been suggested by the Environment Agency and authorities in Scotland and Wales (Sing *et al.*, 2018; Broadmeadow *et al.*, 2019; Manzoor *et al.*, 2019), the differences in planting criteria means it is not possible to systematically compare hydrological changes across our chosen catchments. Here we attempt to create afforestation scenarios related to both catchment river network structure and land use that are directly comparable across a range of catchments. Afforestation was in grassland areas to reduce the complexity of the decisions made and enable an understanding behind catchment sensitivity to land cover changes related to soil and catchment structure.

Three metrics were selected to discretise the catchment into distinct areas for afforestation: the Topographic Wetness Index (TWI) (Beven and Kirkby, 1979), Strahler (Strahler, 1957) and Shreve orders (Shreve, 1966). These metrics capture different parts of the catchment such as propensity for saturation, drainage network location and relative contributing areas. TWI is calculated by:

$$TWI = \ln \frac{a}{\tan \gamma} \tag{17}$$

where a is the upslope area draining through a point, per unit contour length, and γ is the local surface topographic slope in radians. All three metrics were calculated using the 50 m IHDTM (Morris and Flavin, 1990), thresholding stream formation at an accumulation of ten pixels using the D8 flow direction algorithm within ArcGIS 10.6.1 (O'Callaghan and Mark, 1984). Strahler order ranges from one (headwaters) to seven (lowlands). Due to the continuous nature of TWI (0.05 – 31.49) and large ordinal range of Shreve order (1 – 9523) calculated for the entire British Isles, we group TWI orders into five quantiles and seven quantiles for Shreve. Increasing TWI order in this case indicates increasing propensity for saturation, or potential maximum saturation level, and increasing Shreve order indicates increasing contributing area. Catchments were broken down to watersheds from the downstream point of the Shreve and Strahler orders. Due to the nature of the data, this led to some first order Strahler catchments being incorrectly generated for some catchments [Supplementary Table S3.7]. Using these generated catchment areas, we plant both inside and outside of these watersheds to understand the hydrological difference between opposing planting locations. In each of the catchment

areas, two different levels of afforestation were tested of approximately 25 and 50 % of the possible planting area. Planted area was assigned at random in the catchment and was produced by calculating the area available for afforestation and randomly producing points that covered the area required using the Create Random Points tool in ArcGIS 10.6.1.

Discussions exist about where to plant woodland in relation to existing land cover, to provide ecosystem services, including around watercourses (Thomas and Nisbet, 2007; de Sosa *et al.*, 2018), urban areas (Fuller *et al.*, 2016; Gunnell *et al.*, 2019) and woodland (Woodland Expansion Advisory Group, 2012; Burton *et al.*, 2018). Therefore, in this study we try to understand how these potential planting scenarios will affect hydrology in general. Using the CEH 2000 land cover map (Fuller *et al.*, 2002) buffers of broadleaf land cover were created at 25 and 50 m around these three land uses [Supplementary Figure S3.7]. These were then discretised according to the catchment areas. As examples, one scenario would be afforesting up to 50 m around existing broadleaf woodland inside the Shreve order one catchment area, whilst another would be randomly afforesting within 25 % of the available area outside of TWI order five area.

Afforestation according to different catchment areas and land cover uses between 234 and 288 scenarios for each catchment and between 0 and c. 40 percentage point increase in broadleaf woodland [Supplementary Figure S3.2 & Table S3.8]. Due to the structure and size of the different catchments, and thus differences in Strahler and Shreve orders, not all catchments had a comparable number of higher orders. Produced scenarios were converted to the 1 km^2 grid scale by altering the fraction of land cover types within each grid cell. It should be noted that this work only considers the impact of mature broadleaf woodland and neglects the influence of the initial planting and growing of the woodland that would likely have its own impact on catchment hydrology as frequently reported (Marc and Robinson, 2007; Birkinshaw *et al.*, 2014). Furthermore, it does not include the period when there would be the highest amount of carbon sequestration. This study seeks to understand the theoretical impact of woodland on catchment hydrology when fully developed to understand the long-term implications of management decisions.

3.5.4. Hydrological Signatures and Analysis

Several hydrologic indices can be used to characterise the influence of afforestation on streamflow regime (Olden and Poff, 2003; Addor *et al.*, 2017). To analyse average streamflow and extremes, we look at the top 1% (very high flow), 5% (high flow), 50% (median flow), 90% (low flow) and 95% (very low flow) quantiles of daily streamflow. To quantify flow variability, we use the slope of the flow duration curve (Yadav *et al.*, 2007; Sawicz *et al.*, 2011) calculated thus:

$$FDC = \frac{\ln(Q_{33\%}) - \ln(Q_{66\%})}{(0.66 - 0.33)} \quad (18)$$

where $Q_{33\%}$ is the 33rd flow exceedance quantile and $Q_{66\%}$ is the 66th flow exceedance quantile. To ascertain catchment responsiveness to climatic forcing we use median streamflow elasticity (Sankarasubramanian *et al.*, 2001; Sawicz *et al.*, 2011):

$$MSE = median\left(\frac{dQ}{dP}\frac{P}{Q}\right) \quad (19)$$

where dQ and dP are the annual changes in yearly discharge and precipitation, respectively. Finally, we use the runoff ratio to quantify water balance changes related to streamflow and evapotranspiration (Milly, 1994):

$$RR = \frac{\mu_Q}{\mu_P} \quad (20)$$

where μ_Q and μ_P are the average yearly discharge and precipitation using daily values, respectively. We also qualitatively assess the largest peak flow daily event in the 10-year record used in this study to determine the impact of afforestation on the highest possible flows in each catchment.

To determine how afforestation influences streamflow metrics, percentage changes in flow metrics are plotted as a function of percentage point increases in afforestation (calculated using the difference between original and afforested scenario). Quantile regression is applied to determine the median regression slope of the trend for the entire period (Koenker and Bassett, 1978). The benefit of using quantile regression is that it identifies the median response of the input variable (in this case the level of afforestation in both percentage and absolute terms) without being influenced by extreme outliers. In this way we can estimate the proportional streamflow response to afforestation over the period. We use the regression slope coefficient as a proxy of catchment sensitivity to afforestation for each streamflow metric. The slope coefficient is then correlated to catchment attributes, as stated in the CAMELS-GB dataset (Coxon *et al.*, 2020), using Spearman's rank correlation. This allows us to determine the

direction and significance of the catchment property influences on the sensitivity of catchments to afforestation for the different hydrologic signatures. To determine the impact of different planting locations according to catchment and land cover location a one-way analysis of variance (ANOVA) test is undertaken using R (RStudio Team, 2021).

4. Afforestation impacts on terrestrial hydrology insignificant compared to climate change in Great Britain

---

This chapter has been submitted as a research article to the journal Hydrology and Earth System Sciences. Marcus Buechel ran the simulations, analysed the results, and created the figures. All co-authors contributed to editing the manuscript.

Citation: Buechel, M. E. H., Slater, L., and Dadson, S.: Afforestation impacts on terrestrial hydrology insignificant compared to climate change in Great Britain, Hydrol. Earth Syst. Sci. Discuss. [preprint], https://doi.org/10.5194/hess-2023-138, in review, 2023.

Responses to initial reviews can be found at https://doi.org/10.5194/hess-2023-138-AC1 and https://doi.org/10.5194/hess-2023-138-AC2 .

4.1. Abstract

Widespread afforestation has been proposed internationally to reduce atmospheric carbon dioxide, however the specific hydrological consequences and benefits of such large-scale afforestation (e.g., Natural Flood Management) are poorly understood. We use a high-resolution land surface model, JULES, with realistic potential afforestation scenarios to quantify possible hydrological change across Great Britain in both present and projected climate. We assess whether proposed afforestation produces significantly different regional responses across regions; whether hydrological fluxes, stores and events are significantly altered by afforestation relative to climate; and how future hydrological processes may be altered up to 2050. Additionally, this enables determination of the relative sensitivity of land surface process representation in JULES compared to climate changes. For these three aims we run simulations using: (i) past climate with proposed land cover changes and known floods and drought events; (ii) past climate with independent changes in precipitation, temperature, and CO_2; and (iii) a potential future climate (2020-2050). We find the proposed scale of afforestation is unlikely to significantly alter regional hydrology, however it can noticeably

decrease low flows whilst not reducing high flows. The afforestation levels minimally impact hydrological processes compared to changes in precipitation, temperature, and CO_2. Warming average temperatures (+ 3 °C) decreases streamflow, while rising precipitation (130%) and CO_2 (600 ppm) increase streamflow. Changes in high flow are generated because of evaporative parameterisations whereas low flows are controlled by runoff model parameterisations. In this study, land surface parameters within a land surface model do not substantially alter hydrological processes when compared to climate.

4.2. Introduction

Land cover (e.g., grassland and bare ground) exerts a strong control on catchment hydrology (Blöschl *et al.*, 2007; Pattison and Lane, 2012; Rogger *et al.*, 2017). A land use or land cover change (LULC) can obscure the impact of climate on streamflow. LULC alters streamflow by changing hydrological processes (e.g., subsurface flow) over multiple spatial and temporal scales. One example of LULC is afforestation, which can lower catchment water tables (Kellner and Hubbart, 2018; Shuttleworth *et al.*, 2019; Peskett *et al.*, 2020), increase precipitation downwind (Teuling *et al.*, 2019; Meier *et al.*, 2021; Xu *et al.*, 2022) and alter transpiration rates over time (Newson and Calder, 1989; Hudson *et al.*, 1997; Marc and Robinson, 2007). Many studies suggest afforestation can reduce overall streamflow, however, land management practices (e.g., artificial ditching and road cutting) may also increase peak streamflow (Beschta *et al.*, 2000; Bathurst *et al.*, 2018). It is therefore important to understand all the hydrological processes of afforestation (and other LULC), especially as the climate changes and the hydrological cycle intensifies (Kundzewicz, 2011; IPPC, 2019; Hung *et al.*, 2020). Changing rainfall (Gao *et al.*, 2018; Fowler *et al.*, 2021), temperature (Wasko, 2021) and carbon dioxide (Gedney *et al.*, 2006; Betts *et al.*, 2007) could all influence how large-scale afforestation impacts hydrology.

Potential afforestation benefits include the reduction of atmospheric CO_2 (Griscom *et al.*, 2017; Hawes, 2018; Cook-Patton *et al.*, 2020; Palmer, 2021); moderation of temperature extremes (O'Briain *et al.*, 2020; Schwaab *et al.*, 2020); reduction of air and noise pollution (Oldfield *et al.*, 2013; Fenner, 2017); provision of areas of societal wellbeing (Dick *et al.*, 2019); and reduction of flood risk as a form of Natural Flood Management (NFM) (Dadson *et al.*, 2017; Cooper *et al.*, 2021). These potential benefits have led governments and businesses to pledge

woodland acreage increases (Lewis *et al.*, 2019; Seddon *et al.*, 2020), but there is a need to quantify the actual (and not merely perceived) advantages of planting the right trees in the right place (Grassi *et al.*, 2017; Seddon *et al.*, 2021). The UK government plans to expand woodland from 13% to 17% of land cover by 2050 to reach Net Zero (Committee on Climate Change, 2019b, 2019a). As the UK experiences more frequent and larger floods (Griffin *et al.*, 2019; Hannaford *et al.*, 2021), it is important to learn how afforestation could reduce flood peaks. Therefore, additional research is required to interrogate the hydrological response to afforestation over regional to continental scales.

Determining woodland influence on hydrology is not new (Andréassian, 2004). Studies investigating afforestation impact on streamflow have used global streamflow datasets (Bradshaw *et al.*, 2007; Do *et al.*, 2017), paired catchments (Bosch and Hewlett, 1982; Brown *et al.*, 2013; Bathurst *et al.*, 2018) and modelling (Iacob *et al.*, 2017; Li *et al.*, 2018; Speich *et al.*, 2018). Recent UK studies show how wet canopy evaporation can reduce high runoff (Page *et al.*, 2020) and afforestation can increase saturated soil hydraulic conductivity in upland areas (Murphy *et al.*, 2021). These results, and others, have been taken by some to suggest that afforestation can reduce flooding with greater water usage, higher infiltration rates and increased floodplain hydraulic roughness (Nisbet *et al.*, 2011; Cooper *et al.*, 2021). However, it remains unclear whether hydrological afforestation effects have a detectable hydrological impact over areas larger than 50 km^2 due to the small scales of existing studies of afforestation hydrology (Dadson *et al.*, 2017; Rogger *et al.*, 2017; Nisbet and Thomas, 2021). Further uncertainty exists between empirical studies and model results regarding peak streamflow generation following afforestation (Stratford *et al.*, 2017; Carrick *et al.*, 2019), making it difficult to transfer afforestation impacts on catchment hydrology over large regions.

Process-based numerical models provide one way to understand the consequences of afforestation (Gush *et al.*, 2002; Bonan, 2008). They incorporate known processes to determine system responses to scenarios (e.g., projected climate). Many studies have applied numerical models to determine afforestation's role in reducing flood risk, although few have considered areas larger than a single catchment (Stratford *et al.*, 2017). Land surface models (LSMs) incorporate a suite of known Earth system processes and have been used to study countrywide and continental hydrology (Prudhomme *et al.*, 2012; Blyth *et al.*, 2021). Inclusion of plant functional types, nutrient cycling, physiological forcing and surface energy fluxes mean LSMs are well suited to investigate afforestation mechanistic impacts on the hydrosphere compared

to simpler models. This is essential to assess the hydrological response to a system as complex as vegetation change (Rogger *et al.*, 2017). LSMs should therefore quantify projected hydrological changes whilst modellers determine if outputs are realistic. Previous work using an LSM has shown tree planting location has a minimal impact compared to the extent planted within catchments (Buechel *et al.*, 2022). It is unknown whether this finding is true across all regions of Great Britain in a changing climate and the fidelity of the model parameterisations.

In this study, the impact of increasing broadleaf afforestation on Great Britain's hydrology is analysed with a high-resolution LSM. The approach allows direct comparison of streamflow with and without afforestation on a country-wide scale, whilst determining processes and catchment attributes driving modelled hydrological changes. Three central questions are investigated about realistic afforestation scenarios influencing country-wide hydrology:

1. What is the hydrological response to afforestation across Great Britain and how does this vary regionally?

2. How much of an impact would realistic afforestation scenarios have on hydrological processes compared to potential changes in climate?

3. How might realistic afforestation alter future hydrological scenarios up to 2050?

We evaluate these questions by quantifying how plausible afforestation across Great Britain could influence catchment hydrology, identifying changes across the streamflow spectrum, and testing the fitness for purpose of model process representation.

4.3. Methods

4.3.1. Plausible Afforestation Scenarios

Several afforestation scenarios have been used to investigate the hydrological consequences of afforestation, such as the 'global restoration potential' dataset (Bastin *et al.*, 2019; Meier *et al.*, 2021; Hoek van Dijke *et al.*, 2022) but its realism has been questioned (Friedlingstein *et al.*, 2019; Wilkes *et al.*, 2020). Hydrological conclusions derived from such unlikely scenarios are

therefore equally questionable. The UK Government's Net Zero strategy includes planting 30 000 hectares of trees, equivalent to sequestering 14 $MtCO_2e$, a year from 2024 onwards (Committee on Climate Change, 2018). This roughly approximates to 900 000 hectares of additional woodland across the country by 2050. Plausible afforestation scenarios for Great Britain should emphasis planting trees in areas that accomplish maximal societal benefits (Bradfer-Lawrence *et al.*, 2014; Burke *et al.*, 2021). This study produces credible afforestation extents with multiple purposes and minimal resistance [Figure 4.1] by altering three previously developed afforestation scenarios for the countries of Great Britain: England, Wales, and Scotland. Northern Ireland is not included as model driving datasets do not cover this region. The scenario for England is the Environment Agency's Working with Natural Processes program, which aims to reduce flood risk and restore the natural regulating function of catchments (Environment Agency, 2018). In Wales the Glastir Woodland Creation opportunities map is utilised that aims to plant trees for maximal benefits (Welsh Government, 2021). Finally for Scotland, the Woodland Expansion Advisory Group's map is used that identified areas with the greatest potential for woodland expansion (Sing and Aitkenhead, 2020).

Woodland extent is spatially constrained for the chosen afforestation scenarios, however further limits are applied to promote afforestation in low-risk locations. Principles to expand woodland into areas that minimally interfere with existing land practices are used, developed by the Scottish Woodland Expansion Advisory Group and the Forestry Commission (Sing and Aitkenhead, 2020). Afforestation takes place in: acid grassland, arable and horticultural areas, heather, heather grassland, improved grassland and neutral grassland as defined by the CEH Land Cover 2000 (Fuller *et al.*, 2002) [Figure 4.1]. Woodland expansion does not encroach on urban areas, existing woodland, shrubland, bare ground, inland water, or upon biodiversity-rich grasslands (by excluding it from priority habitat areas). To note, grassland afforestation can decrease soil carbon and not sequester additional carbon over the short term (Don *et al.*, 2009). Other spatial constraints for woodland expansion are summarised in Figure 4.1. Across Great Britain, this afforestation criteria creates a geographical imbalance with largest potential afforestation areas in Scotland followed by Wales then England [Figure 4.2]. This is due to more land being initially identified in Scotland and Wales for afforestation and greater areal constraints to afforestation in England. A maximal potential afforestation area of 3.53 million hectares is generated in Great Britain using these afforestation constraints (approximately 700 000 hectares less than the 'global restoration potential').

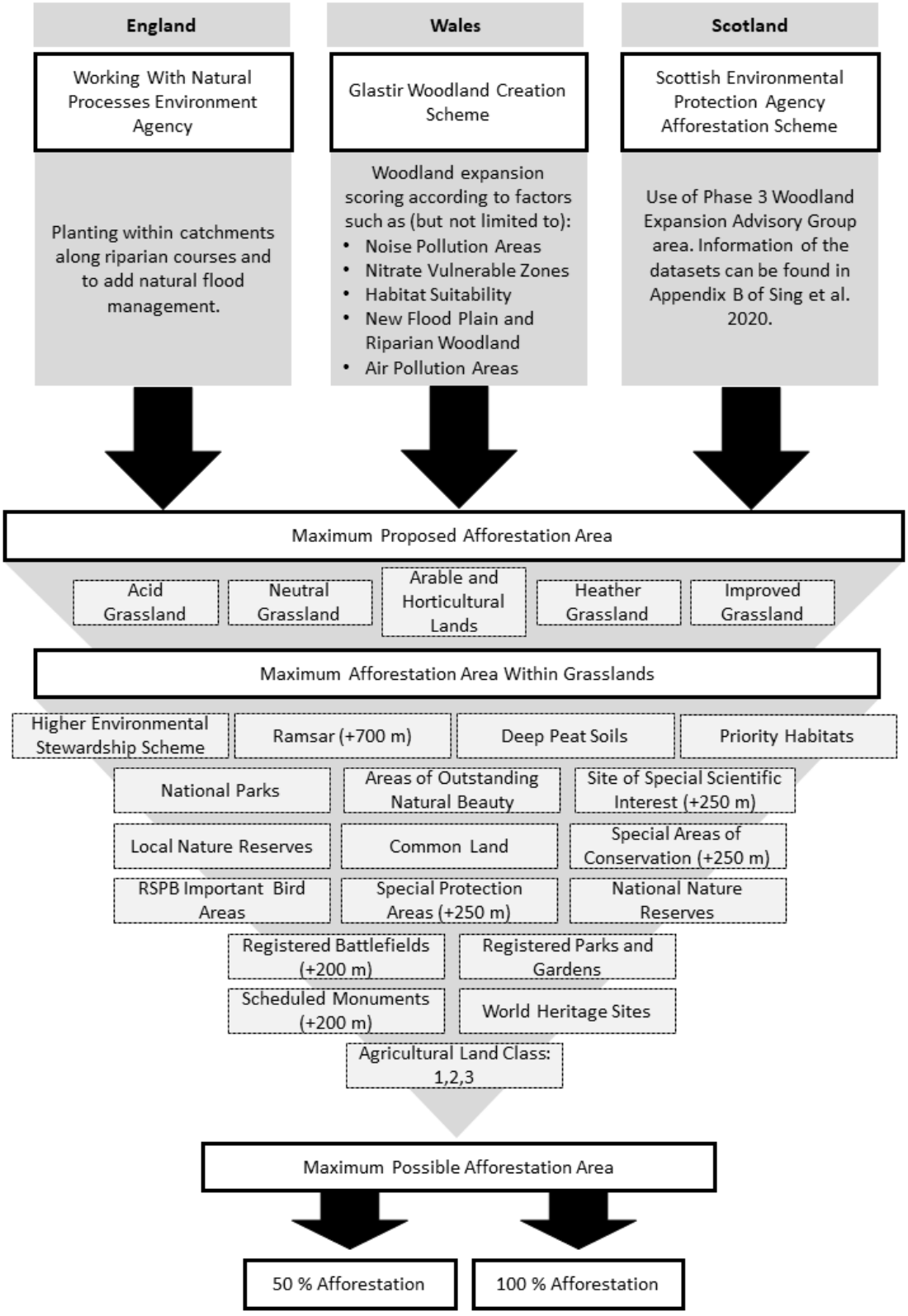

Figure 4.1: Flow diagram explaining the creation of the two realistic afforestation scenarios. *The top row indicates the three afforestation scenarios developed for England, Scotland, and Wales. The spatial extent of these scenarios is reduced by selecting the scenario areas that intersect with grasslands (as defined by the CEH Landcover 2000 map) and several other*

factors as shown above (such as Areas of Outstanding Natural Beauty and Special Protection Areas). 100 % and 50 % scenarios are created from the maximum possible afforestation area calculated.

900 000 hectares of broadleaf woodland is randomly 'planted', at a 25 m resolution, within the generated maximum afforestation extent (on the same projected coordinate system as the CEH 2000 landcover map (Fuller *et al.*, 2002)). In addition, another scenario with approximately 450 000 hectares of woodland is made to represent afforestation at similar present rates (Forest Research, 2021a). Woodland extent across Great Britain changes from 12.3% to 14.3% and 16.2% for the 50% and 100% afforestation scenarios respectively (using the CEH 2000 land cover). These two afforestation scenarios are combined with the CEH 2000 landcover map (Fuller *et al.*, 2002) and scaled to a 1 km^2 grid, similar to the CHESS-land dataset (Martinez-de la Torre *et al.*, 2018), by calculating the fraction of eight different land cover types detailed in the following section. Arguably these scenarios are a restrictive level of afforestation, but they appear ambitious when compared to current afforestation rates of approximately 10 000 hectares per year (Forest Research, 2021b).

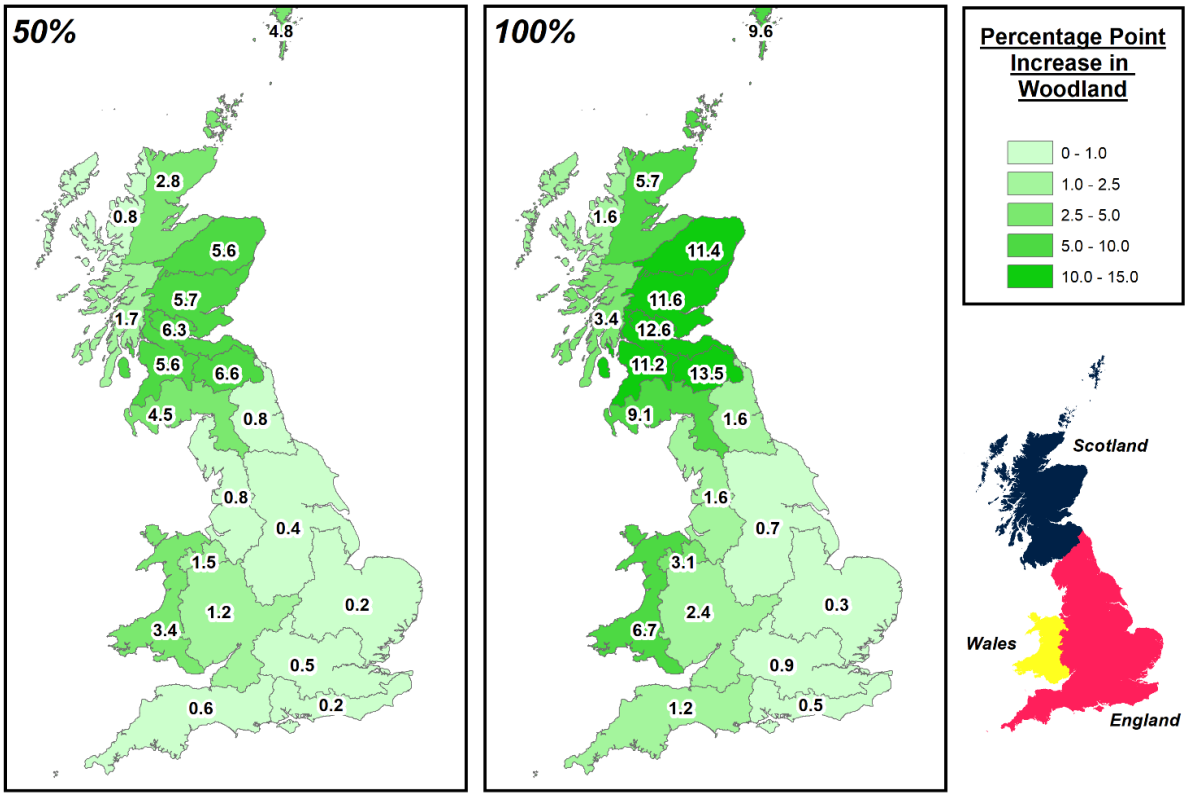

Figure 4.2: Percentage point increase in broadleaf woodland for the two realistic afforestation scenarios generated for each of the twenty UKCP18 hydro-regions in Great Britain.

4.3.2. Modelling Methodology

This study is split into three parts for each research question. This enables a coherent understanding of afforestation on potential past, present and future hydrology within the model domain. First, the potential hydrological benefits, and drawbacks, of afforestation scenarios are considered under present climate conditions. Second, a simple factorial sensitivity analysis is undertaken to ascertain the relative importance of afforestation and climate on future hydrological changes, and model process parameterisation. Finally, a future climate scenario is utilised to project how plausible future afforestation may alter hydrology in Great Britain up to 2050.

4.3.2.1. Model Description

The Joint UK Land Environment Simulator (JULES), a physically based LSM, is used and simulates water, carbon and energy stores and fluxes (Best *et al.*, 2011; Clark *et al.*, 2011). JULES has been used many times previously, for example: determining the climatic impact of the Montreal protocol (Young *et al.*, 2021); assessing trends in evapotranspiration across Great Britain since the 1960s (Blyth *et al.*, 2019); and aiding production of high-resolution UK soil moisture datasets (Peng *et al.*, 2021). Due to the complexity and high number of free and fixed parameters of JULES the base validated model configuration of Buechel *et al.* (2022), Robinson *et al.* (2017) and Martínez-de la Torre *et al.* (2019) is utilised. Configuration details are found in Buechel *et al.* (2022) and accessible as Rose suite u-ce663 from the Met Office Rose/Cylc suite control system (https://metomi.github.io/rose/doc/html/index.html). The CHESS-land dataset specifies JULES' bounding conditions including soil hydraulic, thermal, vegetation and orographic properties at a 1 km^2 spatial resolution (Martinez-de la Torre *et al.*, 2018). CHESS-met provides the meteorological information of air temperature, pressure, specific humidity as well as short- and long-wave radiation for the first two parts of the study (Robinson *et al.*, 2017). In the final study section, we utilise CHESS-SCAPE (Robinson *et al.*, 2022), a 1 km^2 downscaled UKCP18 projection (Lowe *et al.*, 2018) with all the same variables and spatial and temporal resolution of CHESS-met.

JULES runs at a numerical timestep of 30 minutes. The land surface is divided into eight possible types, five vegetated (broadleaf, needleleaf, C3 grass, C4 grass (crops), shrubs) and three non-vegetated (urban, inland water, bare soil). Precipitation covers a grid cell according to a constant dependent on temperature (Best *et al.*, 2009) and is intercepted by vegetation, as a function of the leaf area index (LAI). Canopy throughfall is a function of the existing canopy water, rainfall, and the maximum amount of canopy water (related to LAI). Evapotranspiration is calculated using effective surface resistance (water stored in the canopy compared to the maximum canopy capacity) and stomatal conductance is modelled using soil moisture, atmospheric carbon dioxide and the vapour pressure deficit (Cox *et al.*, 1998). Water at the surface is routed as infiltration excess overland flow, at a rate controlled by the soil hydraulic conductivity, or as saturation-excess overland flow calculated by the Probability Distributed Model (PDM) (Moore, 2007; Clark and Gedney, 2008). A topography-derived parametrisation of soil water storage in the PDM is used to calculate grid fraction saturation, which is used as a multiplier to convert excess water reaching the surface to saturation-excess overland flow (Martínez-De La Torre *et al.*, 2019; Lewis and Dadson, 2021). Water flux through the four soil layers (3 m deep) is calculated by the Darcy-Richards equation and the van Genuchten scheme calculates suction and soil conductivity (van Genuchten, 1980). Vegetation extracts excess water from the different soil layers as a function of root density and soil moisture critical and wilting points. As soil layers become progressively saturated water is passed downwards until excess water at the base becomes subsurface runoff. The River Flow Model (RFM) implementation of the kinematic wave equation solution routes both the surface and subsurface runoff according to a D8 flow direction grid (Davies *et al.*, 2022). The model is spun-up for ten years in all experiments so that soil moisture content equilibrates (Martínez-de la Torre *et al.*, 2018; Blyth *et al.*, 2019).

Model output (soil moisture, evaporation and streamflow) is validated with twelve COSMOS-UK stations (Cooper *et al.*, 2021) and the National River Flow Archive database for the investigated catchments (Vitolo *et al.*, 2016) [Supplementary Material: Figures S1 & S2]. The Kling-Gupta Efficiency Measure (KGE) (Gupta *et al.*, 2009) quantifies model accuracy where scores better than -0.41 show model performance greater than the mean seasonal cycle (Knoben, Freer and Woods, 2019). Several model outputs are validated to determine whether JULES is providing the right result for the right reason across model parameterisation domains (Mai *et al.*, 2020; Lane *et al.*, 2021). We find JULES performs satisfactorily: streamflow has a median KGE of 0.50 (minimum: 0.08; maximum 0.76), soil moisture 0.44 (minimum: 0.20;

maximum: 0.82) and potential evaporation 0.53 (minimum: 0.22; maximum: 0.72). These are not perfect scores and so caution must be applied when considering results. KGE scores illustrate the challenges in producing a 'model of everywhere' when there is so much uncertainty in model parameterisations and parameters (Beven, 2007; Blair *et al.*, 2019). Furthermore, any changes in model results are relative to simulations and are not compared to realistic absolute values due to limitations of model process representation. Refer to Buechel *et al.* (2022) for further details on model validation and Supplementary Material [Tables S4.1,S4.2,S4.3].

4.3.2.2. Streamflow Analysis

Streamflow is the combined output of upstream hydrological processes and thus invaluable to explore afforestation effects. Fifty-one catchments are selected to assess streamflow across all regions [Supplementary Material: Figure S4.1 & Table S4.4]. Ten are from the previous work of Buechel *et al.* (2022), Crooks *et al.* (2014), and Martínez-De La Torre et al. (2019), thirty-nine are from the UKBN2 gauging station network (Harrigan *et al.*, 2018), and two of the largest catchments in the Dee region (as there were no rivers fitting our criteria). UKBN2 catchments are near natural with minimal human interference; important for isolating changes due to LULC and climate with minimal anthropogenic interference (Villarini and Wasko, 2021), which may be unrepresented within JULES. Chosen catchments are larger than 150 km^2 in size so that processes simulated are more faithful at JULES' spatial (1 km^2) and temporal (30 minute) resolution, apart from two rivers in Scotland which were needed so that all regions would have streamflow simulations. Chosen catchments cover all UKCP18 regions to enable analysis of how countrywide drought and flood conditions change with afforestation.

Flow percentiles at the 1, 5, 10, 50, 90, 95, 99 % are calculated to observe flow change across the whole flow spectrum with afforestation over the full hydrological year and not just individual events. The slope of the flow duration curve (FDC) is calculated to understand flow variability changes:

$$FDC = \frac{\ln(Q_{33\%}) - \ln(Q_{66\%})}{(0.66 - 0.33)} \quad (1)$$

Where $Q_{33\%}$ and $Q_{66\%}$ are the 33rd and 66th percentile of streamflow respectively. Chosen streamflow metrics enable quantification of extreme and average changes induced by afforestation to learn how flow regimes could changes at present and the future.

4.3.3. Present Hydrological Response to Afforestation

The period of 2000-2015 is chosen for the first study part. This is a flood-rich period, including several drought events, allowing determination of the role afforestation would have on these events across the country (Wilby and Quinn, 2013; Dadson *et al.*, 2017). Hydrological processes are disaggregated by the twenty UKCP18 river basin boundaries (Lowe *et al.*, 2018) [Figure 4.2], which are hydrologically distinct to compare afforestation influence across Great Britain. Water flux and store changes (evaporation, soil moisture and runoff) are calculated seasonally and the whole period for each region. The Theil-Sen slope estimator (Sen, 1968; Theil, 1992) is employed to obtain the percentage change in the hydrological variable relative to the percentage point increase in woodland for each region. For example, a catchment where its woodland area increased from 10% to 17% of its overall area would represent a 7% percentage point increase. This allows the sensitivity and relative hydrological response to afforestation to be quantified regarding the spatial scales of afforestation and catchments considered. Theil-Sen, a form of nonparametric regression, is more robust than ordinary least squares regression as it is less sensitive to outliers (Helsel *et al.*, 2020), and it is frequently used in other studies (Gudmundsson *et al.*, 2019; Griffin *et al.*, 2022). The Theil-Sen slope estimators quantify both the direction and size of the response in water stores, fluxes and metrics to afforestation. Spearman's rank correlation coefficient (ρ) is used to identify the strength of the association between afforestation and different hydrological fluxes across regions, where each data point represents an afforestation scenario of a region. The values of ρ reveals the extent to which afforestation, or factors other than afforestation (e.g. regional effects such as soil properties) influences the hydrology. For example, a weak Spearman's rank correlation (e.g., between 0.4 and -0.4) indicates that afforestation is not strongly associated with hydrological change, implying that regional effects are more important than the level of woodland planted.

4.3.4. Proportional Influence of Afforestation Compared to Climate

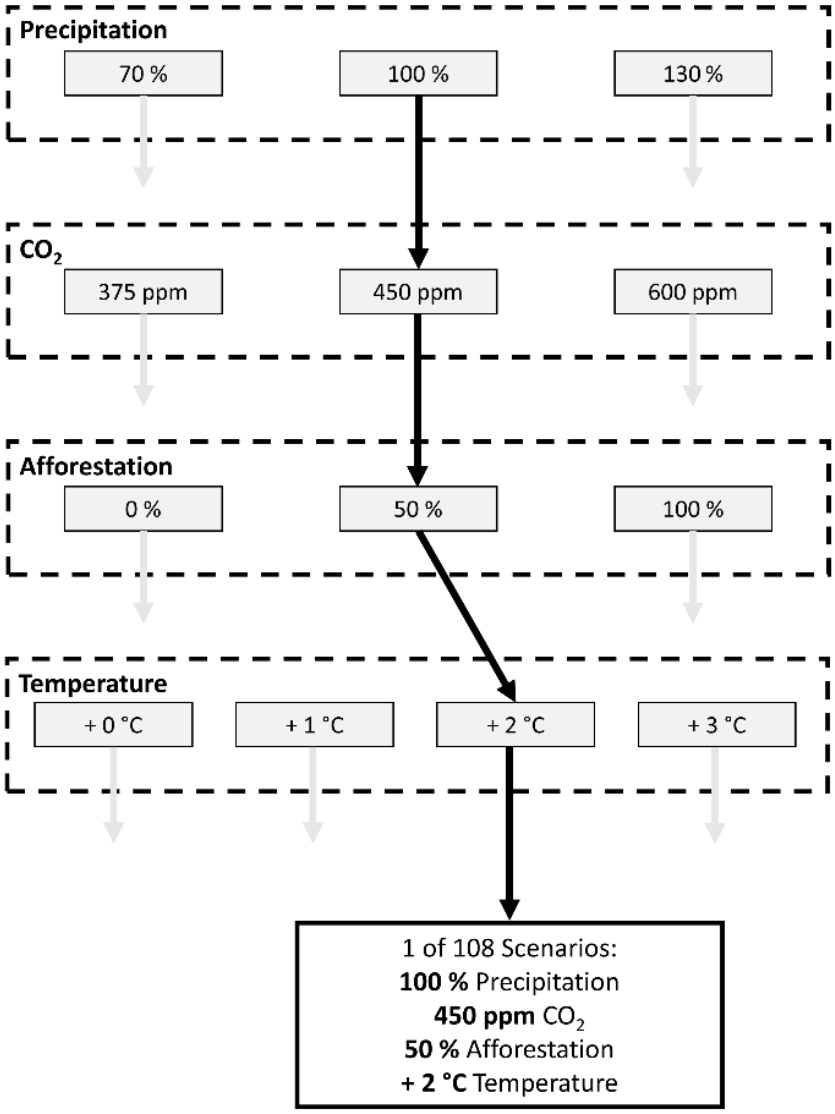

Figure 4.3: Flowchart illustrating the potential scenarios generated with differences in precipitation, CO_2, afforestation, and temperature.

An indicated pathway of one of the 108 scenarios is shown with the thick black arrows. Not all the scenarios seen here are possible or likely. A scenario of 0% afforestation, 100 % precipitation, 375 ppm and + 0 °C temperature would take us to a situation like the start of the 21st Century. A scenario of 0 % afforestation, 130 % precipitation, 600 ppm and + 3 °C temperature would lead us to a situation of SSP5 ('business as usual' or extreme emissions scenario).

JULES' hydrological sensitivity to potential future atmospheric and afforestation changes is determined by undertaking a factorial sensitivity analysis. This allows the terrestrial hydrological response to afforestation, within the model domain, to be verified relative to

atmospheric drivers. Three variables are independently altered in the base meteorological driving data (CHESS-met) for the period of 2000-2015: precipitation, temperature, and carbon dioxide. The model is spun-up for ten years (using 2000-2001) with the perturbed meteorological parameters. Maximal projected changes in precipitation and temperature, as stated in the UKCP18 scenarios, are the baseline for changing the meteorological data (Lowe *et al.*, 2018). In this way, atmospheric variables are altered within a range deemed physically plausible by a validated climate model to observe maximal sensitivity within a credible realm. From the original CHESS-met data, precipitation (in mm day^{-1}) is altered by 70 %, 100 % and 130 %; temperature is raised by 1 °C, 2 °C and 3 °C; atmospheric carbon dioxide is enhanced from 375 ppm to 450 ppm and 600 ppm. For temperature and precipitation, these are the approximate maximal changes in the UKCP18 scenarios up to 2050 under the RCP 8.5 scenario for the 95^{th} percentile of the UKCP18 probabilistic projections (1981-2000 compared to 2041-2060). Current carbon dioxide levels are approximately 415 ppm, up from 375 ppm at the start of the 21^{st} Century (NOAA, 2022). Both Gedney et al. (2006) and Blyth et al. (2019) have explored the atmospheric carbon dioxide impacts on hydrology using JULES (or its predecessor) before, however this approach goes further to see how it relates to potential future climate and LULC. An ensemble of 108 different scenarios per region is generated [Figure 4.3], although this produces the full set of potential scenarios including unlikely ones. For example, an increase in carbon dioxide emissions with a decrease in both temperature and precipitation. Including the whole range not only accounts for the response to extremes in certain seasons, but also provides enough data to decompose the contribution of each driver to hydrological change. This form of factorial sensitivity analysis was also undertaken due to the nonlinearity of hydrological process nonlinearity.

4.3.5. Hydrological Response to Potential Future Climate

The CHESS-SCAPE dataset is used to study future climate impacts (Robinson *et al.*, 2022). CHESS-SCAPE is a 1 km resolution dataset downscaled from the 12 km UKCP18 climate projections (Met Office, 2018) used previously to investigate the influence of climate change on future UK hydrology (Kay, 2021; Griffin *et al.*, 2022). The 12 km simulations were generated using a perturbed parameter ensemble of the Met Office Hadley Centre Global Climate Model (HadGEM3-GA705) under the RCP 8.5 scenario (J. Murphy *et al.*, 2019) which is nested and forced by the wider 60 km global simulations. The CHESS-SCAPE dataset is

created by selecting four model ensembles spanning the range of the original 12 model perturbed parameter ensemble of UKCP18, and then downscaled according to the CHESS-met methodology using local topography (Robinson *et al.*, 2022). The RCP 8.5 uncorrected meteorological dataset for the period 2020-2050 forces JULES with the land cover scenarios across the 20 regions to enable identification of tree planting effect on modulating climatic extremes produced by the worst-possible case of CO_2 concentration in the atmosphere. RCP 8.5 is increasingly recognised as an unlikely and extreme scenario (Hausfather and Peters, 2020), however it is useful for detecting the climate signal from the influence of afforestation and the only scenario available in UKCP18. Vegetation is fixed with no dynamic competition between the different vegetation types in our model setup of JULES and so vegetation does not need to be recalibrated to this new climate regime. The model is spun-up for the period 2010 to 2020 so that the hydrological system is in equilibrium.

4.4. Results

4.4.1. Changes in Regional Hydrology with Afforestation

Broadleaf afforestation across Great Britain clearly changes modelled evaporative processes [Figure 4.4] [Table 4.1]. Canopy and soil evaporation increase on average for the entire year which decreases canopy and soil water stores; however, the direction of change varies seasonally [Figure 4.4]. Averaged over the entire study period, overall canopy evaporation rises by 0.40 % (0.40 mm yr^{-1}) per percentage point of afforestation (PPPoA) with a moderate influence of location ($\rho = 0.59$) and is greater in winter and less in summer months for almost all regions [Figure 4.4]. To reiterate, weaker Spearman rank correlation coefficients indicate factors other than afforestation extent are causing the variation in the hydrological response to afforestation. Canopy storage decreases by 0.73 % (0.001 mm) PPPoA and is minimally affected by afforestation location ($\rho = -0.94$). Simulated soil evaporation, including both evaporation from the soil surface and plant transpiration, increases with afforestation by 0.26 % (0.54 mm yr^{-1}) PPPoA and is partially dependent on geographic region ($\rho = 0.53$). Soil evaporation is projected to increase substantially during winter and decrease in summer, particularly in Scottish regions. By contrast, modelled transpiration decreases with afforestation consistently throughout the period (-0.59 % PPPoA) regardless of location ($\rho = -0.97$). Stomatal conductance decreases in summer and increases in winter and whilst it is

sensitive to location no systematic pattern could be discerned ($\rho = -0.021$, $p < 0.01$). Notable variation is seen in the representation of stomatal conductance amongst LSMs and so this response could be particular to the configuration used here.

Table 4.1: Changes in the average water fluxes and stores with afforestation across Great Britain for each percentage point increase in broadleaf woodland for both the present climate and potential future climate.

ρ (Spearman) correlations indicate the strength of association between increased afforestation and changes in the flux and stores where each data point represents an afforestation scenario in a region. High absolute values (e.g., above 0.7) indicate planting location has a minimal influence on altering the response to afforestation. Values in bold are greater than an absolute value of 0.7.

		Present (For each percentage point increase in woodland)			**Future (For each percentage point increase in woodland)**		
		Percentage Change (%)	Absolute Change (mm yr^{-1} and mm)	ρ Correlation	Percentage Change (%)	Absolute Change (mm yr^{-1} and mm)	ρ Correlation
Flux (mm yr^{-1})	Canopy Evaporation	0.40	0.40	0.59	0.33	0.47	0.66
	Soil Evaporation	0.26	0.54	0.53	0.11	0.29	0.51
	Runoff	-0.30	-1.9	**-0.85**	-0.27	-1.84	**-0.74**
	Surface Runoff	-0.20	-0.27	**-0.73**	-0.16	-0.35	-0.53
	Subsurface Runoff	-0.34	-1.0	**-0.85**	-0.26	-0.95	**-0.78**
	Throughfall	-0.34	-1.0	**-0.87**	-0.33	-1.23	**-0.83**
Store (mm)	Total Soil Moisture	-0.05	-0.4	**-0.83**	-0.047	-0.41	**-0.77**
	Canopy Storage	-0.73	-0.001	**-0.94**	-0.64	-0.001	**-0.94**

Table 4.2: Changes in flow metrics with afforestation across Great Britain for each percentage point increase in broadleaf woodland for both the present climate and potential future climate.

ρ (Spearman) correlations indicate the strength of association between increased afforestation and changes in the afforestation extent.

Flow Metric	Present (For each percentage point increase in woodland)		Future (For each percentage point increase in woodland)	
	Percentage Change (%)	ρ Correlation	Percentage Change (%)	ρ Correlation
Very High (1%)	-0.054	-0.2	-0.11	-0.44
High (5%)	-0.11	-0.54	-0.11	-0.66
High (10%)	-0.11	-0.6	-0.09	-0.63
Median (50%)	-0.18	-0.65	-0.14	-0.68
Low (90%)	-0.24	-0.66	-0.25	-0.64
Lower (95%)	-0.32	-0.71	-0.34	-0.75
Very Low (99%)	-0.57	-0.81	-0.72	-0.84
Duration Curve	0.09	-0.2	0.053	-0.37

Afforestation across Great Britain moderately reduces average river flow by 0.17 % PPPoA over the year with only a slight locational variation (ρ = -0.9). This decline in river flow is caused by decreasing surface and subsurface runoff (-0.20 %; -0.27 mm yr^{-1} and -0.34 %; -1.03 PPPoA respectively) [Table 4.1]. Despite the consistent reduction in runoff components throughout the year, the response varies minimally by region (surface: ρ = -0.73, subsurface: ρ = -0.85) [Table 4.1]. Canopy throughfall, the simulated source of water for runoff, decreases with afforestation (-0.34 %; -1.00 mm yr^{-1} PPPoA) regardless of planting location (ρ = -0.87) [Table 4.1], and its reduction is consistent throughout the year. Whilst average total soil moisture decreases with afforestation minimally (0.046 %, -0.40 mm PPPoA) and without influence of planting location (ρ = -0.83) [Table 4.1], the moisture available to vegetation from the uppermost soil layer is noticeably influenced by planting location (ρ = -0.59).

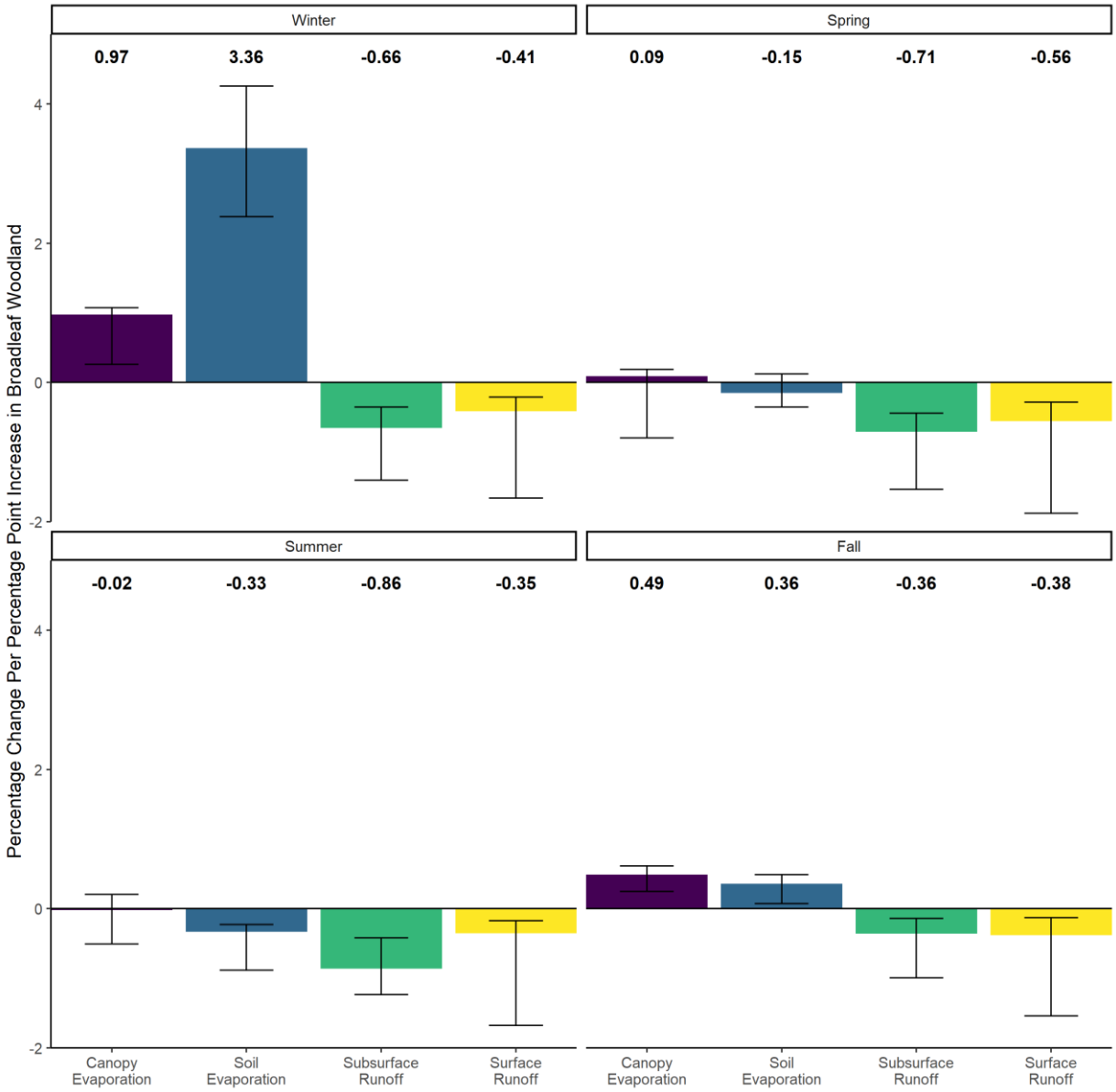

Figure 4.4: Changes in the evaporative and runoff fluxes per percentage point of afforestation (e.g., 10% to 11% of a region afforested) by season with all other variables held constant.

Error bars represent one standard deviation from the median value for the changes in hydrometeorological variables for the UKCP18 hydro-regions investigated with afforestation. This uses both afforestation scenarios and the appropriate change in afforestation is calculated per region for each scenario as well as the corresponding percentage change in the water fluxes compared to the original land cover, for each season, relative to the percentage point increase of afforestation.

At lower streamflow quantiles the influence of afforestation location diminishes [Table 4.2]. At the top 1 % of flows there is no strong response to afforestation (-0.054 % PPPoA; ρ = -0.2, p = 0.012), whereas the top 5 % of flows reduce by 0.11 % PPPoA (ρ = -0.54, p < 0.01) with an even stronger median flow drop of -0.18 % PPPoA (ρ = -0.65, p < 0.01) [Table 4.2]. At the lowest flow exceedances there are clearer patterns between streamflow reductions and afforestation with a decrease of -0.24 % PPPoA (ρ = -0.66, p < 0.01) and -0.57 % PPPoA (ρ = -0.81, p < 0.1) for the 90th and 99th flow percentiles accordingly [Table 4.2]. We find an unclear picture of flow variability changes with afforestation extent, with a decrease 0.09 % PPPoA in the flow duration curve that appears more strongly related to differences in regional factors than afforestation itself (ρ = -0.2, p = 0.012).

4.4.2. Hydrological Sensitivity to Climate and Land Cover Changes

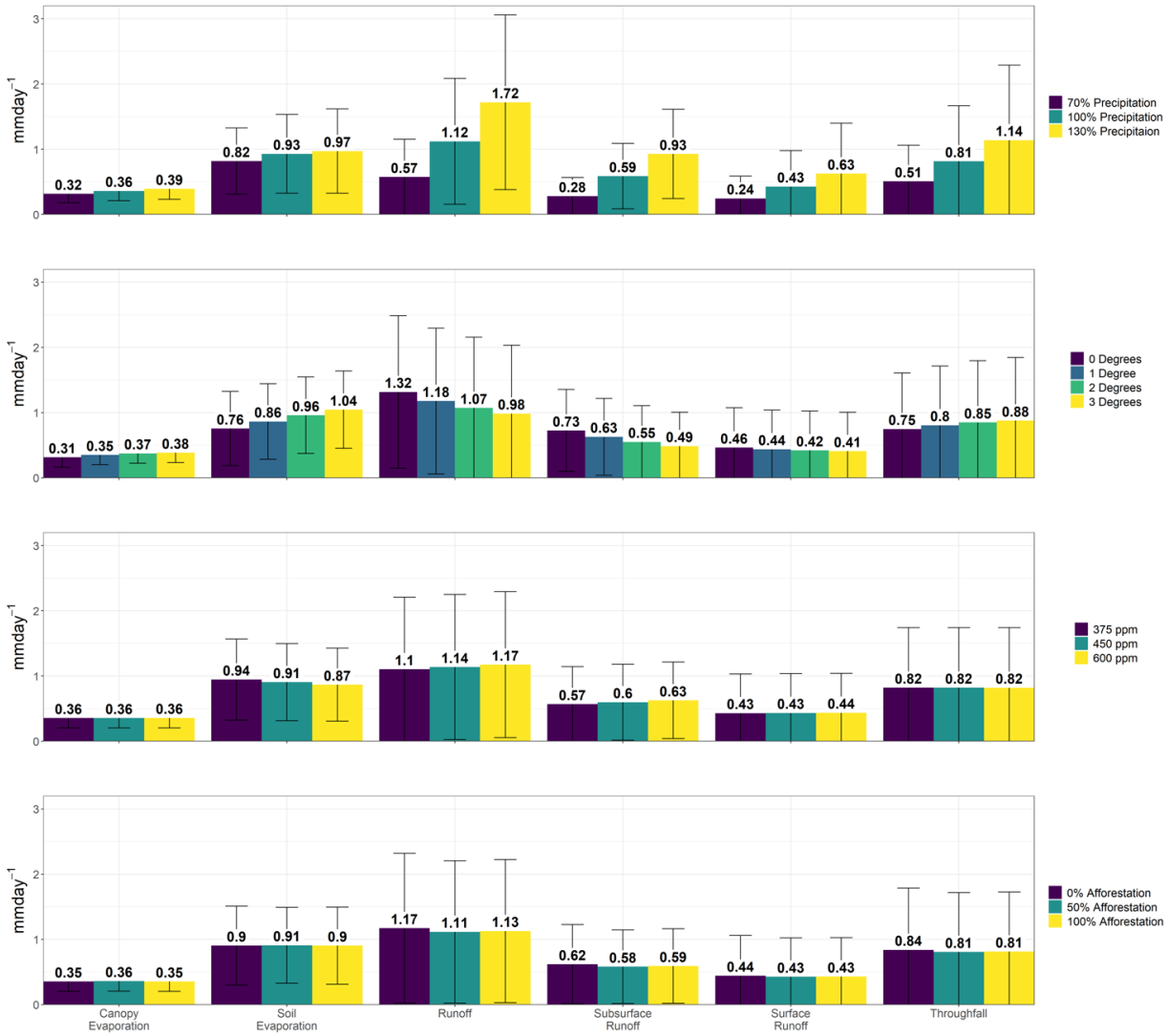

Figure 4.5: Mean hydrological fluxes across all UKCP18 regions for each of the four variables altered relative to present climate and landcover: precipitation, temperature, CO_2 and landcover.

Error bars indicate one standard deviation. Supplementary Figures S4.5 and S4.6 show how these change in summer and winter respectively.

As the climate changes, land cover is also expected to change. Although it is expected that hydrological systems will respond significantly to climate change it is unknown what the relative response to concurrent land cover changes will be. Hydrological processes in JULES show strong sensitivity to climate relative to LULC across the range of scenarios tested [Figure 4.5]. ANOVA reveals significant differences in hydrological variables in all regions with proposed changes in precipitation and temperature ($p < 0.01$). When compared to projected changes in precipitation, temperature and CO_2, the effects of LULC are almost undetectable. Only in a few isolated regions in winter are canopy storage, stomatal conductance and soil moisture significantly altered by LULC ($p < 0.01$) [Supplementary Material: Figures S3 & S4]. Interestingly, rising carbon dioxide only notably reduces transpiration and stomatal conductance in some regions (ANOVA, $p < 0.01$) [Supplementary Material: Figure S3]. Although not substantial, higher CO_2 suppresses soil evaporation, which increases soil moisture and therefore runoff.

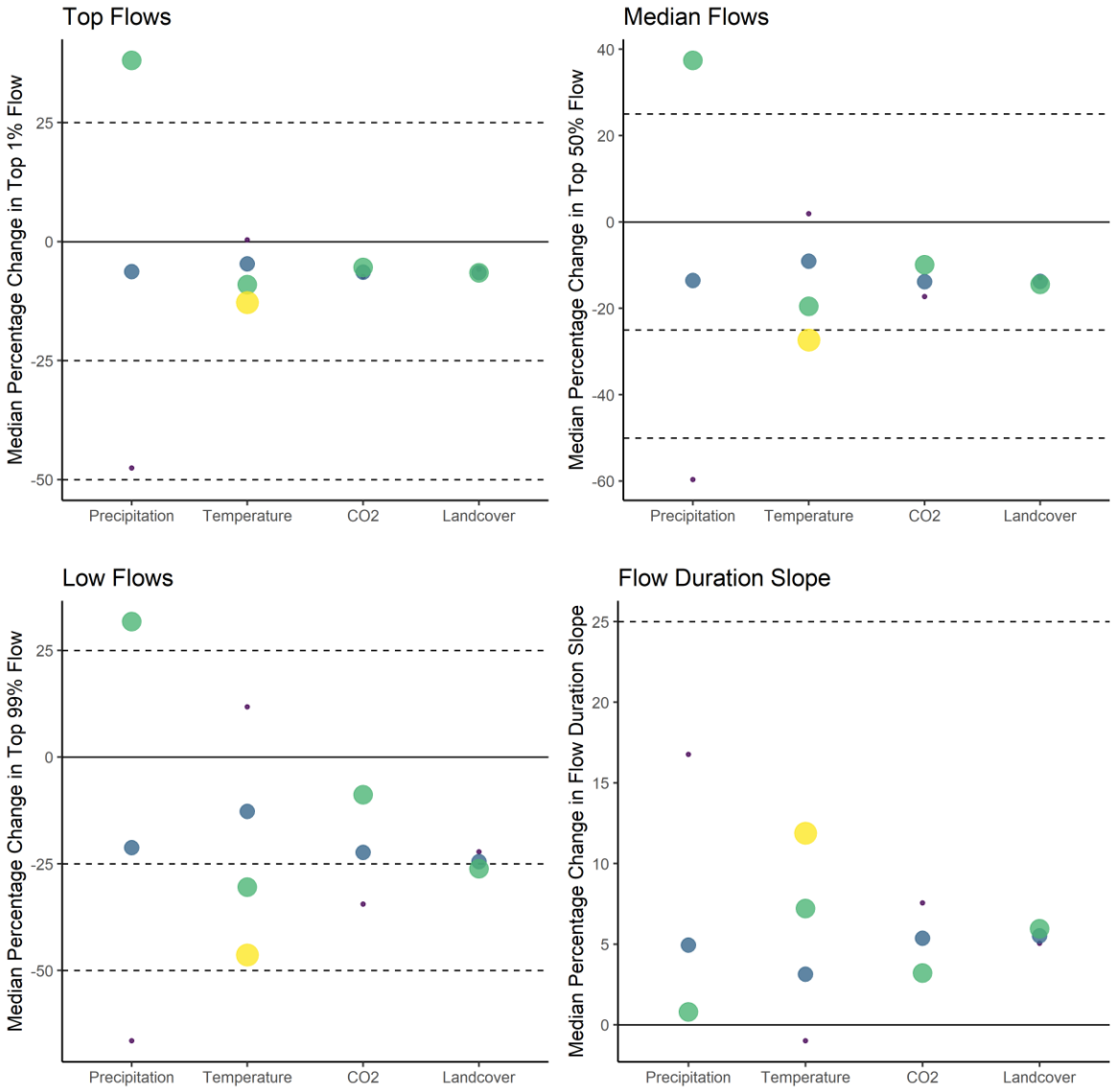

Figure 4.6: Median percentage change in the indicated four metrics for catchments based on precipitation, temperature, CO2, and afforestation changes.

Increasing dot size and lighter colour indicate larger changes in the variables explored (precipitation: 70%, 100%, 130%; temperature: 0 °C, +1 °C, +2 °C, +3 °C; CO2: 375 ppm, 425 ppm, 600 ppm; afforestation: 0%, 50%, 100%). Colours are used to further differentiate variable quantity and are not relative to the size of the variable. The solid black horizontal line indicates a 0 % change for all variables whereas the dashed lines indicate defined intervals of change.

Enhanced precipitation across Great Britain greatly increases hydrological fluxes and stores compared to all other factors altered [Figure 4.5]. When averaged across the whole period, precipitation does not have a significant impact on soil evaporation and transpiration, except

in northwest Scotland. However, in summer, enhanced precipitation significantly increases soil evaporation across many regions (1.4 to 1.7 mm day^{-1} from 70 % to 130 % precipitation) [Supplementary Material: Figure S4.5]. Both canopy and soil moisture stores increase with precipitation, enhancing runoff (0.7 to 1.7 mm day^{-1} from 70 % to 130 % precipitation) [Figure 4.5].

Rising temperatures appreciably alter many of JULES' hydrological parameterisations. Soil and canopy evaporative processes rise in winter with higher temperatures (both by 0.2 to 0.4 mm day^{-1} with 3°C extra). In summer, soil evaporation continues to increase (1.4 to 1.7 mm day^{-1} with 3°C extra) but canopy evaporation stays approximately the same. This slightly enlarges the canopy store, although not significantly for many regions. In winter, throughfall increases (0.8 to 1.2 mm day^{-1} with 3°C extra) likely due to more intense rainfall which is parameterised by temperature. The higher throughfall further reduces canopy storage. Stomatal conductance decreases throughout the entire period with rising temperatures but is not significant for all regions and transpiration clearly increases with temperature in winter. Soil moisture reduces in the summer with rising temperature which minimises subsurface runoff (0.4 to 0.2 mm day^{-1} with 3°C extra). However, there are no statistically significant changes in river flow and surface runoff in winter and summer for almost all regions as temperatures rise.

Precipitation is a first order control on flood and drought formation in JULES, as expected. Precipitation significantly (Kruskal-Wallis (KW) test, $p < 0.001$) influences the top 1 % of flows: reducing precipitation by 30% decreases them by 48 % whilst increasing precipitation by 30% enlarges them by 38 % [Figure 4.6]. Rising temperatures significantly (KW test, $p < 0.001$) reduce high flows (+ 3°C reduces high flows by 13 %) [Figure 4.6]. Enhanced CO_2 insignificantly amplifies the top flows whereas afforestation insignificantly reduces them [Figure 4.6]. Findings are similar at the lowest (top 99%) flows, but the modelled flow response range is a greater with climate and land cover perturbations. Increasing precipitation significantly increases low flows (KW test, $p < 0.001$) by 32 % for a 30 % precipitation increase (-67 % for a 30 % precipitation decrease). Rising temperatures substantially reduce low flows by 46 % for an additional 3°C. Greater CO_2 increases low streamflow across all 108 scenarios (KW test, $p < 0.001$) from -34 % for 375 ppm of CO_2 to -8.8 % for 600 ppm. Across all the proposed environmental disturbances, LULC has the smallest impact on streamflow. Afforestation only weakly decreases low flows from -22 % (0 % afforestation) to -26 % (100 % afforestation) insignificantly across all scenarios in comparison to all scenarios (KW test, p

> 0.1). Flow regimes became less variable with increasing precipitation ($p < 0.001$, from 18 % to 0.60 %) and CO_2 ($p < 0.001$, reduction of 7.6 % to 3.2 %) [Figure 4.6]. In contrast, rising temperature increases flow variability ($p < 0.001$) from -1.0 % to 12 % and afforestation increases flow variability by only a small amount which is not statistically significant ($p > 0.1$).

4.4.3. Potential Influence of Afforestation in the Future

In the future, afforestation has a similar influence on hydrology as in the present climate [Table 4.1]. Therefore, projected climate changes are insufficient to substantially alter simulated vegetation's interaction with water fluxes. Canopy evaporation and storage are similarly influenced by land cover change location in the future ($\rho = 0.66$; $\rho = -0.94$ respectively) and increase by 0.33 % (0.47 mm yr^{-1}) and decrease by 0.64 % (0.001 mm yr^{-1}) PPPoA respectively [Table 4.1]. However, soil evaporation increases at half the present rate at 0.11 % (0.29 mm yr^{-1}) PPPoA and is strongly influenced by afforestation location ($\rho = 0.51$). Transpiration robustly decreases at a rate of -0.78% PPPoA regardless of planting location ($\rho = -0.98$). Regional influence on stomatal conductance is increased compared to present ($\rho = 0.40$) and rises more rapidly at 0.14 % PPPoA.

Average simulated river flow, compared to present, drops at a slightly lower rate of -0.12 % PPPoA ($\rho = -0.82$) [Table 4.1]. Runoff decreases with afforestation at a comparable rate to present (-0.27 %; 1.84 mm yr^{-1} PPPoA) however, location has a greater effect ($\rho = -0.74$) and surface runoff (-0.16 %; -0.35 mm yr^{-1}) is greatly influenced by location ($\rho = -0.53$) [Table 4.1]. Subsurface runoff also becomes slightly more influenced by location ($\rho = -0.78$) with a decrease of 0.26 % (-0.95 mm yr^{-1}) PPPoA. Both throughfall and soil moisture respond to afforestation in a similar manner to as at present regarding their trends and connection to planting location (-0.33 %, -1.23 mm yr^{-1} PPPoA, $\rho = -0.83$; -0.047 %, -0.41 mm PPPoA, $\rho = -0.77$ respectively) [Table 4.1].

In the future, planting location has a reduced influence on streamflow when compared to increases with afforestation compared to present [Table 4.2]. Median streamflow reduces by -0.14 % PPPoA ($\rho = -0.68$), low flows decrease by -0.25 % PPPoA ($\rho = -0.64$) at the 90th percentile of flow and -0.72 % PPPoA ($\rho = -0.84$) at the 99th percentile of flow [Table 4.2]. The effect of afforestation is more complicated at the highest flows with the top 1 % and 5 %

of flows reducing by 0.11 % PPPoA (ρ = -0.44 and ρ = -0.66). Flow variability does not substantially change in the future, with insignificant change (0.053 % PPPoA) and a strong regional influence (ρ = -0.37).

4.5. Discussion

4.5.1. Afforestation Influence Across Great Britain

Regional hydrological response to afforestation does not significantly vary across Great Britain. Proposed countrywide afforestation is projected with JULES to have a detectable, but not substantial, impact on hydrology. However, slight nuances occur depending on afforestation location and the time of year (discussed later). LULC has a diminishing impact on streamflow further from the intervention area, however the scale of afforestation considered here (large compared to realistic afforestation rates) means modelled large-scale hydrological processes are detectable at multiple spatial scales (Blöschl *et al.*, 2007; Pattison and Lane, 2012; Dadson *et al.*, 2017). The realism of the afforestation scenarios herein illustrates how large-scale hydrological changes demonstrated by improbable widespread afforestation scenarios considered in the literature, have minor relevance to the debate of probable afforestation rate impacts (Meier *et al.*, 2021; Denissen *et al.*, 2022). Despite a broader modelling domain and greater hydrological diversity than in Buechel *et al.* (2022), we find little difference in catchment water output sensitivity to afforestation location, suggesting potential reductions in water yield can be directly estimated from the areal extent of woodland planted rather than its location. However, this finding may simply demonstrate the relative insensitivity of terrestrial processes to landcover changes modifying terrestrial processes within an LSM. No modelled hydrological change is exactly equivalent to afforestation, for example a one percent woodland increase does not equal a one percent change in canopy evaporation. This is also seen in observational studies where a 1 % increase in upstream afforestation area does not detectably change streamflow (Anderson *et al.*, 2022).

The lack of regional variability in catchment hydrological response to afforestation could be due to terrestrial hydrological similarity across the UK (Wagener *et al.*, 2021). Alternatively, the large epistemic uncertainty within JULES means that highly sensitive hydrological parameters are not included that would lead to diverging regional afforestation responses, such

as variable vertical soil column properties (Beven and Cloke, 2012; Beven, 2018). LSMs scale physical processes from very small areas and so the lack of sensitivity to widespread afforestation, and detected nuances related to location, could also be due to inaccurate representations of model processes, such as the use of pedotransfer functions (Beven, 1989; Clark *et al.*, 2009). Another consideration is the uncertainty in soil products where there is large disagreement in the amount of organic material which significantly influences soil hydraulics (Feeney *et al.*, 2022). As an offline model (i.e., the land surface is not coupled to the atmosphere) factors that enhance regional importance with land parameterisations, such as orographic rainfall, are not represented. Importantly for this work, overall soil moisture dryness may be overestimated as the rain seeding effect of afforestation is not included (Teuling *et al.*, 2017; Xu *et al.*, 2022). Modelling widespread afforestation with JULES has revealed further questions about the adequacy of LSM parameterisations.

The overall reduction in simulated runoff (and streamflow) by afforestation is a consequence of soil and canopy evaporation increases [Figure 4.4]. Although evaporative processes are more influenced by regional properties [Table 4.1], JULES' land surface parameterisations screen atmospheric differences leading to diminished locational impacts on runoff compared to LULC. However, JULES systematically overestimates evaporation and so these results must be treated cautiously (Van den Hoof *et al.*, 2013; Blyth *et al.*, 2019). Rising evaporation rates are likely due to albedo reduction with afforestation, enhancing surface temperatures, and larger canopy stores with the higher LAI, and turbulence, compared to grasslands. Increases in canopy storage, evaporation and interception reduce throughfall reaching the soil surface, which minimises regional climate differences relative to afforestation [Table 4.1]. Reduced throughfall means less soil moisture, runoff, and streamflow. The declining soil moisture with afforestation diminishes subsurface runoff and results in more water-stressed vegetation. The lower stomatal conductance, and thus transpiration, particularly in summer months, is evidence of the diminished soil moisture store. In JULES, broadleaf woodland has deeper roots than grasslands and shrublands, which leads to water being extracted lower in the soil column to maintain growth (Best *et al.*, 2011; Harper *et al.*, 2021). In reality, tree root depths would be much deeper and vary according to the soil type (Vereecken *et al.*, 2022) and implementing woodland in this manner could lead to more accurate evaporation rates (Roebroek *et al.*, 2020; Harper *et al.*, 2021). In summer, moisture in the uppermost soil layer slightly increases which could be a function of lower roots, compared to grasslands, and reduced stomatal conductance (Buechel *et al.*, 2022). The slight association of afforestation with topsoil moisture increases

and location could be the result of different soil types (e.g., organic) which facilitate differences in hydraulic conductivity related to afforestation. The runoff model in this setup of JULES enhances runoff during high precipitation events with increased topsoil saturation, however, the proportionally small rise in topsoil moisture with simulated afforestation would make it potentially unobservable within natural uncertainty. Several limitations and assumptions should be considered when using LSMs such as JULES. The model domain only includes known hydrological processes. Unincluded, or undiscovered, processes may have important consequences on afforestation's hydrological impact, unknown to the modeller (Beven *et al.*, 2011). Furthermore, processes within the model may inaccurately be implemented numerically or physically (Hrachowitz and Clark, 2017). Results therefore could potentially be affected by inadequate process representation and implementation.

Some regions in Great Britain exhibit slightly stronger effects of afforestation. In southeast England and Anglia, there are significantly larger hydrological variations, likely due to underlying soil properties and climate regime, similar to Buechel *et al.* (2022) with more sensitive catchments in drier regions. Afforestation therefore could strain water resources in regions of low water yield (Ellison *et al.*, 2012). However, the model representation of hydrological processes in groundwater-based catchments (found in these regions) is known to be inadequate (Le Vine *et al.*, 2016). Therefore in reality, afforestation may have a muted influence on streamflow in these regions with roots accessing the deeper groundwater (Roberts and Rosier, 2005). Evaporation rates are partially impacted by afforestation location, particularly in Scottish regions and parts of the west coast, which could enable flood magnitude reduction with spatially targeted broadleaf afforestation. The higher levels of wind turbulence and speed likely enable high evaporation rates to be maintained with additional woodland. Page et al. (2020) suggested canopy evaporation could reduce flood peaks in upland regions; alignment between model and observations suggests further analysis to quantify evaporative processes over countrywide scales to mitigate flood risk. Regional differences in modelled stomatal conductance are due to climatic conditions, such as temperature and humidity as well as soil moisture and resulting vegetation water stress (Betts *et al.*, 2007; Best *et al.*, 2011). The similar connection of surface runoff with location suggests soil hydrology is an important control on stomatal conductance and runoff [Table 4.1]. JULES' modelling paradigm for simulating stomatal conductance is not applied in all other models, and therefore other studies may find different projected stomatal conductance and thus resulting evaporation. However,

JULES poses interesting questions for further exploration on the impact of widespread afforestation on regional hydrology and whether simulated changes are observable.

Afforestation across Great Britain influences the entire simulated streamflow spectrum (high to low flows) [Table 4.2]. It is often observed significantly reducing the low to median flows, while high flow changes are frequently undetectable or inconsistent (Farley *et al.*, 2005; Do *et al.*, 2017; Anderson *et al.*, 2022). Afforestation's impact on streamflow is complex within JULES. Afforestation decreases the lowest flows and suggests locational factors have a minimal impact, similar to other research (Birkinshaw *et al.*, 2014; Bathurst *et al.*, 2020; Buechel *et al.*, 2022). If our projections are correct, water managers need to prepare for worse hydrological droughts with proposed afforestation in conjunction with those already predicted in the future (Lowe *et al.*, 2018; Kay *et al.*, 2021). The mechanisms generating low flow response to afforestation are therefore more likely to be driven by runoff and soil moisture parameterisations compared to evaporative processes. This is because both runoff and soil moisture are more influenced by afforestation extent than location [Table 4.1] which is then replicated in the similar Spearman's rank correlation coefficients for the lower streamflow percentiles [Table 4.2]. To re-emphasise, larger Spearman's rank correlation coefficients indicate that afforestation extent, rather than locational influences, impact the hydrological response. This highlights that the hydrological model structure within an LSM is likely to govern the model's ability to produce accurate drought predictions compared to other system parameterisations (Van Kempen *et al.*, 2021). In comparison, at the simulated very highest flows (top 1% of flows), afforestation both decreases and increases streamflow. This result is significant as more simple, and conceptually-based hydrological modelling often suggest afforestation reduces the highest flows (Stratford *et al.*, 2017). The regional differences in the hydrological response of the highest flows to afforestation suggests evaporation rates are controlling the response, which is seen with the lower Spearman's rank correlation coefficients with afforestation extent and high flows, and evaporative processes. However, floods are often generated by extreme precipitation which generate 'numerical daemons' where the numerical implementation of hydrological processes generate implausibly high responses (Clark, Zolfaghari, *et al.*, 2021; La Follette *et al.*, 2021). Therefore, floods could be more sensitive to terrestrial model parameters which could also lead to strong regional influences on afforestation impact. Increases in small and large floods suggest similar generation mechanisms. Top flows usually decrease in catchments that are predominantly grass and pasture, where the chosen woodland planting criteria allow for larger areas to be afforested.

Greater afforestation reduces simulated soil moisture, reduces throughfall and increases interception and canopy evaporation. When over five percentage points of a catchment's area is afforested, total soil and canopy evaporation rise, enhancing the catchment capacity to store and remove precipitation. During high magnitude precipitation events, initial woodland planting reduces the overall effectiveness of the catchment to reduce flood peaks. Preliminary afforestation reduces the overall simulated maximal catchment water storage capacity in winter, due to decreased LAI, thus reducing water usage and evaporative fluxes.

These results have three major outcomes for future work. Firstly, models that encapsulate more known earth surface dynamic processes (e.g., dynamic vegetation coupled with soil hydraulics and river runoff routines) produces a more nuanced understanding of how afforestation could impact hydrology (Cooper *et al.*, 2021). Although not perfect, particularly at hydrological extremes (Cuntz *et al.*, 2016; Brunner *et al.*, 2021), LSMs allow us to propose new hypotheses related to the influence of afforestation (and LULC) on hydrological processes as a form of multiple working hypotheses (Clark *et al.*, 2011). Secondly, analysis of median hydrological fluxes across hydro regions reveals reductions in overall runoff and streamflow over an entire year which would lead to the incorrect assertion that afforestation could effectively act as to mitigate peak flows over extensive areas as higher flows were less influenced. Targeted afforestation locations within large catchments (> 150 km^2) may be ineffective for NFM downstream unless extensive or coupled with other flood mitigation measures. Finally, model parameterisations have a significant bearing on our derived conclusions, with hydrological model structure being more significant than other model parameters for determining afforestation impacts on streamflow. Evaporative processes strongly influence simulated floods whereas runoff model implementations are more important for calculating droughts with LULC change. Future work should therefore continue to investigate the role of hydrological model structure within LSMs to assess its impact on quantifying the hydrological response to LULC change (Clark, Zolfaghari, *et al.*, 2021).

4.5.2. Sensitivity to Climate and Afforestation Changes

Compared to the most extreme proposed atmospheric changes, the impact of afforestation on Great Britain's hydrology is relatively limited, with precipitation being the greatest driver of hydrological change compared to other variables studied [Figure 4.5]. All water fluxes and

stores rise in JULES with enhanced precipitation; in a projection of greatly increased rainfall, flooding will likely increase, regardless of plausible land cover and other climate changes. For example, with heavier rainfall, hotter temperatures and more CO_2 in winter (such as under the high-emissions Shared Socioeconomic Pathway 5 (SSP5) – 'Taking the Highway' (Riahi *et al.*, 2017)) countrywide afforestation would not reduce flood magnitude. Conversely, in summer, an overall decrease in precipitation (with increased temperatures and CO_2) could greatly reduce runoff, which is only slightly diminished further by afforestation. In the UK, more intense rainfall (convective) is predicted in the summer (Fosser *et al.*, 2020; Kay *et al.*, 2021; E. J. Kendon *et al.*, 2023) and our results indicate realistic afforestation is likely to be ineffective for flood management during these events. The use in the present study of JULES without atmospheric coupling, and no vegetation competition in this model configuration, means there is no large-scale moisture recycling or vegetation mortality that would modulate model precipitation response further (e.g. Cui *et al.*, 2022). For example, reduced rainfall could result in large-scale vegetation dieback, amplifying the effect of high precipitation with reduced interception and less infiltration. Precipitation decreases demonstrate the nonlinear parameterisations of JULES' hydrology with larger reductions at smaller streamflow percentiles [Figure 4.8] (further justifying the factorial sensitivity analysis). Increased precipitation saturates the canopy and topsoil which quickly routes excess water to rivers. There are two consequences of JULES' hydrological implementation. Firstly, uncertainty in precipitation products measurably alters conclusions derived using JULES. Any small differences in precipitation used to drive JULES will lead to larger differences in the modelled hydrological outputs. As a result, secondly, slight precipitation product differences could negate the impact of LULC using JULES (or other similar LSMs) when comparing studies that utilise different precipitation datasets. This is important as it suggests that work using LSMs to determine countrywide changes in hydrology over periods where there have been relatively small land cover changes, can justify not using evolving land cover as that would be likely to minimally reduce uncertainty (e.g. Blyth *et al.*, 2019). Further attention is therefore required to minimise uncertainty in meteorological datasets to predict floods and droughts as terrestrial processes within LSMs will have a comparatively minor influence.

Previous work has illustrated the minor influence land cover has on hydrological processes compared to other atmospheric processes, both in models and in observational studies (Oudin *et al.*, 2008; Gedney *et al.*, 2014), and our results confirm that afforestation has the smallest impact on modelled streamflow compared to climate changes [Figure 4.5]. Therefore, to detect

afforestation influence upon streamflow, one must be aware of climate changes over the same period and be able to accurately remove any climatic effect which could obscure the LULC signal (Milly *et al.*, 2008; Slater *et al.*, 2021). This may explain why observational studies have found an insignificant impact of afforestation on streamflow (e.g., Anderson *et al.*, 2022), particularly with the large number of dependent interacting processes associated with woodland hydrology. Hydrological conclusions using JULES over long time periods therefore can determine that LULC is of minor relevance when compared to climate (e.g., Blyth *et al.*, 2019). With climate change, afforestation is likely to be insufficient to reduce the largest pluvial flood risks. However, some research suggests smaller magnitude floods are becoming more frequent, and so plausible afforestation may mitigate the risk they pose (Griffin *et al.*, 2019; Wasko, Nathan, *et al.*, 2021). Our results emphasise LSMs pushing to be 'models of everywhere' are relatively insensitive to terrestrial process parameterisations in relation to climate drivers (Blair *et al.*, 2019). By applying atmospheric changes across the whole country, variations in landcover, topography and soil type are insufficient to substantially alter the hydrological response. It is possible that in JULES, overparameterization could be leading to high complexity of interacting processes muting terrestrial parameter impact, or large epistemic uncertainty might be responsible for the minimal response compared to climate (Hrachowitz and Clark, 2017; Beven and Lane, 2022). Nonetheless, the JULES community model is continually being improved, and further work should test whether terrestrial properties, including LULC, are adequately represented.

Simulations of future climate suggest raised atmospheric CO_2 could negate the influence of increasing afforestation on streamflow [Figure 4.6]. With increases in CO_2, simulated streamflow rises across the flow spectrum because of reduced vegetation water usage. Amplified CO_2 decreases vegetation growth as the CO_2 pressure gradient between the stomata and atmosphere diminishes (Gedney *et al.*, 2006; Prudhomme *et al.*, 2014; Blyth *et al.*, 2019), which reduces soil water usage, increasing soil moisture and overall runoff. JULES has exhibited strong sensitivity, be this correct or not, to CO_2 previously (Prudhomme *et al.*, 2014). If these results are accurate, afforestation in a changing climate may not be the silver bullet for mitigating flood risk and reducing atmospheric carbon policy makers envisage, particularly as vegetation becomes less effective at absorbing the additional CO_2 with increased atmospheric CO_2 (IPPC, 2019; Leung *et al.*, 2019; Cook-Patton *et al.*, 2020). A simpler hydrological model, and not an LSM, is unlikely to show the effect of CO_2 seen. Atmospheric CO_2 has a strong control on low flows, which is important to consider in the context of future droughts and

illustrates its strong influence on JULES' runoff mechanisms [Figure 4.6]. CO_2 fertilisation is not currently included within the version of JULES (vn5.6) used here, which would influence the effectiveness of vegetation to interact with water fluxes and potentially minimise the CO_2 impact (Bonan, 2008; Ritchie *et al.*, 2019; Zhang *et al.*, 2022). Therefore, afforestation may have an equivalent or larger impact on streamflow than CO_2, and we encourage further research to test these results.

Temperature is a second order control on hydrological sensitivity within JULES and is more important than afforestation and CO_2 changes [Figure 4.5]. Streamflow is significantly reduced across the whole flow regime by increasing temperatures due to increased evaporation and water usage by vegetation. Again, looking under the high-emissions SSP5 scenario, afforestation may enhance drought formation (both magnitude and duration) due to warmer temperatures. Increased flow variability with higher temperatures is also likely to make it more difficult to adequately manage water resources. In JULES, precipitation is converted to convective rainfall at a certain temperature (the same amount of rainfall occurs in a smaller fraction of the grid box) (Best *et al.*, 2011). Temperature rises therefore trigger more 'convective' rainfall events but interestingly, even with increased precipitation, top flows do not grow, even with larger throughfall. This suggests that in JULES, greater temperatures reduce antecedent soil moisture, decreasing runoff, and minimising the impact of the more intense rainfall. However, even the largest temperature increases cannot mitigate the impact of greater precipitation on increasing flood magnitude and frequency. Furthermore, this uncoupled model does not include realistic changes in rainfall intensity and magnitude which might be expected with increases in temperature and could change land surface responses to floods and droughts (Wasko *et al.*, 2019; Lee *et al.*, 2022).

4.5.3. Afforestation Impact with Climate Change

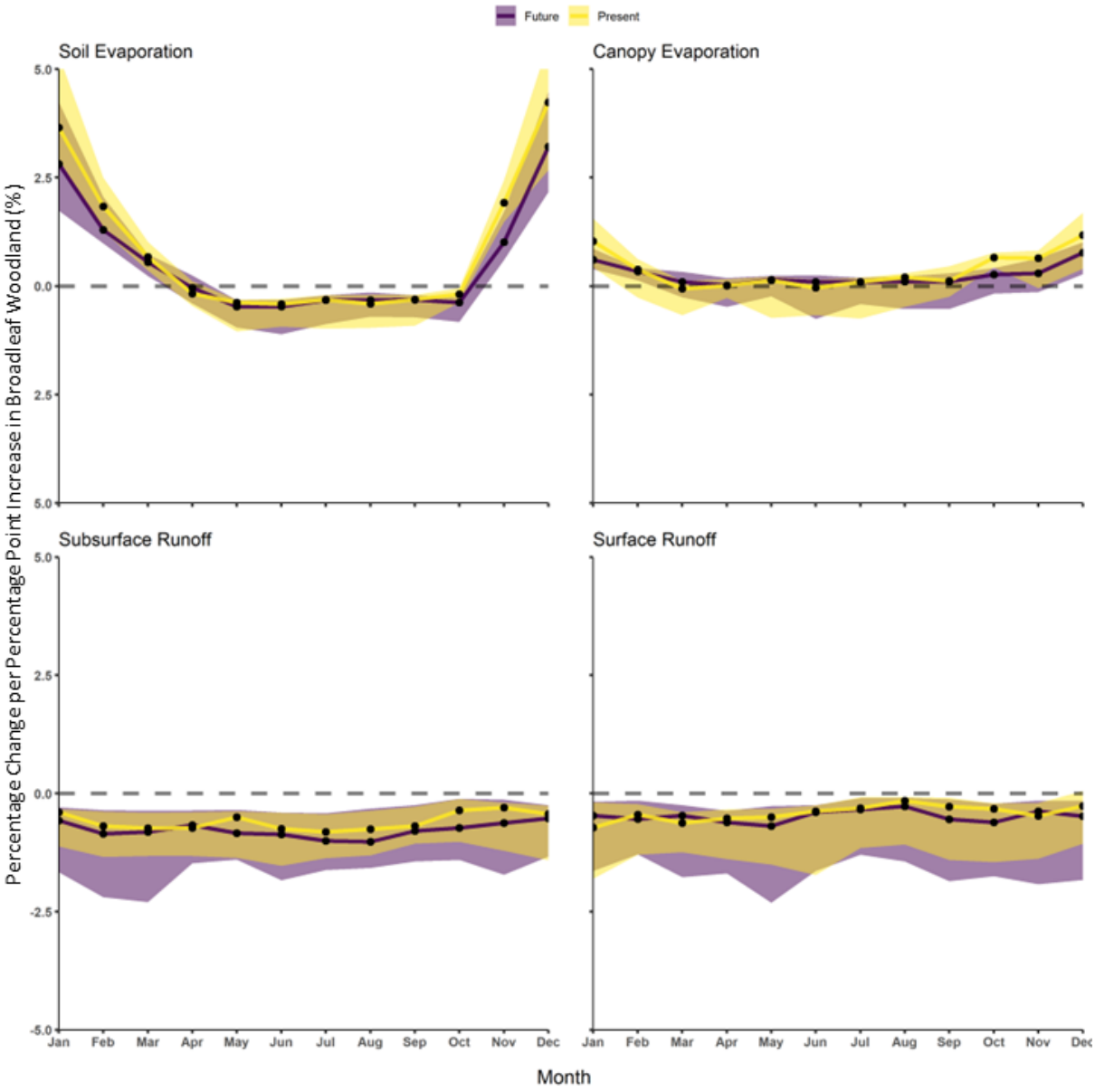

Figure 4.7: Hydrological flux changes with PPPoA between the present (yellow) of 2000-2015 and future of 2020-2050 (purple).

Use of an unpaired two-samples Wilcoxon test reveals no significant difference in the above hydrological fluxes between the future and present ($p > 0.1$). Shaded regions represent the 10th and 90th percentile of hydrological flux changes across all regions.

In an extreme potential future climate scenario (RCP 8.5 / SSP 5), we find afforestation is unlikely to alter hydrological processes differently than under our present climate [Figure 4.7]. There are no statistically significant differences (KW test, $p > 0.5$) between the hydrological impacts for the same amount of afforestation in the present climate and the future [Figure 4.7]. Although future precipitation, temperature and CO_2 could have altered the woodland

hydrological response, as seen in the previous part of the study, the average climate changes are insufficient to induce significant changes. Afforestation is therefore unlikely to provide any greater protection from projected increases in hydrological extremes (Lane and Kay, 2021; Griffin *et al.*, 2022). This finding suggests that current estimates of the impact of afforestation on hydrology can also be used for the future; catchments where afforestation has reduced the largest floods are likely to continue to experience some protection for future events of similar magnitude. This is important as other work using extreme land cover and climate scenarios suggest significantly different hydrological systems in the future. Projected climate changes are unlikely to be large enough to generate differing responses from land surface parameterisations in JULES, compared to the simple sensitivity analysis undertaken. Future studies should justify and utilise plausible land cover scenarios for policy recommendations to determine the future effect of changing climate and land cover more credibly on extremes when using numerical methods.

Some future impacts of afforestation on hydrological fluxes in JULES depart from present estimates. Transpiration decreases in the future, driven by lower summer precipitation, which mitigates the impact of growing broadleaf woodland relative to grasslands. Future rising temperatures, in conjunction with reduced albedo from more woodland, may therefore reduce stomatal conductance, due to the increased vapour pressure deficit. Decreases in both average river flow and runoff appear to be more influenced by regional effects with a reduced correlation between amount of afforestation and percentage reduction in runoff across the studied regions. This is likely due to greater differences in precipitation and temperatures (previously shown as the main differentiator of streamflow response) leading to changes in evaporation and runoff. It might also suggest that evaporative processes have a stronger effect on runoff generation which have been shown to be driven by regional controls [Table 4.1]. However, a stronger correlation between the top 1 % of flows and afforestation extent in the future [Table 4.2] suggests climate is likely to alter the modulating role of land cover during extreme events. Current implementations of land cover into LSMs need to ensure land cover parameterisations are accurate to ensure modelled responses to climate are faithful. If they are not, we are projecting further uncertainty into future scenarios.

4.6. Conclusion

Modelling ‘realistic’ countrywide afforestation in line with UK Government ambitions shows only small changes in hydrological processes and streamflow. Afforestation could generate unintended reductions in low flows in some locations, both at present and in the future. Although there are not significantly divergent regional responses to afforestation, catchment attributes and climate do produce nuanced hydrological responses (such as soil moisture). Evaporative processes govern high flow generation, while runoff parameterisation controls lower streamflow generation. Our sensitivity analysis shows large-scale plausible afforestation has only a minimal impact on hydrology compared to possible climate changes. Precipitation changes have the largest impact on the modelled streamflow regime whereas temperature and CO_2 have a discernible impact on the lowest flows only. Furthermore, this study illustrates the epistemic uncertainties within the JULES model and potentially under-sensitive land surface parameters and parameterisations. Finally, the effects of afforestation on land surface hydrology and the terrestrial hydrosphere are similar in the present and future. Climate changes (e.g., precipitation and temperature) do not alter woodland regulation of hydrological extremes and only slightly alter regional differences in the hydrological response to afforestation. Future research should use fully coupled land surface – atmosphere LSMs to assess how afforestation influences hydrology over larger spatial scales than the catchments studied to elucidate the strength and spatial extent of water cycling from increased canopy evaporation.

5. Afforestation leads to a wetter UK: findings from a kilometer-scale climate model

---

This chapter has been submitted as a research article to the journal Environmental Research Letters. Marcus Buechel ran the simulations, analysed the results, and created the figures. All co-authors contributed to editing the manuscript. Marcus Buechel generated afforestation scenarios (with help from Ségolène Berthou), analyzed model output, and wrote the manuscript. Marcus Buechel, Simon Dadson, Huw Lewis and Ségolène Berthou conceived the project. Will Keats ran the model simulations. Ségolène Berthou, Louise Slater, Simon Dadson, Huw Lewis and Will Keats all contributed to editing the manuscript. Co-authorship statements can be found in Appendix 6.

This is the first proposed revision of the manuscript.

5.1. Abstract

Afforestation is of international interest for its positive benefits on carbon storage, ecology, and society, but its impacts on terrestrial and atmospheric processes are still poorly understood. This study presents the first use of a coupled land surface and convection permitting atmospheric model (CPM) to quantify hydrometeorological afforestation effects across the United Kingdom, focusing on atmospheric processes often missing in hydrological modeling. Generating a scenario of 93 000 km^2 (40%) additional woodland across the UK, the periods of 2042-2052 and 2062-2072 are analyzed. Simulated afforestation significantly alters seasonal and regional UK hydrometeorology. Countrywide runoff increases in all seasons (between 5.4-11 mm and 4.3-8.6% per season) due to elevated subsurface flows from greater soil moisture. Evaporation decreases in summer (-20.6 mm, -10%) but increases in winter (8.1 mm, 15%) whereas rainfall increases throughout all seasons (between 2.2-6.86 mm and 0.9-2.2% per season). Greater winter rainfall is detected along Great Britain's west coastline as increased surface roughness produces prolonged and heavier rainfall. In the summer, increased albedo leads to increased potential evapotranspiration and reduced near surface specific humidity:

water is locked in deeper soil layers as transpiration diminishes and the topsoil dries out. However, the magnitude of hydrometeorological change due to altered land cover is smaller than the uncertainty in local climate change projections. This work sets a precedent in illustrating the impacts of afforestation on hydrology using a high-resolution CPM and highlights the importance of coupled hydrometeorological processes when investigating land cover impacts on hydrological processes.

5.2. Introduction

Widespread afforestation is receiving growing international interest and could substantially change global land cover (Griscom *et al.*, 2017; Hawes, 2018). Its proposed societal benefits include reducing atmospheric CO_2 and pollution (Bonan, 2008; Forster *et al.*, 2021), improving biodiversity (Burton *et al.*, 2018), and mitigating floods (Carrick *et al.*, 2019). However, the ramifications of afforestation on the Earth system at large spatial scales are not entirely known related to their magnitude and direction of change.

It is not fully understood how afforestation influences the water cycle (Wang-Erlandsson *et al.*, 2018). Gaps exist between modelled and observed terrestrial impacts of afforestation (Andréassian, 2004), especially when considering the hydrological consequences of using afforestation as Natural Flood Management (NFM) (Dadson *et al.*, 2017; Lane, 2017). Whether the benefits of NFM outweigh the water resource demand of widespread afforestation is undetermined (Ellison *et al.*, 2012). Direct measurements of woodland on land surface processes (e.g., evaporative fluxes and streamflow) continue to educate us on how afforestation could influence energy and water fluxes (Marc and Robinson, 2007; Osborne and Weedon, 2021; Monger *et al.*, 2022). However, studies often take place over relatively small spatial scales (< 50 km^2) using a paired catchment approach which compares process differences between afforested and unaltered land cover in similar catchments (Bosch and Hewlett, 1982; Bathurst *et al.*, 2018). Many observational studies suggest afforestation reduces overall runoff, although its effects are more complex at the highest flows (Do *et al.*, 2017; Bathurst *et al.*, 2020). However, data driven analysis of afforestation consequences are difficult to extrapolate

both in time and space due to the number of interacting dependent processes with nonstationary forcing, such as climate change (Slater, Anderson, *et al.*, 2021; Anderson *et al.*, 2022).

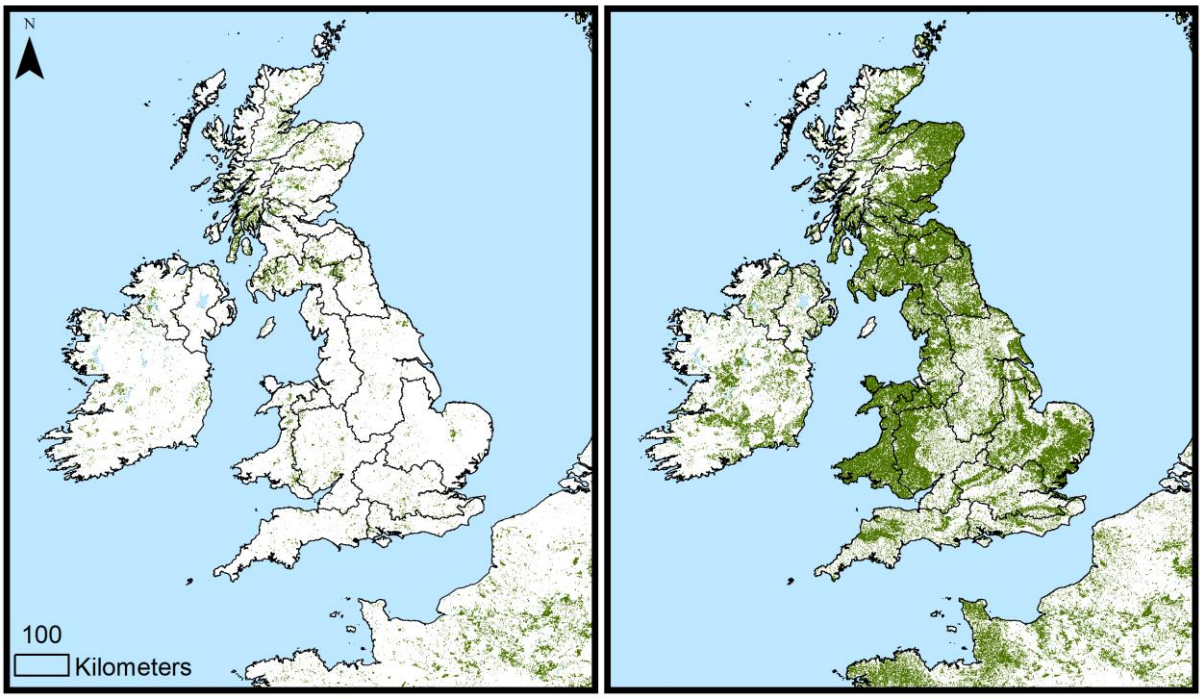

Figure 5.1: Maps illustrating the amount of land cover before (left) and after (right) afforestation.

For the periods simulated, forest cover is the only variable that changes between the model runs. Green represents both broadleaf and needleleaf woodland. Disaggregation between the two species can be found in Supplementary Figure S5.1 and the areal increase in woodland in for each region in Supplementary Table 5.1.

Conceptual and simple process-based models, used to explore larger spatial scales, broadly agree that afforestation reduces overall and peak streamflow (Bulygina *et al.*, 2013; Stratford *et al.*, 2017). These results however do not necessarily provide a full physically-based understanding of afforestation on hydrology, as observed (Soulsby *et al.*, 2017; M. Cooper *et al.*, 2021). Recently, process-based land surface models have been used to explore terrestrial consequences of countrywide land cover change (Blyth *et al.*, 2019; Ritchie *et al.*, 2019), and show afforestation generates complex hydrological responses (Buechel *et al.*, 2022; Zhang *et al.*, 2022). Those studies only consider terrestrial hydrology and thus intra-catchment afforestation impacts, consequently neglecting significant atmospheric feedbacks (Lacombe *et al.*, 2016; Meier *et al.*, 2021; Cui *et al.*, 2022). Therefore, it is essential to look beyond individual catchment boundaries to fully comprehend afforestation's impact on the water cycle.

Earth system models (ESMs) have illustrated the far reaching consequences of afforestation on atmospheric and ocean circulation (Breil *et al.*, 2020; Davin *et al.*, 2020; De Hertog *et al.*, 2022) but are limited by their coarse grid spacing and provision of continental-scale information, such as orography. This work is the first to use a high spatial resolution (2.2 km) regional convection-permitting model (CPM), coupling the land and atmosphere, to assess the potential hydrometeorological consequences of widespread afforestation at a countrywide scale. We focus on the United Kingdom which plans widespread afforestation and is considered an ideal location for European afforestation (Bastin *et al* 2019; Committee on Climate Change, 2019). We focus on three main questions. Firstly, do the most extreme plausible afforestation scenarios significantly change hydrometeorological processes: rainfall, evaporation, and runoff? Existing work suggests significant changes in hydrology with widespread afforestation (e.g. Hoek van Dijke *et al* 2022), however further work is required to determine if this is reasonable. Secondly, we question whether significant regional patterns in hydrometeorological processes occur with afforestation, and whether terrestrial properties mediate this response. Previous work has shown afforestation impacts on meteorological processes over continental scales (e.g., Teuling *et al* 2017; Cerasoli *et al* 2021) but greater spatial granularity and model diversity is needed. Finally, we assess whether afforestation generates significant seasonal differences in hydrometeorological processes with increased woodland. This study will assess the hydrometeorological consequences of widespread afforestation within the UK and model sensitivity to land cover changes, whilst providing a base understanding of afforestation on the formation of convective rainfall, something previously parameterized in models (Fisher and Koven, 2020; Blyth *et al.*, 2021).

5.3. Methods

5.3.1. Model

A CPM is run at a 2.2 km grid spacing and 60 second timestep for a model domain centered over the UK. The configuration is the same one used for the local CPM projections in the UK Climate Projections (UKCP18). Full details are provided by Kendon *et al* (2019) and Keat *et al* (2021). Two model ensembles are used from the twelve-model ensemble of UKCP18 in this study. Running at kilometer-scale enables a more detailed representation of the land surface than typically resolved in climate models, and convection is explicitly simulated rather than

parameterized, which leads to significantly improved physical representation of precipitation extremes at an hourly scale (Kendon *et al.*, 2014; Prein *et al.*, 2015). No prior work investigating afforestation impact has used this model type. Lateral boundaries are forced by a regional climate model (RCM; 12 km spatial resolution) which is driven by a global climate model (GCM; 60 km spatial resolution) (J. Murphy *et al.*, 2019). These boundaries are different between the two model ensembles. A variable resolution grid allows showers to grow before entering the CPM (Tang *et al.*, 2013) and nesting in the RCM reduces precipitation biases compared to directly coupling with the GCM (J. Murphy *et al.*, 2019). The model is run with a 360-day calendar for the periods 2040-2060 and 2060-2080 using the RCP 8.5 transient projection. Although this scenario is potentially beyond what is considered plausible (Hausfather and Peters, 2020), it allows identification of hydrological response to extreme climatological conditions.

The land surface scheme is JULES, the Joint UK Land Environment Simulator (Best *et al.*, 2011; D. B. Clark *et al.*, 2011), in its regional land and atmospheric science configuration (detailed in Bush *et al* (2020, 2023), but with three significant hydrological differences. One, Brooks and Corey (1964) soil hydraulics are used, two, excess moisture is moved downwards in soil layers and finally, the rainfall-runoff model TOPMODEL is used (Clark and Gedney, 2008). Soil hydraulic conductivity is derived from the fraction of silt, sand and clay. Landscape heterogeneity is represented using a surface tiling scheme within each grid box and independent water and energy fluxes are calculated for each tile, or land cover type. There are five plant functional types (PFTs): broadleaf and needleleaf trees, C3 and C4 grasses and shrubs; and four non-plant functional types: urban, lake, bare soil, and ice. The Met Office Reading Urban Surface Exchange Scheme represents roofs and street canyons as two separate tiles (Porson *et al.*, 2010). Stomatal conductance is dependent on the humidity deficit and CO_2 concentration, which is related to plant type, and the availability of soil moisture (Cox *et al.*, 1998). If net photosynthesis is less than zero, or stomatal conductance is below a defined threshold, stomata close and conductance is set to the threshold. The two-stream radiation approach calculates direct and diffuse Photosynthetically Available Radiation at each of the ten layers specified within the canopy (Sellers, 1985). Albedo is calculated for each PFT by using transmission and reflection coefficients in the visible and near-infrared regions for individual leaves and the leaf area index (LAI). LAI for each month and PFT is based on climatology between 2005-2009 and the MODIS LAI product (J. Murphy *et al.*, 2019; Wiltshire *et al.*, 2020). Although LAI is kept constant, stomatal conductance varies according to atmospheric and surface conditions.

The surface has a sensible heat capacity and evaporation from the soil, water and transpiration combine to generate the surface latent heat fluxes. Energy and water fluxes are calculated in four soil layers with depths of 0.1, 0.25, 0.65 and 2 m. Underneath, there is a layer where drainage slows to form groundwater. Information on precipitation interaction with the canopy and soils is found in Buechel *et al.* (2022).

5.3.2. Land Cover Scenarios

Three approaches have been taken to predict afforestation influence: model all available land as afforested (e.g. De Hertog *et al.*, 2022), use scenario-driven afforestation with models (e.g. Hoek van Dijke *et al.*, 2022), or extrapolate woodland observations (e.g. Schwaab *et al.*, 2020). To maximize the likelihood of detecting a signal, we use maximal proposed afforestation scenarios determined by the United Kingdom's individual nations: in England, the working with natural processes Environment Agency afforestation scenario (Environment Agency, 2018); in Wales, the woodland opportunity map created by the Welsh Government (Welsh Government, 2021); in Scotland, the land suitability map for woodland expansion (Sing and Aitkenhead, 2020); and for Northern Ireland, afforestation extent is created using the method of Buechel et al. (2023) [Figure 5.1]. Landcover fractions are constant for the baseline and afforestation scenarios.

Afforestation scenarios for continental Europe and Ireland in the model domain are also created. 50 % of the afforestation area proposed by Bastin *et al.* (2019) is randomly wooded for continental Europe, acknowledging its potential over-ambition. In Ireland, an afforestation scenario is created based on Farrelly and Gallagher (2015). In reality, tree species planting is due to socio-economic, political and landowner choices (Sing *et al.*, 2018; Sutherland and Huttunen, 2018; Brown, 2020). Accurately modelling these factors is impossible considering the large uncertainty in future environmental and societal conditions. Only broadleaf and needleleaf woodland vegetation classifications are used and so nearest neighbor interpolation is utilized to expand similar species to those nearby, working on the principle woodland is locally similar which is preferable for ecological functioning (e.g. Hughes *et al.*, 2023). Seventeen land cover types from the Climate Change Initiative 2020 land cover map (ESA, 2017) are converted to the nine modelled, and each land cover type is calculated as a fraction of each grid cell (Bush *et al.*, 2020). A total of 93 290 km^2 (c. 40%) additional woodland is

generated across the UK [Figure 5.1; Supplementary Table 5.1]. To note, this is an unrealistically large afforestation extent and ignores the hydrological effect of growing vegetation as all additional woodland is mature within the model domain.

5.3.3. Analysis

Analysis is disaggregated into the 23 UKCP18 hydro-regions and individual nations [Figure 5.1] for two time periods, 2042-2052 and 2062-2072, to identify the response of individual hydrologically distinct areas to afforestation (J. Murphy *et al.*, 2019). The period chosen ensures water stores are equilibrated at the start of the period and there is a long enough period for analysis given computational resources. Each CPM period is driven by the same perturbed climatology RCM providing data for 40 years (two model ensembles of 20 years of data each).

Quantile regression (Koenker and Bassett, 1978) is used to ascertain direction and magnitude of rainfall, evaporation and runoff changes across regions and countrywide for the overall time period, and seasonally. Quantile regression is nonparametric and minimally influenced by extreme outliers. Spearman's rank correlation coefficient quantifies the strength of association between afforestation extent and hydrometeorological variable changes. Weaker correlations (-0.5 – 0.5) indicate that regional properties have a greater influence than afforestation extent on simulated changes in hydrometeorology. A full set of the quantile regression and Spearman correlations can be found in Supplementary Tables 5.2 and 5.3. To determine if hydrometeorological alterations due to afforestation are statistically significant in time and space a Shapiro-Wilk test (Shapiro and Wilk, 1965) is applied; if the data are normally distributed, a two-sided Student's t test is used, and if not, a Wilcoxon test.

5.4. Results

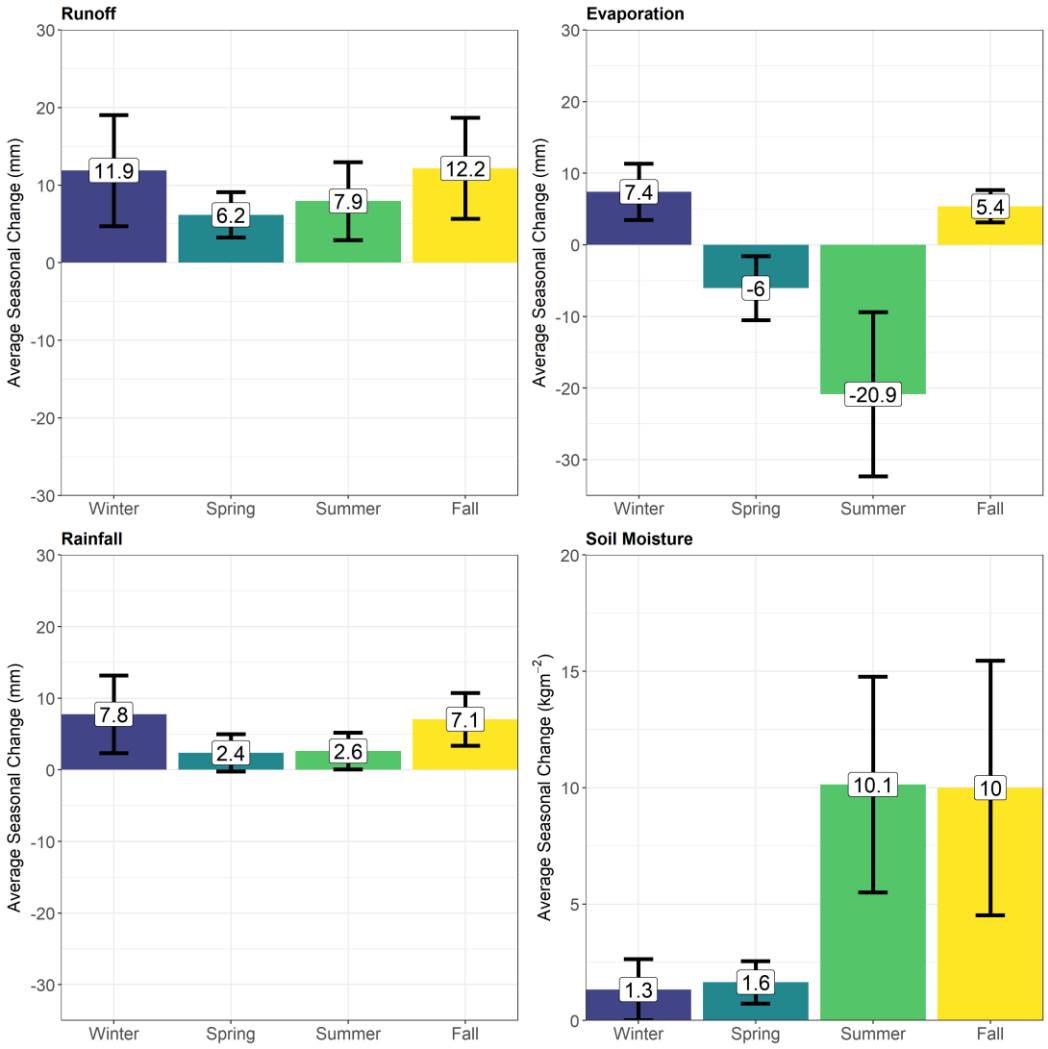

Figure 5.2: Average absolute change in rainfall, evaporation, runoff, and soil moisture following afforestation across the 23 regions.

Error bars represent one standard deviation from the mean of changes in the hydrometeorological variables with afforestation across the 23 UKCP18 regions. A corresponding plot as percentage change can be found as Supplementary Figure S5.2. These values are different to the averages reported for just the UK which can be found in Supplementary Table 5.4. The absolute changes recorded here are from the entire period for all of the UKCP18 regions using monthly output from the simulations and calculating the absolute change between the base land cover and afforestation scenarios, for the corresponding ensemble member and period [Table 2.1].

Afforesting the UK increases average rainfall between 2.19 and 6.86 mm (0.88%-2.24%) more per season [Supplementary Table: 5.4]. Comparing across regions the maximum average

absolute rainfall increases by approximately 7 mm in winter and fall [Figure 5.2]. Rainfall increases along the west coast of Great Britain, particularly in winter [Figure 5.3]. In spring and winter, statistically significant increases in rainfall occur ($p < 0.025$, over 0.2 mm day^{-1} | 0.9%), but not for the rest of the year across the whole of the UK [Figure 5.3]. Decreases in precipitation are simulated in the east of Great Britain but are not statistically significant ($p > 0.025$). An insignificant correlation between afforestation and precipitation changes over the period, and for seasons, suggests that precipitation response to afforestation is not exactly co-located ($\rho = 0.15$, $p > 0.1$). Heavier rainfall occurs with afforestation as the western coastline of Great Britain has over 3 days of additional heavy rain days over a 10-year period [Figure 5.4].

Afforestation substantially influences seasonal evaporative processes [Figure 5.2]. In the winter and fall, overall evaporation increases in the UK per season on average by 8.1 mm (15.6%) and 5.6 mm (6.5%) respectively, however in summer and spring it dramatically reduces by 20.6 mm (10%) and 4.9 mm (3.2%) [Supplementary Table 5.4]. Soil evaporation, which includes transpiration, is the predominant driver of seasonal changes in overall evaporation [Figure 5.5]. Soil evaporation reduces by 0.11% for each PPI of woodland and the pattern is strong ($\rho = -0.75$, $p < 0.001$) across regions. Soil evaporation significantly increases in almost all regions across the UK in winter ($\rho = 0.91$, $p < 0.001$, 0.53% PPI), but decreases in summer ($\rho = -0.94$, $p < 0.001$, -0.28% PPI). Afforestation broadly increases overall canopy evaporation over the period with a 0.08% increase with each percentage point increase (PPI) of woodland ($\rho = 0.48$, $p < 0.025$). Winter has the largest increase in canopy evaporation of 0.13% ($\rho = 0.65$, $p < 0.01$), whereas spring has the least discernible trend with afforestation. Potential evapotranspiration effectively doubles with afforestation across all regions, all year ($\rho = 0.85$, $p < 0.001$, 2.44% PPI), with the largest absolute increase in summer [Supplementary Table 5.2]. Soil moisture changes are predominantly driven by evaporation alterations with afforestation: decreased summer and spring evaporation increases absolute soil moisture, while winter and fall increases lead to a reduction.

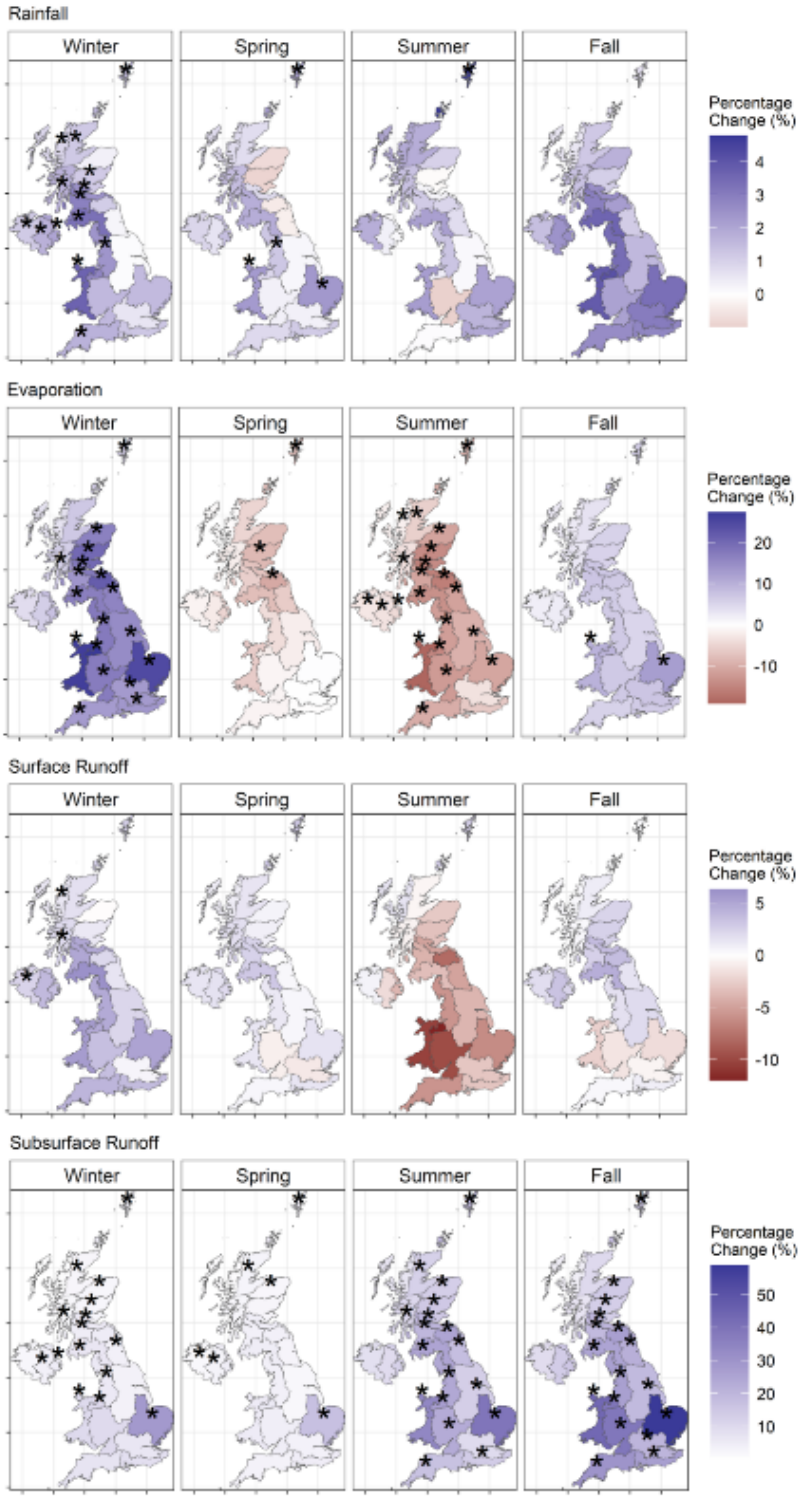

Figure 5.3: Percentage change in rainfall, evaporation and turnover ratio following afforestation for each season.

The difference is between the variables in the simulations for original compared to afforested simulated variables. The stars represent regions where the change is significant ($p < 0.025$). Supplementary Figure S5.3 shows this as absolute changes.

Surface runoff has a strong seasonal directional change with afforestation [Figure 5.5] but there are no significant regional changes across regions [Figure 5.3]. Surface runoff slightly increases in winter due to rainfall, but not significantly ($\rho = 0.4$, $p > 0.5$, 0.05% PPI), indicating strong regional variation in the increase. In summer, a clear reduction in surface runoff is attributable to afforestation with a drying of the topsoil ($\rho = -0.74$, $p < 0.001$, -0.14% PPI), however, changes are insignificant across regions. Subsurface runoff increases across the entire period and all regions with the most statistically significant increases observed on the western side of Great Britain and in Anglia for all seasons [Figure 5.3]. Overall, subsurface runoff increases by 0.15% PPI of afforestation ($\rho = 0.75$, $p < 0.001$) with the largest increases observed in summer months ($\rho = 0.87$, $p < 0.001$, 0.31% PPI) and the smallest in winter ($\rho = 0.5$, $p < 0.025$, 0.08% PPI) due to soil moisture.

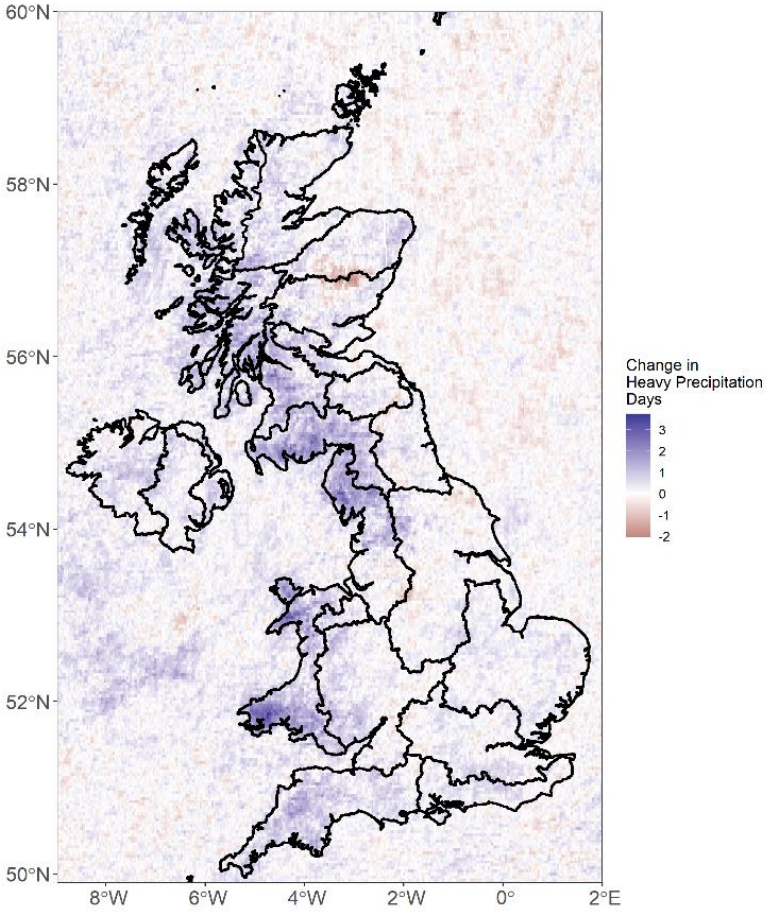

Figure 5.4: Average increase in the number of days where precipitation is greater than 20 mm for the 20-year period across all run scenarios.

Supplementary Figure S5.4 indicates the average number of days with heavy precipitation disaggregated across regions.

5.5. Discussion

Widespread afforestation extensively alters UK hydrometeorological processes. However, changes are strongly regional with significant nearfield effects as a result of afforestation, unlike previous studies (e.g., Li *et al.*, 2018; Teuling *et al.*, 2019). Greater winter rainfall in the west of Great Britain is simulated with afforestation [Figure 5.4], due to increased roughness length, humidity, and temperature [Figure 5.6]. Indeed, wind speeds predominantly decrease up to the first 3 km of the atmosphere with additional woodland [Supplementary Figure 5.5]. Winter fronts and convective showers advect inland from the sea, and the orography and roughness of the western coastline stalls their progress travelling along the westerlies within the CPM (Berthou *et al.*, 2020; Kendon *et al.*, 2020). Woodland enhances the sea-land roughness contrast further, likely slowing the progressing systems (Belušić *et al.*, 2019). Additional woodland also decreases the land snow-free albedo, increasing surface temperatures and potential evapotranspiration [Supplementary Figures 5.6 & 5.7] (*cf.* Lejeune *et al.*, 2017; Cerasoli *et al.*, 2021). Transpiration and soil evaporation rise, enhancing atmospheric moisture as tree roots access deeper soil moisture stores compared to shorter vegetation. Larger soil moisture stores are available from summer and fall periods (discussed later) [Figure 5.2]. Canopy evaporation continues to be elevated providing further atmospheric moisture [Figure 5.5]. Higher temperatures and humidity provide conditions more favorable to intense and larger rainfall events with increased air buoyancy and instability (illustrated by moist static energy [Supplementary Figure 5.8]). Higher winter humidity promotes increased transpiration due to the reduced humidity deficit (Cox *et al.*, 1998). These factors combine to increase cloud cover (and total overall cloud liquid volume) over afforested regions for the first few kilometers [Supplementary Figure 5.9]. A slight rain shadow effect is detectable on the northeast side of the UK, although not significant [Figure 5.3], and so precipitation does not significantly increase downstream of westerlies. Increases in winter turnover rate suggest hydrological cycle intensification in afforested regions [Supplementary Figure 5.10]. Thus, although afforestation is being used as a measure to mitigate climate extremes, it could make rainfall-driven climate change impacts worse with increased flooding events. Enhanced rainfall and antecedent soil moisture (from the summer) elevates surface and subsurface runoff, which would increase streamflow. During winter, absolute soil moisture reduces with increased evaporation and runoff, providing the conditions for hydrometeorological process changes which occur in the summer [Figure 5.2].

In summer, rainfall, evaporation, and runoff function differently with afforestation compared to winter [Figure 5.6]. Topsoil moisture decreases, whereas the lower soil column becomes increasingly saturated (aided by reduced drainage promoted to form groundwater table) [Supplementary Figure 5.11]. Reduced topsoil moisture is likely due to over-drying, caused by the large increase in potential evapotranspiration. An increase in the 1.5 m temperature decreases relative humidity [Supplementary Figure 5.12], and combined with lowered soil evaporation, reinforces the transpiration reduction by increasing the humidity deficit (-1.64% in specific humidity across the UK in summer) (Cox *et al.*, 1998). As topsoil moisture decreases, surface runoff and soil evaporation reduce. Reduced topsoil moisture further decreases transpiration due to the soil root mechanisms in JULES (Best *et al.*, 2011), particularly with grass roots accessing any available moisture in the topsoil. As summer continues, subsurface runoff gradually increases with rising absolute soil moisture lower in the column [Figure 5.5]. In winter, overall soil moisture stores are diminished as additional precipitation saturates the soil which increases runoff [Figure 5.5]. However, this UKCP18 RCP 8.5 scenario is at the upper limit of temperature plausibility (Hausfather and Peters, 2020) and thus feedbacks may be over-exaggerated. The distribution of soil moisture within the soil column aids an increase in the Bowen Ratio [Supplementary Figure 5.12]. If this is the case, the hydrological implementation is directly influencing energy balances meaning greater attention is needed to ensure accurate hydrological results (Clark *et al.*, 2011; Clark *et al.*, 2016). To note, the increase in soil moisture could be due to the configuration of soil moisture routing implemented in this model configuration (Bush *et al.*, 2020; 2023). Formation of lower-level clouds [Supplementary Figure 5.9] do not appear to counteract the influence of decreased albedo with afforestation on temperatures (e.g. Cerasoli *et al.*, 2021). In summer, RCMs exhibit divergent temperature and evaporative fraction changes with afforestation, which has been attributed to land surface model parameterizations (Lejeune *et al.*, 2017; Davin *et al.*, 2020), such as root distributions and soil water uptake formulas (Meier *et al.*, 2018). In this setup, stomatal conductance is the primary driver of transpiration change. Changing the root depth, and including lateral subsurface flows, or including more accurate plant hydraulics would enable more accurate calculation of evaporation (Chang *et al.*, 2018b; Harper *et al.*, 2021; Picourlat *et al.*, 2022) and may alter our results by enabling plants to access deeper and locally adjacent soil moisture.

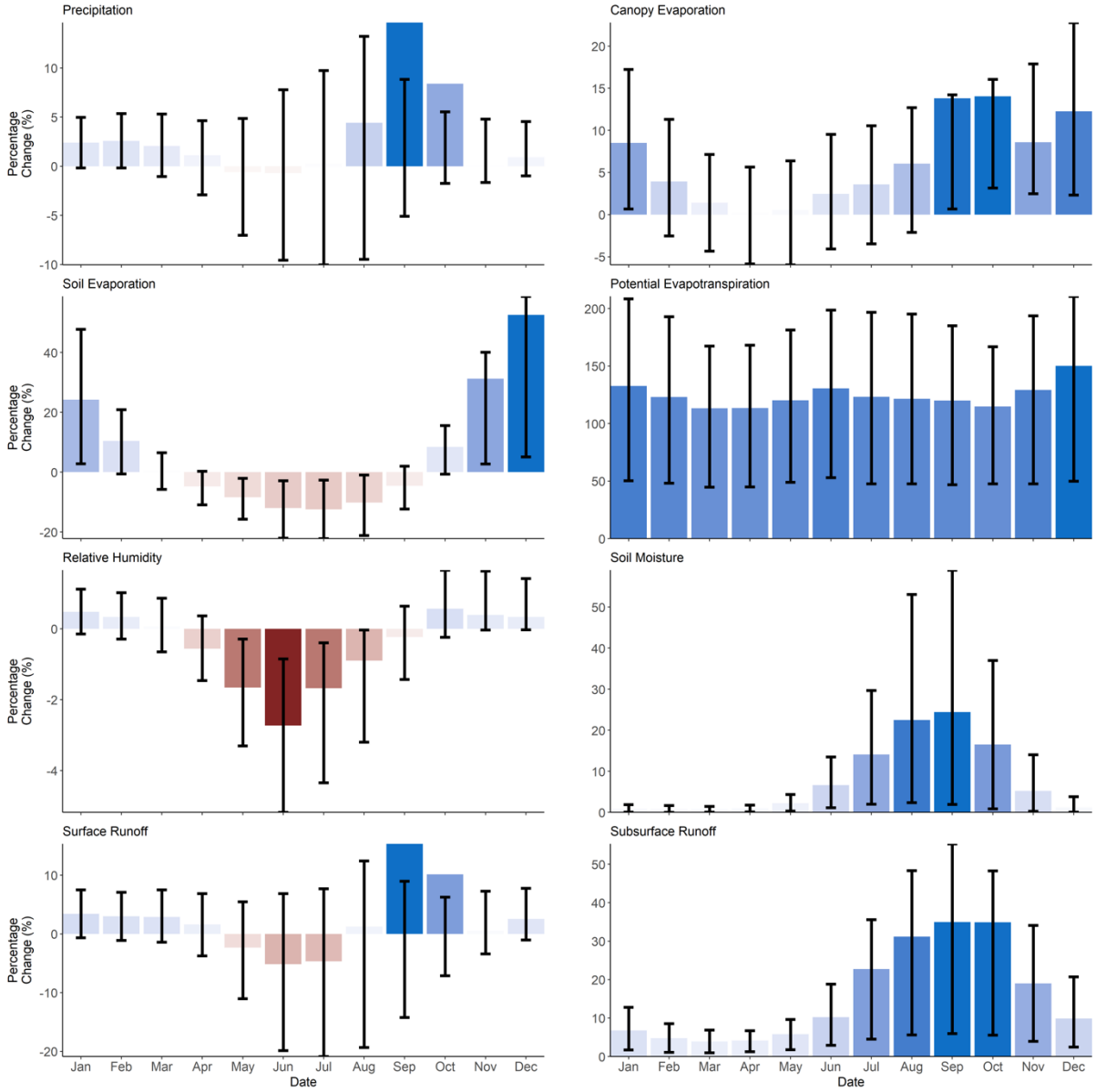

Figure 5.5: Percentage changes in hydrometeorological processes (precipitation, canopy and soil evaporation, potential evapotranspiration, relative humidity, soil moisture, surface, and subsurface runoff) for the 20-year period for all regions with afforestation.

Error bars represent the 10th and 90th percentiles for the 23 UKCP18 regions. Supplementary Figure S5.13 provides the figure as absolute changes. These are calculated with the monthly output data from the simulations and are the percentage difference between the base land cover scenario and the afforestation scenario, across the simulation suites for the corresponding ensemble member and period [Table 2.1].

Compared to winter, there is not a similar summer precipitation increase, and regional differences occur. Woodland reduces wind speed, however, humidity, soil evaporation and transpiration decreases. The lessened atmospheric moisture contributes to the reduced rainfall in summer and exemplified by the turnover ratio decline [Supplementary Figure 5.10]. Decreases in relative humidity are driven by summer increases in temperature and reductions in soil evaporation due to the reduced albedo and greater sensible heat fluxes [Supplementary Figures 5.7 & 5.14]. These temperature increases would also be detrimental to human life, particularly in a climate scenario where temperatures are expected to be elevated. Summer temperatures increases are not seen in winter due to larger latent and reduced sensible heat fluxes. Some inland regions receive intense summer precipitation, and this leads to the divergence in the mean precipitation across regions observed in Figure 5.5.

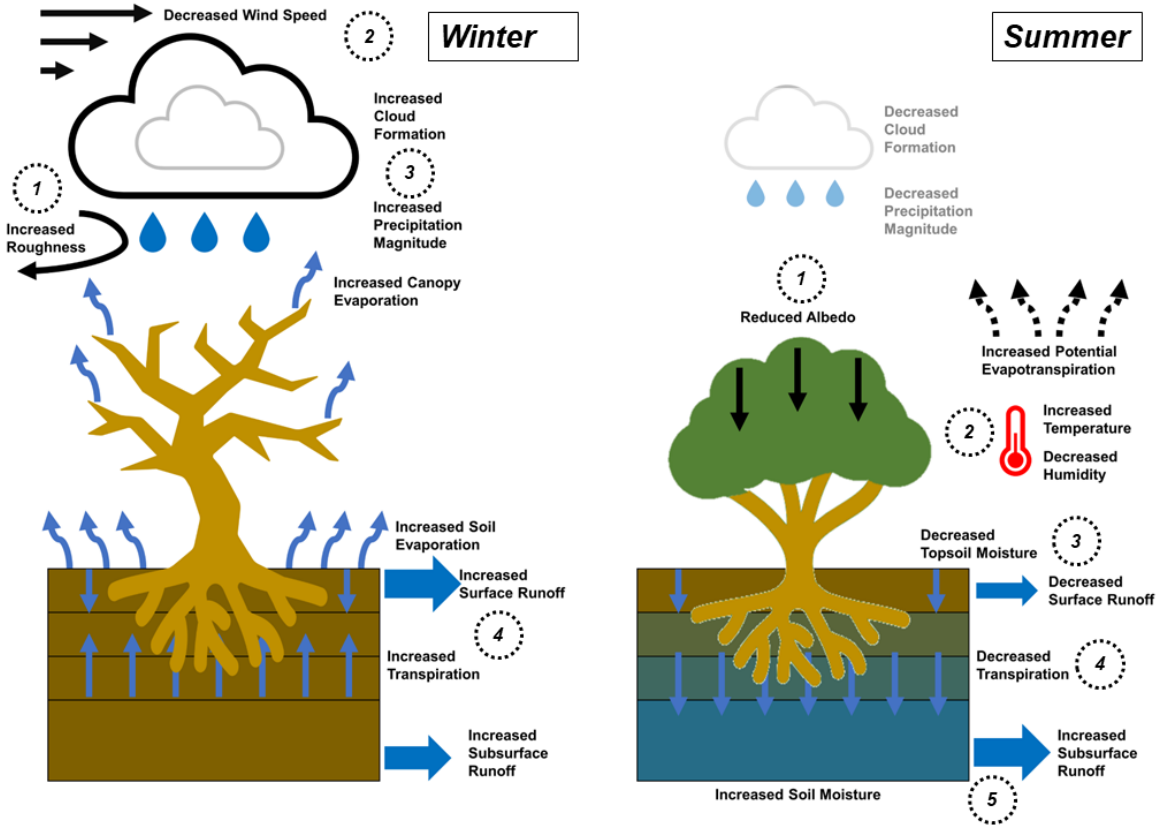

Figure 5.6: Conceptual diagram of the hydrometeorological changes that occur on average with afforestation in winter and summer.

In winter, (1) the increased roughness length of woodland (2) decreases wind speed, which (3) stalls convective cells and leads to increased precipitation and (4) generates increased surface runoff. In summer, woodland (1) decreases albedo that (2) increases temperatures, reduces relative humidity, and increases potential evapotranspiration. This (4) over-dries the topsoil and results in (4) reduced transpiration and stomatal closure (along with reduced humidity).

The root profile parameterizations (5) increase soil moisture deeper in the column and enhance subsurface runoff. In some regions, summer precipitation decreases, but it is not significant and thus is shown muted.

Despite the large areal coverage of afforestation undertaken here, not all hydrometeorological processes changed comparatively. For example, surface runoff changes were minimal compared to land cover changes. However, there were significant changes in radiative fluxes, demonstrated by the significant decrease in albedo [Supplementary Figure 5.7] and increase in potential evapotranspiration for the entire period [Figure 5.5]. When compared to projected changes in climate, afforestation is of minor importance. For the period 2060-2080 compared to 1981-2000, precipitation is projected to decrease over the entire UK between 46% and 16% in summer, whilst increasing between 16% and 43% in winter across the UKCP18 model ensemble. The relatively small range of rainfall changes induced by widespread afforestation in this study (-1% to 4% across regions) indicate the relatively minor role of significant land cover changes in altering predominant climate atmospheric signals. This emphasizes the potential difficulty in attributing hydrometeorological changes to land cover in a nonstationary climate. However weak the signal may be, the afforestation response of rainfall, runoff and evaporation is the same across different model ensembles and periods (i.e. no statistical difference based on ANOVA tests; $p > 0.1$), further emphasizing these results are not an artefact of model internal variability.

A coupled land-atmosphere model reveals the noticeable feedback between vegetation and the atmosphere. This approach dynamically calculates evaporation and rainfall according to land surface processes. Previous hydrological work evaluating afforestation impacts on terrestrial hydrology with fixed forcing indicated that vegetation parameterization generates similar responses where increased LAI reduces throughfall, increases the canopy store, and increased transpiration, reduces streamflow (Stratford *et al.*, 2017; Buechel *et al.*, 2022). However, in this study, afforestation, particularly in western regions, increases throughfall because of more intense winter precipitation. Thus, epistemic uncertainty caused by not including relevant processes within hydrological models completely reverses intended benefits, particularly as increased precipitation with afforestation (and decrease with deforestation) has been observed before (Staal *et al.*, 2020; Cerasoli *et al.*, 2021). Furthermore, although canopy evaporation was relatively heightened, with increased surface temperatures and canopy store, the magnitude of change is so minimal it cannot counteract precipitation and soil evaporation changes. The clear

impact on hydrological and atmospheric processes with afforestation means continued effort is required to improve ESM representation to ensure hydrometeorological outputs are given for the right reasons (Beven, 2007).

This work has shown the novel application of a CPM to determine the impact of afforestation on hydrometeorological processes. However, future work should explore and compare these results to other CPMs to determine how land surface components, such as the hydrological parameterizations, alter hydrometeorology, similar to CMIP5 (Lejeune *et al.*, 2017). Radiative balance changes with afforestation are due to tree parameterizations and so need to be accurate for predicting climate. Caveats to note are excessive evaporation generated by JULES (Blyth *et al.*, 2019), inaccurate rooting profile representation (Harper *et al.*, 2021), and the lack of an accurate representation of groundwater (Le Vine *et al.*, 2016). The limited number of tree species and stand age would also significantly impact calculated evapotranspiration (Bentley and Coomes, 2020). Using this model from a hydrological perspective illustrates the epistemic uncertainty of determining the impacts of largescale land cover change when using simple terrestrial hydrological models which lack critical biophysical parameterizations. It also reveals that the current practice of driving hydrological models with atmospheric outputs is a somewhat circular endeavor, as the hydrological models originally embedded within RCMs will have left their mark by imprinting processes into the energy and water fluxes.

5.6. Conclusion

This work demonstrates the impacts afforestation could have on hydrometeorology by using a novel regional convective-permitting model. Clear seasonal and regional differences exist in how afforestation alters hydrometeorology within the UK, particularly in western regions of Great Britain. In winter, the increased roughness length of woodland stalls convective cells and fronts from the sea, which are then very slightly enhanced by increased moisture and temperature inland. In summer, changes in precipitation are not significant but reduced albedo diminishes transpiration and elevates soil moisture in deeper soil layers. Greater soil moisture produces larger subsurface runoff. Soil evaporation greatly varies with season and is the predominant driver of hydrometeorological changes. Despite vast increases in woodland, the impacts on hydrometeorology are insignificant when compared to uncertainties in climate projections. This work illustrates that although coupled systems are not as sensitive to land

cover changes as to driving atmospheric forces in this geographical setting, they can produce very different results to uncoupled systems. Our afforestation scenarios suggest the UK would become a slightly wetter place and further work should compare results with other modelling approaches.

6. Conclusion

6.1. Chapter Summaries

6.1.1. Hydrological impact of widespread afforestation in Great Britain using a large ensemble of modelled scenarios

In the first part of the research, JULES was employed for its ability to capture several relevant Earth systems required to simulate the influence of widespread afforestation upon the hydrological response of catchments across Great Britain. Twelve catchments ranging in size from approximately 500 km^2 to 10 000 km^2 were simulated and for each, a suite of up to 288 afforestation scenarios was created according to catchment structure and existing land cover. This work firstly enabled the demonstration of using an LSM to determine potential afforestation influence on hydrology across regions in Great Britain at a high spatial and temporal resolution. Results indicate that afforestation extent was more important than location when influencing streamflow and drier catchments, receiving lower rainfall, were more responsive to the effect of woodland increases. Areas that are water and not energy-limited would therefore have an increase in evaporation with additional woodland removing more water out of the catchment. However, there is a lack of information on the consequences of this increased water in the atmosphere on catchments further afield due to the uncoupled nature of this model setup.

This work provides further evidence that woodland would likely reduce low and median streamflow but have little impact on the most extreme flood events. This is important as this was a finding not always supported by the hydrological numerical modelling literature, suggesting that for such a complex question, an appropriately complex model is required. The fact this modelling work broadly aligns with observations on woodland impact on streamflow also demonstrates the fact that this LSM encapsulates a significant proportion of the necessary processes responsible for catchment response to vegetation changes. However, there are still many epistemic uncertainties within JULES that require a deeper look into the processes occurring.

6.1.2. Afforestation impacts on terrestrial hydrology insignificant compared to climate change in Great Britain

The second research part took the initial findings of the first work forwards and attempted to explore the hydrological processes driving streamflow response to afforestation. Using the principle woodland extent is broadly more important than its location considering streamflow, a realistic afforestation scenario was created for the entirety of Great Britain (if the UK Government planted up to 30 000 hectares of trees a year up to 2050). The JULES model, in the same configuration as the first research piece, simulated a greater variety of catchments across the country. Both the potential streamflow response, and hydrological fluxes and stores, were analysed. Land cover representation within JULES and its comparative sensitivity to atmospheric drivers with extreme climate scenarios was then explored. In this manner, the model was run in areas and realms it was not specifically tested with. This allows investigation of JULES' progress of becoming a 'model of everywhere'.

Land cover changes did not produce significantly different regional hydrological responses across the country. This could either suggest that the driving data is not sufficiently accurate enough to represent the hydrological diversity of the UK (such as the soil ancillaries), or that process representation in JULES is unable to replicate the hydrological diversity, or that the UK is not a hydrologically diverse space. It is likely to be a partial combination of all three factors and so attempting to improve process representation within JULES will be a cyclical endeavour. For example, if we attempt to improve the accuracy of input data, the UK may not be hydrologically diverse enough or JULES's process representations may not be accurate enough to provide clarification on how it might have improved the model output sufficiently.

In addition, LULC had minimal impacts on hydrological processes when compared to potential changes in climate, which either highlights the minimal impact of land cover or process parameterisations within JULES. Furthermore, the fact that future climate would not significantly alter hydrological processes illustrates that future projected climate is not sufficient to enable JULES to project considerably different hydrology. This either supports the notion there will be little effect of future climate on water resources or that changes in climate are not enough to precipitate a significant shift in parameterisation output.

Differences in high flows are predominantly aided by evaporation parameterisations whereas low flows were generated by runoff parameterisations in JULES. This is important for determining the focus required on improving JULES' hydrology when considering its use for estimating floods and droughts. Understandably, precipitation and temperature play a substantial role in altering JULES' hydrological processes and subsequent responses. However, CO_2 followed by LULC changes are of minimal consequence comparatively. This has important ramifications when considering how these factors may change in future and the resulting consequences, particularly when using similar models to predict future climate. Is this an accurate depiction of their relevance for future climate systems, or is their significance being misrepresented?

Essentially this work provided evidence for the potential implications of widespread afforestation in Great Britain and delved into the generating mechanisms. Furthermore, it provided additional insight into the complex nature of LSMs regarding how hydrology is represented within such models.

6.1.3. Afforestation leads to a wetter UK: findings from a kilometer-scale climate model

In the final research part, we use the most advanced coupled, regional land-atmosphere model available at present, coupling both the land surface and the atmosphere. The modelling is performed at a spatial and temporal scale not previously attempted with this methodology and analyses the effects of afforestation on all hydrometeorological processes. Running a model configuration whereby JULES is coupled to the atmosphere enables interpretation of whether the results of the previous uncoupled runs are valid, and if there are detectable system feedbacks. Unlike in previous chapters, an extreme afforestation scenario with two tree types was utilised. Therefore, any responses detected from this work are likely to be far more severe than reality but enables examination into whether the model responds realistically to severe disturbances.

The model setup predicts significant changes in runoff, rainfall and evaporation and several unanticipated responses occur. In summer, water became trapped in lower layers of the soil out of the atmosphere and the sensible heat flux increased as the topsoil dried out. Whether this is due to the large extent of additional woodland or if this could occur even with a small amount

is unknown. Due to the geographical positioning of afforestation and orography, there is increased heavier rainfall on the western coastline of Great Britain and a slight rain shadow forms in the north-eastern side of the country. However, similar to the uncoupled JULES experiments with the atmosphere, the effect of LULC on terrestrial hydrology is insignificant in comparison to climate changes. This is especially acute as the percentage change in hydrometeorological processes with extreme afforestation is less than the uncertainty in the range in potential future climate scenarios. Climate stochasticity produces stronger changes in rainfall and runoff than the effect of changing land-cover.

6.2. Overarching Themes

6.2.1. Hydrological Influence of Widespread Afforestation

Water resources would be noticeably impacted by widespread afforestation, however the use of both coupled and uncoupled model configurations has not provided definitive evidence for one side of the demand- and supply-side debate. The first two chapters suggest that, despite looking at catchments over 1000 km^2, increasing the amount of woodland would noticeably reduce downstream streamflow. In these scenarios, additional woodland enabled more extraction of water from lower in the soil, in comparison to the shorter vegetation which was replaced. As a result, subsurface runoff decreased and thus streamflow. Consequently, planting woodland raises the possibility of exacerbating hydrological droughts. Across the streamflow spectrum, there are continual reductions in flow but once we approach the most extreme high flow events, a minimal influence of woodland is simulated. This is likely because extreme events in the UK are often generated by high antecedent soil moisture after a prolonged period of precipitation. In these conditions, woodland cannot sufficiently reduce the soil moisture or minimise high saturated-excess flow events. In contrast, when running a coupled model simulation, the geographical location of the afforestation came into play. Along the western side of the UK, the increase in woodland led to an increase in overall runoff which would reduce the likelihood of hydrological droughts. Although no streamflow analysis could be undertaken, it is also likely that this would inevitably worsen flood events. However, it is unlikely that such afforestation rates could ever be achieved that would produce such responses. No definitive conclusion can be given on whether additional woodlands would

negatively impact water resources, but this work does suggest that they should not be used to mitigate the most extreme floods as NFM.

As shown with both the coupled and uncoupled model configuration, landcover (in the form of woodland) has a minimal influence on hydrological processes compared to atmospheric drivers. This suggests two things. Firstly, land cover could have a relatively minimal impact on hydrological processes, even when at a scale that is significant to society. Even in the final research piece, an extreme afforestation extent that is incredibly unlikely produced a situation where the smaller percentage change in climate created a stronger response. Secondly, in the quest to make atmospheric outputs accurate, LSMs could still potentially be 'soaking' up and minimising any errors that would reduce their accuracy. Any process extremes could have been diminished to ensure that on average the model outputs are accurate as metrics are used to quantify model outputs, rather than realism (Clark, Vogel, *et al.*, 2021). In the quest for accuracy, models could have forgone fidelity and in so doing ensnared the process of model evolution as we continue to develop models within the echoes of our initial perceptual frameworks.

The hydrometeorological consequences of both a realistic and tremendous extent of afforestation highlight the need for appropriate land cover representation when understanding past, present and future climates. Woodland in the UK covered a much greater extent in the past (thousands of years ago) and so if models are to be validated against previous climate data, then an accurate land cover ancillary is required. If this is not the case, then the significance of planting woodland would be muted or incorrectly represented within models during validation and calibration. However, if small amounts of woodland change (e.g., < 5%) then although the model may not be 100% accurate, it would be adequate within the bounds of other uncertainty. As such, other work which has modelled landscapes where there has not been a considerable change in land cover (e.g., Blyth *et al.*, 2019), do not need to explicitly represent the land cover change. However, as previously noted this could be due to an inaccurate representation of woodland and vegetation within our models. If largescale changes in woodland extent do go ahead, then this does need to be implemented within LSMs and ESMs for accurate predictions.

6.2.2. Representation of Woodland in LSMs and ESMs

All three research chapters fundamentally tested woodland representation in LSMs and ESMs, providing a broad indication of how proposed afforestation could influence both terrestrial and atmospheric water resources. The inclusion of multiple Earth systems relevant to woodland interaction with hydrology such as carbon and energy fluxes demonstrated a more nuanced and complex approach to understanding its impact. This has a key and defining tenet: any change in process representation or parameter value between model instances can generate a significant divergence in results, even if the models themselves share a common ancestor. A key example of this is the generation of streamflow across the entire flow spectrum using JULES. The findings across the first two chapters are consistent that increased woodland extent reduces low and median flow but has a relatively minor impact at high flows. More simple numerical hydrological models find a reduction of the highest flows as well, despite observations (Stratford *et al.*, 2017). Therefore, the application of JULES in this manner has been shown to be appropriate as it is clearly picking up on actual system properties and not just echoing our simple perceptual frameworks back to us. It illustrates that contemporary scientific questions require models that acknowledge and incorporate the interdisciplinary nature of research. No longer is it necessarily possible to develop models within fields without branching into adjacent, intertwined ones. For example, the question of hydrological effects of afforestation requires an understanding and representation of hydrology, climate and ecology. The impact of vegetation on hydrology, both spatially and temporally, requires inclusion of biophysical factors to represent its direct and indirect influence accurately and faithfully. Vegetation types, phenology, stomatal conductance and root representation are key variables that created these results (e.g., decreases in low and median, but not high streamflow) and therefore require inclusion, and development, in existing hydrological models. These factors ensured that water stores dynamically evolved more realistically than the temporally static stores often calibrated and utilised in models. We therefore need future models to embrace the nonstationary nature of catchments if we are to accurately predict present and future water resources. Although this work just addresses this through surface vegetation it should also incorporate the fields of geomorphology, geochemistry and limnology.

Taking the idea of including known, relevant Earth system interactions further, the final research chapter yields differing results to the initial research chapters. It is known that large woodland areas generate substantial changes in rainfall patterns and by coupling the land surface with the atmosphere, similar results were obtained. In this manner we removed another layer of epistemic uncertainty when just modelling the land surface and provided runoff outputs

contradictory to initial conclusions. With increased surface roughness, evaporation and efficient energy exchange, there was an increase in runoff with afforestation due to the increase in (particularly intense) precipitation. Returning to the principle of parsimony, does this model configuration represent the minimal simplicity that is required to represent the influence of afforestation on hydrology, or are these processes more complex than required? This work advances deeper into utilising the most current, complex numerical models available to answer contemporary questions over afforestation on hydrology. However, by doing so, it has opened 'Pandora's box' and revealed the challenge in trying to isolate one Earth system when they are all intrinsically connected. Whenever statements are made on the influence of woodland on hydrology using models there not only needs to be an acknowledgement of epistemic uncertainty induced by model structure and implementation, but also what key features are missing. This would not only aid development of our understanding of both the world and models, but also challenge our perceptual models to ensure their accuracy and relevance.

There are still some improvements to be made within JULES. The hydrological representation continues to improve but this work has demonstrated emergent system responses that are not necessarily likely and more due to the current representation of vegetation and surfaces within the model. Of critical note, are the dynamics of soil moisture within the column which substantially altered the conclusions derived for all research chapters. Suggestions for potential improvements are found in the following chapter. Although arguably adequate for this work, further work is required to improve the representation of woodland PFTs in JULES as there is a large hydrological diversity in tree species (McCulloch and Robinson, 1993; M. Cooper *et al.*, 2021). If there is a continual push into 'models of everywhere' there will need to be a drive into more straightforward implementation of PFTs. Whilst we continue to group such diverse PFTs into singular groups, hydrological responses will continue to be muted and unrealistic. The monotone hydrological response to increasing woodland demonstrates that at 'hyper-resolutions' we also must dig into the finer granularity of grid-cell heterogeneity, such as vegetation species. This is critical if we are to correctly identify feedbacks and tipping points within the Earth system.

6.3. Outlook and Future Work

6.3.1. Afforestation and Hydrology

This work provides a positive step forward in illuminating new pathways for future discovery as we seek further answers into the potential hydrological impact of afforestation on UK hydrology.

The application of a land surface model at this spatial and temporal scale to investigate the hydrological impact of a particular land cover change cannot be understated. At our current ability and understanding it has provided a methodology and benchmark from which further studies can model and compare the potential hydrological implications of afforestation country-wide, and even, continental-wide. It is true that with better computational resources and a process understanding of the world around us, this work will be surpassed in its accuracy and conclusion granularity, however we have provided an example of running one of the most complex Earth system models that we currently have at our disposal. We therefore lay the gauntlet down for future studies to use improved models to observe whether similar conclusions are derived. This would not only help narrow down and identify the precise influence of afforestation on catchment hydrology, but also whether our models are improving to produce the *right result for the right reason*. This of course extends to other potential land cover changes such as agricultural and urban areas, but there is much further work to be done on their representation within LSMs and ESMs.

This work has attempted to provide evidence about the potential hydrological consequences of afforestation at a scale previously neglected within the literature. Studies range from 0.1 -1 km^2 to 100 km^2 when investigating afforestation effect at catchment scales to continental and global scales of over 1 000 000 km^2. We have therefore provided a datapoint in the middle of this continuum, considering small country-wide scale and catchments of approximately 10 000 km^2. This was important to provide both scientists and policymakers with evidence from which to test and develop scientific and practical hypotheses. Whether the answers are accurate is currently unknown as there is not the observational experiment from which we can fully compare these results with. At the small, paired catchment observational experiments such as Plynlimon and Coalburn, comparing the output of JULES is not appropriate or wise as the model is meant to answer questions at larger spatial scales. We therefore require more observational data at greater spatial granularity and extents to fully validate models as they travel towards hyper resolution models of everywhere (Beven *et al.*, 2019).

The final chapter given here is groundbreaking and novel within the field. No other work has utilised a LSM and a CPM at this spatial scale (c. 2.2 km^2) to answer the question of widespread afforestation influence on both climate and terrestrial hydrology. It therefore, similar to the first research piece, provides an evidence point from which further work can compare, contrast and improve, to develop our understanding of afforestation on water resources. Undertaking this work also provided vital information on how altering the epistemological uncertainty within the numerical model (in this case adding an atmosphere) can produce divergent responses despite a similar underlying model architecture. It illustrates that even methodology with the same ancestry does not provide identical results and thus in our quest to learn more about afforestation impact on hydrology, we must turn to a range of methodologies to provide evidence from a continuum of perspectives.

6.3.2. Improving JULES

Further work is required to improve the accuracy and fidelity of JULES. Soil and vegetation representation, and its numerical implementation are noted as particular avenues in which improvement within JULES can take place.

6.3.2.1. Soil Representation

Firstly, there the representation of water in the soil needs further attention. As noted in previous studies, the level of soil moisture has direct ramifications on biological, chemical, nutrient and energy cycles. If not correctly calculated, then other dependent systems will not react appropriately. Soil moisture has moved beyond being a 'fudge' factor with which the model is tuned with to produce a singular accurate output and into a critical model component. Increasing the amount of woodland directly exacerbates any issues in the calculation of soil moisture as this PFT has deep roots and high levels of momentum and energy exchanges to enable efficient evaporation rates. Any plant parameterisations significantly alter how the PFT interacts with adjacent Earth systems, such as those that predict energy and nutrient fluxes. If the soil moisture store is incorrect, plant parameterisations, such as leaf area indices, could be adjusted to compensate for inaccurate soil moisture and thus incorrectly impact other model outputs. Following this research, and the recommendations of others, soil moisture in LSMs

and ESMs could be improved in several ways. These demonstrations of altering land cover within these particular model domains have clearly evidenced the challenges we face as a community for improving soil hydraulics.

A deeper soil column is required for more realistic tree root depths and for water to percolate lower. In combination with this, more accurate implementations of root water extraction mechanisms are needed. Currently JULES' hydraulics, and those in other LSMs, are relatively simple. This allowed situations seen here where water is not appropriately extracted from the soil column. For example, water became trapped in lower layers in summer in the work of Chapter 5 as trees appeared unable to efficiently draw water from lower layers after the topsoil dried out and created a situation of water stressed vegetation. In reality, if trees become water stressed water would likely be drawn from below, but in this situation the trees over relied on the topsoil to govern evapotranspiration and stomatal conductance. The addition of lateral subsurface flow could also help improve soil moisture and thus the ability of vegetation to use it. Implementing a groundwater element to the model similarly would also enable vegetation to draw upon deeper water reserves in periods where the topsoil becomes desiccated. Finally, regarding soil moisture representation, PTFs need to not only vary over time according to soil conditions but also developed so that they are more accurate than their current implementation as discussed in the Literature Review.

Organic soil representation within LSMs also requires attention. At several points the hydrology in areas of high organic soils had dramatic responses to afforestation. This is even though it has been illustrated that data collected about organic-rich soils is often highly inaccurate. Attempts to try and improve the parameters of soils do not necessarily lead to accurate representations within plausible realms. Furthermore, the parameterisation of flow over organic soils is not necessarily correct and so further work should focus on improving our hydrological models in regions where these soils exist.

6.3.2.2. Vegetation Representation

Further work should improve the implementation of trees within JULES. It has already been noted that the current implementation of tree parameterisations are not necessarily accurate (but are broadly correct) in their interaction with the hydrological cycle (Nisbet, 2005).

Phenology in the model runs of this work are prescribed as the currently implemented methodology to calculate phenology in JULES is not correct. This provides a clear avenue for future improvement as terrestrial hydrology will alter the LAI, consequently changing the interception rate and canopy storage. Ideally all the parameters used in JULES to represent PFTs should be established in the literature and easily implemented. This would then also enable the inclusion of more varieties of trees which have been shown to have different interactions within the water cycle. Including varying soil infiltration enhancement factors for the different tree types would also account for species' impact on infiltration.

Another factor to consider is the time-varying nature of vegetation and how its growth modulates its hydrological impact. Although LSMs can have dynamic global vegetation models which predict the shift and competition between PFTs, there is no growth phase which is critical in determining the hydrological impact of vegetation. Improvements on the radiation and momentum exchange with the canopy is ongoing and this work does not add anything further to that debate. However, the current albedo calculated with afforestation may be slightly too high and leading to the extreme responses seen particularly in Chapter 5. This leads to potential overestimation of evaporation rates and the dramatic shifts in soil moisture simulated.

In essence, this work calls for further PFTs within JULES to represent the vegetation diversity present more accurately in woodland, from species to age. A critical step in this journey will require PFT parameters to both be accurate and fidelious. To do this, a methodology should be researched and developed that explicitly concentrates on the representation of vegetation within LSMs and how it would be more efficient and accessible to implement necessary PFTs for scientific endeavours.

6.3.2.3. Numerical Implementation

The numerical implementation of LSMs, particularly JULES, needs to evolve. Already comments arise on the haphazard nature of constructing many LSMs where concepts, systems and parameterisations have all been 'bolted on' over time. This has led to two major consequences.

Firstly, on a scientific front it has made them increasingly difficult to analyse the exact system processes occurring. This is for several reasons. There is such a 'spaghetti' of interactions it is almost impossible to follow the entire chain of events across the parameterisations. Within these parameterisations there can be unnamed variables and hard-coded constants which are unrealistic. If run at high resolutions, data memory outputs can be very high which limits the infrastructure able to hold and analyse outputs.

Secondly, the current nature of LSMs creates a very high bar for entry, particularly when trying to fully understand them. Due to the number of parametrisations, compiling and running the model can lead to multiple errors in which it is not possible to fully detect where the issue arises, and whether this is a computer, or process, issue. Breaking LSMs back down into their constituent parts to enable models to run independent of all other parts would allow more thorough identification and sensitivity analyses of what, and why, things occur within them. Initial work is separating processes within JULES, but this is an undertaking that needs to be replicated across all LSMs. Ideally, a community should continue growing to share and implement common practices and concepts. With the rise of machine learning being implemented within LSMs, this becomes increasingly important to enable efficient implementation and experimentation. Furthermore, machine learning should hopefully provide further opportunities to learn more about the world around us and enlighten new relationships and representations that could improve our most complex system models.

As time has progressed and computing power has increased in conjunction with our ability to implement our understanding of the world, we have disaggregated the numerical world into finer spatial and temporal units. However, this has potentially come at the expense of efficient and parsimonious implementations within LSMs. Grid cell complexity and heterogeneity are resolved by averaging and using tiles to represent different surfaces. This leads to two major problems evident in the sort of query developed here. Firstly, energy exchanges between the surface and atmosphere are averaged across the entire grid. When we increase one set of PFTs, its impact on energy fluxes is averaged across the grid and not applied to just the precise planting area. This could produce more extreme feedbacks becoming muted or minor surface impacts becoming amplified above certain other land surfaces. Secondly, there is no association with PFT location and local area properties (e.g., orography and soil). This is particularly important for the hydrological system as it dictates the vegetation response to atmospheric changes. One approach to improve hydrology in LSMs is to use hydrological

response units (HRUs) to group areas that function hydrologically similarly. Work is underway to disaggregate JULES into HRUs, and it may provide a step forward in both understanding model systems and accurately representing regional hydrology. This approach has been shown to be more efficient and at much lower computational cost than traditional LSMs (Torres-Rojas *et al.*, 2022). The solution may appear to run models at finer resolutions to produce more accurate answers, however this is likely to lead to effective parameters and parameterisations which produce inaccurate answers as they were unfaithful to begin with. As the community pushes towards 'hyper-resolution' models, this must be at the fore of LSM and ESM development.

Of minor, but important note, is the useability of JULES and LSMs in general. Although they are still often complicated to utilise due to computational expense and computer programming barriers, the ability to learn, implement and analyse the results in a few years should not be neglected. LSM evolution enables future collaboration and interdisciplinary work to take place which will be critical when improving future models and our understanding of Earth systems. Continued effort should improve the accessibility of such models as they provide the necessary focus for tackling the contemporary scientific challenges of our time.

6.4. Concluding Remarks

This work has provided an important step forward in helping us understand how widespread afforestation could influence hydrology in temperate climates. The approach employed to answer this question is novel and unique by using some of the most advanced Earth system numerical models to date at the limit of their capability. It has illuminated the need for a sufficiently complex representation of the hydrological system when asking questions about its current and potential future state.

Considering the work's wider impact, critically it has, using our proposed representation of the hydrosphere, demonstrated the relevant insignificance of land cover changes on terrestrial hydrology relative to potential climate changes. In the context of NFM, the spatial extent of afforestation required to substantially reduce high streamflow impacts on downstream communities is unlikely to be achieved. Therefore, although afforestation can be suggested to provide benefits for smaller flood events, it should not be advocated as flood management that

can prepare us for the most extreme future flood events caused by climate change. Furthermore, at large catchment scales (< 1000 km^2) specific planting locations of woodland could be indetectable in reducing flooding and this should also be accounted for when considering afforestation as an NFM measure.

The spatial extent of this inquiry, at a country scale, is unique in providing evidence at a scale not often explored at this process granularity when exploring woodland hydrology. There are many studies observing small catchments and those modelling at global and continental scales, but the gap in between has been neglected. Hopefully, the balance has been addressed here and generated impetus for others to explore woodland impact at a scale relevant to policymakers.

Using a LSM at such a high temporal and spatial resolution, and subsequently coupling it with a CPM, has also provided key lessons for the hydrological numerical modelling community. The implementation of soil and vegetation mechanics within LSMs has been tested by introducing a significant land cover disturbance and analysing the resulting output. We should continue to use these advanced models to find answers to contemporary challenges whilst critically examining outputs to enable improvements in model accuracy and fidelity. Additionally, the work here illustrates that when benchmarking our models, we should consider responses to the extremes and not just average conditions.

The final research piece is unique in coupling an LSM to a CPM to project the hydrometeorological consequences of widespread afforestation across the UK. No other work has explicitly simulated convection with these land cover changes in a future climate. In doing so this work has produced results of increased rainfall and runoff with afforestation that can be explored and compared with other future studies to determine their broad accuracy.

It should not be ignored that covering a significant area of the UK in woodland within these model domains has not only provided a glimpse of potential futures, but also a window into the past when there was a greater woodland coverage. Findings produced therefore have consequences that stretch further than the field of hydrology and could be used in any study attempting to unravel past processes (e.g., geomorphology).

To conclude, work here provides an extra thread in the overall tapestry of knowledge which ranges from hydrology to numerical models. It has pushed boundaries on previous attempts

and investigations, and lays foundations for future research into the complex relationship between woodland and hydrology.

Appendix 1: Understanding hydrological change with land surface models

This appendix section has been published as a Tools of the Trade article in Nature Reviews Earth and Environment. Marcus Buechel wrote the article which was further improved with review comments from Simon Dadson, Louise Slater and Erin Scott.

Citation: Buechel, M. Understanding hydrological change with land surface models. Nat Rev Earth Environ 2, 824 (2021). https://doi.org/10.1038/s43017-021-00241-0

The impact of anthropogenic climate change makes it increasingly necessary to elucidate land surface–atmosphere interactions to mitigate potential hazards such as flooding or wildfires. Observational data of the land surface can be spatially scarce, such as the global distribution of streamflow monitoring stations. This spatially scarce data, in combination with multiple inter-connected processes that affect the land surface, makes it difficult or impossible to identify the individual driving forces of these hazards.

Land surface models allow for investigations of the impact of climate change on hydrological cycles over a broad range of spatial (hundreds of metres to kilometres) and temporal (daily to decadal) scales that go beyond current observations. The Joint UK Land Environment Simulator (JULES) is a free to use, consistently evolving, community physics-based land surface model that is used to assess how various land surface processes interact with each other. There is a working environment for JULES to run on the supercomputer JASMIN, for high-resolution simulations. These simulations require meteorological, land cover and soil data inputs for the area under study. Each grid box within the model can be discretized into different tiles such as ‘plant functional types’ (broadleaf trees, needleleaf trees, grassland) or ‘non-vegetation types’ (urban, bare soil, inland water). During a simulation, carbon, energy and water fluxes are calculated for each surface type in the grid. By coupling JULES with atmospheric numerical models, such as the Met Office’s Unified Model, investigations can be tested on how changes in land cover and climate can impact hydrological and carbon land–atmosphere connections.

Land surface models like JULES will help further understanding and quantification of environmental hazards. For example, whether increasing afforestation could provide natural flood management in the future. By comparing theoretical worlds with and without climate interventions, JULES has also been used to determine the role international agreements have on reaching climate targets (for example, the Paris Agreement and Montreal Protocol). However, no numerical model can fully represent the complexity of the natural world. As anthropogenic climate change leads to unknown tipping points and feedbacks within land surface processes, such as the hydrological cycle, it will become more crucial for JULES to become increasingly interdisciplinary and to continually ground truth numerical models with observational data.

Appendix 2: Supplementary Tables and Figures for Chapter 3

Supplementary Table S3.1: Catchment properties for the twelve studied catchments as reported in the CAMELS-GB database (Coxon et al., 2020).

The lettering codes for the catchments are as labelled in Figure 3.1.

Catchment	Code	Mean Precipitation (mm day^{-1})	Mean PET (mm day^{-1})	Runoff Ratio	Stream Elasticity	Flow Duration Curve Slope	Baseflow Index	Area (km^2)	Mean Elevation (m)
Thames	A	1.99	1.42	0.27	1.9	3.56	0.59	9930.8	109
Severn-HB	B	2.22	1.4	0.42	1.65	2.61	0.58	9885.46	145
Tay	C	4.16	1.12	0.81	1.26	2.23	0.65	4586.79	411
Severn-B	D	2.55	1.38	0.46	1.49	2.87	0.55	4329.9	175
Ouse	E	2.52	1.35	0.53	1.61	2.78	0.45	3300.8	185
Clyde	F	3.28	1.22	0.68	1.27	2.65	0.46	1901.23	265
Dee	G	3.11	1.11	0.71	1.15	1.97	0.52	1833.21	447
Avon	H	2.33	1.43	0.44	1.23	1.99	0.86	1712.31	120
Derwent	I	2.15	1.37	0.42	1.18	2.04	0.7	1594.24	128
Ribble	J	3.73	1.32	0.67	1.32	3.1	0.34	1144.7	220
Tamar	K	3.43	1.44	0.62	1.43	3.39	0.47	920.22	155
Ure	L	3.76	1.28	0.73	1.43	3.33	0.32	510.94	366

Supplementary Table S3.2: Estimated changes in flow with afforestation, percentage and absolute for the streamflow quantiles, and just percentage for the three flow regime metrics. *These values are regression coefficients as calculated using median quantile regression.*

Catchment	Very High Flow		High Flow		Median Flow		Low Flow		Very Low Flow		Runoff Ratio	Flow Duration Slope	Median Elasticity
	%	mm day^{-1}	%	mm day^{-1}	%	mm day^{-1}	%	mm day^{-1}	%	mm day^{-1}	%	%	%
Dee	-0.056	-0.004	-0.101	-0.005	-0.178	-0.003	-0.287	-0.001	-0.384	-0.001	-0.145	0.043	-0.232
Tay	-0.127	-0.016	-0.192	-0.016	-0.120	-0.003	-0.030	0.000	-0.343	-0.002	-0.128	0.004	-0.312
Ouse	-0.099	-0.007	-0.131	-0.005	-0.273	-0.002	-0.219	0.000	-0.930	-0.001	-0.196	0.219	-0.323
Ure	-0.150	-0.027	-0.033	-0.003	-0.251	-0.003	-0.403	-0.001	-0.514	-0.001	-0.121	0.102	-0.278
Derwent	-0.100	-0.004	-0.161	-0.004	-0.465	-0.003	-0.718	-0.001	-1.263	-0.001	-0.273	0.169	-0.624
Thames	-0.175	-0.006	-0.225	-0.005	-0.277	-0.002	-0.319	-0.001	-0.413	0.000	-0.224	0.076	-0.384
Avon	-0.141	-0.008	-0.049	-0.002	-0.399	-0.002	-1.154	-0.001	-0.450	0.000	-0.213	0.072	-0.435
Tamar	-0.046	-0.005	-0.080	-0.005	-0.242	-0.002	-0.685	-0.001	-0.238	0.000	-0.130	0.119	-0.282
Severn-B	-0.140	-0.008	-0.145	-0.005	-0.292	-0.003	-0.339	-0.001	-0.565	-0.001	-0.232	0.213	-0.444
Severn-HB	-0.266	-0.010	-0.207	-0.005	-0.369	-0.003	-0.462	-0.001	-0.454	-0.001	-0.261	0.135	-0.578
Ribble	-0.089	-0.011	-0.074	-0.006	-0.247	-0.004	-0.473	-0.002	-0.224	-0.001	-0.142	0.151	-0.343
Clyde	-0.131	-0.010	-0.170	-0.009	-0.191	-0.003	-0.061	0.000	-0.374	-0.002	-0.181	0.090	-0.361

Supplementary Table S3.3: Spearman correlation coefficients between flow metric and percentage point increase in afforestation for each catchment.

All correlations are at least $p < 0.01$.

Catchment	Very High Flow	High Flow	Median Flow	Low Flow	Very Low Flow	Runoff Ratio	Flow Duration Slope	Median Elasticity
Dee	-0.15	-0.26	-0.66	-0.44	-0.33	-0.99	0.15	-0.95
Tay	-0.37	-0.75	-0.63	-0.50	-0.46	-0.99	0.02	-0.90
Ouse	-0.34	-0.63	-0.81	-0.74	-0.90	-0.96	0.75	-0.86
Ure	-0.51	-0.35	-0.87	-0.91	-0.90	-0.99	0.51	-0.98
Derwent	-0.29	-0.60	-0.75	-0.68	-0.65	-0.77	0.40	-0.48
Thames	-0.64	-0.72	-0.65	-0.60	-0.43	-0.79	0.26	-0.40
Avon	-0.59	-0.11	-0.88	-0.81	-0.81	-0.97	0.57	-0.95
Tamar	-0.35	-0.60	-0.84	-0.79	-0.59	-0.99	0.22	-0.94
Severn-B	-0.56	-0.56	-0.90	-0.85	-0.87	-0.98	0.75	-0.97
Severn-HB	-0.77	-0.68	-0.94	-0.77	-0.75	-0.96	0.38	-0.84
Ribble	-0.41	-0.56	-0.91	-0.92	-0.89	-0.99	0.53	-0.99
Clyde	-0.53	-0.60	-0.67	-0.64	-0.69	-0.80	0.55	-0.77

Supplementary Table S3.4: Conversion table of CEH Land cover 2000 (Fuller et al., 2002) land cover types to the eight types used by JULES in this study.

Left column indicates the twenty-six land cover types in the original CEH land cover dataset, and right column indicates the eight JULES land cover types that these original land cover types are converted to.

Type	Assigned Type
Broad-leaved / mixed woodland	Deciduous
Coniferous woodland	Coniferous
Arable cereals	Crop
Arable horticulture	Crop
Arable non-rotational	Shrub
Improved grassland	Grassland
Set-aside grass	Grassland
Neutral grass	Grassland
Calcareous grass	Grassland
Acid grassland	Grassland
Bracken	Shrub
Dense dwarf shrub heath	Shrub
Open dwarf shrub heath	Shrub
Fen, marsh, swamp	Grassland
Bog (deep peat)	Shrub
Water (inland)	Inland Water
Montane habitats	Shrub
Inland bare ground	Bare
Suburban / rural development	Urban
Continuous urban	Urban
Supra-littoral rock	Bare
Supra-littoral sediment	Bare
Littoral rock	NA
Littoral sediment	NA
Saltmarsh	Inland Water
Sea / Estuary	NA

Supplementary Table S3.5: Original land cover percentages for the eight land cover types without any additional afforestation for the year 2000.

Catchment	Deciduous	Coniferous	Grass	Shrub	Crop	Urban	Inland Water	Bare
Dee	3.21	16.27	14.74	54.64	2.89	0.48	0.5	7.36
Tay	4.29	11.82	35.91	31.28	7.64	0.55	2.79	5.8
Ouse	4.53	1.53	39.99	18.11	32.09	3.38	0.43	0.09
Ure	2.2	2.21	63.4	30.21	1.05	0.67	0.13	0.25
Derwent	8.13	9.06	25.28	14.23	40.94	2.29	0.13	0.06
Thames	11.31	2.1	33.82	0.58	37.06	14.01	1.15	0.12
Avon	6.94	2.43	41.53	2.81	42	3.86	0.36	0.18
Tamar	7.78	3.8	69.24	0.95	15.76	2.1	0.45	0.09
Severn-B	7.22	4.32	55.81	2.11	25.97	4.07	0.57	0.09
Severn-HB	7.06	2.7	48.96	1.16	32.48	7.23	0.49	0.08
Ribble	4.97	2.71	68.5	14.57	1.2	6.85	0.61	0.7
Clyde	4.4	12.43	57.26	12.25	4.98	7.41	0.68	0.72

Supplementary Table S3.6: Error metrics for the twelve catchments, ordered by Nash-Sutcliffe Efficiency (NSE) score [Methods].

Catchment	NSE	Log(NSE)	KGE	1/KGE	MAE	RMSE
Avon	-0.27	-1.14	0.41	-5.54	0.64	0.95
Derwent	0.50	-0.14	0.71	-3.32	0.38	0.57
Severn-B	0.53	0.52	0.71	0.28	0.58	0.92
Dee	0.55	0.69	0.56	0.50	0.79	1.54
Ure	0.63	0.52	0.70	-0.06	1.36	2.63
Tay	0.71	0.63	0.79	0.04	0.99	1.53
Ouse	0.71	0.66	0.72	0.03	0.54	0.90
Thames	0.71	0.51	0.63	0.29	0.25	0.36
Tamar	0.71	-Inf	0.71	NaN	0.97	1.44
Ribble	0.72	0.72	0.67	-0.20	0.96	1.96
Severn-HB	0.73	0.67	0.71	0.47	0.36	0.54
Clyde	0.75	0.65	0.72	0.67	0.80	1.19

Supplementary Table S3.7: Number of afforestation planting locations according to catchment structure.

Catchment	Strahler		Shreve		TWI	
	Inside	**Outside**	**Inside**	**Outside**	**Inside**	**Outside**
Dee	6	5	7	6	5	5
Tay	6	1,3,4,5	7	6	5	5
Ouse	6	5	7	6	5	5
Ure	5	4	7	6	5	5
Derwent	6	5	7	6	5	5
Thames	6	5	7	6	5	5
Avon	6	5	7	6	5	5
Tamar	6	From 2 to 5	7	6	5	5
Severn-B	7	6	7	6	5	5
Severn-HB	7	6	7	6	5	5
Ribble	6	From 2 to 5	7	6	5	5
Clyde	From 2 to 5	From 2 to 4	7	6	5	5

Supplementary Table S3.8: Area translation of what one percentage point area increase in broadleaf equates to in each catchment.

Catchment	Percentage Point Area (km^2)
Dee	18
Tay	46
Ouse	33
Ure	5
Derwent	16
Thames	99
Avon	17
Tamar	9
Severn[1]	43
Severn[2]	99
Ribble	11
Clyde	19

Supplementary Table S3.9: Topsoil moisture error metrics for the twelve COSMOS-UK sites, ordered by Nash-Sutcliffe Efficiency (NSE) score [Methods].

COSMOS-UK Site	NSE	KGE	R^2
Gisburn Forest	-33.58	0.26	0.36
Chobham Common	-7.93	0.23	0.62
Stiperstones	-6.32	0.20	0.70
Wytham Woods	-5.13	0.29	0.15
Hollin Hill	-4.93	0.34	0.61
Heytesbury	-4.63	0.52	0.73
Sheepdrove	-1.15	0.57	0.67
Alice Holt	-0.86	0.43	0.21
Chimney Meadows	0.29	0.68	0.79
Hartwood Home	0.47	0.45	0.51
Waddesdon	0.49	0.58	0.61
Rothamsted	0.81	0.82	0.84

Supplementary Table S3.10: Potential evapotranspiration error metrics for the twelve COSMOS-UK sites, ordered by Nash-Sutcliffe Efficiency (NSE) score [Methods].

COSMOS-UK Site	NSE	KGE	R^2
Hartwood Home	-0.46	0.22	0.55
Chimney Meadows	-0.23	0.27	0.62
Rothamsted	-0.13	0.32	0.62
Sheepdrove	0.11	0.46	0.62
Alice Holt	0.11	0.54	0.53
Heytesbury	0.13	0.51	0.57
Hollin Hill	0.20	0.55	0.59
Gisburn Forest	0.28	0.60	0.59
Stiperstones	0.43	0.70	0.61
Wytham Woods	0.44	0.47	0.67
Chobham Common	0.45	0.72	0.60
Waddesdon	0.46	0.69	0.57

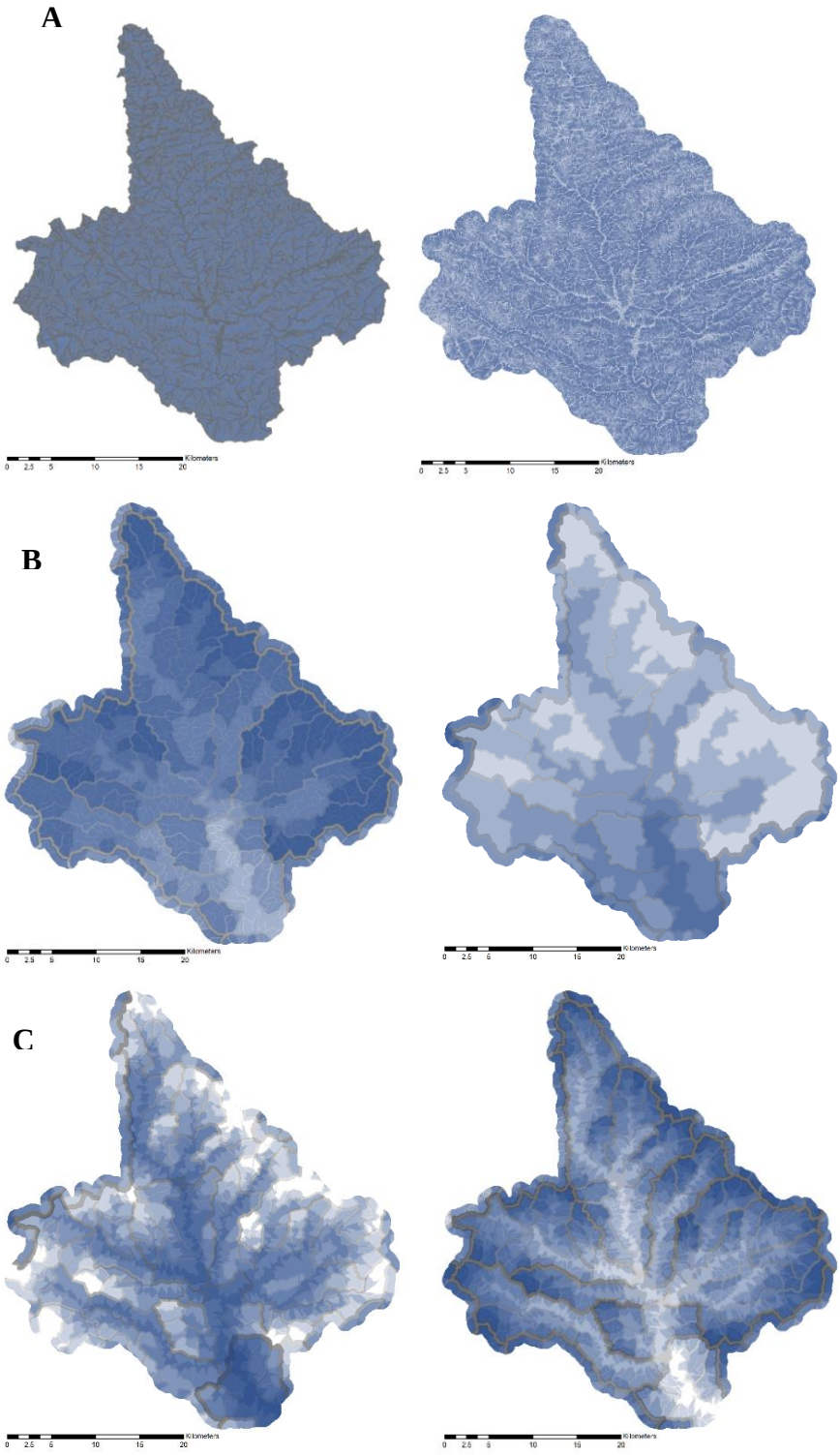

Supplementary Figure S3.1: Illustration of how the River Tamar was discretised into the different planting areas according to catchment structure.

Propensity for saturation (A), stream orders: Shreve (B) and Strahler (C). It shows inside (left) and outside (right) planting areas.

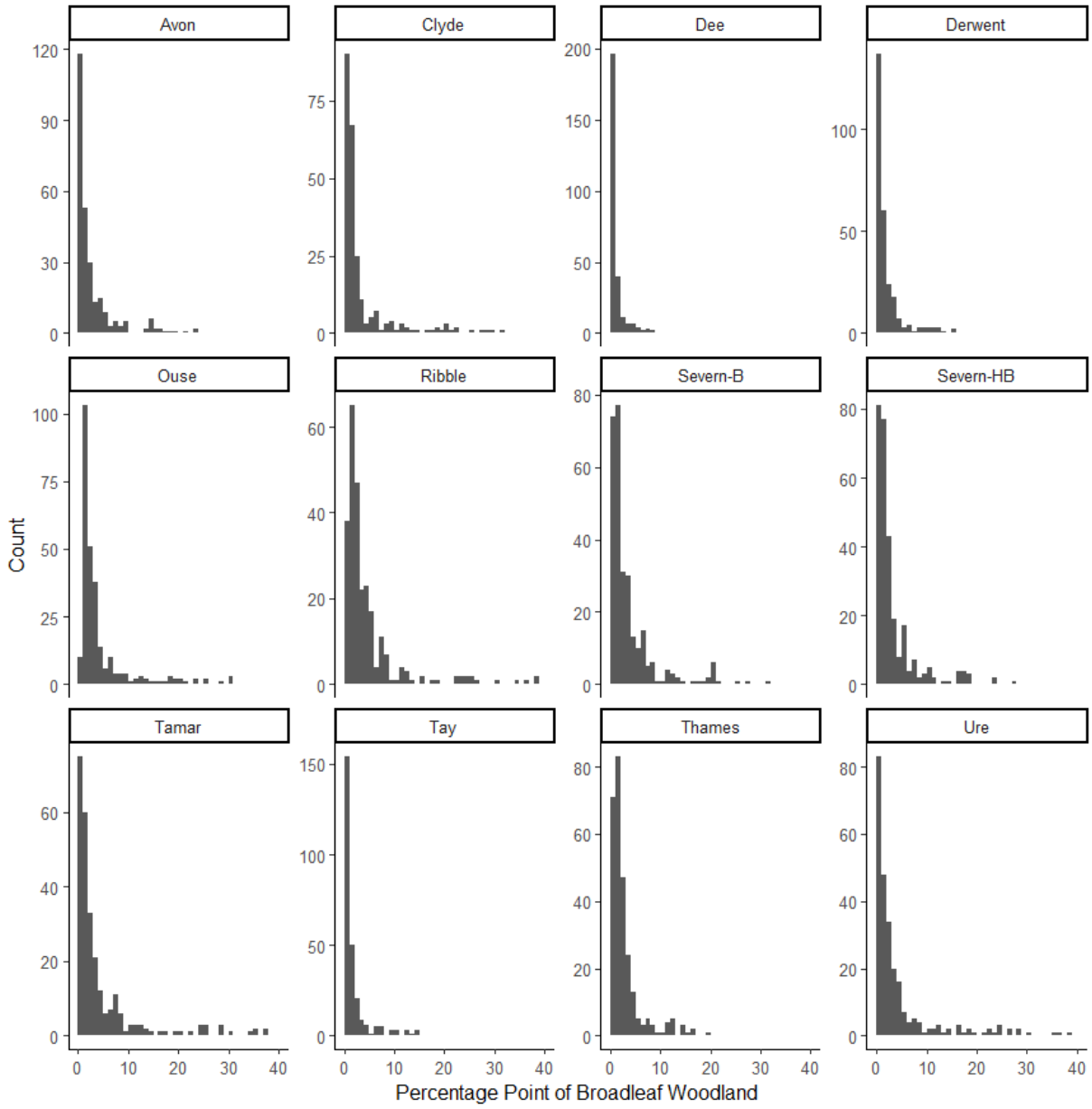

Supplementary Figure S3.2: Histograms illustrating the positive skew in generated afforestation scenarios.

This is driven by the conditions enforced on the planting scenarios.

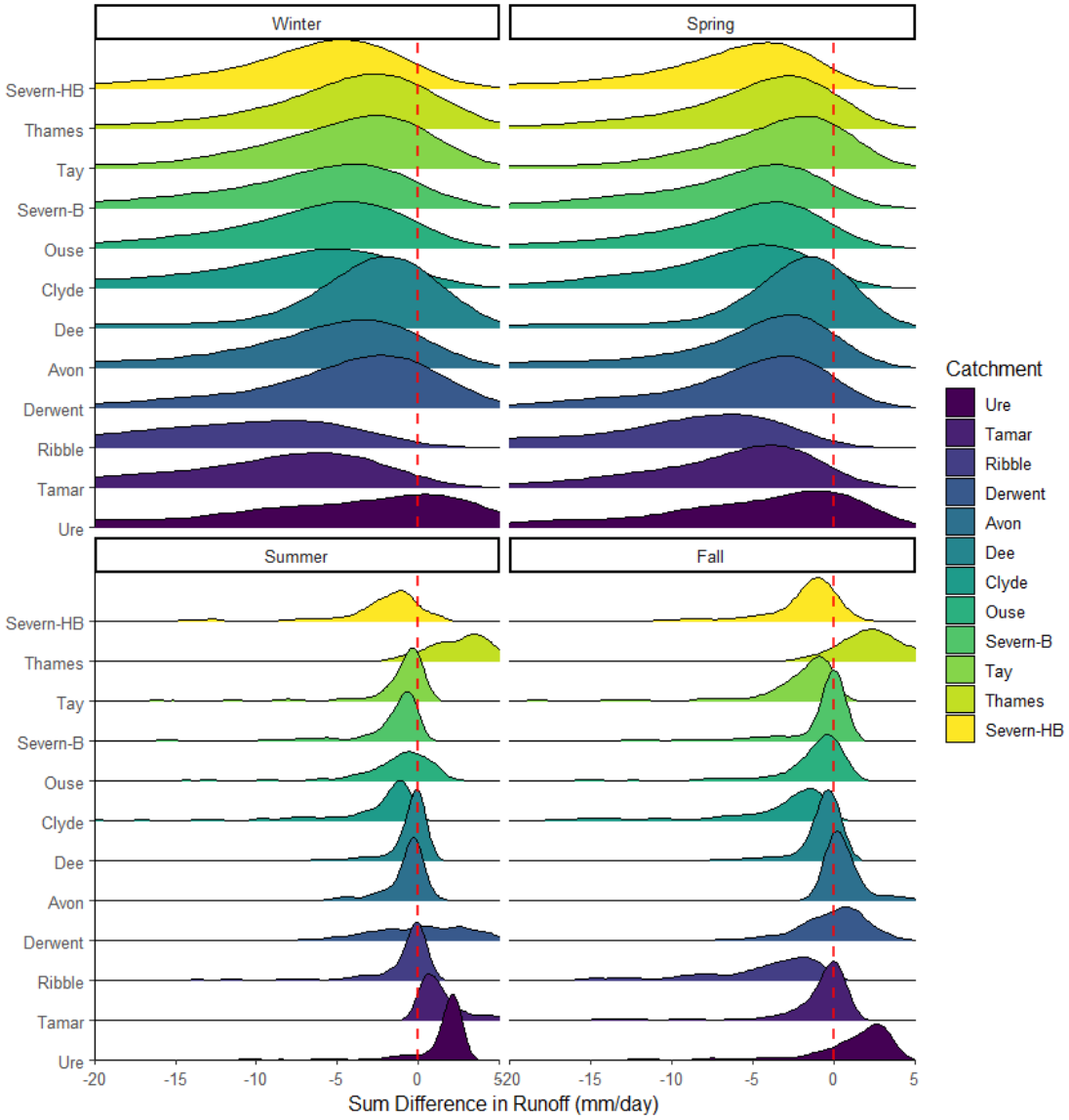

Supplementary Figure S3.3: Distributions of total seasonal runoff difference per catchment for all the afforestation scenarios within each catchment.

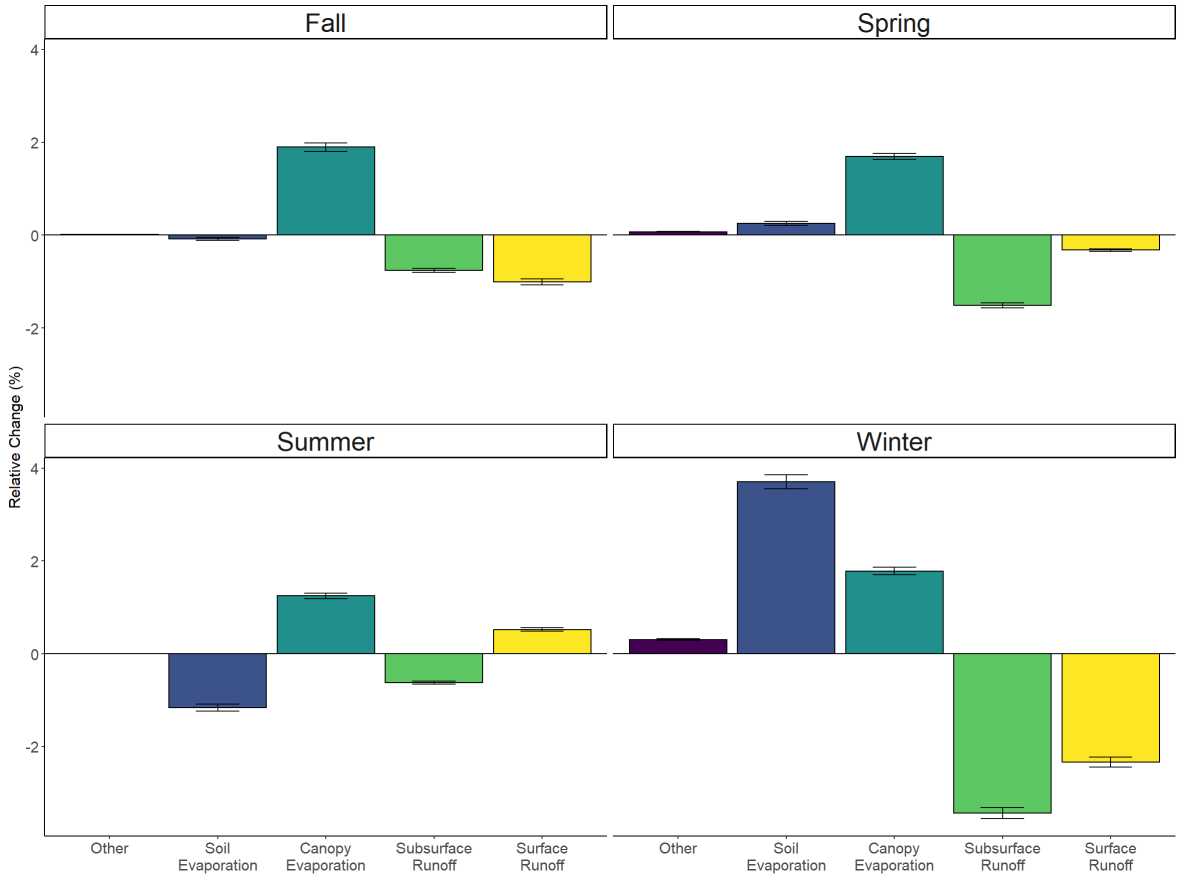

Supplementary Figure S3.4: Median percentage change in the relative fluxes for all catchments, except for the Ure and the Severn at Bewdley.

Error bars represent the standard error in the different catchments. This is the difference between the original land cover and 50 % possible increase in Shreve order 7, or the largest stream.

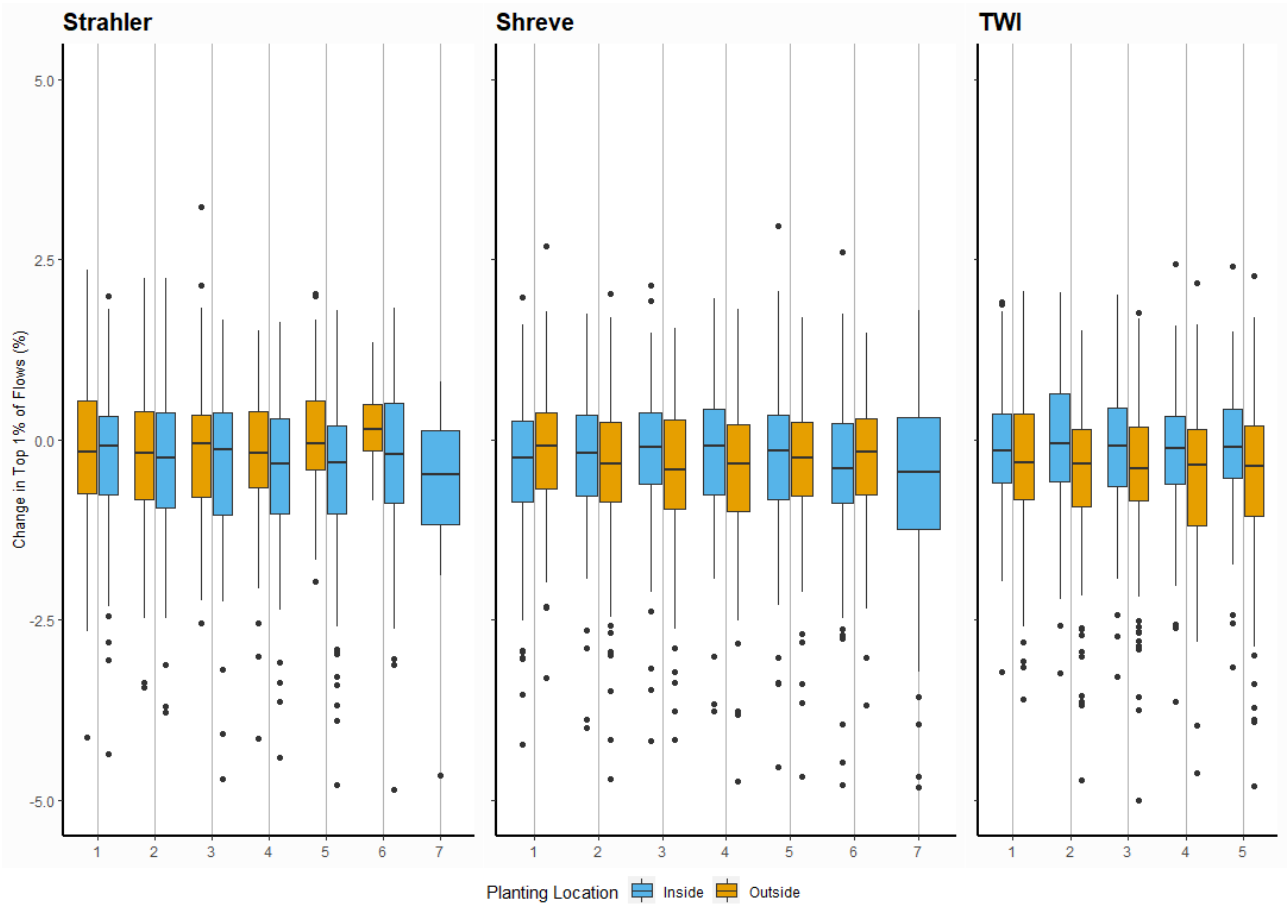

Supplementary Figure S3.5: Change in the very high flows inside and outside of the different catchment structure areas.

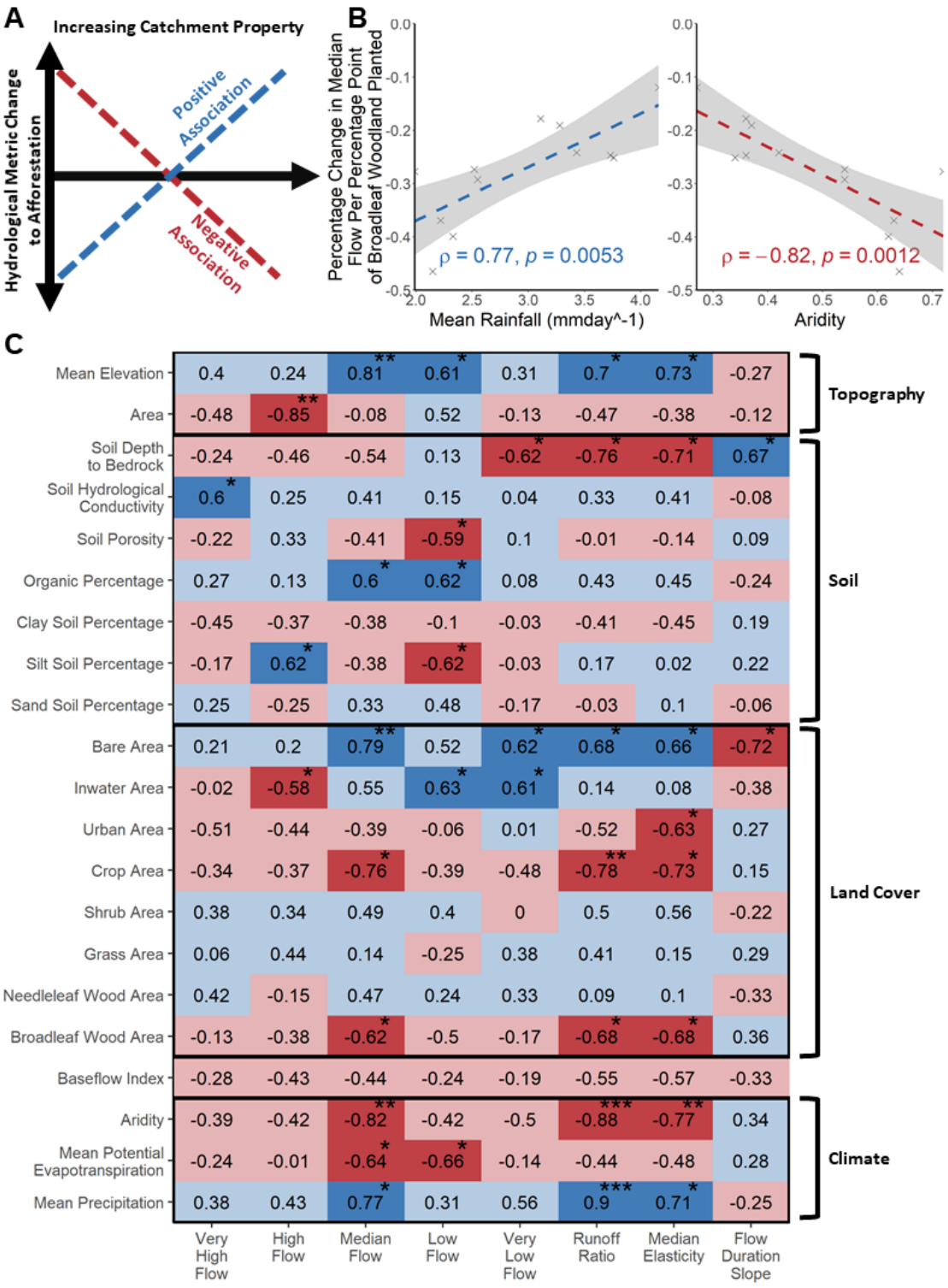

Supplementary Figure S3.6: Correlation table of factors with catchment attributes.

A) Shows the theoretical positive and negative associations of catchment response to afforestation. B) Illustrates the association of reductions in the median flow with mean

precipitation and aridity. C) Is the correlation table grouped by the different factors of climate, land cover, soil, and topography.

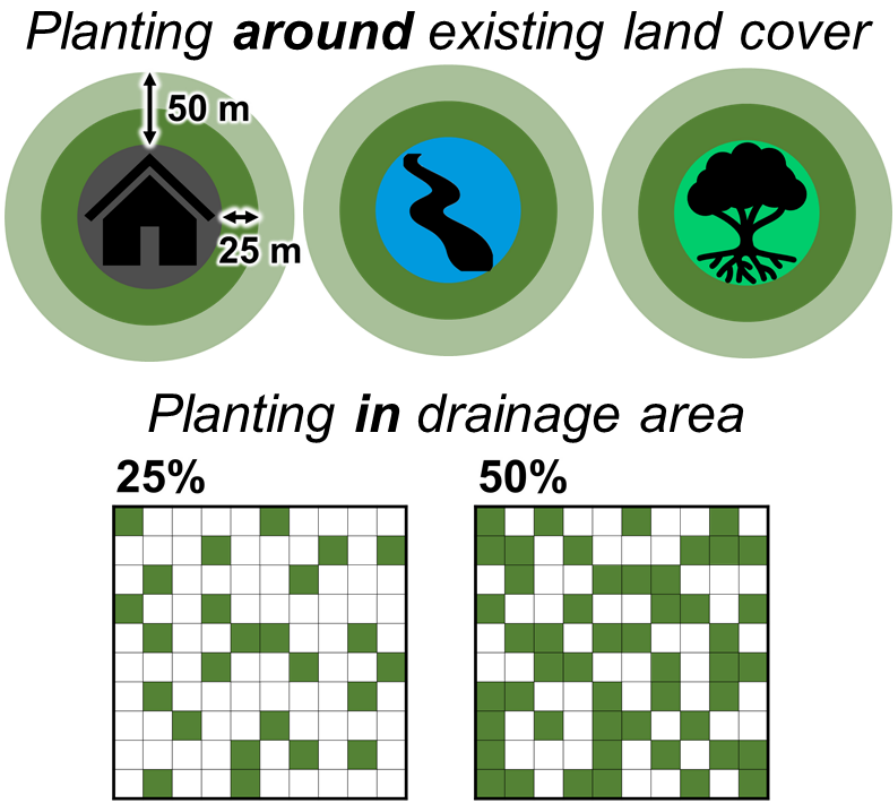

Supplementary Figure S3.7: Theoretical planting options for afforestation scenarios.

Either planting at 25 and 50 m buffers around existing urban, watercourses and broadleaf woodland or 25 or 50 % of a watershed.

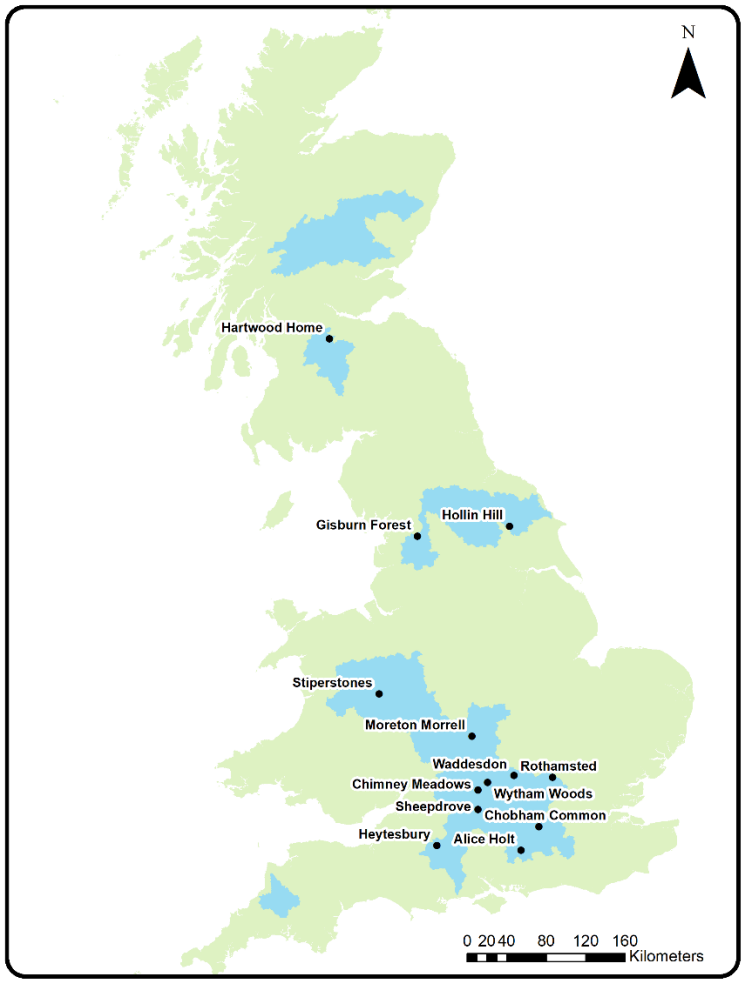

Supplementary Figure S3.8: Location of the COSMOS-UK sites used to validate model outputs.

Appendix 3: Supplementary Tables and Figures for Chapter 4

Supplementary Table S4.1: Error metrics for the 51 catchments in this study for the period 2000-2015.

Station	NSE	KGE	R^2
2002	0.36	0.43	0.39
7001	0.14	0.21	0.20
8004	0.06	0.28	0.19
8009	0.18	0.37	0.26
8013	0.10	0.40	0.26
11004	-0.11	0.47	0.39
12002	0.23	0.38	0.27
15006	0.48	0.68	0.53
17005	0.20	0.15	0.34
18001	0.41	0.48	0.48
21006	0.44	0.60	0.45
22001	0.16	0.39	0.23
23004	0.12	0.35	0.19
27009	0.45	0.61	0.48
27035	0.50	0.59	0.53
27041	0.46	0.70	0.59
33019	-0.18	0.15	0.42
34011	-0.03	0.30	0.64
37005	0.62	0.70	0.64
39001	0.66	0.63	0.78
40005	0.60	0.48	0.67
40011	0.47	0.64	0.70
43021	-0.27	0.40	0.44
45005	0.04	0.48	0.27
46003	0.49	0.53	0.53
47001	0.46	0.61	0.49
50002	0.42	0.49	0.43
53006	0.60	0.51	0.66
53008	0.55	0.53	0.61
54057	0.63	0.68	0.63
55014	0.05	0.55	0.41
55026	0.43	0.65	0.48
55029	0.23	0.58	0.35
60003	0.35	0.57	0.46
62001	0.67	0.66	0.70
64001	0.45	0.58	0.49
67033	0.58	0.76	0.64
68005	0.16	0.08	0.60
71001	0.19	0.42	0.24
72005	0.16	0.39	0.25
73005	0.25	0.50	0.34
79002	0.37	0.53	0.39

81002	0.25	0.48	0.30
81004	0.36	0.26	0.54
83006	0.22	0.30	0.23
84013	0.48	0.50	0.50
94001	0.39	0.67	0.61
96002	0.44	0.54	0.46
106001	0.38	0.35	0.64
107001	0.20	0.11	0.67

Supplementary Table S4.2: Topsoil moisture error metrics for the twelve COSMOS-UK sites [Supplementary Figure S4.2], ordered by Nash-Sutcliffe Efficiency (NSE) score.

COSMOS-UK Site	NSE	KGE	R^2
Gisburn Forest	-33.58	0.26	0.36
Chobham Common	-7.93	0.23	0.62
Stiperstones	-6.32	0.20	0.70
Wytham Woods	-5.13	0.29	0.15
Hollin Hill	-4.93	0.34	0.61
Heytesbury	-4.63	0.52	0.73
Sheepdrove	-1.15	0.57	0.67
Alice Holt	-0.86	0.43	0.21
Chimney Meadows	0.29	0.68	0.79
Hartwood Home	0.47	0.45	0.51
Waddesdon	0.49	0.58	0.61
Rothamsted	0.81	0.82	0.84

Supplementary Table S4.3: Potential evapotranspiration error metrics for the twelve COSMOS-UK sites [Supplementary Figure S4.2], ordered by Nash-Sutcliffe Efficiency (NSE) score.

COSMOS-UK Site	NSE	KGE	R^2
Hartwood Home	-0.46	0.22	0.55
Chimney Meadows	-0.23	0.27	0.62
Rothamsted	-0.13	0.32	0.62
Sheepdrove	0.11	0.46	0.62
Alice Holt	0.11	0.54	0.53
Heytesbury	0.13	0.51	0.57
Hollin Hill	0.20	0.55	0.59
Gisburn Forest	0.28	0.60	0.59
Stiperstones	0.43	0.70	0.61
Wytham Woods	0.44	0.47	0.67
Chobham Common	0.45	0.72	0.60
Waddesdon	0.46	0.69	0.57

Supplementary Table S4.4: Catchment attributes for those in this study as derived from the CAMELS-GB dataset.

Also included is the percentage increase in woodland for the catchments.

Station	Mean Precipitation (mm day^{-1})	Mean Potential Evapotranspiration (mm day^{-1})	Runoff Ratio	Area (km^2)	Mean Elevation (m)	Percentage Increase in Woodland	Percentage Point Increase in Woodland
2002	3.41	1.11	0.72	423.48	259.00	2400.56	6.31
7001	3.42	1.07	0.87	415.59	560.00	279.83	5.06
8004	3.08	1.07	0.75	540.75	525.00	191.08	6.99
8009	2.83	1.09	0.69	272.20	461.00	513.50	6.66
8013	3.68	1.03	0.78	229.63	618.00	243.06	1.10
11004	2.44	1.20	0.59	195.44	206.00	649.39	18.38
12002	3.11	1.11	0.71	1833.21	447.00	197.31	5.86
15006	4.16	1.12	0.81	4586.79	411.00	137.37	7.11
17005	2.87	1.25	0.65	194.81	161.00	165.89	13.64
18001	4.10	1.20	0.72	160.29	245.00	446.06	13.37
21006	3.35	1.21	0.64	1505.54	358.00	282.73	11.75
22001	2.39	1.32	0.53	578.25	225.00	33.76	2.28
23004	3.18	1.26	0.66	749.89	350.00	16.95	0.69
27009	2.52	1.35	0.53	3300.80	185.00	13.87	0.76
27035	3.18	1.33	0.63	283.39	230.00	132.47	6.42
27041	2.15	1.37	0.42	1594.24	128.00	2.82	0.23
33019	1.76	1.48	0.30	311.37	39.00	13.93	1.28
34011	1.94	1.47	0.23	162.93	62.00	2.95	0.17
37005	1.61	1.47	0.25	235.88	66.00	2.02	0.13
39001	1.99	1.42	0.27	9930.80	109.00	9.23	1.25
40005	1.94	1.40	0.33	278.05	45.00	1.75	0.23
40011	2.10	1.40	0.38	341.26	84.00	0.68	0.10
42016	2.41	1.41	0.67	234.17	123.00	0.04	0.00
43021	2.33	1.43	0.44	1712.31	120.00	0.43	0.04
45005	2.75	1.45	0.50	202.83	144.00	2.28	0.25
46003	5.16	1.42	0.75	249.99	327.00	0.03	0.00
47001	3.43	1.44	0.62	920.22	155.00	69.29	6.09
50002	3.37	1.43	0.61	664.25	160.00	44.87	5.23
53006	2.29	1.43	0.44	151.63	73.00	11.16	0.55
53008	2.27	1.44	0.42	305.17	119.00	10.48	0.76
54057	2.22	1.40	0.42	9885.46	145.00	24.56	2.20
55014	2.84	1.36	0.59	202.54	299.00	181.38	7.88
55026	4.61	1.33	0.76	172.12	387.00	337.28	6.18

55029	2.73	1.38	0.54	355.01	228.00	11.03	1.27
60003	4.02	1.43	0.76	216.44	125.00	381.18	18.33
62001	3.85	1.37	0.74	897.59	209.00	193.36	12.63
64001	5.18	1.32	0.85	464.61	281.00	70.36	6.30
67033	3.11	1.35	0.51	1800.75	242.00	50.66	3.28
68005	1.96	1.41	0.34	201.38	89.00	13.30	0.54
71001	3.73	1.32	0.67	1144.70	220.00	55.52	4.12
72005	4.72	1.27	0.85	219.24	317.00	40.66	1.37
73005	4.88	1.29	0.78	212.24	234.00	69.51	3.89
79002	4.22	1.22	0.74	797.71	294.00	432.43	14.44
81002	5.20	1.25	0.73	366.21	238.00	63.01	2.21
81004	3.87	1.33	0.67	329.07	105.00	140.46	4.29
83006	3.51	1.23	0.66	579.03	219.00	552.96	12.03
84013	3.28	1.22	0.68	1901.23	265.00	334.33	13.56
94001	6.49	1.07	0.90	441.21	311.00	6.01	0.08
96002	3.81	1.08	0.75	474.01	224.00	358.55	5.03
106001	4.16	1.13	0.78	44.93	100.00	0.00	0.00
107001	3.16	1.07	0.73	19.60	99.00	1.75E+20	5.58

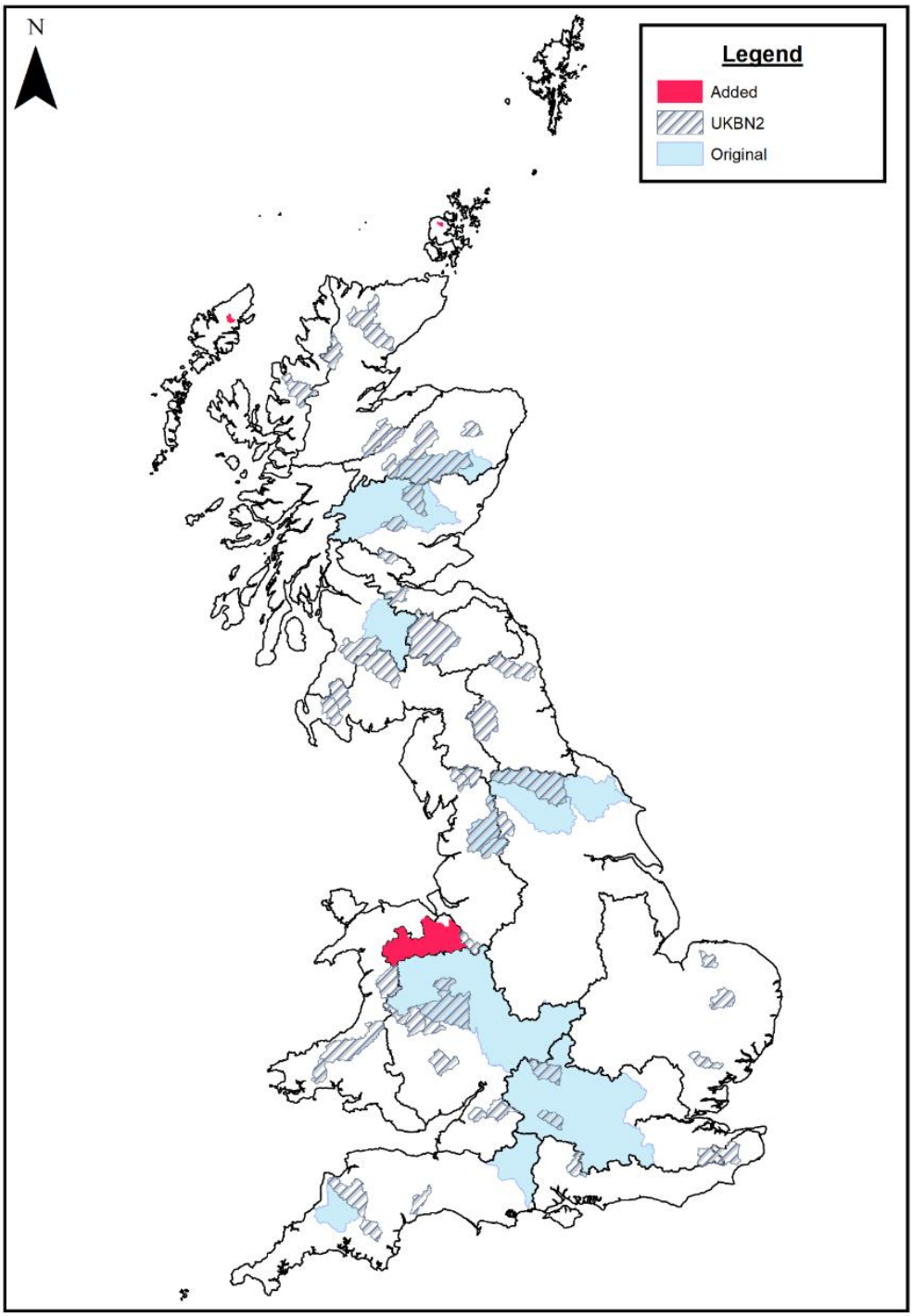

Supplementary Figure S4.1: Map of the 51 catchments used to study streamflow changes to afforestation and climate.

They include the original catchments studied in Buechel et al. (2022), near-natural catchments over 150 km2 from the UKBN2 network and the catchment for the Dee and regions in Scottish hydro-regions where there were no catchments from the initial selection.

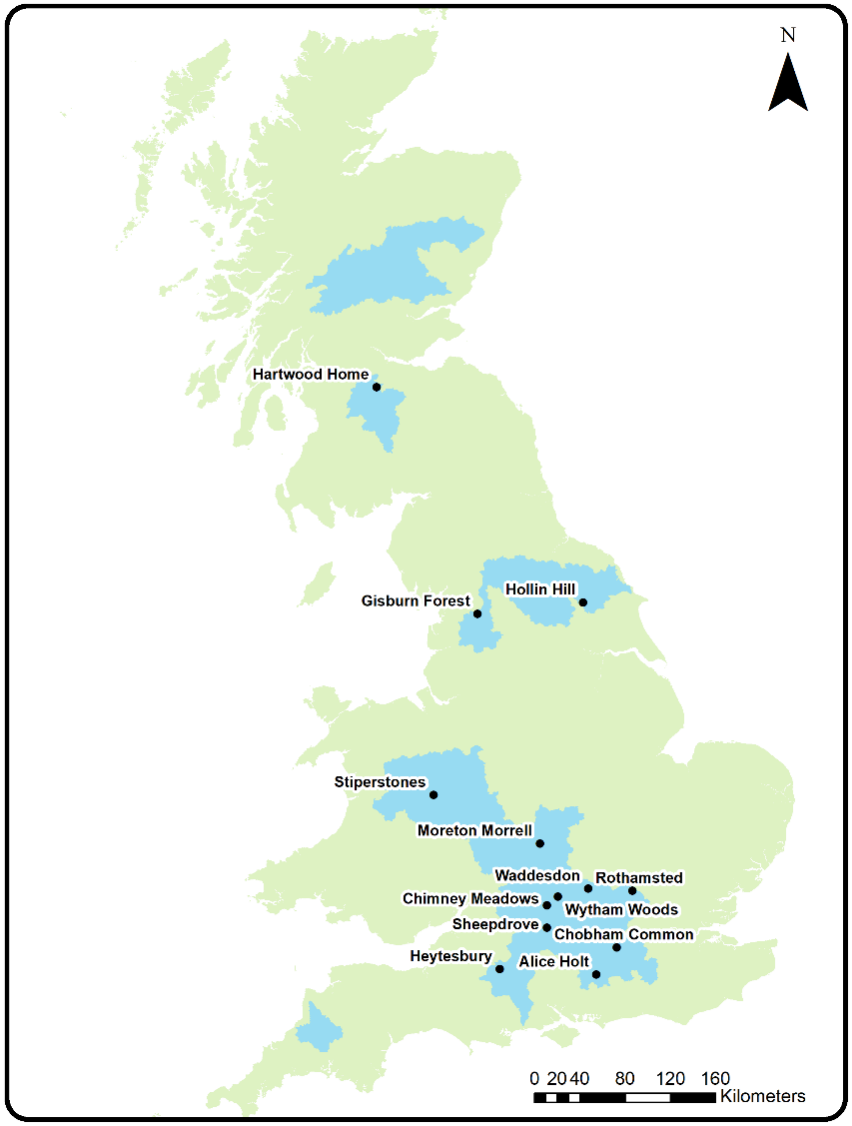

Supplementary Figure S4.2: Location of the COSMOS-UK sites used to validate model outputs.

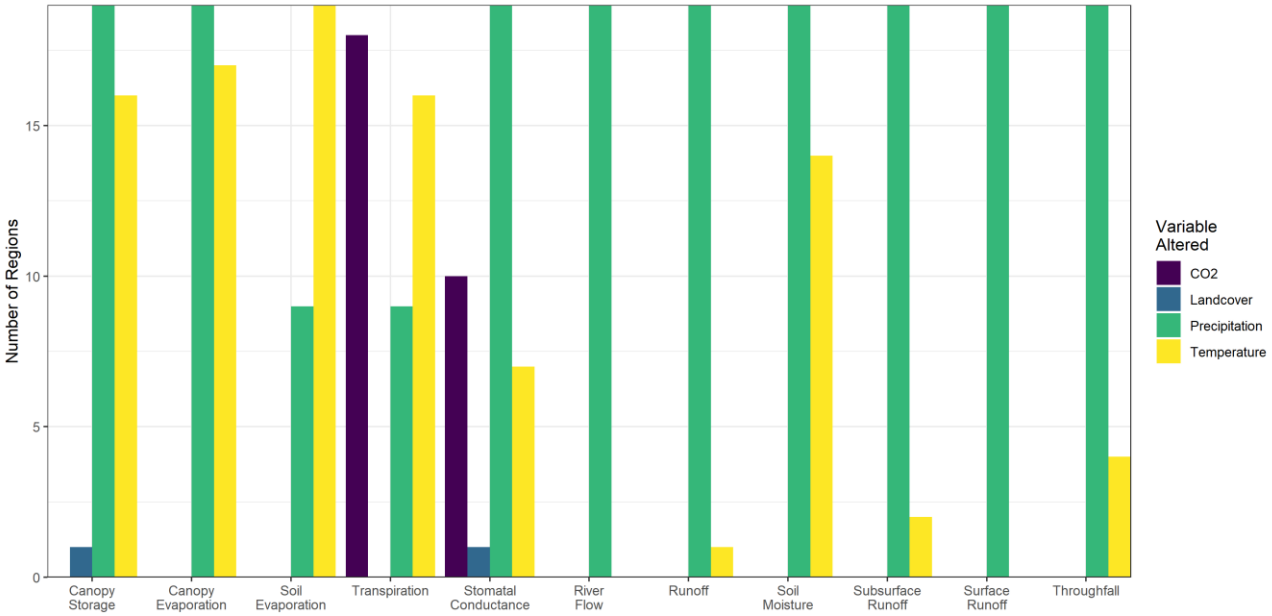

Supplementary Figure S4.3: Number of UKCP18 regions that show significant changes ($p < 0.01$ with ANOVA) in the system states (on the x axis), for the entire period for the four variables altered: CO_2, afforestation (landcover), precipitation and temperature.

Only in the Orkney and Shetland region are significant changes seen due to afforestation. Supplementary Material Figure S4 shows how this varies per season. Northeast Scotland not included due to computational issues.

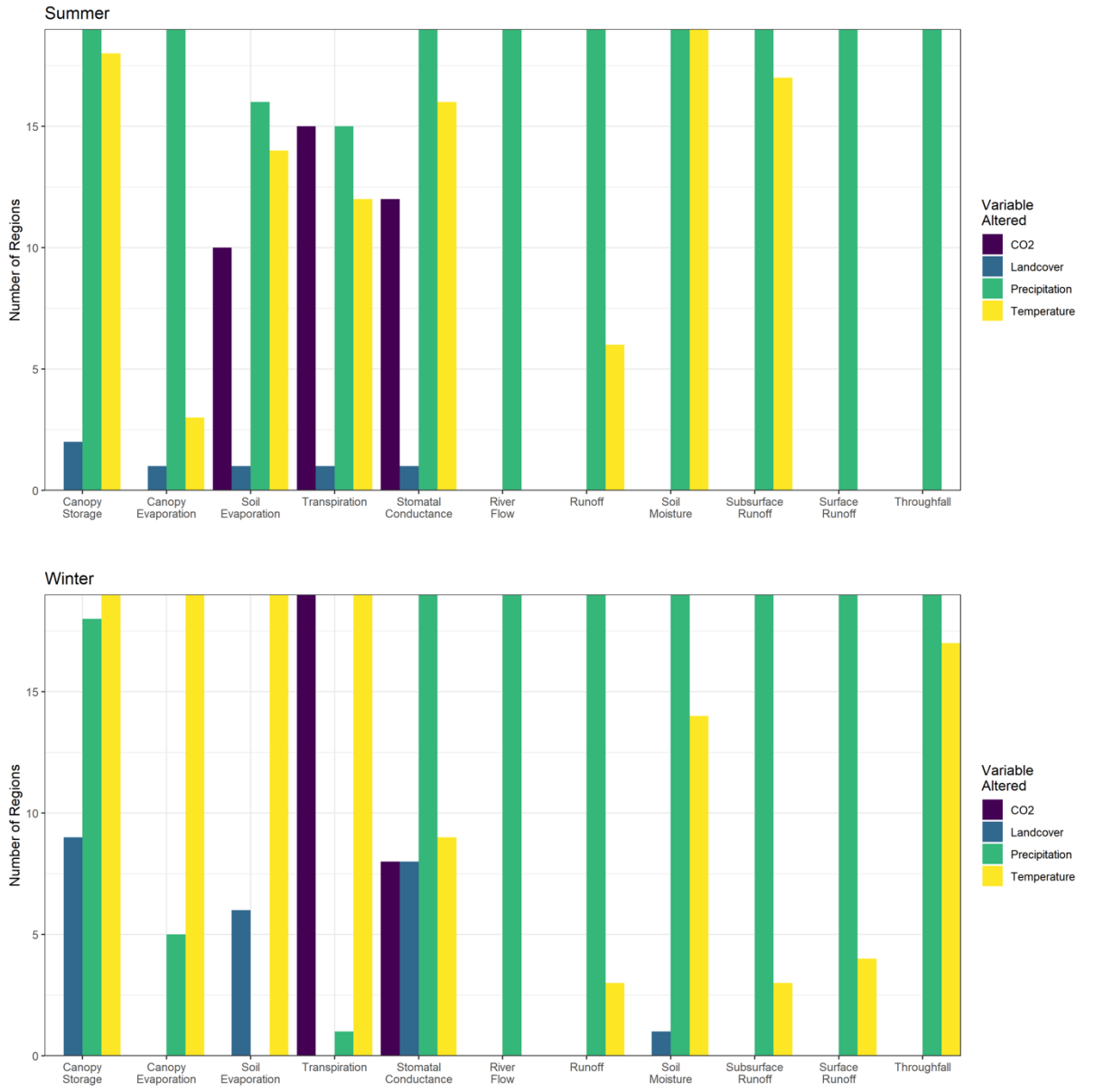

Supplementary Figure S4.4: Number of UKCP18 regions that show significant changes ($p < 0.01$ with ANOVA) in the system states (on the x axis), for the entire period for the four variables altered: CO_2, afforestation (landcover), precipitation and temperature.

The graphs are for winter and summer. Northeast Scotland not included due to computational issues.

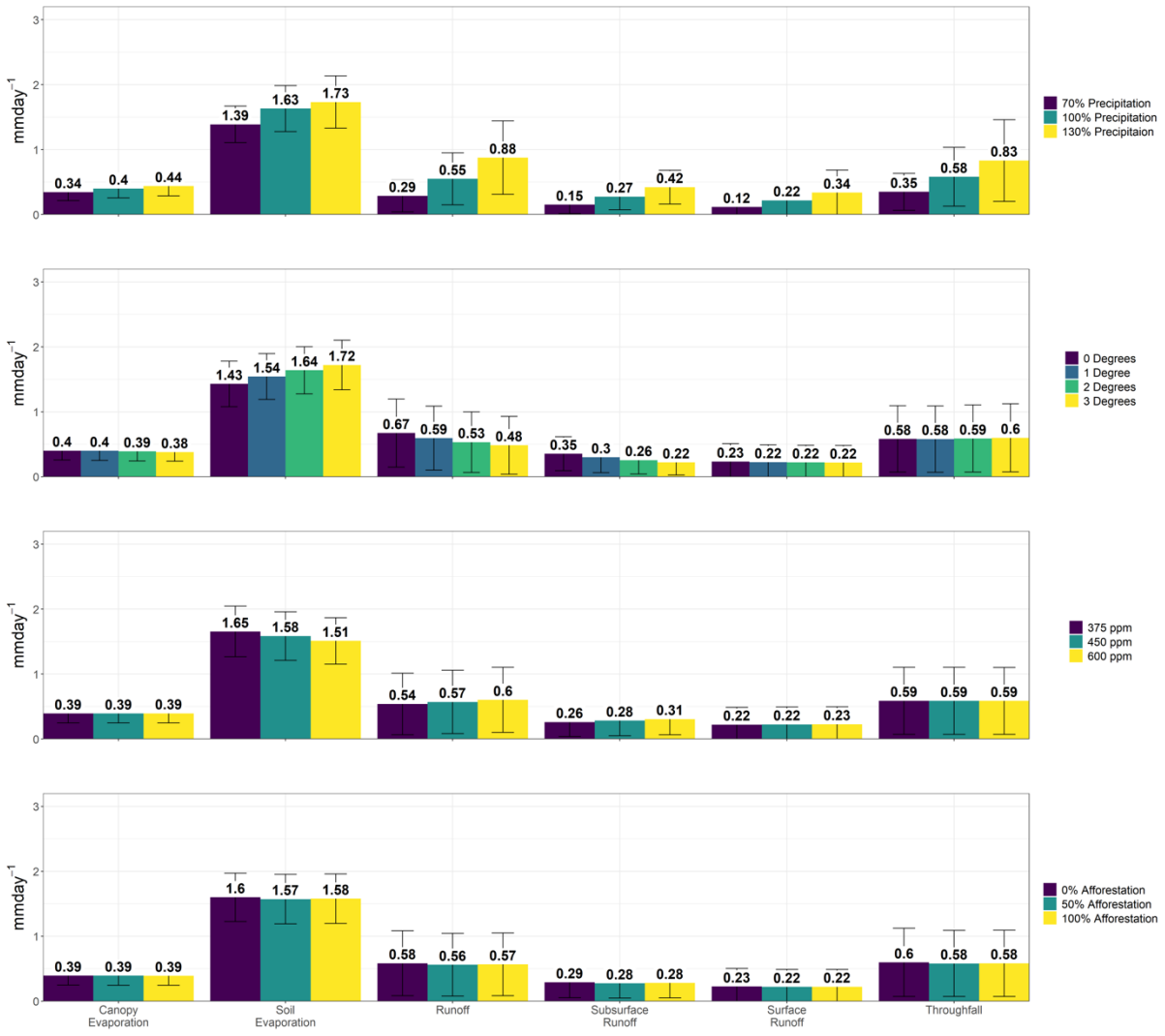

Supplementary Figure S4.5: Mean hydrological fluxes across all UKCP18 regions in summer for each of the four variables altered: precipitation, temperature, CO2 and landcover.

Error bars indicate one standard deviation.

Appendix 4: Supplementary Tables and Figures for Chapter 5

Supplementary Table S5.1: Amount of additional woodland for the 23 UKCP18 hydro-regions.

Region	**Percentage Point Increase in Woodland**	**Absolute Change (km^2)**
Anglian	53.15	11662
Argyll	14.64	1478
Clyde	50.71	3583
Dee	71.99	1270
Forth	59.29	2331
Humber	34.78	8504
Neagh Bann	16.24	1216
Northeast Scotland	51.46	4951
North-eastern Ireland	27.08	798
North Highland	27.06	3927
Northwest England	53.66	5948
North-western Ireland	11.77	1241
Northumbria	52.14	4139
Orkney and Shetland	38.60	1159
Severn	44.42	8323
Solway	55.75	5198
Southeast England	22.18	1589
Southwest England	27.14	4153
Tay	53.83	5378
Thames	27.83	3902
Tweed	66.71	3296
West Highland	7.44	758
Western Wales	77.64	8752

Supplementary Table S5.2: Median percentage change in variables with afforestation for each percentage point increase in woodland, as calculated using the quantile regression coefficient, with associated spearman correlation coefficient and p value.

This is disaggregated by season and calculated using the calculated percentage change in the variable for each region compared to the percentage point increase of woodland.

Variable	Season	Quantile Regression Coefficient	Spearman	P Value
Canopy Evaporation	Winter	0.13	**0.65**	0.00
	Spring	-0.02	-0.31	0.15
	Summer	0.04	0.40	0.06
	Fall	0.15	**0.82**	0.00
Soil Evaporation	Winter	0.53	**0.91**	0.00
	Spring	-0.12	**-0.56**	0.01
	Summer	-0.27	**-0.94**	0.00
	Fall	0.10	**0.53**	0.01
Overall Evaporation	Winter	0.31	**0.93**	0.00
	Spring	-0.11	**-0.56**	0.01
	Summer	-0.24	**-0.95**	0.00
	Fall	0.10	**0.72**	0.00
Soil Moisture	Winter	0.01	0.32	0.14
	Spring	0.01	**0.39**	0.06
	Summer	0.22	**0.63**	0.00
	Fall	0.20	**0.47**	0.03
Potential Evapotranspiration	Winter	2.41	**0.68**	0.00
	Spring	2.32	**0.85**	0.00
	Summer	2.72	**0.91**	0.00
	Fall	2.23	**0.80**	0.00
Precipitation	Winter	0.03	**0.56**	0.01
	Spring	0.01	0.07	0.76
	Summer	-0.01	-0.05	0.83
	Fall	0.04	0.48	0.02
Total Liquid Cloud Volume	Winter	0.03	**0.73**	0.00
	Spring	0.01	0.19	0.38
	Summer	-0.02	-0.41	0.05
	Fall	0.02	**0.51**	0.01
Specific Humidity	Winter	0.01	**0.79**	0.00
	Spring	0.00	-0.07	0.74
	Summer	-0.02	**-0.80**	0.00
	Fall	0.01	**0.56**	0.01
Rainfall	Winter	0.02	0.33	0.12
	Spring	0.00	0.03	0.90
	Summer	-0.02	-0.06	0.79
	Fall	0.04	0.50	0.02

Variable	Season	Quantile Regression Coefficient	Spearman	P Value
	Winter	0.01	**0.66**	0.00
	Spring	-0.01	-0.16	0.45
	Summer	-0.03	**-0.83**	0.00
Relative Humidity	Fall	0.01	**0.55**	0.01
	Winter	0.08	0.50	0.02
	Spring	0.04	**0.54**	0.01
	Summer	0.31	**0.87**	0.00
Subsurface Runoff	Fall	0.36	**0.62**	0.00
	Winter	0.05	0.41	0.06
	Spring	-0.01	-0.15	0.50
	Summer	-0.14	**-0.74**	0.00
Surface Runoff	Fall	0.03	0.09	0.67
	Winter	-0.08	**-0.62**	0.00
	Spring	-0.14	**-0.80**	0.00
	Summer	-0.18	-0.13	0.55
Snow	Fall	-0.02	0.06	0.78
	Winter	-3.90E-05	0.12	0.59
	Spring	6.49E-04	**0.75**	0.00
	Summer	1.60E-03	**0.80**	0.00
Temperature at 1.5 m	Fall	3.09E-04	0.48	0.02

Supplementary Table S5.3: Median percentage change in variables with afforestation for each percentage point increase in woodland, as calculated using the quantile regression coefficient, with associated spearman correlation coefficient and p value.

This is calculated using the calculated percentage change in the variable for each region for the overall period compared to the percentage point increase of woodland.

Variable	**Quantile Regression Coefficient**	**Spearman**	**P Value**
Canopy Evaporation	0.076	0.48	0.022
Soil Evaporation	-0.114	-0.75	0.000
Soil Moisture	0.093	0.66	0.001
Potential Evapotranspiration	2.438	0.85	0.000
Precipitation	0.020	0.40	0.058
Total Liquid Cloud Volume	0.008	0.45	0.034
Specific Humidity	0.001	0.01	0.959
Relative Humidity	-0.004	-0.07	0.754
Subsurface Runoff	0.151	0.75	0.000
Surface Runoff	-0.018	-0.26	0.227
Snow	-0.099	-0.69	0.000
Temperature at 1.5 m	0.001	0.72	0.000

Supplementary Table S5.4: Absolute and percentage changes in rainfall, evaporation, runoff and soil moisture across the different countries of the United Kingdom for the entire period following afforestation.

Region	**Season**	**Rainfall**		**Runoff**		**Evaporation**		**Soil Moisture**	
		mm	**%**	**mm**	**%**	**mm**	**%**	**Kg m^{-2}**	**%**
United Kingdom	Winter	6.86	1.63	11.03	4.31	8.06	15.62	1.64	1.11
	Spring	2.24	0.88	5.40	2.82	-4.87	-3.17	1.71	1.27
	Summer	2.19	1.10	6.55	6.24	-20.64	-9.98	10.87	12.52
	Fall	6.67	2.24	10.56	8.59	5.58	6.45	11.34	11.72
Great Britain	Winter	6.76	1.61	11.00	4.31	8.34	16.14	1.67	1.14
	Spring	2.17	0.85	5.31	2.79	-4.86	-3.15	1.69	1.27
	Summer	2.21	1.12	6.58	6.32	-21.37	-10.35	11.20	13.05
	Fall	6.61	2.22	10.59	8.61	5.77	6.68	11.71	12.25
England	Winter	4.09	1.23	7.90	5.31	9.29	16.68	2.28	1.63
	Spring	1.65	0.80	3.39	2.75	-2.46	-1.52	1.90	1.49
	Summer	1.16	0.77	2.80	3.86	-19.00	-9.50	12.08	16.56
	Fall	5.51	2.50	6.36	9.08	5.93	7.24	13.85	17.81
Scotland	Winter	8.46	1.60	11.47	2.81	4.98	11.68	0.51	0.33
	Spring	2.23	0.69	7.24	2.51	-7.85	-5.67	1.32	0.95
	Summer	3.70	1.33	11.52	7.37	-19.59	-9.39	8.27	7.95
	Fall	6.84	1.66	15.17	7.15	4.50	5.00	6.40	5.25
Wales	Winter	17.17	3.15	28.73	8.28	14.95	24.93	2.22	1.32
	Spring	5.17	1.75	10.11	4.10	-8.80	-5.35	1.78	1.16
	Summer	3.15	1.64	11.86	11.12	-42.97	-18.05	16.72	16.94
	Fall	12.71	3.61	20.11	16.44	9.55	9.45	18.18	16.64
Northern Ireland	Winter	8.44	1.92	11.61	4.21	3.53	7.02	1.06	0.68
	Spring	3.41	1.28	6.88	3.21	-5.03	-3.46	1.91	1.33
	Summer	1.98	0.92	6.14	5.16	-8.89	-4.12	5.54	5.37
	Fall	7.57	2.44	10.11	8.19	2.47	2.76	5.30	4.60

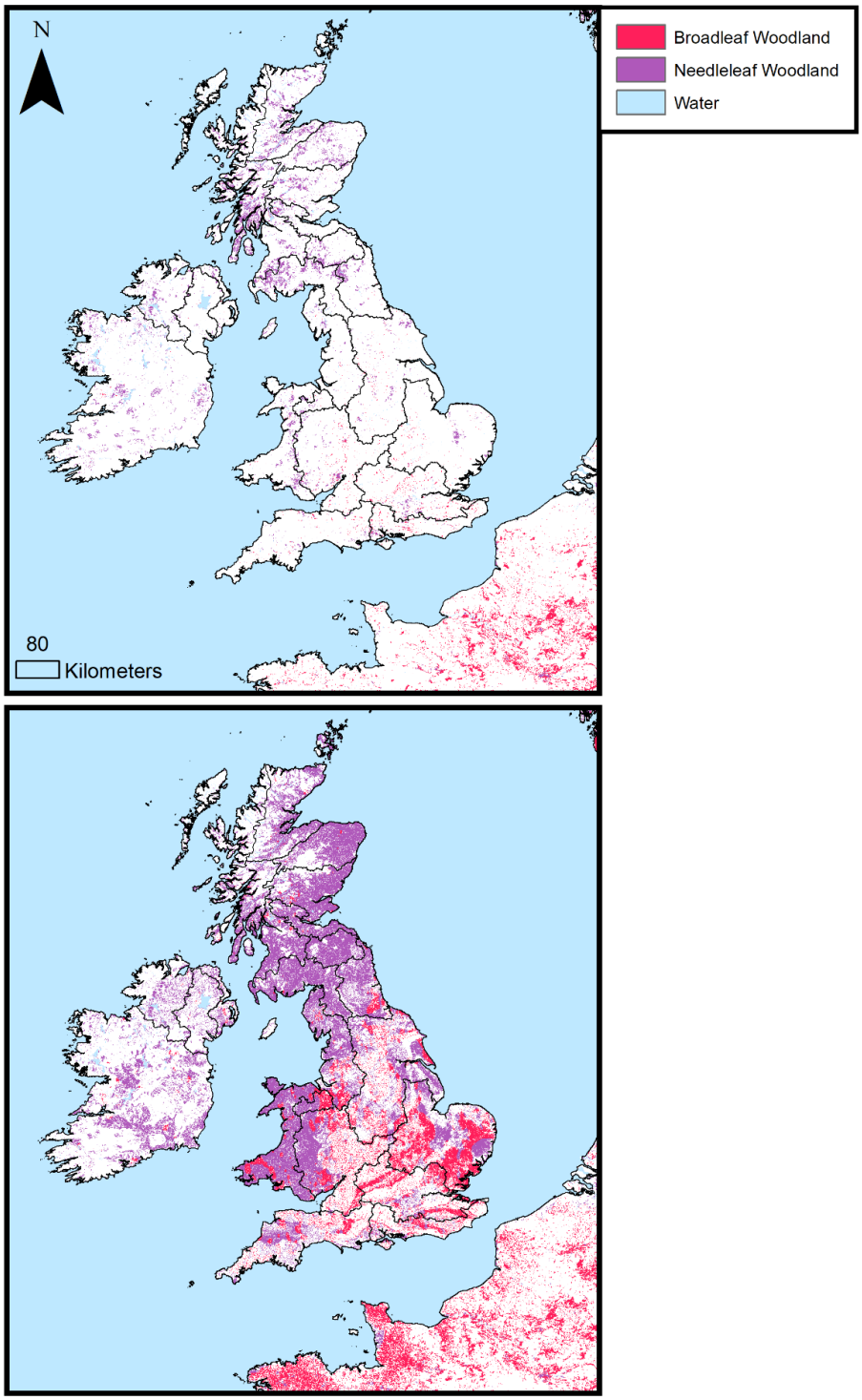

Supplementary Figure S5.1: The top panel shows the initial distribution of broadleaf and needleleaf woodland areas within the model domain and the bottom panel shows the afforestation expansion scenario disaggregated by the two tree types.

Figure S5.15 shows the original distribution of land cover.

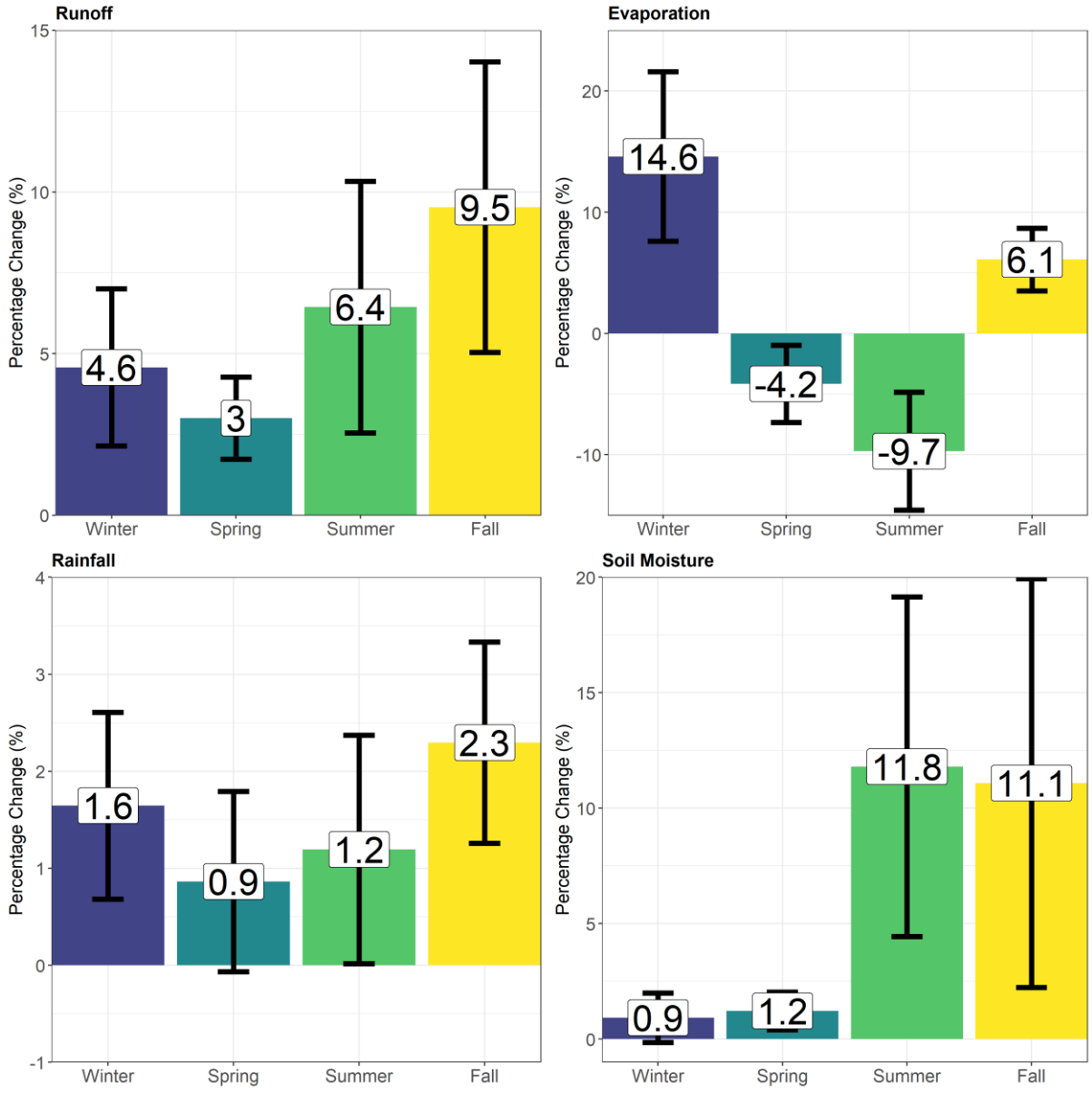

Supplementary Figure S5.2: Average percentage change in rainfall, evaporation, runoff, and soil moisture following afforestation across the 23 regions.

Error bars represent one standard deviation from the mean. The absolute change version can be found in the main text as Figure 2.

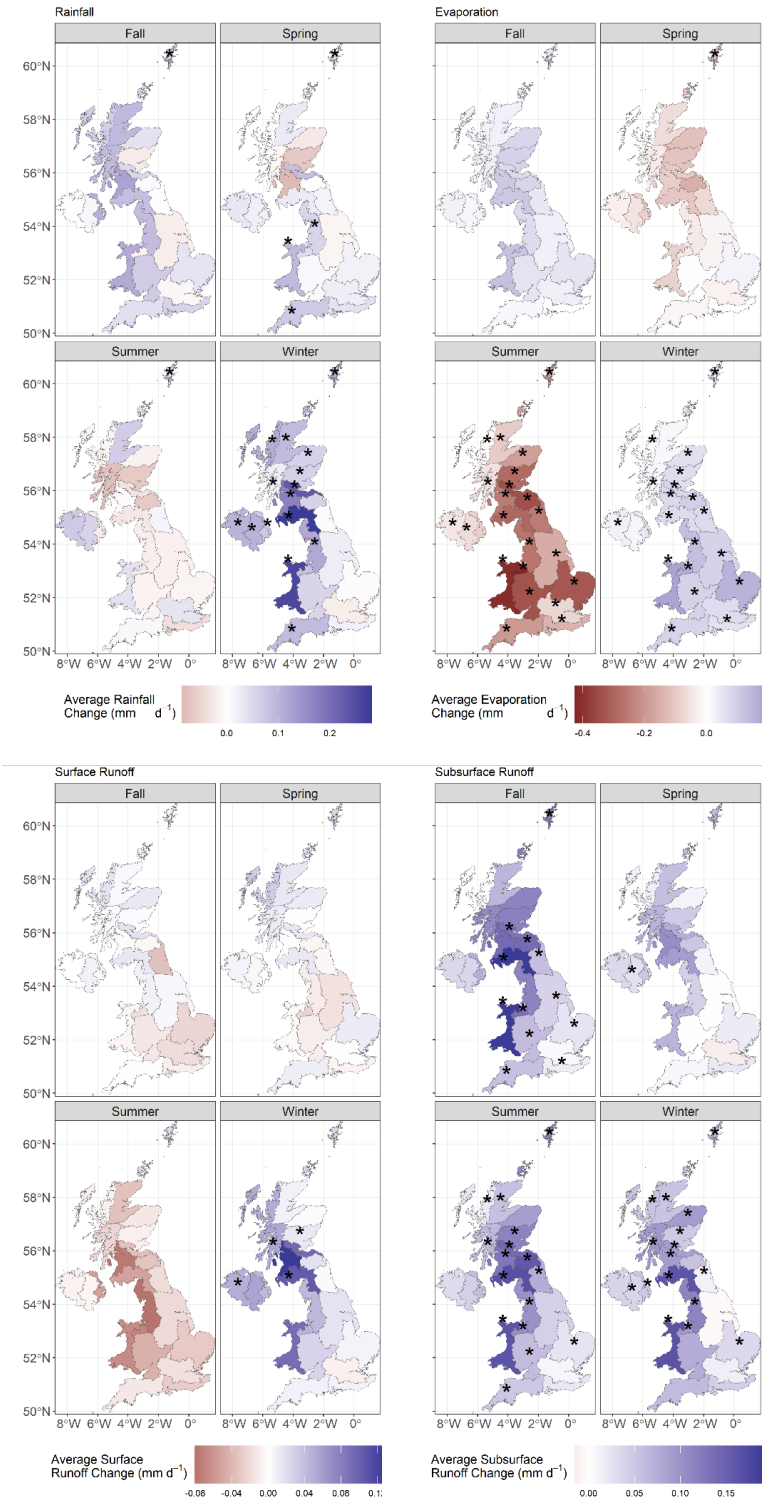

Supplementary Figure S5.3: Absolute change in rainfall, evaporation and turnover ratio following afforestation for each season.

The stars represent regions where the change is significant ($p < 0.025$). Figure 3 in the main manuscript shows this as percentage changes.

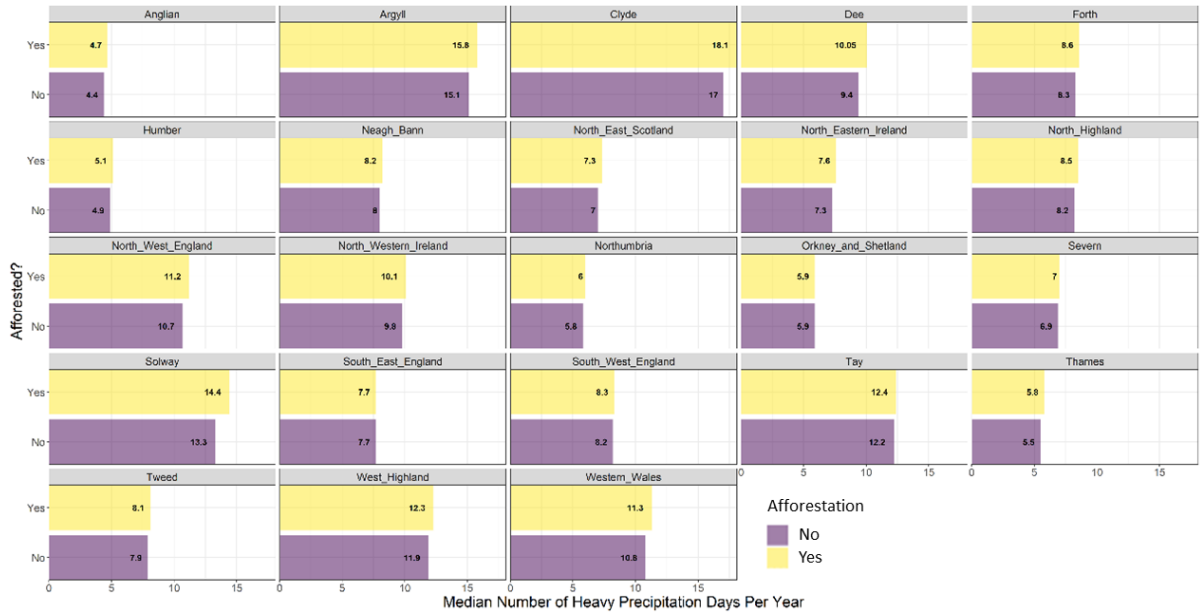

Supplementary Figure S5.4: Change in the median number of heavy precipitation days (20 mm of rainfall) per year for the period 2062-2072 for each UKCP18 region.

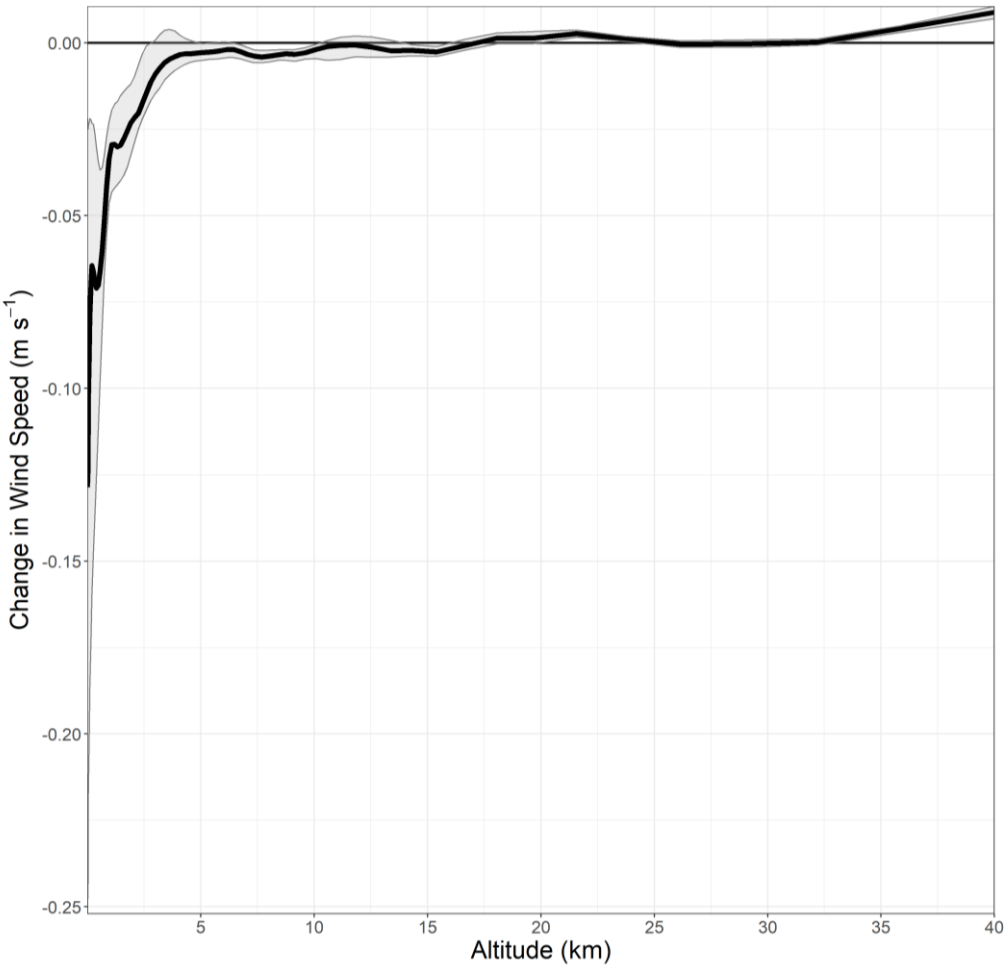

Supplementary Figure S5.5: Median change in wind speed over western Wales with afforestation.

Grey shading represents the 90th and 10th percentile whilst the black line represents the median change in wind speed.

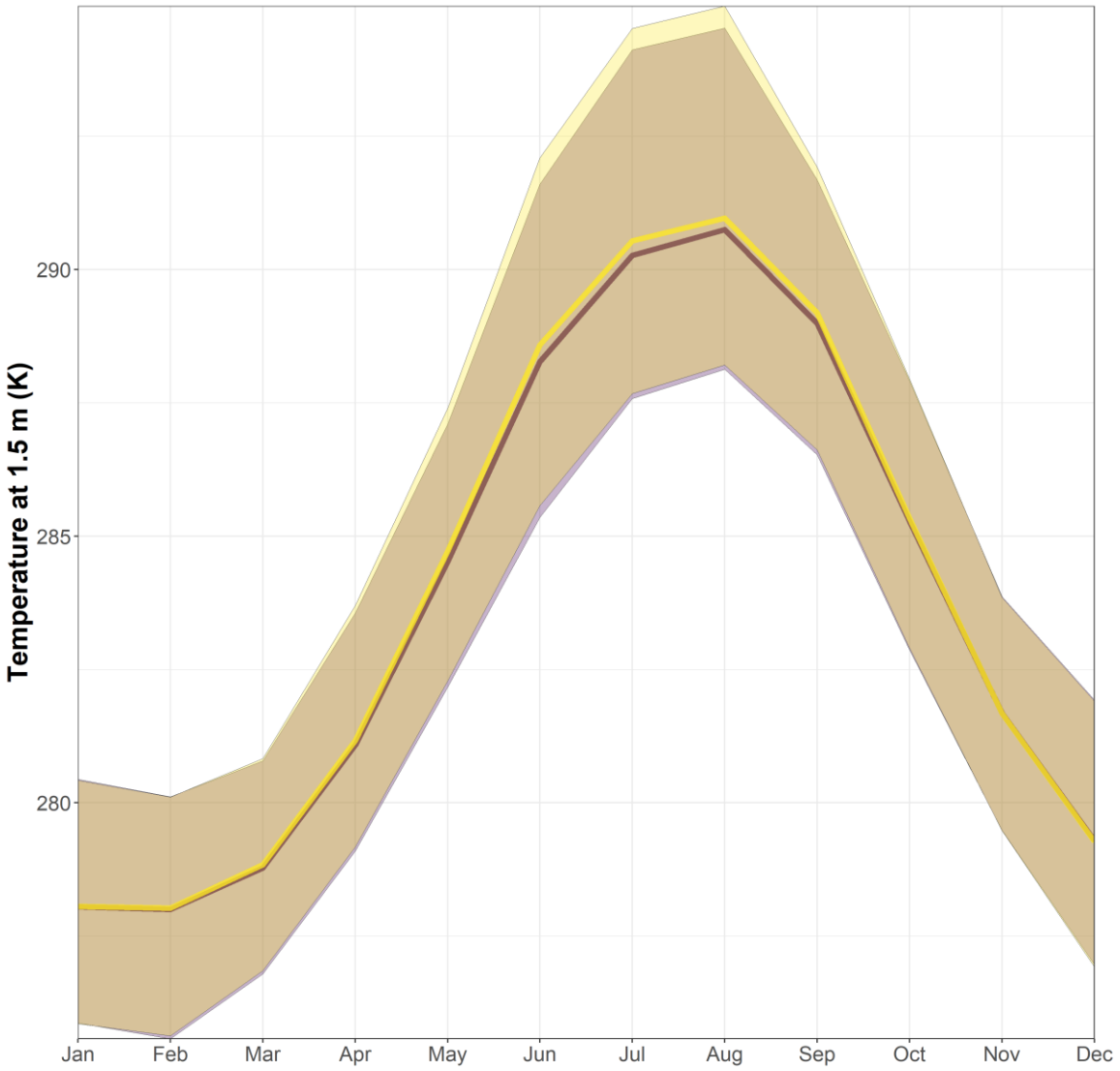

Supplementary Figure S5.6: Temperature at 1.5 m (K) between afforestation (yellow) and no land cover change (purple).

Bands represent the 90th and 10th percentiles of the regions and the middle line represents the median value.

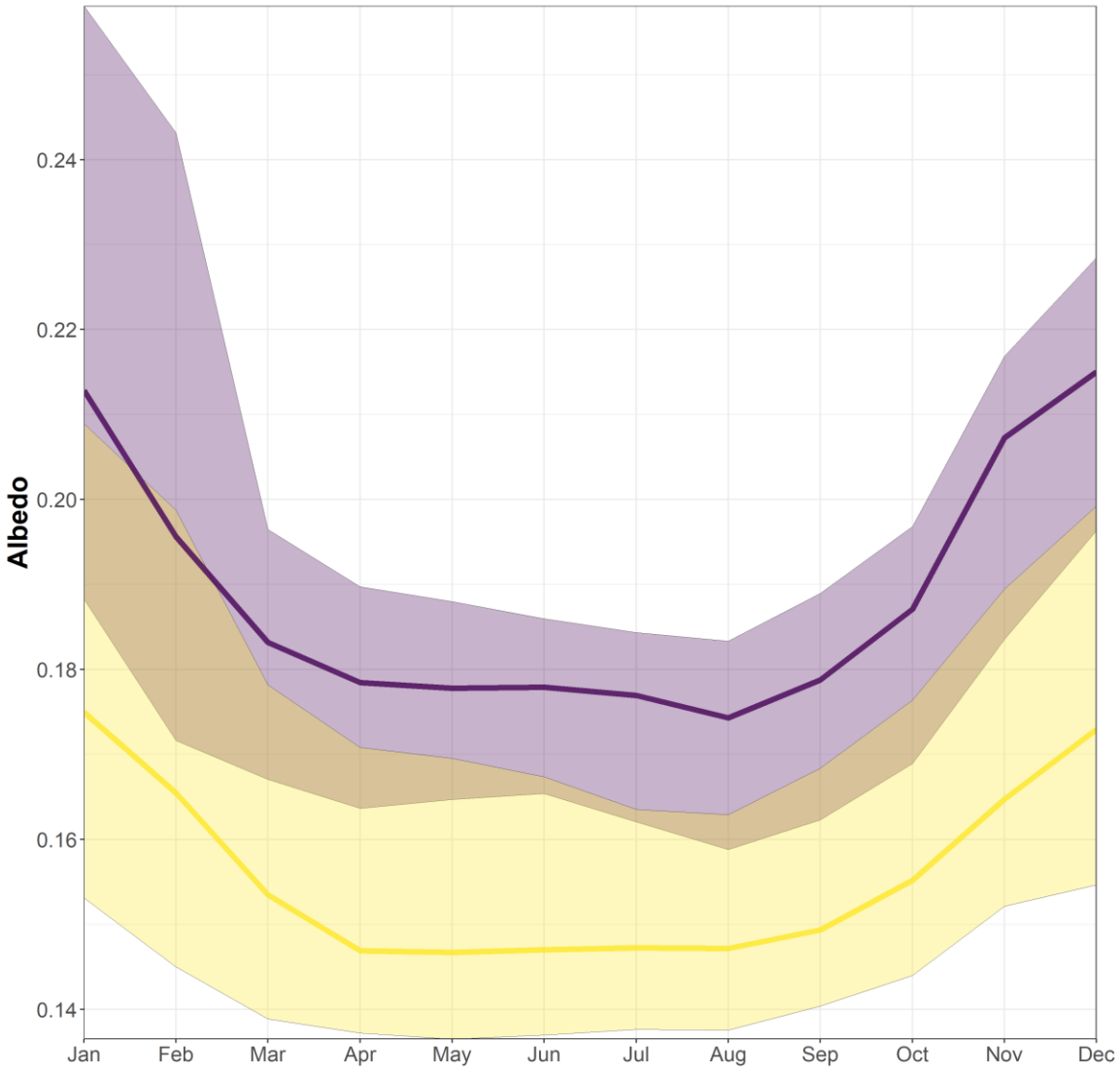

Supplementary Figure S5.7: Albedo reduction between afforestation (yellow) and no land cover change (purple).

Bands represent the 90th and 10th percentiles of the regions and the middle lines represent the median values.

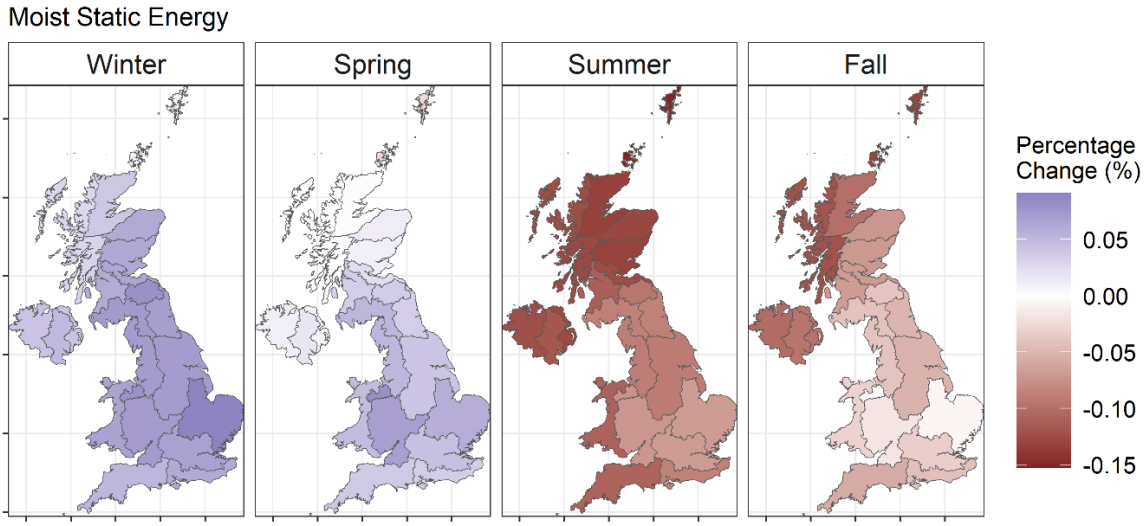

Supplementary Figure S5.8: Percentage change in the moist static energy.

Blue indicates increase, red decrease. A star represents where the change is significant $p < 0.025$. Calculation of moist static energy can be found in Supplementary Text.

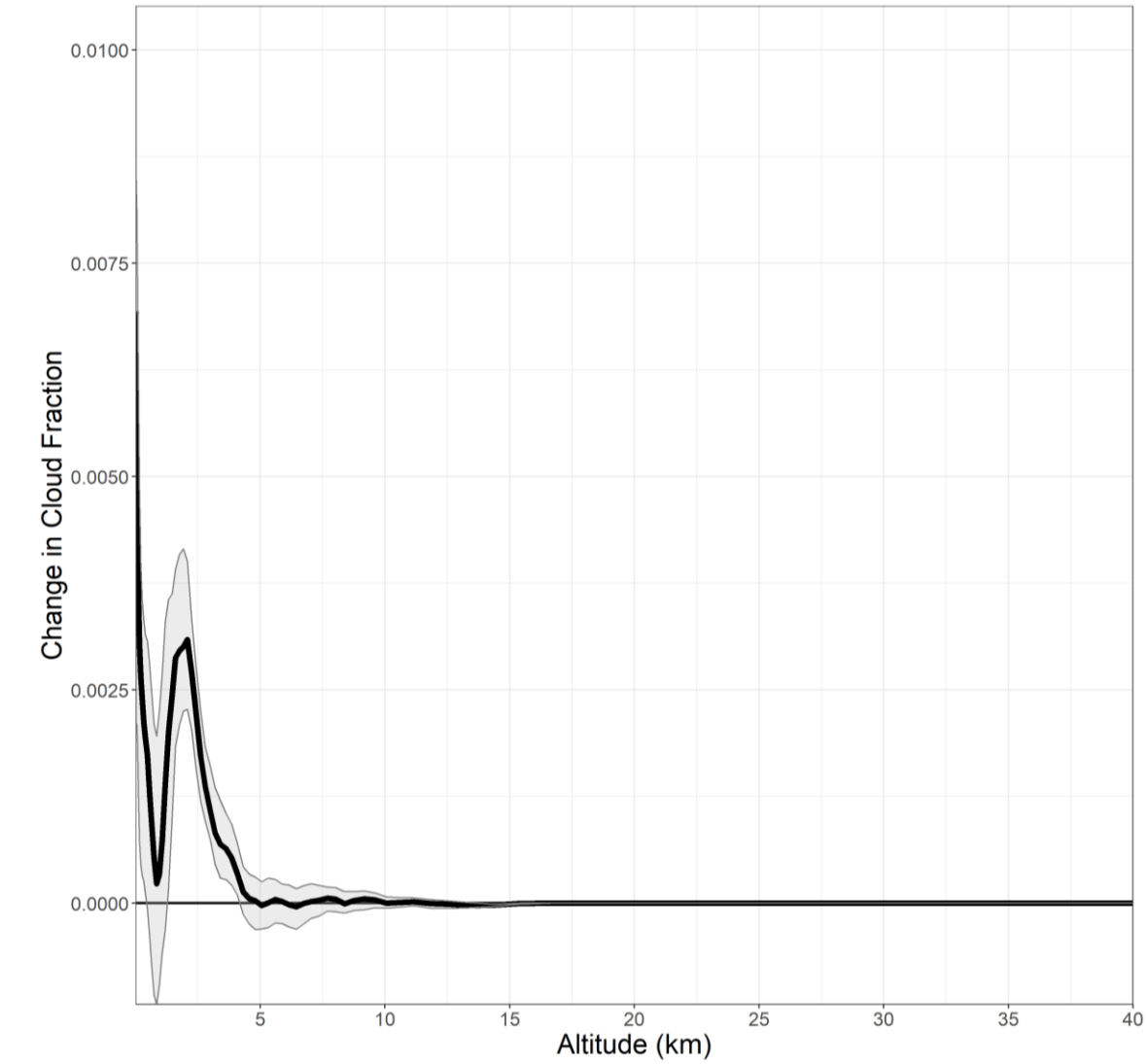

Supplementary Figure S5.9: Median change in cloud fraction over western Wales with afforestation.

Grey shading represents the 90th and 10th percentile and the black line represents the median value.

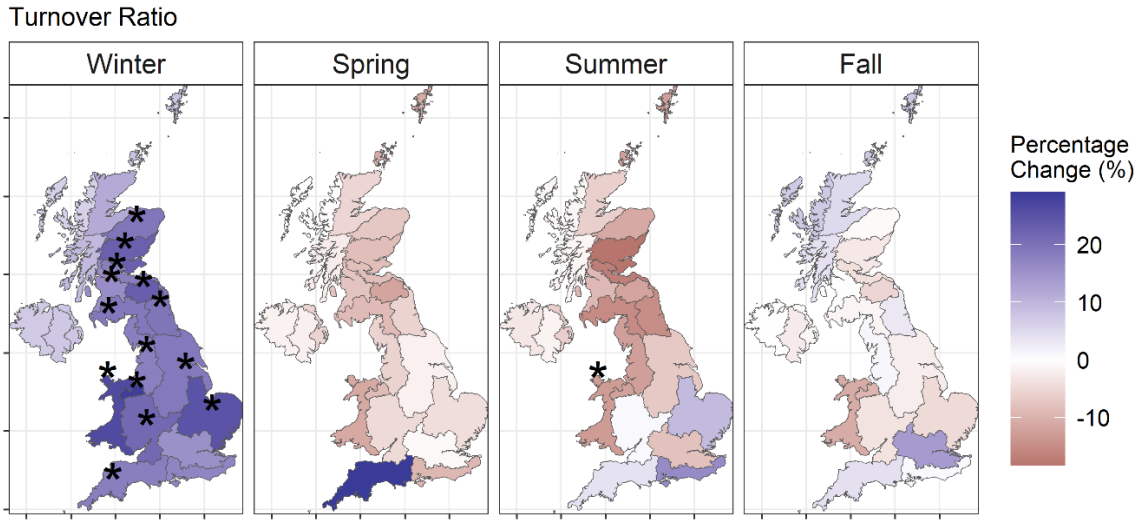

Supplementary Figure S5.10: Change in the Turnover Ratio for the different regions.

Blue indicates increase, red decrease. A star represents where the change is significant $p < 0.025$. Calculation of the Turnover Ratio can be found in Supplementary Text.

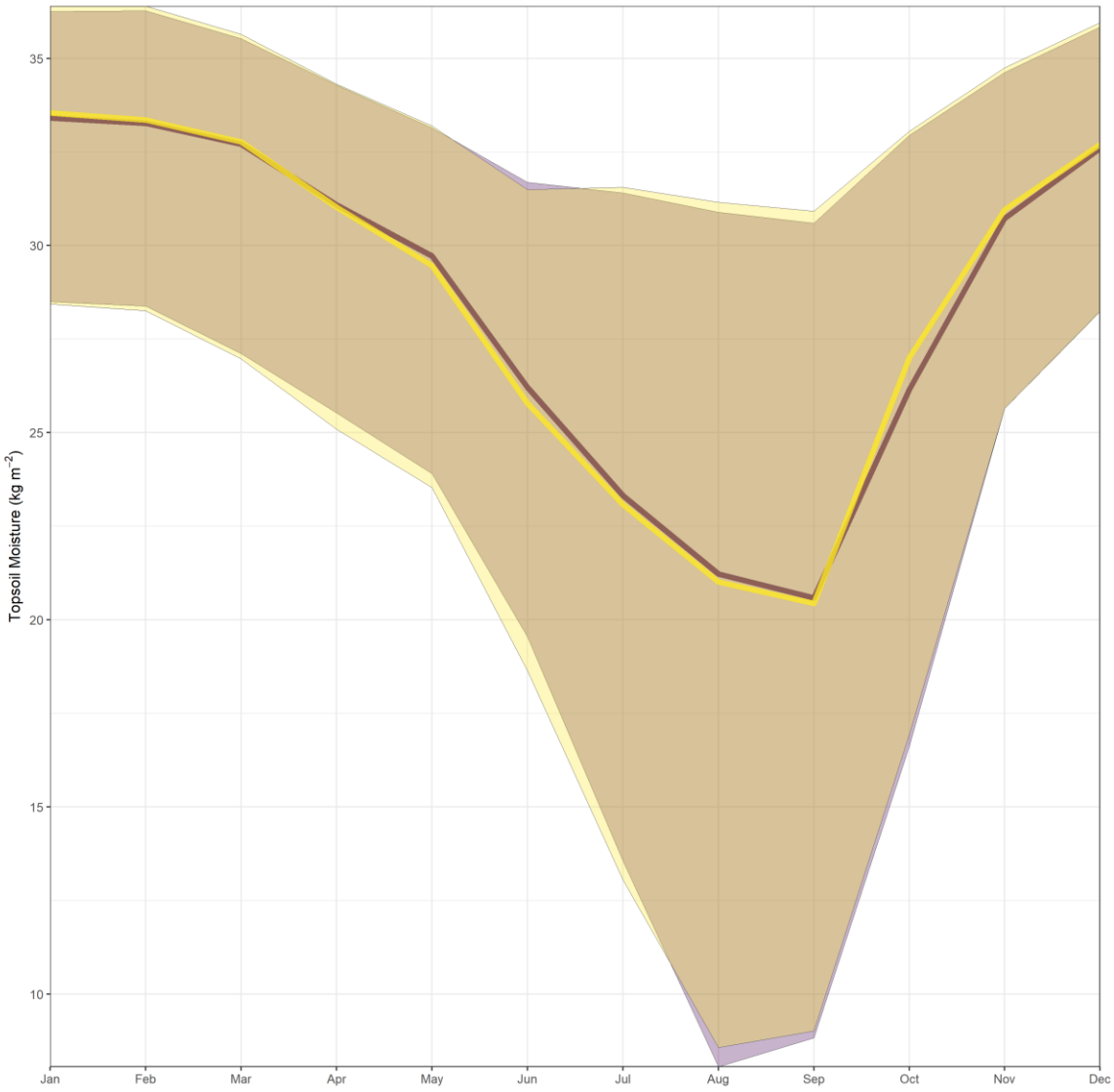

Supplementary Figure S5.11: Topsoil moisture between afforestation (yellow) and no land cover change (purple).

Bands represent the 90th and 10th percentiles of the regions and the middle lines represent the median values.

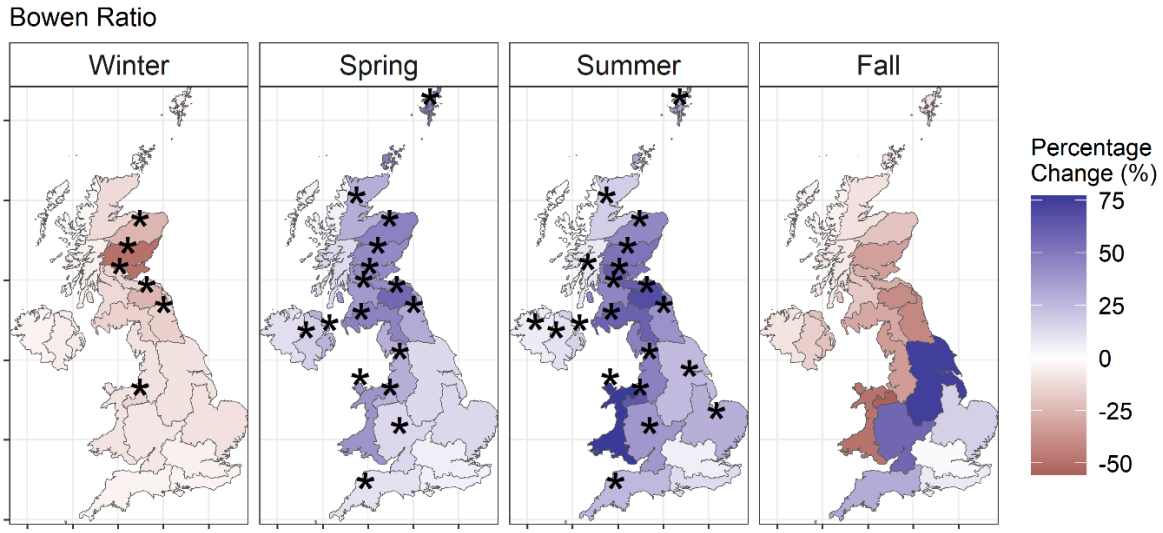

Supplementary Figure S5.12: Change in the Bowen Ratio for the different regions.

Blue indicates increase, red decrease. A star represents where the change is significant $p < 0.025$. Calculation of the Bowen Ratio can be found in Supplementary Text.

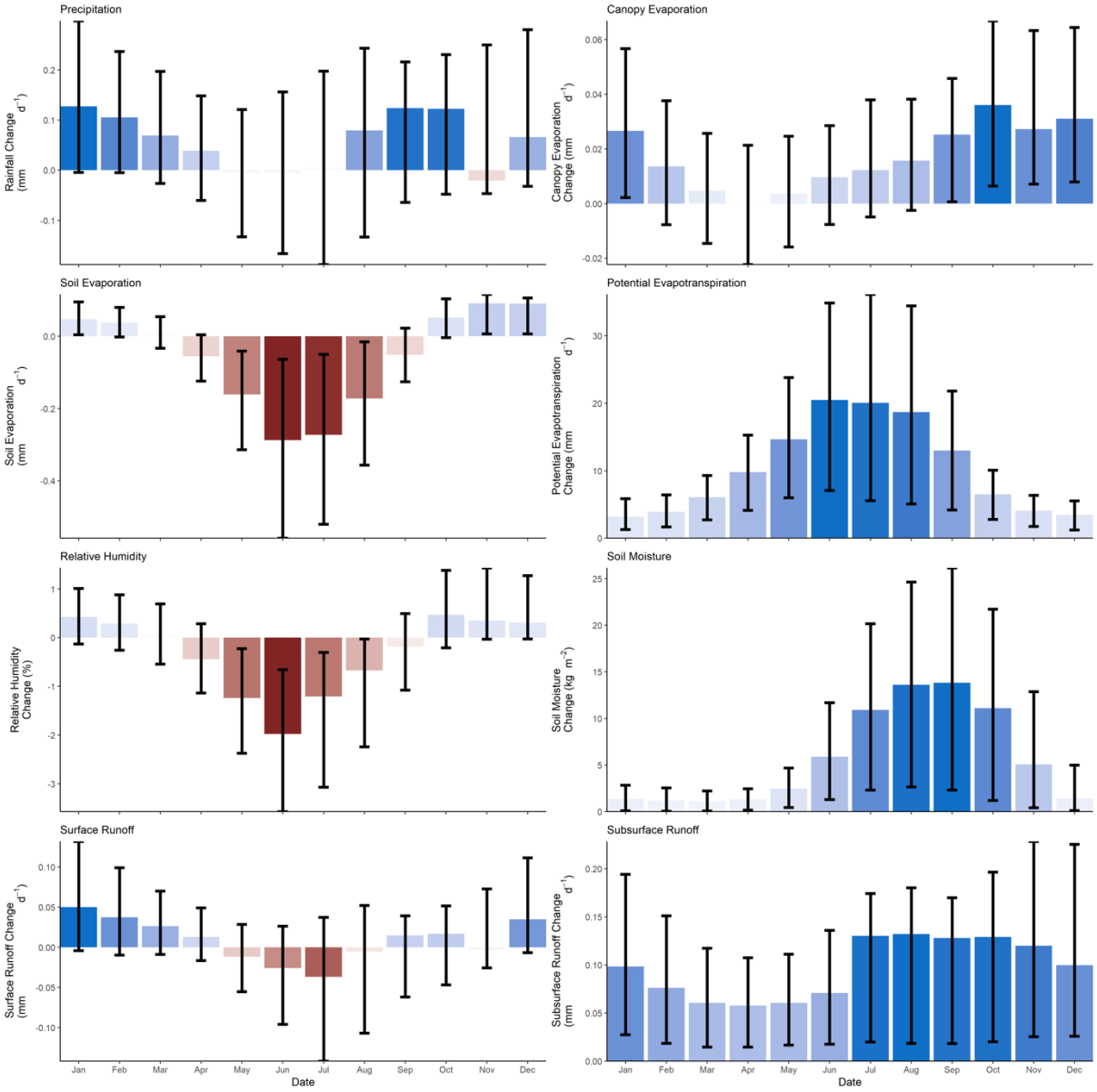

Supplementary Figure S5.13: Absolute changes in hydrometeorological processes (precipitation, canopy and soil evaporation, potential evapotranspiration, relative humidity, soil moisture, surface, and subsurface runoff) for the 20-year period for all regions with afforestation.

Error bars represent the 10th and 90th percentiles for the 23 regions. Figure 5 in the manuscript provides the figure as percentage changes.

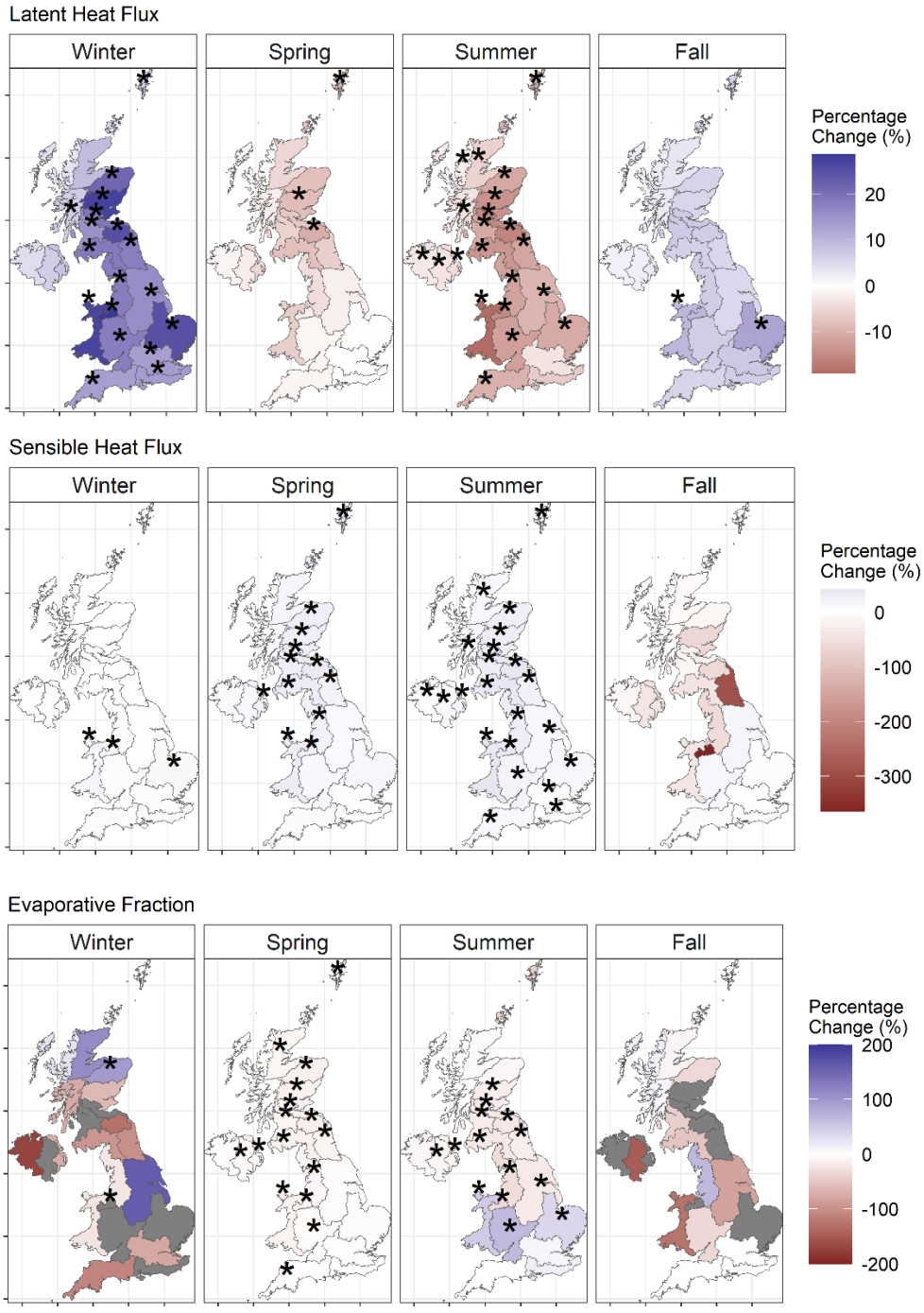

Supplementary Figure S5.14: Changes in the latent heat flux, sensible heat flux and evaporative fraction following afforestation for each season.

Evaporative fraction calculation can be seen in Supplementary Text.

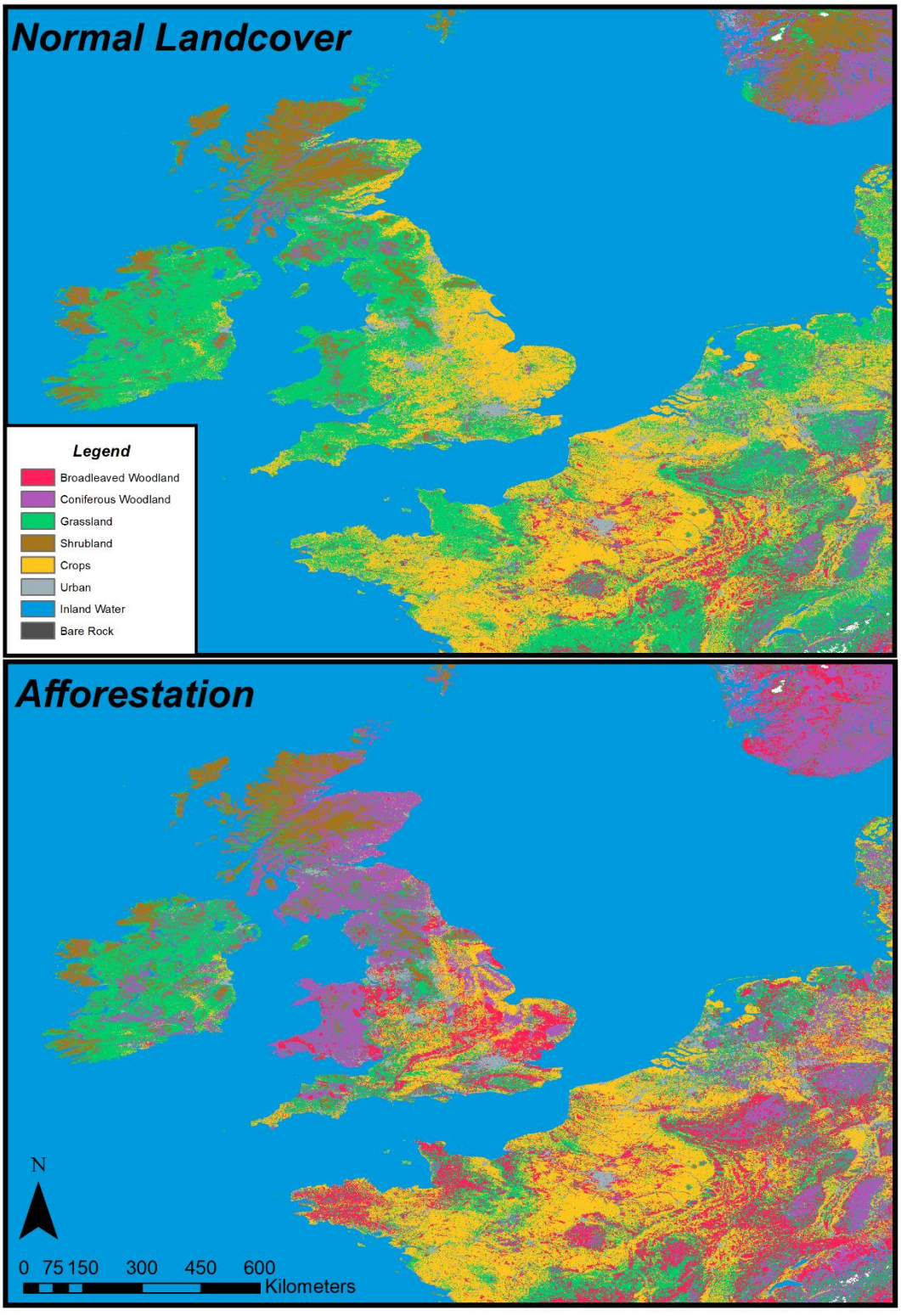

Supplementary Figure S5.15: Map of the increase in afforestation in the bottom panel compared to the baseline original landcover (top panel).

Supplementary Text

To determine land-atmosphere interactions there are several metrics. The Bowen Ratio quantifies the heat lost in the form of moisture:

$$B_R = \frac{H}{L}$$

Where H is the sensible heat flux and L is the latent heat flux. The Evaporative Fraction provides an understanding of the distribution of the available energy at the surface and removes the albedo influence:

$$E_F = \frac{L}{L + H}$$

The Turnover Ratio calculates rate of the moisture cycle with afforestation which is simply the ratio of evaporation to rainfall:

$$T = \frac{E}{R}$$

Moist Static Energy is calculated as an indicator of conditions favorable for generating convective rainfall events:

$$MSE = C_P T + gz + L_v r$$

C_P is the specific heat capacity of air at a constant pressure, T is the absolute observed temperature, g is gravitational acceleration, z is the height above the surface, L_V is the latent heat of vaporization and r is the water vapor mixing ratio in the air.

Appendix 5: Base Namelist for JULES Configuration

The following is a copy and description of the initial base namelist configuration for JULES used in the first two pieces of research (Chapters 3 & 5). It is however not the exact configuration due to the variety of experiments undertaken and therefore should be used for reference rather than using it to run JULES as in this research. The configuration is based on Rose suites **u-bi090** and **u-au394**, which can be found using the Rose/Cylc suite control system: https://metomi.github.io/rose/doc/html/index.html. Information is based on notes from https://jules-lsm.github.io/latest/index.html and some text is from this document. Any 'notes' referenced relate to those produced by the Met Office as climate science technical notes: https://www.metoffice.gov.uk/research/library-and-archive/publications/science/climate-science-technical-notes.

---

jules_lsm_switch.nml

&jules_lsm_switch
lsm_id=1,

The JULES land surface model has been used instead of CABLE.

---

jules_surface_types.nml

&jules_surface_types
ice=-1,
lake=7,
nnvg=3,
npft=5,
soil=8,
urban=6,

1. Ice surface type index = -1. This is because we do not want any ice surface type in this model.
2. Lake surface type index = 7.
3. Three non-plant surface types will be modelled. These are the urban, bare rock/soil and inland water/lake surfaces.
4. Five plant functional types will be modelled. These are broadleaf and needleleaf trees, C3, shrubs and crops.
5. Soil surface type index = 8.
6. Urban surface type index = 6.

N.B.
Neither elev_ice or elev_rock have been used as l_elev_land_ice has not been set to true.
Neither urban_canyon or urban_roof have been used as l_urban2t has not been set to true.

---

model_environment.nml

&jules_model_environment
l_jules_parent=0,

JULES is being run standalone and not with the Unified Model.

---

jules_surface.nml

&jules_surface
all_tiles=0,
beta1=0.83,
beta2=0.93,
cor_mo_iter=1,
fwe_c3=0.5,
fwe_c4=2.0e4,
hleaf=5.7e4,

hwood=1.1e4,
iscrntdiag=0,
l_aggregate=.false.,
l_anthrop_heat_src=.true.,
l_elev_land_ice=.false.,
l_elev_lw_down=.false.,
l_epot_corr=.true.,
l_land_ice_imp=.false.,
l_point_data=.false.,
l_urban2t=.false.,

1. Calculations are not performed on all tiles for all gridpoints even when the tile fraction is zero.
2. Coupling coefficient for co-limitation in photosynthesis is set to 0.83; refer to Cox et al., 1999, eq61.
3. Coupling coefficient for co-limitation in photosynthesis is set to 0.93; refer to Cox et al., 1999, eq61.
4. Correct convective gustiness in low winds is performed according to the Monin-Obukhov surface exchange calculation. Referenced in the UMDP24 section 8.4.1.
5. 0.5 is the constant in expression for limitation of photosynthesis by transport of products for C3 plants; refer to Cox et al., 1999, eq60.
6. 20000 is the constant in expression for limitation of photosynthesis by transport of products for C4 plants; refer to Cox et al., 1999, eq60. Note, there are no C4 plants in this model configuration of JULES.
7. Specific heat capacity of leaves is set to 5.7e4 $JK^{-1}kg^{-1}$ of carbon refer to Technical Note 30, pg6.
8. Specific heat capacity of wood is set to 1.1.e4 $JK^{-1}kg^{-1}$ of carbon refer to Technical Note 30, pg6.
9. Surface similarity theory is used for diagnosing screen temperature. This is the recommended option when JULES is in standalone mode.
10. A separate energy balance is calculated for each surface type so that ntiles= ntype. This switch is about controlling the number of tiles in each gridbox.
11. Anthropogenic influence/contribution to surface heat flux from urban surface types is included.

12. Multiple ice tiles are not allowed to exist in ice gridbox. This is because they do not exist in this model setup.
13. As there is no elevation data included with this model run, no adjustments are made to the elevation offset influence on downwelling longwave radiation.
14. Potential evaporation calculation is corrected.
15. Explicit numerics are used to update land ice temperatures.
16. Driving data are area averages and not point data.
17. The two-tile urban scheme with urban canyons and roofs is not used.

---

jules_radiation.nml

&jules_radiation
l_albedo_obs=.false.,
l_cosz=.true.,
l_embedded_snow=.false.,
l_mask_snow_orog=.false.,
l_spec_albedo=.false.,
wght_alb=0.0,0.5,0.0,0.5,

1. Albedo values on tiles is not scaled (as there is no prescribed data to drive).
2. The solar zenith angle is calculated.
3. The embedded canopy snow albedo model is not used.
4. Orographic masking of snow is not included.
5. A single averaged waveband albedo is calculated.
6. This is the prescribed list of the overall albedo from its components.

N.B.
As l_spec_albedo is set as false, this means that the options l_spec_alb_bs, l_niso_direct and l_snow_albedo are not used.

---

jules_hydrology.nml

```
&jules_hydrology
b_pdm=2.0,
dz_pdm=1.0,
l_pdm=.true.,
l_spdmvar=.true.,
l_top=.false.,
slope_pdm_max=6.0,
/
```

1. 2.0 is used as the shape parameter for the probability distribution function.
2. A 1 m depth of soil is considered.
3. The Probability Distributed Model of Moore 1985 is used.
4. A linear function to calculated topographic slope is used to calculate the S0/Smax.
5. A TOPMODEL-type scheme is not used.
6. The maximum topographic slope in the linear function is set to 6.0.

N.B.
Both of l_spdmvar and slope_pdm_max have been tested on catchments in Great Britain.
By selecting the TOPMODEL function, there would be more options that are not detailed above.

---

jules_soil.nml

```
&jules_soil
confrac=1.0,
cs_min=1.0e-6,
dzsoil_io=0.1,0.25,0.65,2.0,
l_bedrock=.false.,
l_dpsids_dsdz=.false.,
l_holdwater=.true.,
l_soil_sat_down=.false.,
```

l_vg_soil=.true.,
sm_levels=4,
soilhc_method=2,
zsmc=1.0,
zst=1.0,

1. The entire fraction of the gridbox is assumed to be covered by convective precipitation (taken due to the resolution of 1 km grid).
2. The minimum allowed soil carbon is taken as 1.0e-6kgm^{-2}.
3. The soil layer depths as defined by sm_levels are taken as 0.1, 0.25, 0.65 and 2.0 m below the surface.
4. No bedrock is modelled below the soil column in terms of thermal conductivity.
5. Vertical gradient of soil suction is not calculated.
6. Supersaturated soil moisture goes into an adjacent layer.
7. Any excess water in the supersaturated soil is put into the layer above. This is in line with the paper that said this option leads to better surface runoff and less excessive soil moisture.
8. The Van Genuchten soil hydraulic model is used.
9. 4 soil layers are used.
10. The thermal conductivity model of Dharssi et al., 2009 is used.
11. Depth-averaged soil moisture is calculated from this surface to 1.0 m below the surface.
12. The soil temperature is averaged to a depth of 1.0 m for the calculation of wetland methane emissions.

---

jules_vegetation.nml

&jules_vegetation
can_model=4,
can_rad_mod=6,
fsmc_shape=0,
ilayers=10,
l_bvoc_emis=.true.,

l_gleaf_fix=.false.,
l_ht_compete=.false.,
l_inferno=.false.,
l_irrig_dmd=.false.,
l_landuse=.false.,
l_leaf_n_resp_fix=.false.,
l_limit_canhc=.false.,
l_nitrogen=.false.,
l_o3_damage=.false.,
l_phenol=.true.,
l_recon=.false.,
l_scale_resp_pm=.false.,
l_spec_veg_z0=.false.,
l_stem_resp_fix=.false.,
l_trait_phys=.false.,
l_trif_crop=.false.,
l_trif_fire=.false.,
l_triffid=.false.,
l_use_pft_psi=.false.,
l_vegcan_soilfx=.false.,
l_vegdrag_pft=.false.,
phenol_period=1,
stomata_model=1,

1. The canopy model chosen is that of the radiative canopy with heat capacity and snow representation below the canopy.
2. Canopy radiation treatment:
    - 2-stream approach
    - Accounts for:
        - Leaf angle distribution
        - Zenith Angle
        - Absorption differences between direct and diffuse radiation

- Exponential decline of leaf nitrogen through the canopy proportional to LAI following Beer's Law
- Inhibition of lead respiration in the light
- Sunfleck penetration
- Division of sunlit and shaded leaves within the canopy level
- Modified version of inhibition of leaf respiration in the light

3. Soil moisture stress function on vegetation is piece-wise linear in volume soil moisture.
4. 10 layers are used to calculate in the canopy radiation model.
5. BVOC (biogenic volatile organic compound) emissions are calculated.
6. Veg1 does not accumulate g_leaf_phen_acc between calls to TRIFFID as TRIFFID is not being used.
7. The INFERNO fire model is not used.
8. Irrigation demand code is not used.
9. The bug fix for leaf nitrogen content is not used in the calculation of plant maintenance respiration as can_rad_mod is not 1,4 or 5 that are affected by this bug.
10. The vegetation areal heat capacity is unlimited as the area is not the Amazon/tropical forests.
11. Ozone damage is not included in this model run.
12. Phenology method is used.
13. Minimum vegetation fractions are not applied as some points on a 1km grid will be either 100% lake or urban.
14. Soil moisture stress only reduces leaf maintenance respiration and not leaf, root and stem maintenance respiration.
15. Vegetation roughness lengths are calculated using canopy heights and parameter dz0v_dh_io.
16. The respiring stem mass varies with seasonal LAI.
17. Related to trait-based physiology. Vcmax is calculated on parameters nl0 and neff.
18. Dynamic vegetation model TRIFFID is not used meaning a single soil carbon pool is used.
19. Vegetation competition is calculated for natural and crop PFTs together, with natural PFTs excluded from the agricultural area that is defined by the frac_agr variable.
20. FSMC is calculated from sm_wilt and sm_crit that are defined in JULES_SOIL_PROPS and fsmc_p0_io.
21. No conduction from the canopy into the soil is calculated.

22. The vegetative drag scheme is not used.
23. Phenology model is called every (1) day.
24. The model used for stomatal conductance is the same as that given in the original JULES papers of 2011.

N.B.

As TRIFFID is not used there are a lot of functions that have not been included above.

As the irrigation demand code is not used, l_irrig_limit and irr_crop are not used.

---

jules_soil_biogeochem.nml

```
&jules_soil_biogeochem
 soil_bgc_model = 1,
 q10_soil = 2.0,
 kaps = 0.5e-8,
 l_q10 = .true.,
 l_soil_resp_lev2 = .false.,
 l_ch4_tlayered = .false.,
 l_ch4_interactive = .false.,
 ch4_substrate = 1,
 t0_ch4 = 273.15
 const_ch4_cs = 7.41e-12
 q10_ch4_cs = 3.7
```

1. 7.41e-12 is the scale factor for wetland CH_4 emissions when soil carbon is taken as the substrate for CH_4 emissions.
2. Dummy value for scale factor for wetland CH_4 emissions when NPP is taken as the substrate for CH_4 emissions.
3. Dummy value for scale factor for wetland CH_4 emissions when soil respiration is taken as the substrate for CH_4 emissions.
4. Specific soil respiration rate at 25 degrees Celsius and optimum soil moisture. Refer to note 24, eq16.

5. The Q10 approach is used when calculating soil respiration.
6. Temperature and unfrozen moisture content of the first (topmost) soil layer are used.
7. 3.7 set for the Q10 value for wetland CH_4 emissions as carbon is taken from the soil carbon substrate.
8. Dummy value Q10 value for wetland CH_4 emissions when npp is taken as the substrate for CH_4 emissions.
9. Dummy value Q10 value for wetland CH_4 emissions when soil respiration is taken as the substrate for ch4 emissions (ch4_substrate = 3).
10. Q10 factor for soil respiration is set at 2.0 (default). Refer to note 24, eq17.
11. A single-pool model of soil carbon turnover is used and not updated. This is because TRIFFID has not been selected.
12. Reference temperature for the Q10 function CH_4 emission calculation is set to 273.15 K.

N.B.
ch4_substrate =1 is not written but is taken as default where the model is run with a single-pool of carbon substrate.

---

jules_soil_ecosse.nml

&jules_soil_ecosse

This namelist is not populated the soil Ecosse model it is not meant to be used at this stage.

---

jules_deposition.nml

&jules_deposition
l_deposition=.false.,

Model deposition is turned off in JULES.

---

jules_snow.nml

```
&jules_snow
aicemax=0.78,0.36,
cansnowpft=.false.,.true.,.false.,.false.,.false.,
dzsnow=0.1,0.15,0.2,
frac_snow_subl_melt=1,
graupel_options=0,
i_basal_melting_opt=0,
i_grain_growth_opt=0,
i_relayer_opt=0,
i_snow_cond_parm=1,
l_et_metamorph=.false.,
l_snow_infilt=.false.,
l_snow_nocan_hc=.false.,
l_snowdep_surf=.true.,
lai_alb_lim_sn=5*0.5,
maskd=50.0,
nsmax=3,
rho_firn_albedo=550.0,
rho_snow_fresh=100.0,
snow_hcap=0.63e6,
snow_hcon=0.265,
snowinterceptfact=0.7,
snowliqcap=0.05,
snowloadlai=4.4,
snowunloadfact=0.4,
unload_rate_cnst=5*0.0,
unload_rate_u=5*0.0,
```

1. Although aicemax should only be used when l_elev_land_ice = true, this model did not run without these values. Therefore, the default values have been added for VIS and NIR wavebands respectively.

2. Cansnowpft is used as can_model = 4 which means that snow can be under the canopy for each of the plant functional types. At the moment the model is only suitable for coniferous trees and so the snow is only held under pft 2, which is for needleleaf trees.
3. The heights of the three snow layers are: 0.1, 0.15 and 0.2 metres, when they are not the bottom layer. Refer to the manual for 5.5 to understand better what the scheme is.
4. Snow-cover fraction is used in the calculation of sublimation and melting.
5. Graupel is included as snowfall in the snow scheme. This is because in the standalone model of JULES there is no separate snow and graupel driving data.
6. Basal melting of the snow takes place if the temperature of the first soil layer is above freezing until the snow is removed or the temperature of the soil layer is reduced to freezing.
7. The original snow grain growth calculation of Marshall 1989 is used to speed up the simulation.
8. Original scheme with relayering of the grain size is used which involved the grain size itself to increase the speed.
9. Conductivity of snow is used.
10. The effect of thermal metamorphism on the snow density is not included.
11. Rainfall and melting from the canopy is not passed to the snowpack as infiltration.
12. The canopy heat capacity is included in the surface energy balance at the top of the snowpack.
13. Equivalent canopy snow depth for surface calculations on tiles with a snow canopy are used.
14. The values for the minimum LAI in calculation of albedo in the presence of snow are taken from the GL4 versions that include this as part of the namelist.
15. The default value of 50.0 is used as exponent of equation that weights snow-covered and snow-free albedo.
16. Number of snow layers is set to three. The minimum recommended amount.
17. Rho_firn_albedo is set to 550.0.
18. Density of fresh snow is taken to be 100.0 kgm^{-3}.
19. Thermal capacity of lying snow is 0.63e6 $JK^{-1}m^{-3}$.
20. Thermal conductivity of lying snow is taken to be 0.265 $Wm^{-1}K^{-1}$. Refer to note 30m eq 42.
21. 0.7 is the constant in the relationship between mass if intercepted snow and snowfall rate that is used because can_model = 4.

22. Liquid water holding capacity of lying snow as a fraction of snow mass is 0.05.
23. Ratio of maximum canopy snow load to LAI is 4.4 kgm^{-2}, used as can_model =4.
24. Default value for the constant in the relationship between mass of intercepted snow and snowfall rate. Used as can_model =4.
25. Unload rate constant is 0 for the unloading rate for snow on the canopy as seen in the GL4 examples for tiles where cansnowpft = true.
26. The term, proportional to wind speed, in unloading rate for snow in the canopy, is also taken as 0 for all plant functional types as seen in the GL4 models.

N.B.
As l_snow_albedo in the radiation namelist is not set to true, there are a load of parameters that have not been included in this namelist that are related to the radiation properties of snow. L_snow_albedo is not used as l_spec_albedo is not set to TRUE which would have used a spectral albedo with VIS and NIR components.
As l_elev_land_ice is not set to TRUE there are further features that are not included such as the maximum albedo for ice.
Can_clump not used as l_embedded_snow = .false.
Many parameters not used that would have if l_et_metamorph had been included.

This file contains two separate namelists. These being the main rivers options and the jules_overbank options.

jules_rivers.nml

```
&jules_rivers
a_thresh=13,
cbland=0.05,
cbriver=0.05,
cland=0.4,
criver=0.5,
i_river_vn=2,
l_inland=.false.,
```

l_rivers=.true.,
nstep_rivers=1,
retl=0.005,
retr=0.005,
runoff_factor=1.0,
slfac=0.0,

&jules_overbank
l_riv_hypsometry=.false.,
l_riv_overbank=.false.,
riv_a=7.20,
riv_b=0.50,
riv_c=0.27,
riv_f=0.30,
use_rosgen=.false.,

JULES_RIVERS

1. 13 gridcells are taken to be the threshold drainage area draining into a gridbox above which the grid cell is considered to be a river point.
2. Subsurface land wave speed is taken to be 0.05 ms^{-1}.
3. Subsurface river wave speed is taken to be 0.05 ms^{-1}.
4. The kinematic wave speed for surface flow in a land grid cell is 0.4 ms^{-1}.
5. The river wave speed for surface flow in a river grid cell is 0.5 ms^{-1}.
6. The standalone JULES implementation of the RFM kinematic wave model is used that can be read about in Dadson & Bell, 2010.
7. Inland basin water is not re-routed back into soil moisture.
8. The river routing algorithm is used that is specified in i_river_vn.
9. At every model timestep the routing scheme is implemented. This means that the model is accumulating water every timestep and then it is routed. This can be changed to increase the speed of the model.
10. Bell et al. 2007 suggest a value of 0.005 for the land return flow fraction for a 1 km scale.
11. Similar to above, 0.005 is taken for the river return flow fraction.

12. Runoff factor is taken as 1.0 so that there is no runoff adjustment as advised. This is normally used to correct biases in the precipitation when the model is forced with observed data.
13. Slope factor is taken as 0.

JULES_OVERBANK

1. Overbank inundation gridbox is not included.
2. Inundated area is not calculated at present using estimates of the inundated area from simple river width scaling (ignoring topography).
3. The four factors included are those that are suggested for when using a 1 km grid.
4. Rosgen entrenchment ratio approach is not included.

---

science_fixes.nml

This namelist is just to fix things temporarily that alter science results.

```
&jules_temp_fixes
l_dtcanfix=.false.,
l_fix_alb_ice_thick=.false.,
l_fix_albsnow_ts=.false.,
l_fix_ctile_orog=.false.,
l_fix_moruses_roof_rad_coupling=.false.,
l_fix_osa_chloro=.false.,
l_fix_ustar_dust=.false.,
l_fix_wind_snow=.false.,
```

These fixes were not documented well when this document was compiled so all are set to false for now.

l_fix_moruses_roof_rad_coupling is related to the MORUSES model and so as it is not being used, this function is set to false.

---

timesteps.nml

```
&jules_time
l_360=.false.,
l_leap=.true.,
main_run_end='2015-01-01 00:00:00',
main_run_start='2005-01-01 00:00:00',
print_step=480,
timestep_len=1800,

&jules_spinup
max_spinup_cycles=4,
nvars=2,
spinup_end='2005-01-01 00:00:00',
spinup_start='2004-01-01 00:00:00',
terminate_on_spinup_fail=.false.,
tolerance=-1.0,-0.1,
use_percent=.false.,.false.,
var='smcl','t_soil',
```

JULES_TIME

1. Each year consists of either 365 or 366 days.
2. Leap years are modelled.
3. The main run end is: '2015-01-01 00:00:00'
4. The main run start is: '2005-01-01 00:00:00'
5. 480 timesteps will occur before information is printed to the screen.
6. The timestep length of the model is 1800 seconds. This is the same as 30 mins.

JULES_SPINUP

1. The spin-up period is repeated 4 times. It spins up until the change is less than the amount between years as specified in tolerance.
2. Two variables, moisture content and temperature of each soil layer, are used to test if the model has spun-up.

3. Spinup end is: 2005-01-01 00:00:00
4. Spinup start is: 2004-01-01 00:00:00
5. The model will not terminate if the model does not pass the spin-up test after the max_spinup_cycles. This can be set in other models.
6. These are the two absolute values which the model spinups should be within to ensure that the model has spun up.
7. The tolerance is not a percentage.
8. The names of the two variables used to check on the spinup.

---

model_grid.nml

&jules_input_grid
grid_is_1d=.false.,
nx=656,
ny=1057,
pft_dim_name='pft',
sclayer_dim_name='sclayer',
scpool_dim_name='scpool',
soil_dim_name='z',
time_dim_name='time',
type_dim_name='z',
x_dim_name='x',
y_dim_name='y',

&jules_latlon
file='/group_workspaces/jasmin2/jules_bd/data/CHESS_v1.0/ancils_uncompressed/chess_landfrac.nc',
lat_name='lat',
lon_name='lon',

&jules_land_frac

file='/group_workspaces/jasmin2/jules_bd/data/CHESS_v1.0/ancils_uncompressed/chess_landfrac.nc',
land_frac_name='landfrac',

&jules_model_grid
force_1d_grid=.false.,
land_only=.true.,
use_subgrid=.false.,

&jules_nlsizes
bl_levels=1,

&jules_surf_hgt
zero_height=.true.,

&jules_z_land

JULES_INPUT_GRID

1. Variables that are in the input grid have a 2D format.
2. ‘nvg’ used as a dimension for nnvg.
3. The x dimension has a size of 656.
4. The y dimension has a size of 1057.
5. ‘pft’ is used as a dimension for npft.
6. The ‘sclayer’ is called ‘sclayer’ which is the soil carbon layer.
7. The ‘scpool’ is called ‘scpool’ which is the soil carbon pool.
8. Additional dimension of size sm_levels (which is z).
9. The time varying dimension has the name time.
10. ‘ntype’ is dimension z.
11. The x dimension is called ‘x’.
12. The y dimension is called ‘y’.

JULES_LATLON

1. The chess landfraction is used as the file to read latitude and longitude from.
2. Latitude is called ‘lat’ in this file.

3. Longitude is called ‘lon’ in this file.

JULES_LAND_FRAC

1. The chess landfraction is used as the file to read landfraction from. This is the amount of the gridbox that is actually land and in this model run, where the model will actually run calculations.
2. ‘landfrac’ is the name of the variable with the landfraction data.

JULES_MODEL_GRID

1. The model then takes its default grid shape.
2. Land points are the ones that are only modelled.
3. A subgrid is not used.

JULES_NLSIZES

One boundary layer is modelled.

JULES_SURF_HGT

All tile elevations are set to 0. However, this has been done already due to l_aggregate being set to TRUE.

JULES_Z_LAND

There is no information given in the jules_z_land namelist as there is no elevation data.

---

ancillaries.nml

This file has all the time varying ancillary values and so it has 11 namelists.

&jules_frac
file='/home/users/mehb/input_files/landcover_scenarios/landcover_c.nc',
frac_name='frac',

&jules_soil_props

const_val=6.63,0.049460,0.004715,0.458150,0.242433,0.136328,1185676.0,
0.226873,0.150000,
const_z=.false.,
file='/group_workspaces/jasmin2/jules_bd/data/CHESS_v1.0/ancils_uncompressed/chess_soilparams_hwsd_vg.nc',
nvars=9,
use_file=8*.true.,.false.,
var='b','sathh','satcon','sm_sat','sm_crit','sm_wilt','hcap',
'hcon','albsoil',
var_name='oneovernminusone','oneoveralpha','satcon','vsat','vcrit',
'vwilt','hcap','hcon','albsoil',

&jules_pdm
file='/group_workspaces/jasmin2/jules_bd/data/CHESS_v1.0/ancils_uncompressed/uk_ihdtm_topography+topoindex_1km.nc',
nvars=1,
use_file=.true.,
var='slope',
var_name='slope',

&jules_agric

&jules_rivers_props
file='/home/users/albmar/UKEP/data/routing/chess_riverparams.nc',
nvars=4,
nx=656,
nx_grid=656,
ny=1057,
ny_grid=1057,
rivers_dx=1000,
rivers_reglatlon=.false.,
rivers_regrid=.false.,
use_file=.true.,.true.,.true.,.true.,
var='direction','area','latitude_2d','longitude_2d',

var_name='dir','acc','lat','lon',
x_dim_name='x',
y_dim_name='y',

&jules_overbank
l_riv_hypsometry=.false.,
l_riv_overbank=.false.,
riv_a=7.20,
riv_b=0.50,
riv_c=0.27,
riv_f=0.30,
use_rosgen=.false.,

&jules_co2
co2_mmr=5.94100e-4,

JULES_FRAC

1. The land cover fraction is currently pointed to a folder in my directory that is simulated with 100% crops.
2. The land fraction cover name in the netCDF file is called 'frac'.

JULES_SOIL_PROPS

1. These are the 9 constant values given for when there is a false given in use_file.
2. Soil characteristics are set to vary with depth.
3. The soil properties are currently pointed to that used in the CHESS dataset. There are nine variables which are:
    - b- exponent in the soil hydraulic characteristics.
    - Sathh- as we are using the van Genuchten model, sathh = 1/*alpha* where *alpha* is a parameter in the model.
    - Satcon- hydraulic conductivity at saturation
    - Sm_sat- volumetric soil moisture content at saturation
    - Sm_crit- volumetric soil moisture content at the critical point

- Sm_wilt- volumetric soil moisture content at saturation
- Hcap- Dry heat capacity
- Hcon- dry thermal conductivity
- Albsoil- soil albedo

4. The first 8 variables are taken from the file. However, albsoil is not taken from the file and therefore is just taken as the constant value.
5. Variable names are given in the file.

JULES_PDM

1. This points to the file found in the CHESS dataset.
2. There is only one variable.
3. The variable is read in from the file.
4. The variable is slope and its name in the file is given.

JULES_AGRIC

This namelist has been populated with nothing as TRIFFID is not being used in the model.

JULES_RIVER_PROPS

1. Currently pointing the file to that created by Alberto with the needed variables.
2. There are four variables.
3. The x dimension is 656 big.
4. The x dimension is 656 big on a 2D regular lat/lon grid.
5. The y dimension is 1057 big.
6. The y dimension is 1057 big on a 2D regular lat/lon grid.
7. Latitude spacing of the grid containing the model input grid is 0.
8. Longitude spacing of the grid containing the model input grid is 0.
9. Lower left bottom corner of regular 2D grid is 0.
10. Longitude of left bottom corner of 2D grid is 0.
11. The constant size of the rivers grid is 1000m (i.e.1km).
12. River routing grid is not regular as it is projected onto OSGB36/national grid.
13. River routing and model input grids are identical.
14. No tuple name is given as there is no string to substitute into the file name.
15. All four variables come from the file specified.

16. The variables are:
    - Direction
    - Accumulation
    - 2d latitude
    - 2d longitude
17. The four variable names in the file are given.
18. The x dimension is called x.
19. The y dimension is called y.

JULES_OVERBANK

1. Overbank inundation gridbox is not included.
2. Inundated area is not calculated at present using estimates of the inundated area from simple river width scaling (ignoring topography).
3. The four factors included are those that are suggested for when using a 1 km grid.
4. Rosgen entrenchment ratio approach is not included.

JULES_CO2

A constant mass mixing ratio of 5.241e-4 is used.

---

pft_params.nml

The five classes that are represented here are:

1. Deciduous woodland
2. Evergreen woodland
3. Grass and Pasture (C3 grass)
4. Medium scale vegetation (shrubs)
5. Crops

&jules_pftparm

a_wl_io=0.65,0.65,0.005,0.10,0.005,

a_ws_io=10.00,10.00,1.00,10.00,1.00,

aef_io=0.18,0.21,0.12,0.20,0.12,

albsnc_max_io=0.15,0.15,0.60,0.40,0.60,
albsnc_min_io=0.30,0.30,0.80,0.80,0.80,
albsnf_max_io=0.10,0.10,0.20,0.20,0.20,
alnir_io=0.45,0.35,0.58,0.58,0.58,
alpar_io=0.10,0.07,0.10,0.10,0.10,
alpha_io=0.08,0.08,0.12,0.08,0.12,
b_wl_io=5*1.667,
c3_io=5*1,
can_struct_a_io=5*1.0,
canht_ft_io=19.01,16.38,0.10,1.00,0.79,
catch0_io=5*0.50,
ci_st_io=33.46,33.46,34.26,34.26,34.26,
dcatch_dlai_io=5*0.05,
dgl_dm_io=5*0.0,
dgl_dt_io=9.0,9.0,0.0,9.0,0.0,
dqcrit_io=0.090,0.060,0.100,0.100,0.100,
dust_veg_scj_io=0.0,0.0,1.0,0.5,1.0,
dz0v_dh_io=0.05,0.05,0.10,0.10,0.10,
emis_pft_io=5*0.97,
eta_sl_io=5*0.01,
f0_io=0.875,0.875,0.900,0.900,0.900,
fd_io=5*0.015,
fsmc_mod_io=5*0,
fsmc_of_io=5*0.00,
fsmc_p0_io=0.0,0.0,0.0,0.0,0.0,
g_leaf_0_io=5*0.25,
glmin_io=5*1.0e-6,
gpp_st_io=1.29e-7,2.58e-8,2.07e-7,1.68e-7,2.07e-7,
hw_sw_io=5*0.5,
ief_io=35.0,12.0,16.0,20.0,16.0,
infil_f_io=4.00,4.00,2.00,2.00,2.00,
kext_io=5*0.50,
kn_io=5*0.78,
knl_io=5*0.20,

kpar_io=5*0.50,
lai_alb_lim_io=5*0.50,
lai_io=5.0,4.0,2.0,1.0,2.0,
lma_io=0.0824,0.2263,0.0498,0.1370,0.0695,
mef_io=0.60,0.90,0.60,0.57,0.60,
neff_io=5*0.8e-3,
nl0_io=0.040,0.030,0.060,0.030,0.060,
nmass_io=0.0210,0.0115,0.0219,0.0131,0.0219,
nr_io=0.01726,0.00784,0.0162,0.0084,0.01726,
nr_nl_io=5*1.00,
ns_nl_io=0.10,0.10,1.00,0.10,1.00,
nsw_io=0.0072,0.0083,0.01604,0.0202,0.0072,
omega_io=5*0.15,
omnir_io=0.70,0.45,0.83,0.83,0.83,
orient_io=5*0,
q10_leaf_io=5*2.0,
r_grow_io=5*0.25,
rootd_ft_io=3.00,1.00,0.50,0.50,0.50,
sigl_io=0.0375,0.1000,0.0250,0.0500,0.0250,
tef_io=0.40,2.40,0.80,0.80,0.80,
tleaf_of_io=273.15,243.15,258.15,243.15,258.15,
tlow_io=0.0,-5.0,0.0,0.0,0.0,
tupp_io=36.0,31.0,36.0,36.0,36.0,
vint_io=5.73,6.32,6.42,0.00,14.71,
vsl_io=29.81,18.15,40.96,10.24,23.15,
z0hm_classic_pft_io=5*0.1,
z0hm_pft_io=5*0.10,

1. The allometric coefficient relating the target woody biomass to the LAI are set to those according to suite u-bi090 ($kgCm^{-2}$).
2. Woody biomass values as a multiple of live stem biomass.
3. Acetone emission factor varies by pft ($\mu g\ g^{-1}h^{-1}$).
4. Snow-covered albedo for large leaf area index is set for the five PFTs as l_snow_albedo = false. Refer to note 30 equation 2.

5. Snow-covered albedo for zero leaf area index is set for the five PFTs as l_snow_albedo = false. Refer to note 30 equation 2.
6. Snow-covered albedo for zero lead index is set for each of the PFTs as l_spec_albedo = false. Refer to note 30 equation 1.
7. Leaf reflection coefficient for NIR. Refer to note 30, table 3.
8. Leaf reflection coefficient for VIS (photosynthetically active radiation). Refer to note 30, table 3.
9. Quantum efficiency (molCO_2 per mol PAR photons) of the five PFTs.
10. Allometric exponent relating the target woody biomass to the LAI is set to 1.667 for all PFTs. Refer to note 24 equation 8.
11. All five PFTs are given as being of C3 type vegetation.
12. The canopy is structured as being a homogenous canopy.
13. The five values of canopy height for each PFT is given as TRIFFID is not active.
14. Minimum canopy capacity is set to 0.50 kgm^{-2} for all five PFTs. Refer to note 30, pg7.
15. Leaf-internal CO_2 concentration at standard conditions (Pa) are set to 33.46 for the trees and 34.26 for all other PFTs.
16. Rate of change of canopy capacity with LAI is 0.05 kgm^{-2}. Refer to note 30, pg7.
17. Rate of change of leaf turnover rate with moisture availability is set to 0 for all PFTs.
18. Rate of change of leaf turnover rate with temperature is set to 9 K^{-1} for all PFTs except for grass. This is 9 in note 24, equation 10.
19. Critical humidity deficit (kgH_2O per kg air) is set for all PFTs as the Jacobs model of stomatal conductance has been used (stomata_model = 1).
20. Not in the manual.
21. Rate of change of vegetation roughness length for momentum with height is set to 0.05 for trees and 0.10 for the other 3 PFTs. This is used as l_spec_veg0 is set to FALSE. Refer to note 30 page 5.
22. Surface emissivity is set to 0.97 for all PFTs.
23. Live stemwood coefficient is set to 0.1 kg C/m/m^2 leaf for all PFTs.
24. Refer to note 24, equation 9. CI/CA value for when DQ = 0 is set to 0.875 for trees and 0.900 for the other three plant types.
25. Scale factor for dark respiration is 0.015 for all PFTs.
26. As recommended, the fsmc in each soil layer is calculated and a weighted average is taken, using the fraction of roots in each layer as weights for all PFTs.
27. The moisture availability below which leaves are dropped is 0 for all PFTs.

28. Pft-dependent parameter governing the threshold at which the plant starts to experience water stress due to lack of water in the soil. This is all 0 as l_use_pft_psi is true.
29. Minimum turnover rate for leaves is set to 0.25/360 days.
30. Minimum leaf conductance for H2O (ms^{-1}) is set to 1.0e-6 for all PFTs.
31. GPP at standard conditions (refer to manual) vary according to plant type ($kgC\ m^{-2}s^{-1}$).
32. Ratio of N stem to N heartwood (kgN/kgN) from the TRY database.
33. Isoprene emission factor varies by pft ($\mu g\ g^{-1}\ h^{-1}$).
34. Infiltration enhancement factor is set to 4 for trees and 2 for smaller vegetation This is to represent the influence of these types of vegetation on drainage such as the trees creating macropores in the soil. Refer to note 30 pg 14 for details.
35. Light extinction coefficient is used as 0.5 for all PFTs as a part of the Beer's Law for light absorption through the canopy. Refer to note 30 equation 3.
36. Parameter for decay of nitrogen through the canopy as a function of layers is set to 0.78 for all PFTs as in other suites. This is used as can_rad_mod = 4.
37. Parameter for decay of nitrogen through the canopy, as a function of LAI. This is used as can_rad_mod =6.
38. PAR extinction coefficient is set to 0.50 of m^2 leaf/m^2 ground.
39. Minimum LAI permitted in calculation of the albedo in snow-free conditions is set to 0.50 for all PFTs. This is the same variable that has been put in jules_snow.nml.
40. The leaf area index is given for each PFT.
41. Leaf mass per unit area ($kgLeaf\ m^{-2}$). This should not be used as l_trait_phys is false.
42. Methanol emission factor varies by pft ($\mu g\ g^{-1}h^{-1}$).
43. Scale factor is 0.8e-3 for all PFTs that relates Vcmax with leaf nitrogen concentration. Refer to note 24, equation 51. Used as l_trait_phys is set to FALSE.
44. Top leaf nitrogen concentration (kg N/kg C) is varied depending on pft. Used as l_trait_phys is set to FALSE.
45. Top leaf nitrogen content per unit mass ($kgN\ kgLeaf^{-1}$). This should not be used as l_trait_phys is false.
46. Root nitrogen concentration (kgN/kgC). This should not be used as l_trait_phys is false.
47. Ratio of root nitrogen concentration to leaf nitrogen concentration is set to 1 for all PFTs.
48. Ratio of stem nitrogen concentration to leaf nitrogen concentration is set for 1 for grasses and crops and 0.1 for all other PFTs.

49. Stemwood nitrogen concentration (kgN/kgC). This should not be used as l_trait_phys is false.
50. Leaf scattering coefficient for PAR. This should not be used as l_spec_albedo is false.
51. Leaf scattering coefficient for NIR. This should not be used as l_spec_albedo is false.
52. The leaf angle distribution is indicated as spherical rather than horizontal.
53. Q10 factor leaf respiration is set to 2 for all PFTs. Refer to equation 66, Cox et al., 1999.
54. Growth respiration fraction is set to 0.25 for all PFTs.
55. These are the parameters for determining the root depth (m).
56. The specific heat capacity of leaf carbon (kg c/m^2)
57. Monoterpene emission factor varies by pft (μg $g^{-1}h^{-1}$).
58. In Kelvin, the temperature below which leaves are dropped is 0 degrees C for deciduous, -30 for coniferous, -15 for grass and crops and -30 for shrubs.
59. Lower temperature for photosynthesis is set to 0 degrees Celsius for all PFTs except for coniferous trees where it is set to -5 degrees Celsius.
60. Upper temperature for photosynthesis is 36 degrees Celsius for all PFTs except for coniferous trees where it is set to 31 degrees Celsius.
61. There is a linear relationship between Vcmax and Narea. Previously Vcmax was calculated as the product of nl0 and neff. This is now replaced by a linear regression based on data reported in Kattge et al. 2009. Vint is the y-intercept, vsl is the slope. This should not be used as l_trait_phys is false.
62. Slope in the linear regression between Vcmax and Narea. This should not be used as l_trait_phys is false.
63. The classic aerosol scheme input is here as well, for the ratio of roughness length etc. but this is only needed if tied with the UM.
64. Ratio of the roughness length for heat to the roughness length for momentum is set to 0.1 for all PFTs as assumed. Refer to note 30 pg6.

---

nveg_params.nml

The three non-vegetation surfaces used here are:

6. Urban and Suburban areas
7. Inland water

8. Bare soil and rocks

&jules_nvegparm
albsnc_nvg_io=4.00e-1,6.00e-2,8.00e-1,
albsnf_nvg_io=1.80e-1,6.00e-2,-1.00,
catch_nvg_io=5.00e-1,0.00,0.00,
ch_nvg_io=2.80e+5,4.18e+6,0.00,
emis_nvg_io=9.70e-1,9.70e-1,9.70e-1,
gs_nvg_io=0.00,0.00,1.00e-2,
infil_nvg_io=1.00e-1,0.00,5.00e-1,
vf_nvg_io=1.00,1.00,0.00,
z0_nvg_io=1.00,3.00e-4,3.00e-4,
z0hm_classic_nvg_io=0.1,0.1,0.1,
z0hm_nvg_io=1.00e-7,1.00e-1,1.00e-1,

1. The snow-covered albedos are taken from note 30, table 1. This is used as l_snow_albedo = FALSE.
2. Snow-free albedo is set according to u-bi090 and table 1, note 30.
3. Capacity for water is set to 0.5 for urban areas and 0 for the other types (kgm^{-2}). Refer to note 30, pg7.
4. Heat capacity of the various surface types ($JK^{-1}m^{-2}$) as can_model = 4.
5. Surface emissivity is 0.97 for all surfaces.
6. Surface conductance is set to 0 for urban and inland water and 0.01 for bare soil and rock (ms^{-1}). Refer to note 30m pg 7. Soil conductance is modified by the soil moisture as note 30, equation 35.
7. Infiltration enhancement factor varies according to surface type.
8. The fractional coverage of non-vegetation is set to 1.0 for all surfaces as they are radiatively coupled due to can_model =4.
9. Roughness length for momentum is 1m for urban areas and 3.00e-4 for inland water and bare soil rock.
10. Classic scheme is included, but not needed as JULES is in standalone mode.
11. Ratio of the roughness length for heat to the roughness length for momentum is 0.1 for inland water and bare soil/rock and set to 1.00e-7 for urban areas.

N.B.
Albsnf_nvgu_io, albsnf_nvgl_io is not used as l_albedo_obs is FALSE.

---

jules_soilparm_cable.nml

As the CABLE model is not being used in this model run, this namelist is not been populated.

---

crop_params.nml

As ncpft = 0 (i.e. there are no crops explicitly modelled in this model) this namelist has not been populated.

---

triffid_params.nml

As the TRIFFID model is not being used this namelist has been populated with information from the Loobos example by Dr Toby Marthews.

&jules_triffid
alloc_fast_io=0.6,0.6,1.0,1.0,0.8,
alloc_med_io=0.3,0.4,0.0,0.0,0.2,
alloc_slow_io=0.1,0.0,0.0,0.0,0.0,
crop_io=0,0,1,0,1,
dpm_rpm_ratio_io=0.25,0.25,0.67,0.67,0.33,
g_area_io=0.005,0.004,0.25,0.05,0.25,
g_grow_io=5*20.00,
g_root_io=5*0.25,
g_wood_io=0.01,0.01,0.20,0.05,0.20,
lai_max_io=9.00,9.00,4.00,4.00,4.00,
lai_min_io=3.00,3.00,1.00,1.00,1.00,
retran_l_io=5*0.5,

retran_r_io=5*0.2,

---

urban.nml

As the two-tile urban scheme MORUSES is not being used this namelist has not been populated.

---

fire.nml

As the fire scheme is not used in this model, l_fire is set to false so that the fire module will not be executed.

&fire_switches
l_fire=.false.,

---

drive.nml

This is the main file for driving the data and so care must be taken in making this correct to run with the data that you are driving the model with.

&jules_drive
bl_height=1000.0,
data_end='2016-01-02 00:00:00',
data_period=86400,
data_start='1961-01-01 00:00:00',
diff_frac_const=0.4,
dur_conv_rain=7200.0,
dur_conv_snow=7200.0,
dur_ls_rain=18000.0,
dur_ls_snow=18000.0,

file='/group_workspaces/jasmin2/jules_bd/data/CHESS_v1.2/met_uncompressed/chess_%vv_%y4%m2.nc',
interp=8*'nf',
l_daily_disagg=.true.,
l_disagg_const_rh=.true.,
l_imogen=.false.,
l_perturb_driving=.false.,
nvars=8,
precip_disagg_method=3,
read_list=.false.,
t_for_con_rain=288.15,
t_for_snow=275.15,
tpl_name='rsds','rlds','precip','tas','sfcWind','huss','dtr','psurf',
var='sw_down','lw_down','precip','t','wind','q','dt_range',
'pstar',
var_name='rsds','rlds','precip','tas','sfcWind','huss','dtr','psurf',
z1_tq_in=1.2,
z1_tq_vary=.false.,
z1_uv_in=10.0,

1. IMOGEN is not used to generate meteorological forcing data.
2. The near surface-air temperature at or below which precipitation is assumed to be snowfall is 2 degrees Celsius. This is given as total precipitation is given as a forcing variable.
3. The boundary layer height is assumed to be 1000 m above the ground.
4. Data end of the driving data is taken to be 2016 etc.
5. The period of the data is daily and so 86400 seconds is given.
6. Data start of the driving data is taken to be 1961 etc.
7. The diffuse radiation from the total downward shortwave radiation is given as 0.4 as it is not given in the forcing data.
8. Convective rainfall is kept as 7200 seconds (2 hrs) in the daily aggregator scheme. Refer to section 2.4 in note 96.
9. Convective snowfall event is also modelled as being 7 200 seconds long. Refer to section 2.4 in note 96.

10. The large-scale rainfall events are modelled as being 18 000 seconds (5 hrs) long. Refer to section 2.4 in note 96.
11. The large-scale snowfall events are modelled as being 18 000 seconds (5 hrs) long. Refer to section 2.4 in note 96.
12. File is set to the CHESS meteorological dataset with the template information from which to read the files.
13. All variables are temporally interpolated by using forward averaging values (nf). See the temporal interpolation section given in section 4.5 of the manual.
14. The daily disaggregator is used to convert daily data driving data to driving data at the model timestep. Refer to note 96 for a description of how this methodology works. In this model, the daily data is broken down into 30-minute steps.
15. Relative humidity (the amount of water vapour present in air expressed as a percentage of the amount needed for saturation at the same temperature) is kept constant over the day.
16. No perturbation is applied to the driving method.
17. There are 8 variables to drive the data.
18. Disaggregation method 3 is chosen. Daily precipitation is separated into each type of event of duration dur_conv_rain, dur_ls_rain, dur_conv_snow and dur_ls_snow for convective rain, large-scale rain, convective snow and large-scale snow respectively. The start time of this event is randomly distributed from the beginning of the day to the end of the day minus the event duration. If precipitation rate of any type is greater than a hard-coded maximum (350 mm/day), precipitation is redistributed by the redis routine in IMOGEN. Refer to section 2.4 in note 96.
19. Read list is set to false as a single data for is used at all times.
20. Rainfall is assumed to be convective in origin if the near-surface air temperature is at or above 15 degrees Celsius. At lower temperatures, all the rainfall is assumed to be large-scale in origin. Snow is always assumed to be large-scale in origin. Furthermore, this is used as l_point_data = FALSE and therefore convective precipitation is part of the modelling scheme.
21. The string to substitute into the file name is given.
22. The eight variables used to run the model are:
    1. Downward shortwave radiation (Wm^{-2})
    2. Downward longwave radiation (Wm^{-2})
    3. Precipitation rate ($kg\ m^{-2}s^{-1}$)

4. Air temperature (K)
5. Total wind speed (ms^{-1})
6. Specific humidity ($kg\ kg^{-1}$)
7. Diurnal temperature range (K)
8. Air pressure (Pa)

To run the model, you require at least air pressure, specific humidity, air temperature, precipitation, wind and diurnal temperature range. There are combinations of data inputs that can be given. For example, for radiation variables the following combinations can be given:

- ***Sw_down and lw_down***
- ***Rad_net and sw_down***
- ***Lw_net and sw_net***
- ***Lw_down and sw_net***

With this example the diffuse radiation can be used if given from data for each of the four methods mentioned above. When it is not used, the constant diff_rad_const is used such as in this model configuration.

Precipitation in the model can also be input in four ways:

- ***Precip***
- ***Tot_rain and tot_snow***
- ***Ls_rain, con_rain and tot_snow***
- ***Ls_rain, con_rain, ls_snow and con_snow***

Wind can be given in two ways:

- ***Wind***
- ***U and V (the different components of horizontal wind).***

23. The variable names are given for each of the variables in the file containing the data.
24. 1.2 m is taken to be the height for temperature and humidity constant.
25. The height at which the temperature and humidity data are valid is constant and not spatially varying.
26. 10 m (the default) is taken as the constant value for the height at which the wind data are valid for every point.

N.B. Temperature_abs_perturbation and precip_rel_perturbation are not included as l_perturb_driving is false.

Zl_tq_in and zl_tq_var_name are not used as zl_tq_vary is false.
Nfiles is not used as read_list is false and there is not a list of files to call in.

---

imogen.nml

As IMOGEN is not being used, the namelist is not populated.

---

prescribed_data.nml

This the namelist that is used to give time-varying put data that is not meteorological data as given in by drive.nml. This will include the land varying variables.

&jules_prescribed
n_datasets=1,

&jules_prescribed_dataset
data_end='2017-01-01 00:00:00',
data_period=-2,
data_start='1959-01-01 00:00:00',
file='/work/scratch/emrobi/data/ancils/co2/co2_annmean_comb_chess_1959_2017.nc',
interp='nf',
is_climatology=.false.,
nvars=1,
read_list=.false.,
tpl_name='co2_mmr',
var='co2_mmr',
var_name='co2_mmr',

As the prescribed dataset follow the same routine, this is just an example of one of the prescribed datasets information. The rest can be determined.

1. Data ends at 2017.
2. Data period is -2 as this is the code for annual rather than giving it in seconds.
3. Data starts at 1959.
4. The file directory is given.
5. The interpolation is done by using forward averaging values (nf). See the temporal interpolation section given in section 4.5 of the manual.
6. Indicates whether the data is to be used as a climatology (use the same data for every year). If it is true, you interpret the data as a climatology and data_start and data_end must be such that exactly one year of data is being specified. If it is false, do not interpret the data as a climatology.
7. Number of variables, normally one.
8. The number of layers in the file.
9. Read_list is set to false as a single data file is used.
10. The name of the variable in each of the files.
11. Variable given is one of the supported list variables.
12. The name of the variable in each of the files.

The following variables are the ones that are supported by JULES:

- ***Ozone- surface ozone conc.***
- ***Canht- PFT canopy height***
- ***Lai- PFT leaf area index***
- ***Albobs_sw- observed shortwave diffuse albedo***
- ***Albobs_vis- observed VIS diffuse albedo***
- ***Albobs_nir- observed NIR diffuse albedo***
- ***Co2_mmr- concentration of atmospheric CO2, expressed as a mass mixing ratio***
- ***Sthuf- Soil wetness for each layer***
- ***Frac_agr- Fractional area of agricultural land in each gridbox***
- ***Tracer_field- surface conc. of atmospheric chemical tracers in the atmosphere***
- ***Bl_height- height above surface of top of atmospheric boundary layer***
- ***Level_separation- separation of boundary layer levels***

Technically any value can be given as a prescribed dataset. However, this requires altering populate_var in model_interface_mod. All variables input using prescribed.nml must have a time dimension using time_dim_name.

---

initial_conditions.nml

```
&jues_initial
  dump_file = .false.,
  total_snow = .true.,
  file                                                                    =
/group_workspaces/jasmin2/jules_bd/data/CHESS_v1.0/ancils_uncompressed/chess_soilpara
ms_hwsd_vg_sclayer.nc' ,
  nvars = 12,
  var = 'sthuf','canopy','snow_tile','rgrain','tstar_tile','t_soil','cs','gs','lai','canht','sthzw','zw' ,
  use_file=6*.false.,.true.,5*.false. ,
  var_name                                                                =
'sthuf','canopy','snow_tile','rgrain','tstar_tile','t_soil','cs','gs','lai','canht','sthzw','zw'
  const_val = 0.9,0.0,0.0,50.0,275.0,278.0,10.0,0.0,1.0,2.0,0.9,3.0
```

1. The constant values to use if there are not time-varying variables given in the file given.
2. The file used for the initial conditions is not a JULES dump file.
3. The directory given is the same as used in suite u-bi090.
4. There are 12 start up variables.
5. Only the total mass of snow on each tile is required to be an input and all other variables are assumed such as all snow being on the surface.
6. 11 variables in the file are not used, and instead the constants are used. The only variable to be used is ‘cs’ which is the carbon soil store in the gridbox.
7. The 12 variables used to start up the model are:
    - Soil wetness for each layer
    - **Amount of intercepted water that is held on each tile**
    - **Snow on the tile**
    - *Snow surface grain size on each tile (not needed as l_snow_albedo is not used)*
    - **Temperature of each tile**
    - **Temperature of each soil layer**
    - **Soil carbon**

- *Surface conductance for water vapour (but does not need to be here as can_rad_model != 1)*
- Leaf area index
- *Height of each pft (although not needed as triffid is not active).*
- *Soil wetness in the deep layer (although not needed as l_top = false)*
- *Depth from the surface to the water table (although not needed as l_top = false).*

All those in bold are those that are always required to start up the model. Those that are just italicised do not need to be here and could be removed.

---

output.nml

In some ways this is the most important file as it determines the data that you produce. The one written is just an example.

```
&jules_output
dump_period=1,
nprofiles=4,
output_dir='/home/users/mehb/output_files',
run_id='1km_Crops',
/
&jules_output_profile
file_period=-2,
nvars=46,
output_end='2015-01-01 00:00:00',
output_initial=.false.,
output_main_run=.true.,
output_period=-1,
output_spinup=.false.,
output_start='2005-01-01 00:00:00',
output_type=46*'M',
profile_name='monthly_mean_gridbox',
```

```
sample_period=1800,
var='ecan_gb','ei_gb','esoil_gb','et_stom_gb','fqw_gb','ftl_gb',
'latent_heat','snow_mass_gb','surf_ht_flux_gb','t1p5m_gb',
'q1p5m_gb','tstar_gb','canopy_gb','drain','elake','fsat',
'gpp_gb','gs','npp_gb','rad_net','resp_p_gb','resp_s_gb',
'runoff','smc_avail_top','smc_avail_tot','smc_tot',
'snow_can_gb','snow_depth_gb','snow_frac','snow_grnd_gb',
'snow_melt_gb','sub_surf_roff','surf_roff','tfall','trad',
'zw','fao_et0','precip','sw_down','lw_down','tl1','qw1',
'wind','pstar','rainfall','snowfall',
var_name=46*'',

&jules_output_profile
file_period=-2,
nvars=6,
output_end='2015-01-01 00:00:00',
output_initial=.false.,
output_main_run=.true.,
output_period=-1,
output_spinup=.false.,
output_start='2005-01-01 00:00:00',
output_type=6*'M',
profile_name='monthly_mean_runoff',
sample_period=1800,
var='runoff','rflow','rrun','sat_excess_roff',
'sub_surf_roff','surf_roff',
var_name=6*'',

&jules_output_profile
file_period=-2,
nvars=6,
output_end='2015-01-01 00:00:00',
output_initial=.false.,
output_main_run=.true.,
```

output_period=-1,
output_spinup=.false.,
output_start='2005-01-01 00:00:00',
output_type=6*'X',
profile_name='monthly_max_runoff',
sample_period=1800,
var='runoff','rflow','rrun','sat_excess_roff',
'sub_surf_roff','surf_roff',
var_name=6*",

&jules_output_profile
file_period=-2,
nvars=6,
output_end='2015-01-01 00:00:00',
output_initial=.false.,
output_main_run=.true.,
output_period=-1,
output_spinup=.false.,
output_start='2005-01-01 00:00:00',
output_type=6*'N',
profile_name='monthly_min_runoff',
sample_period=1800,
var='runoff','rflow','rrun','sat_excess_roff','sub_surf_roff',
'surf_roff',
var_name=6*",

JULES_OUTPUT

1. The model creates a dump file every (1) year.
2. The number of output profiles is 4 in this case.
3. The output file directory is given.
4. The run id given is 1km_Crop.

JULES_OUTPUT_PROFILE (this is just for the gridbox)

1. The output period for the files, such that all the outputs are clumped into this one file, are set for annual years of data being produced (with -2. -1 would have been monthly)
2. The number of variables is 46.
3. Output end is 2015.
4. An initial data file is created at the start of the main run as output_main_run = TRUE and output_start = main_run_start.
5. Output is produced for the first model run which is given between output_start and output_end.
6. Output period is every month.
7. No output is given during spinup.
8. Output start is 2005.
9. The variables will all be time mean values. The following letters symbolise the outputs that can be generated:
    - S – snapshot
    - M – mean
    - N – minimum
    - X – maximum
    - A – accumulation
10. The profile name is monthly_mean_gridbox.
11. Sample period for creating time varied statistics is the same as timestep length.
12. The variables given are part of the table that can be found in section 9 of the manual.
13. The variable names are going to be the same as the variables.

Appendix 6: Co-Authorship Statements

I Huw Lewis certify that Marcus Buechel completed the majority of the work in the following journal article below, which forms part of his DPhil thesis:

- Afforestation leads to a wetter UK: findings from a kilometer-scale climate model

Print Name: Huw Lewis

Signature: Date: 24/07/2023

I Will Keat certify that Marcus Buechel completed the majority of the work in the following journal article below, which forms part of his DPhil thesis:

- Afforestation leads to a wetter UK: findings from a kilometer-scale climate model

Print Name: William Keat

Signature : *WKeat* Date: 24/07/2023

UNIVERSITY OF OXFORD

I Ségolène Berthou certify that Marcus Buechel completed the majority of the work in the following journal article below, which forms part of his DPhil thesis:

- Afforestation leads to a wetter UK: findings from a kilometer-scale climate model

Print Name: Ségolène Berthou

Signature: Date: 24/07/23

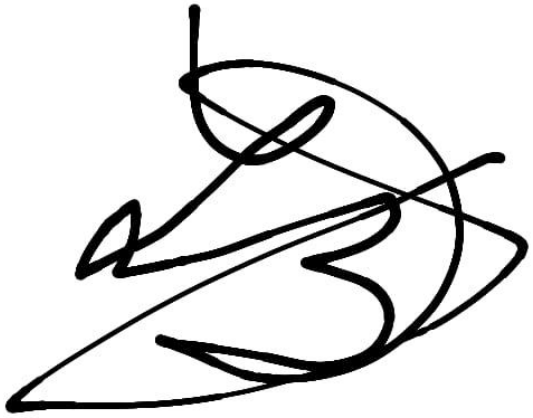

References

Abbott, M.B. *et al.* (1986) ‘An introduction to the European Hydrological System—Systeme Hydrologique Europeen,“SHE”, 1: History and philosophy of a physically-based, distributed modelling system’, *Journal of Hydrology*, 87(1–2), pp. 45–59.

Addor, N. *et al.* (2017) ‘The CAMELS data set: Catchment attributes and meteorology for large-sample studies’, *Hydrology and Earth System Sciences*, 21(10), pp. 5293–5313. doi:10.5194/hess-21-5293-2017.

Addor, N. *et al.* (2020) ‘Large-sample hydrology: recent progress, guidelines for new datasets and grand challenges’, *Hydrological Sciences Journal*, 65(5), pp. 712–725. doi:10.1080/02626667.2019.1683182.

Addor, N. and Melsen, L.A. (2019) ‘Legacy, Rather Than Adequacy, Drives the Selection of Hydrological Models’, *Water Resources Research*, 55(1), pp. 378–390. doi:10.1029/2018WR022958.

Afzal, M. and Ragab, R. (2019) ‘Drought risk under climate and land use changes: Implication to water resource availability at catchment scale’, *Water (Switzerland)*, 11(9). doi:10.3390/w11091790.

Alkama, R. *et al.* (2022) ‘Vegetation-based climate mitigation in a warmer and greener World’, *Nature Communications*, 13(1), pp. 1–10. doi:10.1038/s41467-022-28305-9.

Allan, R.P. *et al.* (2020) ‘Advances in understanding large-scale responses of the water cycle to climate change’, *Annals of the New York Academy of Sciences*, 1472(1), pp. 49–75. doi:10.1111/nyas.14337.

Allen, G.H. and Pavelsky, T. (2018) ‘Global extent of rivers and streams’, *Science*, 361(6402), pp. 585–588. doi:10.1126/science.aat063.

Alton, P. *et al.* (2009) ‘Simulations of global evapotranspiration using semiempirical and mechanistic schemes of plant hydrology’, *Global Biogeochemical Cycles*, 23(4), pp. 1–12. doi:10.1029/2009GB003540.

Anderson, B.J. *et al.* (2022) ‘Statistical Attribution of the Influence of Urban and Tree Cover Change on Streamflow: A Comparison of Large Sample Statistical Approaches’, *Water Resources Research*, 58(5), pp. 1–20. doi:10.1029/2021wr030742.

Andréassian, V. (2004) ‘Waters and forests: From historical controversy to scientific debate’,

Journal of Hydrology, 291(1–2), pp. 1–27. doi:10.1016/j.jhydrol.2003.12.015.

Ares, E., Coe, S. and Uberoi, E. (2021) *House of Commons Briefing Paper: Tree Planting in the UK*. Available at: www.parliament.uk/commons-library%7Cintranet.parliament.uk/commons-library%7Cpapers@parliament.uk%7C@commonslibrary.

Arheimer, B. *et al.* (2020) 'Global catchment modelling using World-Wide HYPE (WWH), open data, and stepwise parameter estimation', *Hydrology and Earth System Sciences*, 24(2), pp. 535–559. doi:10.5194/hess-24-535-2020.

Arora, V.K. and Montenegro, A. (2011) 'Small temperature benefits provided by realistic afforestation efforts', *Nature Geoscience*, 4(8), pp. 514–518. doi:10.1038/ngeo1182.

Astagneau, P.C. *et al.* (2021) 'Technical note: Hydrology modelling R packages - A unified analysis of models and practicalities from a user perspective', *Hydrology and Earth System Sciences*, 25(7), pp. 3937–3973. doi:10.5194/hess-25-3937-2021.

Balsamo, G. *et al.* (2009) 'A Revised Hydrology for the ECMWF Model: Verification from Field Site to Terrestrial Water Storage and Impact in the Integrated Forecast System', *Journal of Hydrometeorology*, 10(3), pp. 623–643. doi:10.1175/2008JHM1068.1.

Bandaragoda, C. *et al.* (2019) 'Enabling Collaborative Numerical Modeling in Earth Sciences using Knowledge Infrastructure', *Environmental Modelling & Software*, 120(February), p. 104424. doi:10.1016/j.envsoft.2019.03.020.

Bastin, J.-F. *et al.* (2019) 'The global tree restoration potential', *Science*, 365(6448), pp. 76–79. doi:10.1126/science.aax0848.

Batelis, S.C. *et al.* (2020) 'Towards the representation of groundwater in the Joint UK Land Environment Simulator', *Hydrological Processes*, 34(13), pp. 2843–2863. doi:10.1002/hyp.13767.

Bates, P.D. *et al.* (2023) 'A climate-conditioned catastrophe risk model for UK flooding', *Natural Hazards and Earth System Sciences*, 23(2), pp. 891–908. doi:10.5194/nhess-23-891-2023.

Bathurst, J. *et al.* (2018) 'Runoff, flood peaks and proportional response in a combined nested and paired forest plantation/peat grassland catchment', *Journal of Hydrology*, 564(April), pp. 916–927. doi:10.1016/j.jhydrol.2018.07.039.

Bathurst, J.C. *et al.* (2020) 'Forests and floods: Using field evidence to reconcile analysis

methods', *Hydrological Processes*, 34(15), pp. 3295–3310. doi:10.1002/hyp.13802.

Beck, H.E. *et al.* (2016) 'Global-scale regionalization of hydrologic model parameters', *Water Resources Research*, 52(5), pp. 3599–3622. doi:10.1002/2015WR018247.

Bell, V.A. *et al.* (2007) 'Development of a high resolution grid-based river flow model for use with regional climate model output', *Hydrology and Earth System Sciences*, 11(1), pp. 532–549. doi:10.5194/hess-11-532-2007.

Belušić, D. *et al.* (2019) 'Afforestation reduces cyclone intensity and precipitation extremes over Europe', *Environmental Research Letters*, 14(7). doi:10.1088/1748-9326/ab23b2.

Bennett, A. and Nijssen, B. (2021) 'Deep Learned Process Parameterizations Provide Better Representations of Turbulent Heat Fluxes in Hydrologic Models', *Water Resources Research*, 57(5), pp. 1–14. doi:10.1029/2020WR029328.

Bentley, L. and Coomes, D.A. (2020) 'Partial river flow recovery with forest age is rare in the decades following establishment', *Global Change Biology*, 26(3), pp. 1458–1473. doi:10.1111/gcb.14954.

Berghuijs, W.R., Allen, S.T., *et al.* (2019) 'Growing Spatial Scales of Synchronous River Flooding in Europe', *Geophysical Research Letters*, 46(3), pp. 1423–1428. doi:10.1029/2018GL081883.

Berghuijs, W.R., Harrigan, S., *et al.* (2019) 'The Relative Importance of Different Flood-Generating Mechanisms Across Europe', *Water Resources Research*, 55(6), pp. 4582–4593. doi:10.1029/2019WR024841.

Berghuijs, W.R. *et al.* (2021) 'Recharge observations indicate strengthened groundwater connection to surface fluxes', pp. 1–9. doi:10.1029/2022GL099010.

Berghuijs, W.R. *et al.* (2022) 'Global Recharge Data Set Indicates Strengthened Groundwater Connection to Surface Fluxes', *Geophysical Research Letters*, 49(23), pp. 1–9. doi:10.1029/2022GL099010.

Bergström, S. and Rapporter, S. (1976) '" Development and Application of a Conceptual Runoff Model for Scandinavian Catchments Utveckling Och Tillämpning Av En Begreppsmässig Avrinningsmodell För Skandinaviska Nederbördsområden', 7.

Berthou, S. *et al.* (2020) 'Pan-European climate at convection-permitting scale: a model intercomparison study', *Climate Dynamics*, 55(1–2), pp. 35–59. doi:10.1007/s00382-018-4114-6.

Beschta, R.L. *et al.* (2000) 'Peakflow responses to forest practices in the western cascades of Oregon, USA', *Journal of Hydrology*, 233(1–4), pp. 102–120. doi:10.1016/S0022-1694(00)00231-6.

Best, M., Essery, R. and Cox, P. (2009) *JULES Technical Documentation MOSES 2.2 Technical Documentation*. Available at: https://jules.jchmr.org/sites/default/files/Technical_documentation_2.pdf.

Best, M.J. *et al.* (2011) 'The Joint UK Land Environment Simulator (JULES), model description – Part 1: Energy and water fluxes', *Geoscientific Model Development*, 4(3), pp. 677–699. doi:10.5194/gmd-4-677-2011.

Best, M.J. *et al.* (2015) 'The plumbing of land surface models: Benchmarking model performance', *Journal of Hydrometeorology*, 16(3), pp. 1425–1442. doi:10.1175/JHM-D-14-0158.1.

Betts, R.A. *et al.* (2007) 'Projected increase in continental runoff due to plant responses to increasing carbon dioxide', *Nature*, 448(7157), pp. 1037–1041. doi:10.1038/nature06045.

Beven, K. (1989) 'Changing ideas in hydrology — The case of physically-based models', *Journal of Hydrology*, 105(1–2), pp. 157–172. doi:10.1016/0022-1694(89)90101-7.

Beven, K. (2006) 'Searching for the Holy Grail of Scientific Hydrology', *Hydrology and Earth System Sciences Discussions*, 3(3), pp. 769–792. doi:10.5194/hessd-3-769-2006.

Beven, K. (2007) 'Towards integrated environmental models of everywhere: Uncertainty, data and modelling as a learning process', *Hydrology and Earth System Sciences*, 11(1), pp. 460–467. doi:10.5194/hess-11-460-2007.

Beven, K. *et al.* (2019) 'Developing observational methods to drive future hydrological science: can we make a start as a community?', *Hydrological Processes*, p. hyp.13622. doi:10.1002/hyp.13622.

Beven, K. (2020) 'Deep learning, hydrological processes and the uniqueness of place', *Hydrological Processes*, 34(16), pp. 3608–3613. doi:10.1002/hyp.13805.

Beven, K. *et al.* (2021) 'A history of TOPMODEL', *Hydrology and Earth System Sciences*, 25(2), pp. 527–549. doi:10.5194/hess-25-527-2021.

Beven, K. *et al.* (2022) 'On (in)validating environmental models. 2. Implementation of a Turing-like test to modelling hydrological processes', *Hydrological Processes*, 36(10), pp. 0–2. doi:10.1002/hyp.14703.

Beven, K. and Freer, J. (2001) 'Equifinality, data assimilation, and uncertainty estimation in mechanistic modelling of complex environmental systems using the GLUE methodology', *Journal of Hydrology*, 249, pp. 11–29. doi:10.1016/S0022-1694(01)00421-8.

Beven, K. and Lane, S. (2022) 'On (in)validating environmental models. 1. Principles for formulating a Turing-like Test for determining when a model is fit-for purpose', *Hydrological Processes*, 36(10), pp. 1–32. doi:10.1002/hyp.14704.

Beven, K., Smith, P.J. and Wood, A. (2011) 'On the colour and spin of epistemic error (and what we might do about it)', *Hydrology and Earth System Sciences*, 15(10), pp. 3123–3133. doi:10.5194/hess-15-3123-2011.

Beven, K.J. (2013) *Rainfall-runoff modeling: The primer (2nd Edition)*. 2nd edn. John Wiley & Sons, Inc.

Beven, K.J. (2018) 'On hypothesis testing in hydrology: Why falsification of models is still a really good idea', *Wiley Interdisciplinary Reviews: Water*, 5(3), p. e1278. doi:10.1002/wat2.1278.

Beven, K.J. and Chappell, N.A. (2021) 'Perceptual perplexity and parameter parsimony', *Wiley Interdisciplinary Reviews: Water*, 8(4), pp. 1–17. doi:10.1002/wat2.1530.

Beven, K.J. and Cloke, H.L. (2012) 'Comment on "Hyperresolution global land surface modeling: Meeting a grand challenge for monitoring Earth's terrestrial water" by Eric F. Wood et al.', *Water Resources Research*, 48(1), pp. 2–4. doi:10.1029/2011wr010982.

Beven, K.J. and Kirkby, M.J. (1979) 'A physically based, variable contributing area model of basin hydrology', *Hydrological Sciences Bulletin*, 24(1), pp. 43–69. doi:10.1080/02626667909491834.

Bierkens, M.F.P. *et al.* (2015) 'Hyper-resolution global hydrological modelling: What is next?: "Everywhere and locally relevant" M. F. P. Bierkens et al. Invited Commentary', *Hydrological Processes*, 29(2), pp. 310–320. doi:10.1002/hyp.10391.

Birkinshaw, S.J., Bathurst, J.C. and Robinson, M. (2014) '45 years of non-stationary hydrology over a forest plantation growth cycle, Coalburn catchment, Northern England', *Journal of Hydrology*, 519(PA), pp. 559–573. doi:10.1016/j.jhydrol.2014.07.050.

Bisht, G. and Riley, W.J. (2019) 'Development and Verification of a Numerical Library for Solving Global Terrestrial Multiphysics Problems', *Journal of Advances in Modeling Earth Systems*, 11(6), pp. 1516–1542. doi:10.1029/2018MS001560.

Bittner, D. *et al.* (2021) 'Temporal Scale-Dependent Sensitivity Analysis for Hydrological Model Parameters Using the Discrete Wavelet Transform and Active Subspaces', *Water Resources Research*, 57(10), pp. 1–40. doi:10.1029/2020WR028511.

Blair, G.S. *et al.* (2019) 'Models of everywhere revisited: A technological perspective', *Environmental Modelling & Software*, 122(September), p. 104521. doi:10.1016/j.envsoft.2019.104521.

Blöschl, G. *et al.* (2007) 'At what scales do climate variability and land cover change impact on flooding and low flows?', *Hydrological Processes*, 21(9), pp. 1241–1247. doi:10.1002/hyp.6669.

Blöschl, G. *et al.* (2019) 'Twenty-three unsolved problems in hydrology (UPH)–a community perspective', *Hydrological Sciences Journal*, 64(10), pp. 1141–1158. doi:10.1080/02626667.2019.1620507.

Blöschl, G. *et al.* (2020) 'Current European flood-rich period exceptional compared with past 500 years', *Nature*, 583(7817), pp. 560–566. doi:10.1038/s41586-020-2478-3.

Blöschl, G. (2022) 'Three hypotheses on changing river flood hazards', *Hydrology and Earth System Sciences*, 26(19), pp. 5015–5033. doi:10.5194/hess-26-5015-2022.

Blöschl, G. and Sivapalan, M. (1995) 'Scale issues in hydrological modelling: A review', *Hydrological Processes*, 9(3–4), pp. 251–290. doi:10.1002/hyp.3360090305.

Blyth, E. (2002) 'Modelling soil moisture for a grassland and a woodland site in south-east England', *Hydrology and Earth System Sciences*, 6(1), pp. 39–47. doi:10.5194/hess-6-39-2002.

Blyth, E. *et al.* (2011) 'A comprehensive set of benchmark tests for a land surface model of simultaneous fluxes of water and carbon at both the global and seasonal scale', *Geoscientific Model Development*, 4(2), pp. 255–269. doi:10.5194/gmd-4-255-2011.

Blyth, E.M. *et al.* (2021) 'Advances in Land Surface Modelling', *Current Climate Change Reports*, 7(2), pp. 45–71. doi:10.1007/s40641-021-00171-5.

Blyth, E.M., Martínez-de la Torre, A. and Robinson, E.L. (2019) 'Trends in evapotranspiration and its drivers in Great Britain: 1961 to 2015', *Progress in Physical Geography*, 43(5), pp. 666–693. doi:10.1177/0309133319841891.

Bonan, G.B. (2008) 'Forests and Climate Change: Forcings, Feedbacks, and the Climate Benefits of Forests', *Science*, 320(5882), pp. 1444–1449. doi:10.1126/science.1155121.

Bond, S. *et al.* (2022) 'The influence of land management and seasonal changes in surface

vegetation on flood mitigation in two UK upland catchments', *Hydrological Processes*, 36(12), pp. 1–20. doi:10.1002/hyp.14766.

Booij, M.J., Schipper, T.C. and Marhaento, H. (2019) 'Attributing changes in streamflow to land use and climate change for 472 catchments in australia and the United States', *Water (Switzerland)*, 11(5). doi:10.3390/w11051059.

Bosch, J.M. and Hewlett, J.D. (1982) 'A review of catchment experiments to determine the effect of vegetation changes on water yield and evapotranspiration', *Journal of Hydrology*, 55(1–4), pp. 3–23. doi:10.1016/0022-1694(82)90117-2.

Box, G.E.P. (1976a) 'Science and Statistics', *Journal of the American Statistical Association*, 71(356), pp. 791–799. doi:10.1080/01621459.1976.10480949.

Box, G.E.P. (1976b) 'Science and Statistics', *Journal of the American Statistical Association*, 71(356), pp. 791–799. doi:10.1080/01621459.1976.10480949.

Bracken, L.J. and Croke, J. (2007) 'The concept of hydrological connectivity and its contribution to understanding runoff-dominated geomorphic systems', *Hydrological Processes*, 21(13), pp. 1749–1763. doi:10.1002/hyp.6313.

Bradfer-Lawrence, T. *et al.* (2014) *Mapping potential areas for woodland creation in the UK*. Available at: https://datastorre.stir.ac.uk/bitstream/11667/179/2/Mapping potential areas for woodland creation.pdf.

Bradshaw, C.J.A. *et al.* (2007) 'Global evidence that deforestation amplifies flood risk and severity in the developing world', *Global Change Biology*, 13(11), pp. 2379–2395. doi:10.1111/j.1365-2486.2007.01446.x.

Breil, M. *et al.* (2020) 'The opposing effects of reforestation and afforestation on the diurnal temperature cycle at the surface and in the lowest atmospheric model level in the European summer', *Journal of Climate*, 33(21), pp. 9159–9179. doi:10.1175/JCLI-D-19-0624.1.

Broadmeadow, S. *et al.* (2018) *Valuing flood regulation services of existing forest cover to inform natural capital accounts, The Research Agency of the Forestry Commission*. Available at: https://www.forestresearch.gov.uk/documents/5499/Final_report_valuing_flood_regulation_services_051218.pdf.

Broadmeadow, S., Thomas, H. and Nisbet, T. (2019) *Opportunity mapping for woodland creation to reduce diffuse water pollution and floof risk in England and Wales.*, *Journal of*

Chemical Information and Modeling.

Brogna, D. *et al.* (2017) 'How does forest cover impact water flows and ecosystem services? Insights from "real-life" catchments in Wallonia (Belgium)', *Ecological Indicators*, 72, pp. 675–685. doi:10.1016/j.ecolind.2016.08.011.

Brooks, R. and Corey, A. (1964) 'Hydraulic properties of porous media', *Hydrology Papers, Colorado State University*, 3(March), p. 37 pp. Available at: http://www.citeulike.org/group/1336/article/711012.

Brown, A.E. *et al.* (2013) 'Impact of forest cover changes on annual streamflow and flow duration curves', *Journal of Hydrology*, 483, pp. 39–50. doi:10.1016/j.jhydrol.2012.12.031.

Brown, I. (2020) 'Challenges in delivering climate change policy through land use targets for afforestation and peatland restoration', *Environmental Science and Policy*, 107(October 2019), pp. 36–45. doi:10.1016/j.envsci.2020.02.013.

Brunner, M.I. *et al.* (2021) 'Challenges in modeling and predicting floods and droughts: A review', *WIREs Water*, 8(3), pp. 1–32. doi:10.1002/wat2.1520.

Buechel, M., Slater, L. and Dadson, S. (2022) 'Hydrological impact of widespread afforestation in Great Britain using a large ensemble of modelled scenarios', *Communications Earth & Environment*, 3(1), pp. 1–10. doi:10.1038/s43247-021-00334-0.

Bulygina, N., McIntyre, N. and Wheater, H. (2013) 'A comparison of rainfall-runoff modelling approaches for estimating impacts of rural land management on flood flows', *Hydrology Research*, 44(3), pp. 467–483. doi:10.2166/nh.2013.034.

Burke, T. *et al.* (2021) 'Achieving national scale targets for carbon sequestration through afforestation: Geospatial assessment of feasibility and policy implications', *Environmental Science & Policy*, 124(December 2020), pp. 279–292. doi:10.1016/j.envsci.2021.06.023.

Burt, T.P., Howden, N.J.K. and Worrall, F. (2016) 'The changing water cycle: hydroclimatic extremes in the British Isles', *Wiley Interdisciplinary Reviews: Water*, 3(6), pp. 854–870. doi:10.1002/wat2.1169.

Burt, T.P. and McDonnell, J.J. (2015) 'Whither field hydrology? The need for discovery science and outrageous hydrological hypotheses', *Water Resources Research*, 51(8), pp. 5919–5928. doi:10.1002/2014WR016839.

Burton, V. *et al.* (2018) 'Reviewing the evidence base for the effects of woodland expansion on biodiversity and ecosystem services in the United Kingdom', *Forest Ecology and*

Management, 430(April), pp. 366–379. doi:10.1016/j.foreco.2018.08.003.

Bush, M. *et al.* (2020) 'The first Met Office Unified Model-JULES Regional Atmosphere and Land configuration, RAL1', *Geoscientific Model Development*, 13(4), pp. 1999–2029. doi:10.5194/gmd-13-1999-2020.

Bush, M. *et al.* (2023) 'The second Met Office Unified Model–JULES Regional Atmosphere and Land configuration, RAL2', *Geoscientific Model Development*, 16(6), pp. 1713–1734. doi:10.5194/gmd-16-1713-2023.

Buytaert, W. and Beven, K. (2011) 'Models as multiple working hypotheses: Hydrological simulation of tropical alpine wetlands', *Hydrological Processes*, 25(11), pp. 1784–1799. doi:10.1002/hyp.7936.

Calder, I.R. (2002) 'Forests and Hydrological Services: Reconciling public and science perceptions', *Land Use and Water Resources Research*, 2, pp. 1–12. doi:10.22004/ag.econ.47860.

Calder, I.R. (2007) 'Forests and water—Ensuring forest benefits outweigh water costs', *Forest Ecology and Management*, 251(1–2), pp. 110–120. doi:10.1016/j.foreco.2007.06.015.

Calder, I.R. and Newson, M.D. (1979) 'Land-Use and Upland Water Resources in Britain - a Strategic Look', *JAWRA Journal of the American Water Resources Association*, 15(6), pp. 1628–1639. doi:10.1111/j.1752-1688.1979.tb01176.x.

Carrick, J. *et al.* (2019) 'Is planting trees the solution to reducing flood risks?', *Journal of Flood Risk Management*, 12(S2), pp. 1–10. doi:10.1111/jfr3.12484.

Cerasoli, S., Yin, J. and Porporato, A. (2021) 'Cloud cooling effects of afforestation and reforestation at midlatitudes', *Proceedings of the National Academy of Sciences of the United States of America*, 118(33), pp. 1–7. doi:10.1073/pnas.2026241118.

Chan, W.C.H. *et al.* (2022) 'Tracking the methodological evolution of climate change projections for UK river flows', *Progress in Physical Geography*, 46(4), pp. 589–612. doi:10.1177/03091333221079201.

Chandler, K.R. *et al.* (2018) 'Influence of tree species and forest land use on soil hydraulic conductivity and implications for surface runoff generation', *Geoderma*, 310(August 2017), pp. 120–127. doi:10.1016/j.geoderma.2017.08.011.

Chaney, N.W., Metcalfe, P. and Wood, E.F. (2016) 'HydroBlocks: a field-scale resolving land surface model for application over continental extents', *Hydrological Processes*, 30(20), pp.

3543–3559. doi:10.1002/hyp.10891.

Chang, L.L. *et al.* (2018a) 'Why Do Large-Scale Land Surface Models Produce a Low Ratio of Transpiration to Evapotranspiration?', *Journal of Geophysical Research: Atmospheres*, 123(17), pp. 9109–9130. doi:10.1029/2018JD029159.

Chang, L.L. *et al.* (2018b) 'Why Do Large-Scale Land Surface Models Produce a Low Ratio of Transpiration to Evapotranspiration?', *Journal of Geophysical Research: Atmospheres*, 123(17), pp. 9109–9130. doi:10.1029/2018JD029159.

Chiverrell, R.C. *et al.* (2019) 'Using lake sediment archives to improve understanding of flood magnitude and frequency: Recent extreme flooding in northwest UK', *Earth Surface Processes and Landforms*, 44(12), pp. 2366–2376. doi:10.1002/esp.4650.

Cioni, G. and Hohenegger, C. (2017) 'Effect of soil moisture on diurnal convection and precipitation in large-eddy simulations', *Journal of Hydrometeorology*, 18(7), pp. 1885–1903. doi:10.1175/JHM-D-16-0241.1.

Clapp, R.B. and Hornberger, G.M. (1978) 'Empirical equations for some soil hydraulic properties', *Water Resources Research*, 14(4), pp. 601–604. doi:10.1029/WR014i004p00601.

Clark, D.B. *et al.* (2011) 'The Joint UK Land Environment Simulator (JULES), model description – Part 2: Carbon fluxes and vegetation dynamics', *Geoscientific Model Development*, 4(3), pp. 701–722. doi:10.5194/gmd-4-701-2011.

Clark, D.B. and Gedney, N. (2008) 'Representing the effects of subgrid variability of soil moisture on runoff generation in a land surface model', *Journal of Geophysical Research*, 113(D10), p. D10111. doi:10.1029/2007JD008940.

Clark, M.P. *et al.* (2008) 'Framework for Understanding Structural Errors (FUSE): A modular framework to diagnose differences between hydrological models', *Water Resources Research*, 44(12), pp. 1–14. doi:10.1029/2007WR006735.

Clark, M.P. *et al.* (2009) 'Consistency between hydrological models and field observations: linking processes at the hillslope scale to hydrological responses at the watershed scale', *Hydrological Processes: An International Journal*, 23(2), pp. 311–319.

Clark, M.P., Nijssen, B., Lundquist, J.D., Kavetski, D., Rupp, D.E., Woods, R.A., Freer, J.E., Gutmann, E.D., Wood, A.W., Brekke, L.D., *et al.* (2015) 'A unified approach for process-based hydrologic modeling: 1. Modeling concept', *Water Resources Research*, 51(4), pp. 2498–2514. doi:10.1002/2015WR017198.

Clark, M.P., Nijssen, B., Lundquist, J.D., Kavetski, D., Rupp, D.E., Woods, R.A., Freer, J.E., Gutmann, E.D., Wood, A.W., Gochis, D.J., *et al.* (2015) 'A unified approach for process-based hydrologic modeling: 2. Model implementation and case studies', *Water Resources Research*, 51(4), pp. 2515–2542. doi:10.1002/2015WR017200.

Clark, M.P. *et al.* (2016) 'Improving the theoretical underpinnings of process-based hydrologic models', *Water Resources Research*, 52(3), pp. 2350–2365. doi:10.1002/2015WR017910.

Clark, M.P., Vogel, R.M., *et al.* (2021) 'The Abuse of Popular Performance Metrics in Hydrologic Modeling', *Water Resources Research*, 57(9). doi:10.1029/2020WR029001.

Clark, M.P., Zolfaghari, R., *et al.* (2021) 'The numerical implementation of land models: Problem formulation and laugh tests', *Journal of Hydrometeorology*, 22(6), pp. 1627–1648. doi:10.1175/JHM-D-20-0175.1.

Clark, M.P. and Kavetski, D. (2010) 'Ancient numerical daemons of conceptual hydrological modeling: 1. Fidelity and efficiency of time stepping schemes', *Water Resources Research*, 46(10). doi:10.1029/2009WR008894.

Clark, M.P., Kavetski, D. and Fenicia, F. (2011) 'Pursuing the method of multiple working hypotheses for hydrological modeling', *Water Resources Research*, 47(9). doi:10.1029/2010WR009827.

Cole, B., Smith, G. and Balzter, H. (2018) 'Acceleration and fragmentation of CORINE land cover changes in the United Kingdom from 2006–2012 detected by Copernicus IMAGE2012 satellite data', *International Journal of Applied Earth Observation and Geoinformation*, 73(February), pp. 107–122. doi:10.1016/j.jag.2018.06.003.

Committee on Climate Change (2018) 'Land use: Reducing emissions and preparing for climate change', (November), p. 100. Available at: www.theccc.org.uk/publications.

Committee on Climate Change (2019a) 'Net Zero: The UK's contribution to stopping global warming', *Committee on Climate Change*, (May), p. 277. Available at: https://www.theccc.org.uk/publication/net-zero-the-uks-contribution-to-stopping-global-warming/.

Committee on Climate Change (2019b) *Net Zero Technical Report*. Available at: https://www.theccc.org.uk/publication/net-zero-technical-report/.

Committee on Climate Change (2020) *Reducing UK emissions - 2019 Progress Report to Parliament*, *Progress Report to UK Parliament*. Available at:

https://www.theccc.org.uk/publication/reducing-uk-emissions-2019-progress-report-to-parliament/%0Awww.theccc.org.uk/publications.

Condon, L.E., Atchley, A.L. and Maxwell, R.M. (2020) 'Evapotranspiration depletes groundwater under warming over the contiguous United States', *Nature Communications*, 11(1), pp. 1–8.

Connelly, A. *et al.* (2020) 'What approaches exist to evaluate the effectiveness of UK-relevant natural flood management measures? A systematic map protocol', *Environmental Evidence*, 9(1), p. 11. doi:10.1186/s13750-020-00192-x.

Cook-Patton, S.C. *et al.* (2020) 'Mapping carbon accumulation potential from global natural forest regrowth', *Nature*, 585(7826), pp. 545–550. doi:10.1038/s41586-020-2686-x.

Cooper, E. *et al.* (2021) 'Using data assimilation to optimize pedotransfer functions using field-scale in situ soil moisture observations', *Hydrology and Earth System Sciences*, 25(5), pp. 2445–2458. doi:10.5194/hess-25-2445-2021.

Cooper, E. *et al.* (2022) 'Improved Hydrology for Regional Environmental Prediction'.

Cooper, H.M. *et al.* (2021) 'COSMOS-UK: National soil moisture and hydrometeorology data for environmental science research', *Earth System Science Data*, 13(4), pp. 1737–1757. doi:10.5194/essd-13-1737-2021.

Cooper, M. *et al.* (2021) 'Role of forested land for natural flood management in the UK: A review', *WIREs Water*, 8(5), pp. 1–16. doi:10.1002/wat2.1541.

Cotterill, D. *et al.* (2021) 'Increase in the frequency of extreme daily precipitation in the United Kingdom in autumn', *Weather and Climate Extremes*, 33, p. 100340. doi:10.1016/j.wace.2021.100340.

Cox, P.M. *et al.* (1999) 'The impact of new land surface physics on the GCM simulation of climate and climate sensitivity', *Climate Dynamics*, 15(3), pp. 183–203. doi:10.1007/s003820050276.

Cox, P.M. *et al.* (2000) 'Acceleration of global warming due to carbon-cycle feedbacks in a coupled climate model', *Nature*, 408(6809), pp. 184–187. doi:10.1038/35041539.

Cox, P.M. (2001) 'Description of the TRIFFID dynamic global vegetation model. Hadley Centre Technical Note 24', *Theoretical and Applied Climatology*, p. 16. Available at: https://jules.jchmr.org/sites/default/files/HCTN_24.pdf.

Cox, P.M., Huntingford, C. and Harding, R.J. (1998) 'A canopy conductance and

photosynthesis model for use in a GCM land surface scheme', *Journal of Hydrology*, 212–213(1–4), pp. 79–94. doi:10.1016/S0022-1694(98)00203-0.

Coxon, G. *et al.* (2019) 'DECIPHeR v1: Dynamic fluxEs and ConnectIvity for Predictions of HydRology', *Geoscientific Model Development*, 12(6), pp. 2285–2306. doi:10.5194/gmd-12-2285-2019.

Coxon, G. *et al.* (2020) 'CAMELS-GB: hydrometeorological time series and landscape attributes for 671 catchments in Great Britain', *Earth System Science Data*, 12(4), pp. 2459–2483. doi:10.5194/essd-12-2459-2020.

Crawford, N.H. and Burges, S.J. (2004) 'History of the Stanford Watershed Model', *Water Resources Impact*, 6(2), pp. 3–6. Available at: https://www.jstor.org/stable/wateresoimpa.6.2.0003.

Crooks, S.M. *et al.* (2014) 'From catchment to national scale rainfall-runoff modelling: Demonstration of a hydrological modelling framework', *Hydrology*, 1(1), pp. 63–88. doi:10.3390/hydrology1010063.

Crutzen, P.J. (2002) 'Geology of mankind', *Nature*, 415(6867), pp. 23–23. doi:10.1038/415023a.

Cui, J. *et al.* (2022) 'Global water availability boosted by vegetation-driven changes in atmospheric moisture transport', *Nature Geoscience*, 15(12), pp. 982–988. doi:10.1038/s41561-022-01061-7.

Cuntz, M. *et al.* (2016) 'The impact of standard and hard-coded parameters on the hydrologic fluxes in the Noah-MP land surface model', *Journal of Geophysical Research: Atmospheres*, 121(18), pp. 10,676-10,700. doi:10.1002/2016JD025097.

Dadson, S.J. *et al.* (2017) 'A restatement of the natural science evidence concerning catchment-based "natural" flood management in the UK', *Proceedings of the Royal Society A: Mathematical, Physical and Engineering Sciences*, 473(2199), p. 20160706. doi:10.1098/rspa.2016.0706.

Dadson, S.J., Bell, V.A. and Jones, R.G. (2011) 'Evaluation of a grid-based river flow model configured for use in a regional climate model', *Journal of Hydrology*, 411(3–4), pp. 238–250. doi:10.1016/j.jhydrol.2011.10.002.

Dandy, N. (2016) 'Woodland neglect as social practice', *Environment and Planning A*, 48(9), pp. 1750–1766. doi:10.1177/0308518X16651266.

Davies, H., Rameshwaran, P. and V, B. (2022) 'Gridded (1km) physical river characteristics for the UK'. NERC EDS Environmental Information Data Centre. doi:10.5285/6da95899-f3b8-4089-b621-560818aa78ba.

Davies, H.N. and Bell, V.A. (2009) 'Assessment of methods for extracting low-resolution river networks from high-resolution digital data', *Hydrological Sciences Journal*, 54(1), pp. 17–28. doi:10.1623/hysj.54.1.17.

Davin, E.L. *et al.* (2020) 'Biogeophysical impacts of forestation in Europe: First results from the LUCAS (Land Use and Climate across Scales) regional climate model intercomparison', *Earth System Dynamics*, 11(1), pp. 183–200. doi:10.5194/esd-11-183-2020.

Denissen, J.M.C. *et al.* (2022) 'Widespread shift from ecosystem energy to water limitation with climate change', *Nature Climate Change*, 12(7), pp. 677–684. doi:10.1038/s41558-022-01403-8.

Devanand, A. *et al.* (2020) 'Land Use and Land Cover Change Strongly Modulates Land-Atmosphere Coupling and Warm-Season Precipitation Over the Central United States in CESM2-VR', *Journal of Advances in Modeling Earth Systems*, 12(9), pp. 1–23. doi:10.1029/2019MS001925.

Dick, J. *et al.* (2019) 'How are nature based solutions contributing to priority societal challenges surrounding human well-being in the United Kingdom: A systematic map protocol', *Environmental Evidence*, 8(1), p. 37. doi:10.1186/s13750-019-0180-4.

van Dijk, A.I.J.M. *et al.* (2009) 'Forest-flood relation still tenuous - Comment on 'Global evidence that deforestation amplifies flood risk and severity in the developing world'by C. J. A. Bradshaw, N.S. Sodi, K. S.-H. Peh and B.W. Brook', *Global Change Biology*, 15(1), pp. 110–115. doi:10.1111/j.1365-2486.2008.01708.x.

Dittrich, R. *et al.* (2019) 'A cost-benefit analysis of afforestation as a climate change adaptation measure to reduce flood risk', *Journal of Flood Risk Management*, 12(4), pp. 1–11. doi:10.1111/jfr3.12482.

Do, H.X., Westra, S. and Leonard, M. (2017) 'A global-scale investigation of trends in annual maximum streamflow', *Journal of Hydrology*, 552, pp. 28–43. doi:10.1016/j.jhydrol.2017.06.015.

Doelman, J.C. *et al.* (2018) 'Exploring SSP land-use dynamics using the IMAGE model: Regional and gridded scenarios of land-use change and land-based climate change mitigation',

Global Environmental Change, 48(December 2017), pp. 119–135. doi:10.1016/j.gloenvcha.2017.11.014.

Döll, P., Kaspar, F. and Lehner, B. (2003) 'A global hydrological model for deriving water availability indicators: Model tuning and validation', *Journal of Hydrology*, 270(1–2), pp. 105–134. Available at: www.elsevier.com/locate/jhydrol%0Ahttp://dx.doi.org/10.1016/S0022-1694(02)00283-4.

Dolman, J.A. and Gregory, D. (1992) 'The Parametrization of Rainfall Interception In GCMs', *Quarterly Journal of the Royal Meteorological Society*, 118(505), pp. 455–467. doi:10.1002/qj.49711850504.

Don, A. *et al.* (2009) 'Impact of afforestation-associated management changes on the carbon balance of grassland', *Global Change Biology*, 15(8), pp. 1990–2002. doi:10.1111/j.1365-2486.2009.01873.x.

Dooge, J.C.I. (1986) 'Looking for hydrologic laws', *Water Resources Research*, 22(9 S), pp. 46S-58S. doi:10.1029/WR022i09Sp0046S.

Eagleson, P.S. (1986) 'The emergence of global-scale hydrology', *Water Resources Research*, 22(9S), pp. 6S-14S. doi:10.1029/WR022i09Sp0006S.

Ellis, N., Anderson, K. and Brazier, R. (2021) 'Mainstreaming natural flood management: A proposed research framework derived from a critical evaluation of current knowledge', *Progress in Physical Geography: Earth and Environment*, 45(6), pp. 819–841. doi:10.1177/0309133321997299.

Ellison, D., Futter, M.N. and Bishop, K. (2012) 'On the forest cover-water yield debate: From demand- to supply-side thinking', *Global Change Biology*, 18(3), pp. 806–820. doi:10.1111/j.1365-2486.2011.02589.x.

Engler, A. (1919) *Untersuchungen über den Einfluss des Waldes auf den Stand der Gewässer, Mitteilungen der Schweizerischen Zentralanstalt für das forstliche Versuchswesen*. . Available at: https://www.dora.lib4ri.ch/wsl/islandora/object/wsl%3A13503/datastream/PDF/Engler-1919-Untersuchungen_über_den_Einfluß_des-%28published_version%29.pdf.

Environment Agency (2018) *Mapping the potential for Working with Natural Processes-technical report Mapping the potential for Working with Natural Processes-technical report SC150005*. Available at: https://assets.publishing.service.gov.uk/media/6036c659d3bf7f0ab2f070c1/Working_with_na

tural_processes_mapping_technical_report.pdf.

Environmental Audit Committee (2023) *Seeing the wood for the trees : the contribution of the forestry and timber sectors to biodiversity and net zero goals*. Available at: https://committees.parliament.uk/publications/40938/documents/199465/default/.

ESA (2017) *Land Cover CCI Product User Guide Version 2. Tech. Rep.* Available at: maps.elie.ucl.ac.be/CCI/viewer/download/ESACCI-LC-Ph2-PUGv2_2.0.pdf.

Essery, R.L.H., Best, M.J. and Cox, P.M. (2001) 'MOSES 2.2 technical documentation. Hadley Centre Technical Note 30'. Available at: http://jules.jchmr.org/sites/default/files/HCTN_30.pdf.

Ewen, J., Parkin, G. and O'Connell, P.E. (2000) 'SHETRAN: Distributed River Basin Flow and Transport Modeling System', *Journal of Hydrologic Engineering*, 5(3), pp. 250–258. doi:10.1061/(ASCE)1084-0699(2000)5:3(250).

Fan, Y. *et al.* (2019) 'Hillslope Hydrology in Global Change Research and Earth System Modeling', *Water Resources Research*, 55(2), pp. 1737–1772. doi:10.1029/2018WR023903.

Farley, K.A., Jobbágy, E.G. and Jackson, R.B. (2005) 'Effects of afforestation on water yield: A global synthesis with implications for policy', *Global Change Biology*, 11(10), pp. 1565–1576. doi:10.1111/j.1365-2486.2005.01011.x.

Farrelly, N. and Gallagher, G. (2015) 'An analysis of the potential availability of land for afforestation in the Republic of Ireland.', *Irish Forestry*, 72, pp. 120–138.

Faulkner, D. *et al.* (2019) 'Can we still predict the future from the past? Implementing non-stationary flood frequency analysis in the UK', *Journal of Flood Risk Management* [Preprint]. doi:10.1111/jfr3.12582.

Feeney, C.J. *et al.* (2022) 'Multiple soil map comparison highlights challenges for predicting topsoil organic carbon concentration at national scale', *Scientific Reports*, 12(1), pp. 1–13. doi:10.1038/s41598-022-05476-5.

Fenner, R. (2017) 'Spatial evaluation of multiple benefits to encourage multi-functional design of sustainable drainage in Blue-Green cities', *Water (Switzerland)*, 9(12). doi:10.3390/w9120953.

Filoso, S. *et al.* (2017) 'Impacts of forest restoration on water yield: A systematic review', *PLoS ONE*, 12(8), pp. 1–26. doi:10.1371/journal.pone.0183210.

Fisher, R.A. and Koven, C.D. (2020) 'Perspectives on the Future of Land Surface Models and

the Challenges of Representing Complex Terrestrial Systems', *Journal of Advances in Modeling Earth Systems*, 12(4). doi:https://doi.org/10.1029/2018MS001453.

La Follette, P.T. *et al.* (2021) 'Numerical daemons of hydrological models are summoned by extreme precipitation', *Hydrology and Earth System Sciences*, 25(10), pp. 5425–5446. doi:10.5194/hess-25-5425-2021.

Folwell, S.S., Taylor, C.M. and Stratton, R.A. (2022) 'Contrasting contributions of surface hydrological pathways in convection permitting and parameterised climate simulations over Africa and their feedbacks on the atmosphere', *Climate Dynamics*, 59(1–2), pp. 633–648. doi:10.1007/s00382-022-06144-0.

Forest Research (2021a) *Forestry Statistics 2021 - Chapter 1: Woodland Area and Planting*. Available at: https://cdn.forestresearch.gov.uk/2022/02/ch1_woodland_fs2021-1.pdf.

Forest Research (2021b) 'Provisional Woodland Statistics. 2021 Edition', (First release), pp. 1–33. Available at: www.forestresearch.gov.uk/statistics/.

Forster, E.J. *et al.* (2021) 'Commercial afforestation can deliver effective climate change mitigation under multiple decarbonisation pathways', *Nature Communications*, 12(1), pp. 1–12. doi:10.1038/s41467-021-24084-x.

Fosser, G. *et al.* (2020) 'Optimal configuration and resolution for the first convection-permitting ensemble of climate projections over the United Kingdom', *International Journal of Climatology*, 40(7), pp. 3585–3606. doi:10.1002/joc.6415.

Foster, I., Anderson, M.G. and Burt, T.P. (Ed. (1986) 'Hydrological Forecasting', *Transactions of the Institute of British Geographers*, 11(4), p. 501. doi:10.2307/621948.

Fowler, H.J. *et al.* (2021) 'Anthropogenic intensification of short-duration rainfall extremes', *Nature Reviews Earth and Environment*, 2(2), pp. 107–122. doi:10.1038/s43017-020-00128-6.

Freeze, R.A. and Harlan, R.L. (1969) 'Blueprint for a physically-based, digitally-simulated hydrologic response model', *Journal of Hydrology*, 9(3), pp. 237–258. doi:10.1016/0022-1694(69)90020-1.

Friedlingstein, P. *et al.* (2019) 'Comment on "The global tree restoration potential"', *Science*, 366(6463), pp. 76–79. doi:10.1126/science.aay8060.

Fuller, L. *et al.* (2016) 'Public acceptance of tree health management: Results of a national survey in the UK', *Environmental Science and Policy*, 59, pp. 18–25.

doi:10.1016/j.envsci.2016.02.007.

Fuller, R. *et al.* (2002) 'Land cover map 2000 - final report'. NERC Environmental Information Data Centre. doi:10.5285/f802edfc-86b7-4ab9-b8fa-87e9135237c9.

Gadian, A.M. *et al.* (2018) 'A case study of possible future summer convective precipitation over the UK and Europe from a regional climate projection', *International Journal of Climatology*, 38(5), pp. 2314–2324. doi:10.1002/joc.5336.

Gao, J., Kirkby, M. and Holden, J. (2018) 'The effect of interactions between rainfall patterns and land-cover change on flood peaks in upland peatlands', *Journal of Hydrology*, 567(April), pp. 546–559. doi:10.1016/j.jhydrol.2018.10.039.

Gedney, N. *et al.* (2006) 'Detection of a direct carbon dioxide effect in continental river runoff records', *Nature*, 439(7078), pp. 835–838. doi:10.1038/nature04504.

Gedney, N. *et al.* (2014) 'Detection of solar dimming and brightening effects on Northern Hemisphere river flow', *Nature Geoscience*, 7(11), pp. 796–800. doi:10.1038/ngeo2263.

van Genuchten, M.T. (1980) 'A Closed-form Equation for Predicting the Hydraulic Conductivity of Unsaturated Soils', *Soil Science Society of America Journal*, 44(5), pp. 892–898. doi:10.2136/sssaj1980.03615995004400050002x.

Gimeno, L. *et al.* (2021) 'The residence time of water vapour in the atmosphere', *Nature Reviews Earth and Environment*, 2(8), pp. 558–569. doi:10.1038/s43017-021-00181-9.

Girardin, C.A.J. *et al.* (2021) 'Nature-based solutions can help cool the planet - if we act now', *Nature*, 593(7858), pp. 191–194. doi:10.1038/d41586-021-01241-2.

Gleeson, T. *et al.* (2020) 'Illuminating water cycle modifications and Earth system resilience in the Anthropocene', *Water Resources Research*, 56(4), pp. 1–24. doi:10.1029/2019WR024957.

Gleeson, T. *et al.* (2021) 'GMD perspective: The quest to improve the evaluation of groundwater representation in continental-to global-scale models', *Geoscientific Model Development*, 14(12), pp. 7545–7571. doi:10.5194/gmd-14-7545-2021.

Godwin, H. (1975) 'History of the natural forests of Britain: establishment, dominance and destruction', *Philosophical Transactions of the Royal Society of London. B, Biological Sciences*, 271(911), pp. 47–67. doi:10.1098/rstb.1975.0034.

Grassi, G. *et al.* (2017) 'The key role of forests in meeting climate targets requires science for credible mitigation', *Nature Climate Change*, 7(3), pp. 220–226. doi:10.1038/nclimate3227.

Griffin, A., Kay, A., Stewart, L., *et al.* (2022) 'Climate change allowances, non-stationarity and flood frequency analyses', *Journal of Flood Risk Management*, (December 2021), pp. 1–12. doi:10.1111/jfr3.12783.

Griffin, A., Kay, A., Sayers, P., *et al.* (2022) 'Widespread flooding dynamics changing under climate change : characterising floods using UKCP18', *Hydrology and Earth System Sciences*, (July), pp. 1–18. doi:https://hess.copernicus.org/preprints/hess-2022-243/.

Griffin, A., Vesuviano, G. and Stewart, E. (2019) 'Have trends changed over time? A study of UK peak flow data and sensitivity to observation period', *Natural Hazards and Earth System Sciences*, 19(10), pp. 2157–2167. doi:10.5194/nhess-19-2157-2019.

Griscom, B.W. *et al.* (2017) 'Natural climate solutions', *Proceedings of the National Academy of Sciences*, 114(44), pp. 11645–11650. doi:10.1073/pnas.1710465114.

Gudmundsson, L. *et al.* (2019) 'Observed Trends in Global Indicators of Mean and Extreme Streamflow', *Geophysical Research Letters*, 46(2), pp. 756–766. doi:10.1029/2018GL079725.

Gudmundsson, L. *et al.* (2021) 'Globally observed trends in mean and extreme river flow attributed to climate change', *Science*, 371(6534), pp. 1159–1162. doi:10.1126/science.aba3996.

Gudmundsson, L., Seneviratne, S.I. and Zhang, X. (2017) 'Anthropogenic climate change detected in European renewable freshwater resources', *Nature Climate Change*, 7(11), pp. 813–816. doi:10.1038/nclimate3416.

Guillod, B.P. *et al.* (2018) 'A large set of potential past, present and future hydro-meteorological time series for the UK', *Hydrology and Earth System Sciences*, 22(1), pp. 611–634. doi:10.5194/hess-22-611-2018.

Gunnell, K. *et al.* (2019) 'Evaluating natural infrastructure for flood management within the watersheds of selected global cities', *Science of the Total Environment*, 670, pp. 411–424. doi:10.1016/j.scitotenv.2019.03.212.

Gupta, H. V *et al.* (2009) 'Decomposition of the mean squared error and NSE performance criteria: Implications for improving hydrological modelling', *Journal of Hydrology*, 377(1–2), pp. 80–91. doi:10.1016/j.jhydrol.2009.08.003.

Gush, M.B. *et al.* (2002) 'A new approach to modelling streamflow reductions resulting from commercial afforestation in South Africa', *The Southern African Forestry Journal*, 196(1), pp. 27–36. doi:10.1080/20702620.2002.10434615.

Hallouin, T. *et al.* (2022) 'UniFHy v0.1.1: a community modelling framework for the terrestrial water cycle in Python', *Geoscientific Model Development*, 15(24), pp. 9177–9196. doi:10.5194/gmd-15-9177-2022.

Hankin, B. *et al.* (2017) 'Strategies for Testing the Impact of Natural Flood Risk Management Measures', *Flood Risk Management*, pp. 1–40. doi:10.5772/intechopen.68677.

Hannaford, J. *et al.* (2021) 'An updated national-scale assessment of trends in UK peak river flow data: How robust are observed increases in flooding?', *Hydrology Research*, 52(3), pp. 699–718. doi:10.2166/nh.2021.156.

Harding, R.J. *et al.* (2014) 'The future for global water assessment', *Journal of Hydrology*, 518(PB), pp. 186–193. doi:10.1016/j.jhydrol.2014.05.014.

Harper, A.B. *et al.* (2016) 'Improved representation of plant functional types and physiology in the Joint UK Land Environment Simulator (JULES v4.2) using plant trait information', *Geoscientific Model Development*, 9(7), pp. 2415–2440. doi:10.5194/gmd-9-2415-2016.

Harper, A.B. *et al.* (2018) 'Land-use emissions play a critical role in land-based mitigation for Paris climate targets', *Nature Communications*, 9(1). doi:10.1038/s41467-018-05340-z.

Harper, A.B. *et al.* (2021) 'Improvement of modeling plant responses to low soil moisture in JULESvn4.9 and evaluation against flux tower measurements', *Geoscientific Model Development*, 14(6), pp. 3269–3294. doi:10.5194/gmd-14-3269-2021.

Harrigan, S. *et al.* (2018) 'Designation and trend analysis of the updated UK Benchmark Network of river flow stations: The UKBN2 dataset', *Hydrology Research*, 49(2), pp. 552–567. doi:10.2166/nh.2017.058.

Haughton, N. *et al.* (2016) 'The plumbing of land surface models: Is poor performance a result of methodology or data quality?', *Journal of Hydrometeorology*, 17(6), pp. 1705–1723. doi:10.1175/JHM-D-15-0171.1.

Hauser, E. *et al.* (2022) 'Global-Scale Shifts in Rooting Depths Due To Anthropocene Land Cover Changes Pose Unexamined Consequences for Critical Zone Functioning', *Earth's Future*, 10(11), pp. 1–14. doi:10.1029/2022ef002897.

Hausfather, Z. and Peters, G.P. (2020) 'Emissions – the "business as usual" story is misleading', *Nature*, 577(7792), pp. 618–620. doi:10.1038/d41586-020-00177-3.

Hawes, M. (2018) 'Planting carbon storage', *Nature Climate Change*, 8(7), pp. 556–558. doi:10.1038/s41558-018-0214-x.

Helsel, D.R. *et al.* (2020) *Statistical methods in water resources: U.S. Geological Survey Techniques and Methods, Book 4, Hydrologic Analysis and Interpretation*. USGS.

Henderson-Sellers, A. *et al.* (1995) 'The Project for Intercomparison of Land Surface Parameterization Schemes (PILPS): Phases 2 and 3', *Bulletin of the American Meteorological Society*, 76(4), pp. 489–503. doi:10.1175/1520-0477(1995)076<0489:TPFIOL>2.0.CO;2.

De Hertog, S.J. *et al.* (2022) 'The biogeophysical effects of idealized land cover and land management changes in Earth system models', *Earth System Dynamics*, 13(3), pp. 1305–1350. doi:10.5194/esd-13-1305-2022.

Hewlett, J.D. (1982) *Principles of forest hydrology*. Athens: University of Georgia Press.

Hoch, J.M. *et al.* (2023) 'Hyper-resolution PCR-GLOBWB: opportunities and challenges from refining model spatial resolution to 1 km over the European continent', *Hydrology and Earth System Sciences*, 27(6), pp. 1383–1401. doi:10.5194/hess-27-1383-2023.

Hoek van Dijke, A.J. *et al.* (2022) 'Shifts in regional water availability due to global tree restoration', *Nature Geoscience*, 15(5), pp. 363–368. doi:10.1038/s41561-022-00935-0.

Hohenegger, C. *et al.* (2009) 'The soil moisture-precipitation feedback in simulations with explicit and parameterized convection', *Journal of Climate*, 22(19), pp. 5003–5020. doi:10.1175/2009JCLI2604.1.

Van den Hoof, C. *et al.* (2013) 'Improved evaporative flux partitioning and carbon flux in the land surface model JULES: Impact on the simulation of land surface processes in temperate Europe', *Agricultural and Forest Meteorology*, 181, pp. 108–124. doi:10.1016/j.agrformet.2013.07.011.

Horton, P., Schaefli, B. and Kauzlaric, M. (2022) 'Why do we have so many different hydrological models? A review based on the case of Switzerland', *Wiley Interdisciplinary Reviews: Water*, 9(1), pp. 1–32. doi:10.1002/wat2.1574.

Hrachowitz, M. and Clark, M.P. (2017) 'HESS Opinions: The complementary merits of competing modelling philosophies in hydrology', *Hydrology and Earth System Sciences*, 21(8), pp. 3953–3973. doi:10.5194/hess-21-3953-2017.

Hudson, J.A., Crane, S.B. and Robinson, M. (1997) 'The impact of the growth of new plantation forestry on evaporation and streamflow in the Llanbrynmair catchments', *Hydrology and Earth System Sciences*, 1(3), pp. 463–475. doi:10.5194/hess-1-463-1997.

Hughes, S. *et al.* (2023) 'New woodlands created adjacent to existing woodlands grow faster,

taller and have higher structural diversity than isolated counterparts', *Restoration Ecology*, pp. 1–9. doi:10.1111/rec.13889.

Humphrey, V. *et al.* (2021) 'Soil moisture–atmosphere feedback dominates land carbon uptake variability', *Nature*, 592(7852), pp. 65–69. doi:10.1038/s41586-021-03325-5.

Hung, C.-L.J. *et al.* (2020) 'Impacts of combined land-use and climate change on streamflow in two nested catchments in the Southeastern United States', *Ecological Engineering*, 143, p. 105665. doi:10.1016/j.ecoleng.2019.105665.

Hurtado-Pidal, J. *et al.* (2022) 'Is forest location more important than forest fragmentation for flood regulation?', *Ecological Engineering*, 183(March), p. 106764. doi:10.1016/j.ecoleng.2022.106764.

Hutton, C. *et al.* (2016) 'Most computational hydrology is not reproducible, so is it really science?', *Water Resources Research*, 52(10), pp. 7548–7555. doi:10.1002/2016WR019285.

Iacob, O., Brown, I. and Rowan, J. (2017) 'Natural flood management, land use and climate change trade-offs: the case of Tarland catchment, Scotland', *Hydrological Sciences Journal*, 62(12), pp. 1931–1948. doi:10.1080/02626667.2017.1366657.

Insua-Costa, D. *et al.* (2022) 'The central role of forests in the 2021 European floods', *Environmental Research Letters*, 17(6). doi:10.1088/1748-9326/ac6f6b.

IPPC (2019) *Climate Change and Land, An IPCC Special Report on climate change, desertification, land degradation, sustainable land management, food security, and greenhouse gas fluxes in terrestrial ecosystems*. doi:10.4337/9781784710644.

Jaramillo, F. *et al.* (2022) 'Fewer Basins Will Follow Their Budyko Curves Under Global Warming and Fossil-Fueled Development', *Water Resources Research*, 58(8). doi:10.1029/2021wr031825.

Jehn, F.U. *et al.* (2020) 'Using hydrological and climatic catchment clusters to explore drivers of catchment behavior', *Hydrology and Earth System Sciences*, 24(3), pp. 1081–1100. doi:10.5194/hess-24-1081-2020.

Kay, A.L. *et al.* (2021) 'Climate change effects on indicators of high and low river flow across Great Britain', *Advances in Water Resources*, 151(January), p. 103909. doi:10.1016/j.advwatres.2021.103909.

Kay, A.L. (2021) 'Simulation of river flow in Britain under climate change: Baseline performance and future seasonal changes', *Hydrological Processes*, 35(4), pp. 1–10.

doi:10.1002/hyp.14137.

Keat, W.J., Kendon, E.J. and Bohnenstengel, S.I. (2021) 'Climate change over UK cities: the urban influence on extreme temperatures in the UK climate projections', *Climate Dynamics*, 57(11–12), pp. 3583–3597. doi:10.1007/s00382-021-05883-w.

Kellner, E. and Hubbart, J.A. (2018) 'Land use impacts on floodplain water table response to precipitation events', *Ecohydrology*, 11(1), p. e1913. doi:10.1002/eco.1913.

Van Kempen, G. *et al.* (2021) 'The impact of hydrological model structure on the simulation of extreme runoff events', *Natural Hazards and Earth System Sciences*, 21(3), pp. 961–976. doi:10.5194/nhess-21-961-2021.

Kendon, E.J. *et al.* (2014) 'Heavier summer downpours with climate change revealed by weather forecast resolution model', *Nature Climate Change*, 4(7), pp. 570–576. doi:10.1038/nclimate2258.

Kendon, E.J. *et al.* (2019) *UKCP Convection-permitting model projections: Science report*. Crown Copyright, Met Office. Available at: https://www.metoffice.gov.uk/pub/data/weather/uk/ukcp18/science-reports/UKCP-Convection-permitting-model-projections-report.pdf.

Kendon, E.J. *et al.* (2020) 'Greater future U.K. winter precipitation increase in new convection-permitting scenarios', *Journal of Climate*, 33(17), pp. 7303–7318. doi:10.1175/JCLI-D-20-0089.1.

Kendon, E.J., Fischer, E.M. and Short, C.J. (2023) 'Variability conceals emerging trend in 100yr projections of UK local hourly rainfall extremes', *Nature Communications*, 14(1), p. 1133. doi:10.1038/s41467-023-36499-9.

Kendon, M. *et al.* (2023) 'State of the UK Climate 2022', *International Journal of Climatology*, 43(S1), pp. 1–82. doi:10.1002/joc.8167.

Kirby, C., Newson, M. and Gilman, K. (1991) *Plynlimon research: the first two decades*. Available at: https://nora.nerc.ac.uk/id/eprint/6052/.

Kirchner, J.W. (2006) 'Getting the right answers for the right reasons: Linking measurements, analyses, and models to advance the science of hydrology', *Water Resources Research*, 42(3), pp. 1–5. doi:10.1029/2005WR004362.

Kirchner, J.W. (2009) 'Catchments as simple dynamical systems: Catchment characterization, rainfall-runoff modeling, and doing hydrology backward', *Water Resources Research*, 45(2),

pp. 1–34. doi:10.1029/2008WR006912.

Kirchner, J.W., Benettin, P. and van Meerveld, I. (2023) 'Instructive Surprises in the Hydrological Functioning of Landscapes', *Annual Review of Earth and Planetary Sciences*, 51(1), pp. 277–299. doi:10.1146/annurev-earth-071822-100356.

Kjeldsen, T.R. and Prosdocimi, I. (2018) 'Assessing the element of surprise of record-breaking flood events', *Journal of Flood Risk Management*, 11(1), pp. S541–S553. doi:10.1111/jfr3.12260.

van der Knijff, J.M., Younis, J. and de Roo, A.P.J. (2010) 'LISFLOOD: A GIS-based distributed model for river basin scale water balance and flood simulation', *International Journal of Geographical Information Science*, 24(2), pp. 189–212. doi:10.1080/13658810802549154.

Knoben, W.J.M., Freer, J.E., Fowler, K.J.A., *et al.* (2019) 'Modular Assessment of Rainfall-Runoff Models Toolbox (MARRMoT) v1.0: an open- source, extendable framework providing implementations of 46 conceptual hydrologic models as continuous space-state formulations', *Geoscientific Model Development Discussions*, pp. 1–26. doi:10.5194/gmd-2018-332.

Knoben, W.J.M. *et al.* (2022) 'Community Workflows to Advance Reproducibility in Hydrologic Modeling: Separating Model-Agnostic and Model-Specific Configuration Steps in Applications of Large-Domain Hydrologic Models', *Water Resources Research*, 58(11), pp. 1–52. doi:10.1029/2021WR031753.

Knoben, W.J.M., Freer, J.E. and Woods, R.A. (2019) 'Technical note: Inherent benchmark or not? Comparing Nash-Sutcliffe and Kling-Gupta efficiency scores', *Hydrology and Earth System Sciences*, 23(10), pp. 4323–4331. doi:10.5194/hess-23-4323-2019.

Koenker, R. and Bassett, G. (1978) 'Regression Quantiles', *Econometrica*, 46(1), p. 33. doi:10.2307/1913643.

Koutsoyiannis, D. and Mamassis, N. (2021) 'From mythology to science: The development of scientific hydrological concepts in Greek antiquity and its relevance to modern hydrology', *Hydrology and Earth System Sciences*, 25(5), pp. 2419–2444. doi:10.5194/hess-25-2419-2021.

Kratzert, F. *et al.* (2019) 'Toward Improved Predictions in Ungauged Basins: Exploiting the Power of Machine Learning', *Water Resources Research*, 55(12), pp. 11344–11354. doi:10.1029/2019WR026065.

Krinner, G. *et al.* (2005) 'A dynamic global vegetation model for studies of the coupled

atmosphere-biosphere system', *Global Biogeochemical Cycles*, 19(1), pp. 1–33. doi:10.1029/2003GB002199.

Kundzewicz, Z.W. (2011) 'Nonstationarity in water resources - Central European perspective', *Journal of the American Water Resources Association*, 47(3), pp. 550–562. doi:10.1111/j.1752-1688.2011.00549.x.

Lacombe, G. *et al.* (2016) 'Contradictory hydrological impacts of afforestation in the humid tropics evidenced by long-term field monitoring and simulation modelling', *Hydrology and Earth System Sciences*, 20(7), pp. 2691–2704. doi:10.5194/hess-20-2691-2016.

Laguë, M.M., Bonan, G.B. and Swann, A.L.S. (2019) 'Separating the impact of individual land surface properties on the terrestrial surface energy budget in both the coupled and uncoupled land–atmosphere system', *Journal of Climate*, 32(18), pp. 5725–5744. doi:10.1175/JCLI-D-18-0812.1.

Lane, P.N.J. *et al.* (2005) 'The response of flow duration curves to afforestation', *Journal of Hydrology*, 310(1–4), pp. 253–265. doi:10.1016/j.jhydrol.2005.01.006.

Lane, R.A. *et al.* (2021) 'Incorporating Uncertainty Into Multiscale Parameter Regionalization to Evaluate the Performance of Nationally Consistent Parameter Fields for a Hydrological Model', *Water Resources Research*, 57(10), pp. 1–19. doi:10.1029/2020WR028393.

Lane, R.A. *et al.* (2022) 'A large-sample investigation into uncertain climate change impacts on high flows across Great Britain', *Hydrology and Earth System Sciences*, 26(21), pp. 5535–5554. doi:10.5194/hess-26-5535-2022.

Lane, R.A. and Kay, A.L. (2021) 'Climate Change Impact on the Magnitude and Timing of Hydrological Extremes Across Great Britain', *Frontiers in Water*, 3(July), pp. 1–14. doi:10.3389/frwa.2021.684982.

Lane, S.N. (2017) 'Natural flood management', *WIREs Water*, 4(3), p. e1211. doi:10.1002/wat2.1211.

Law, F. (1956) 'The effects of afforestation upon water yields of catchment areas', *Journal of British Waterworks Association*, 38, pp. 484–494.

Ledingham, J. *et al.* (2019) 'Contrasting seasonality of storm rainfall and flood runoff in the UK and some implications for rainfall-runoff methods of flood estimation', *Hydrology Research*, 50(5), pp. 1309–1323. doi:10.2166/nh.2019.040.

Lee, D. *et al.* (2022) 'Enhanced Role of Convection in Future Hourly Rainfall Extremes Over

South Korea', *Geophysical Research Letters*, 49(22), pp. 1–11. doi:10.1029/2022GL099727.

Lejeune, Q., Seneviratne, S.I. and Davin, E.L. (2017) 'Historical land-cover change impacts on climate: Comparative assessment of LUCID and CMIP5 multimodel experiments', *Journal of Climate*, 30(4), pp. 1439–1459. doi:10.1175/JCLI-D-16-0213.1.

Lenton, T.M. *et al.* (2008) 'Tipping elements in the Earth's climate system.', *Proceedings of the National Academy of Sciences of the United States of America*, 105(6), pp. 1786–1793. doi:10.1073/pnas.0705414105.

Leopold, L.B. (1977) 'A reverence for rivers', *Geology*, 5(7), pp. 429–430. doi:10.1130/0091-7613(1977)5<429:ARFR>2.0.CO;2.

Leung, J.Y.S., Russell, B.D. and Connell, S.D. (2019) 'Global Warming of 1.5 ºC - Summary for Policymakers', *Intergovernmental Panel on Climate Change*, 1(3), pp. 374–381. Available at: https://www.ipcc.ch/sr15/chapter/spm/.

Levia, D.F. *et al.* (2020) 'Homogenization of the terrestrial water cycle', *Nature Geoscience*, 13(10), pp. 656–658. doi:10.1038/s41561-020-0641-y.

Lewis, H. *et al.* (2019) 'The UKC3 regional coupled environmental prediction system', *Geoscientific Model Development*, 12(6), pp. 2357–2400. doi:10.5194/gmd-12-2357-2019.

Lewis, H.W. and Dadson, S.J. (2021) 'A regional coupled approach to water cycle prediction during winter 2013/14 in the United Kingdom', *Hydrological Processes*, 35(12), pp. 1–24. doi:10.1002/hyp.14438.

Lewis, S.L. *et al.* (2019) 'Regenerate natural forests to store carbon', *Nature*, 568(7750), pp. 25–28.

Li, Y. *et al.* (2018) 'Divergent hydrological response to large-scale afforestation and vegetation greening in China', *Science Advances*, 4(5), pp. 1–10. doi:10.1126/sciadv.aar4182.

Liang, X. *et al.* (1994) 'A simple hydrologically based model of land surface water and energy fluxes for general circulation models', *Journal of Geophysical Research*, 99(D7). doi:10.1029/94jd00483.

Liu, Y. *et al.* (2020) 'Plant hydraulics accentuates the effect of atmospheric moisture stress on transpiration', *Nature Climate Change*, 10(7), pp. 691–695. doi:10.1038/s41558-020-0781-5.

Liu, Y. and Gupta, H. V. (2007) 'Uncertainty in hydrologic modeling: Toward an integrated data assimilation framework', *Water Resources Research*, 43(7), pp. 1–18. doi:10.1029/2006WR005756.

Lorenzo, A. *et al.* (2016) 'Global projections of river flood risk in a warmer world', *Earth's Future*, 5(2), pp. 171–182. doi:10.1002/2016EF000485.

Loritz, R. *et al.* (2020) 'The role and value of distributed precipitation data for hydrological models', *Hydrology and Earth System Sciences Discussions*, 25(2007), pp. 1–38. doi:10.5194/hess-2020-393.

Lowe, J.A. *et al.* (2018) *UKCP18 science overview report*, *Met Office Hadley Centre: Exeter, UK*. Available at: https://www.metoffice.gov.uk/pub/data/weather/uk/ukcp18/science-reports/UKCP18-Overview-report.pdf.

Mai, J., R. Craig, J. and A. Tolson, B. (2020) 'Simultaneously determining global sensitivities of model parameters and model structure', *Hydrology and Earth System Sciences*, 24(12), pp. 5835–5858. doi:10.5194/hess-24-5835-2020.

Maina, F.Z. *et al.* (2022) 'Warming, increase in precipitation, and irrigation enhance greening in High Mountain Asia', *Communications Earth & Environment*, 3(1), pp. 1–8. doi:10.1038/s43247-022-00374-0.

Manabe, S. (1969) 'Climate and the Ocean Circulation 1', *Monthly Weather Review*, 97(11), pp. 739–774. doi:10.1175/1520-0493(1969)097<0739:CATOC>2.3.CO;2.

Manzoor, S.A. *et al.* (2019) 'Scenario-led modelling of broadleaf forest expansion in Wales', *Royal Society Open Science*, 6(5), p. 190026. doi:10.1098/rsos.190026.

Marapara, T.R. *et al.* (2021) 'Disentangling the factors that vary the impact of trees on flooding (a review)', *Water and Environment Journal*, 35(2), pp. 514–529. doi:10.1111/wej.12647.

Marc, V. and Robinson, M. (2007) 'The long-term water balance (1972-2004) of upland forestry and grassland at Plynlimon, mid-Wales', *Hydrology and Earth System Sciences*, 11(1), pp. 44–60. doi:10.5194/hess-11-44-2007.

Martínez-de la Torre, A., Blyth, E.M. and Robinson, E.L. (2018) 'Water, carbon and energy fluxes simulation for Great Britain using the JULES Land Surface Model and the Climate Hydrology and Ecology research Support System meteorology dataset (1961-2015) [CHESS-land]'. NERC Environmental Information Data Centre. doi:10.5285/c76096d6-45d4-4a69-a310-4c67f8dcf096.

Martínez-De La Torre, A., Blyth, E.M. and Weedon, G.P. (2019) 'Using observed river flow data to improve the hydrological functioning of the JULES land surface model (vn4.3) used for regional coupled modelling in Great Britain (UKC2)', *Geoscientific Model Development*,

12(2), pp. 765–784. doi:10.5194/gmd-12-765-2019.

Maxwell, R.M., Condon, L.E. and Kollet, S.J. (2015) 'A high-resolution simulation of groundwater and surface water over most of the continental US with the integrated hydrologic model ParFlow v3', *Geoscientific Model Development*, 8(3), pp. 923–937. doi:10.5194/gmd-8-923-2015.

McCulloch, J.S.G. and Robinson, M. (1993) 'History of forest hydrology', *Journal of Hydrology*, 150(2–4), pp. 189–216. doi:10.1016/0022-1694(93)90111-L.

McDonnell, J.J. (2014) 'The two water worlds hypothesis: ecohydrological separation of water between streams and trees?', *WIREs Water*, 1(4), pp. 323–329. doi:10.1002/wat2.1027.

McDowell, N.G. *et al.* (2020) 'Pervasive shifts in forest dynamics in a changing world', *Science*, 368(6494). doi:10.1126/science.aaz9463.

McMillan, H. (2022) 'A taxonomy of hydrological processes and watershed function', *Hydrological Processes*, 36(3), pp. 1–7. doi:10.1002/hyp.14537.

McMillan, H.K. *et al.* (2022) 'Impacts of observational uncertainty on analysis and modelling of hydrological processes: Preface', *Hydrological Processes*, 36(2). doi:10.1002/hyp.14481.

van Meerveld, H.J.I. *et al.* (2019) 'Expansion and contraction of the flowing stream network changes hillslope flowpath lengths and the shape of the travel time distribution', *Hydrology and Earth System Sciences Discussions*, 2006(April 2008), pp. 1–18. doi:10.5194/hess-2019-218.

Meier, R. *et al.* (2018) 'Evaluating and improving the Community Land Model's sensitivity to land cover', *Biogeosciences*, 15(15), pp. 4731–4757. doi:10.5194/bg-15-4731-2018.

Meier, R. *et al.* (2021) 'Empirical estimate of forestation-induced precipitation changes in Europe', *Nature Geoscience*, 14(7), pp. 473–478. doi:10.1038/s41561-021-00773-6.

Melsen, L.A. *et al.* (2018) 'Mapping (dis)agreement in hydrologic projections', *Hydrology and Earth System Sciences*, 22(3), pp. 1775–1791. doi:10.5194/hess-22-1775-2018.

Melsen, L.A. (2022) 'It Takes a Village to Run a Model—The Social Practices of Hydrological Modeling', *Water Resources Research*, 58(2). doi:10.1029/2021WR030600.

Merz, B. *et al.* (2021) 'Causes, impacts and patterns of disastrous river floods', *Nature Reviews Earth and Environment*, 2(9), pp. 592–609. doi:10.1038/s43017-021-00195-3.

Messager, M.L. *et al.* (2021) 'Global prevalence of non-perennial rivers and streams', *Nature*,

594(7863), pp. 391–397. doi:10.1038/s41586-021-03565-5.

Met Office (2018) 'UKCP18 Regional Projections on a 12km grid over the UK for 1980-2080'. Centre for Environmental Data Analysis. Available at: https://catalogue.ceda.ac.uk/uuid/589211abeb844070a95d061c8cc7f604.

Miguez-Macho, G. and Fan, Y. (2021) 'Spatiotemporal origin of soil water taken up by vegetation', *Nature*, 598(7882), pp. 624–628. doi:10.1038/s41586-021-03958-6.

Miller, J., Kjeldsen, T. and Prudhomme, C. (2011) 'Assessment of flood peak simulations by Global Hydrological Models', (35). Available at: http://www.eu-watch.org/publications/technical-reports/2.

Milly, P.C.D. (1994) 'Climate, soil water storage, and the average annual water balance', *Water Resources Research*, 30(7), pp. 2143–2156. doi:10.1029/94WR00586.

Milly, P.C.D. *et al.* (2008) 'Climate change: Stationarity is dead: Whither water management?', *Science*, 319(5863), pp. 573–574. doi:10.1126/science.1151915.

Milly, P.C.D. *et al.* (2015) 'On Critiques of "Stationarity is Dead: Whither Water Management?"', *Water Resources Research*, 51(9), pp. 7785–7789. doi:10.1002/2015WR017408.

Monger, F. *et al.* (2022) 'The impact of semi-natural broadleaf woodland and pasture on soil properties and flood discharge', *Hydrological Processes*, 36(1), pp. 1–14. doi:10.1002/hyp.14453.

Moore, R.J. (2007) 'The PDM rainfall-runoff model', *Hydrology and Earth System Sciences*, 11(1), pp. 483–499. doi:10.5194/hess-11-483-2007.

Morris, D.G. and Flavin, R.W. (1990) 'A digital terrain model for hydrology', *Proc 4th International Symposium on Spatial Data Handling, Zürich*, 1(23–27), pp. 250–262.

Morris, J. and Benyon, R. (2005) 'Plantation water use', in Nambiar, S. and Ferguson, I. (eds) *New forests: wood production and environmental services*. CSIRO PUBLISHING, pp. 75–104.

Murphy, J. *et al.* (2019) 'UKCP18 Land report', *UKCP18 Land Projections: Science Report*, 2018(November 2018). Available at: https://www.metoffice.gov.uk/pub/data/weather/uk/ukcp18/science-reports/UKCP18-Land-report.pdf.

Murphy, T.R. *et al.* (2019) 'Deviation between projected and observed precipitation trends

greater with altitude', *Climate Research*, 79(1), pp. 77–89. doi:10.3354/cr01583.

Murphy, T.R. *et al.* (2021) 'Native woodland establishment improves soil hydrological functioning in UK upland pastoral catchments', *Land Degradation & Development*, 32(2), pp. 1034–1045. doi:10.1002/ldr.3762.

Myhre, G. *et al.* (2018) 'Sensible heat has significantly affected the global hydrological cycle over the historical period', *Nature Communications*, 9(1). doi:10.1038/s41467-018-04307-4.

Nash, J.E. and Sutcliffe, J.V. (1970) 'River flow forecasting through conceptual models part I — A discussion of principles', *Journal of Hydrology*, 10(3), pp. 282–290. doi:10.1016/0022-1694(70)90255-6.

Nath, S. *et al.* (2022) 'TIMBER v0.1: a conceptual framework for emulating temperature responses to tree cover change', *EGUsphere*, 2022(November), pp. 1–36. Available at: https://egusphere.copernicus.org/preprints/egusphere-2022-1024/.

Nearing, G.S. *et al.* (2021) 'What Role Does Hydrological Science Play in the Age of Machine Learning?', *Water Resources Research*, 57(3), p. e2020WR028091. doi:10.1029/2020WR028091.

Neill, A.J. *et al.* (2021) 'Structural changes to forests during regeneration affect water flux partitioning, water ages and hydrological connectivity: Insights from tracer-aided ecohydrological modelling', *Hydrology and Earth System Sciences*, 25(9), pp. 4861–4886. doi:10.5194/hess-25-4861-2021.

Newson, M.D. and Calder, I.R. (1989) 'Forests and water resources: problems of prediction on a regional scale', *Philosophical Transactions of the Royal Society of London. B, Biological Sciences*, 324(1223), pp. 283–298. doi:10.1098/rstb.1989.0049.

Nisbet, T. (2005) *Water use by trees*. Forestry Commission. Available at: https://cdn.forestresearch.gov.uk/2005/03/fcin065.pdf.

Nisbet, T. *et al.* (2011) *Woodland for Water : Woodland measures for meeting Water Framework Directive objectives, Forest Research*. Available at: https://cdn.forestresearch.gov.uk/2011/01/frmg004_woodland4water.pdf.

Nisbet, T. and Thomas, H. (2021) 'Trees, woodlands and flooding', *Quarterly Journal of Forestry*, 115(1), pp. 55–63.

Niu, G.-Y. *et al.* (2011) 'The community Noah land surface model with multiparameterization options (Noah-MP): 1. Model description and evaluation with local-scale measurements',

Journal of Geophysical Research, 116(D12), p. D12109. doi:10.1029/2010JD015139.

NOAA (2022) *Global Monitoring Laboratory - Carbon Cycle Greenhouse Gases: Trends in CO2*. Available at: https://gml.noaa.gov/ccgg/trends/mlo.html (Accessed: 31 October 2022).

De Noblet-Ducoudré, N. *et al.* (2012) 'Determining robust impacts of land-use-induced land cover changes on surface climate over North America and Eurasia: Results from the first set of LUCID experiments', *Journal of Climate*, 25(9), pp. 3261–3281. doi:10.1175/JCLI-D-11-00338.1.

O'Briain, R. *et al.* (2020) 'The efficacy of riparian tree cover as a climate change adaptation tool is affected by hydromorphological alterations', *Hydrological Processes*, (November 2018), p. hyp.13739. doi:10.1002/hyp.13739.

O'Callaghan, J.F. and Mark, D.M. (1984) 'The extraction of drainage networks from digital elevation data.', *Computer Vision, Graphics, & Image Processing*, 28(3), pp. 323–344. doi:10.1016/S0734-189X(84)80011-0.

Olden, J.D. and Poff, N.L. (2003) 'Redundancy and the choice of hydrologic indices for characterizing streamflow regimes', *River Research and Applications*, 19(2), pp. 101–121. doi:10.1002/rra.700.

Oldfield, E.E. *et al.* (2013) 'FORUM: Challenges and future directions in urban afforestation', *Journal of Applied Ecology*, 50(5), pp. 1169–1177. doi:10.1111/1365-2664.12124.

Osborne, S.R. and Weedon, G.P. (2021) 'Observations and modeling of evapotranspiration and dewfall during the 2018 meteorological drought in southern England', *Journal of Hydrometeorology*, 22(2), pp. 279–295. doi:10.1175/JHM-D-20-0148.1.

Oudin, L. *et al.* (2008) 'Has land cover a significant impact on mean annual streamflow? An international assessment using 1508 catchments', *Journal of Hydrology*, 357(3–4), pp. 303–316. doi:10.1016/j.jhydrol.2008.05.021.

Page, T. *et al.* (2020) 'Assessing the significance of wet-canopy evaporation from forests during extreme rainfall events for flood mitigation in mountainous regions of the United Kingdom', *Hydrological Processes*, 34(24), pp. 4740–4754. doi:10.1002/hyp.13895.

Palmer, L. (2021) 'How trees and forests reduce risks from climate change', *Nature Climate Change*, 11(5), pp. 374–377. doi:10.1038/s41558-021-01041-6.

Paltan, H. *et al.* (2017) 'Global Floods and Water Availability Driven by Atmospheric Rivers', *Geophysical Research Letters*, 44(20), pp. 10,387-10,395. doi:10.1002/2017GL074882.

Papadimitriou, L. V. *et al.* (2017) 'The effect of GCM biases on global runoff simulations of a land surface model', *Hydrology and Earth System Sciences*, 21(9), pp. 4379–4401. doi:10.5194/hess-21-4379-2017.

Pascolini-Campbell, M. *et al.* (2021) 'A 10 per cent increase in global land evapotranspiration from 2003 to 2019', *Nature*, 593(7860), pp. 543–547. doi:10.1038/s41586-021-03503-5.

Pattison, I. and Lane, S.N. (2012) 'The link between land-use management and fluvial flood risk: A chaotic conception?', *Progress in Physical Geography*, 36(1), pp. 72–92. doi:10.1177/0309133311425398.

Peel, M.C. and McMahon, T.A. (2020) 'Historical development of rainfall-runoff modeling', *Wiley Interdisciplinary Reviews: Water*, 7(5), pp. 1–15. doi:10.1002/wat2.1471.

Peng, J. *et al.* (2021) 'Estimation and evaluation of high-resolution soil moisture from merged model and Earth observation data in the Great Britain', *Remote Sensing of Environment*, 264, p. 112610. doi:10.1016/j.rse.2021.112610.

Perrin, C., Michel, C. and Andréassian, V. (2003) 'Improvement of a parsimonious model for streamflow simulation', *Journal of Hydrology*, 279(1–4), pp. 275–289. doi:10.1016/S0022-1694(03)00225-7.

Peskett, L. *et al.* (2020) 'The impact of across-slope forest strips on hillslope subsurface hydrological dynamics', *Journal of Hydrology*, 581(December 2019), p. 124427. doi:10.1016/j.jhydrol.2019.124427.

Picourlat, F., Mouche, E. and Mügler, C. (2022) 'Upscaling Hydrological Processes for Land Surface Models With a Two-Hydrologic-Variable Model: Application to the Little Washita Watershed', *Water Resources Research*, 58(9), pp. 1–19. doi:10.1029/2021wr030997.

Pinnington, E. *et al.* (2021) 'Improving soil moisture prediction of a high-resolution land surface model by parameterising pedotransfer functions through assimilation of SMAP satellite data', *Hydrology and Earth System Sciences*, 25(3), pp. 1617–1641. doi:10.5194/hess-25-1617-2021ormation.

Pitman, A.J. *et al.* (2009) 'Uncertainties in climate responses to past land cover change: First results from the LUCID intercomparison study', *Geophysical Research Letters*, 36(14), pp. 1–6. doi:10.1029/2009GL039076.

Porson, A. *et al.* (2010) 'Implementation of a new urban energy budget scheme into MetUM. Part II: Validation against observations and model intercomparison', *Quarterly Journal of the*

Royal Meteorological Society, 136(651), pp. 1530–1542. doi:10.1002/qj.572.

Portmann, R. *et al.* (2022) 'Global forestation and deforestation affect remote climate via adjusted atmosphere and ocean circulation', *Nature Communications*, 13(1), pp. 1–11. doi:10.1038/s41467-022-33279-9.

Prein, A.F. *et al.* (2015) 'A review on regional convection-permitting climate modeling: Demonstrations, prospects, and challenges', *Reviews of Geophysics*, 53(2), pp. 323–361. doi:10.1002/2014RG000475.

Prosdocimi, I. *et al.* (2019) 'Areal Models for Spatially Coherent Trend Detection: The Case of British Peak River Flows', *Geophysical Research Letters*, 46(22), pp. 13054–13061. doi:10.1029/2019GL085142.

Prudhomme, C. *et al.* (2011) 'How well do large-scale models reproduce regional hydrological extremes: In Europe?', *Journal of Hydrometeorology*, 12(6), pp. 1181–1204. doi:10.1175/2011JHM1387.1.

Prudhomme, C. *et al.* (2012) 'Future flows climate: An ensemble of 1-km climate change projections for hydrological application in Great Britain', *Earth System Science Data*, 4(1), pp. 143–148. doi:10.5194/essd-4-143-2012.

Prudhomme, C. *et al.* (2014) 'Hydrological droughts in the 21st century, hotspots and uncertainties from a global multimodel ensemble experiment', *Proceedings of the National Academy of Sciences of the United States of America*, 111(9), pp. 3262–3267. doi:10.1073/pnas.1222473110.

Rahman, M. *et al.* (2022) 'Hydrology research articles are becoming more topically diverse', *Journal of Hydrology*, 614, p. 128551. doi:10.1016/j.jhydrol.2022.128551.

Raju, E., Boyd, E. and Otto, F. (2022) 'Stop blaming the climate for disasters', *Communications Earth & Environment*, 3(1), pp. 21–22. doi:10.1038/s43247-021-00332-2.

Razavi, S. *et al.* (2020) 'Anthropocene flooding: Challenges for science and society', *Hydrological Processes*, 34(8), pp. 1996–2000. doi:10.1002/hyp.13723.

Refsgaard, J.C., Storm, B. and Mike, S.H.E. (1995) 'Computer models of watershed hydrology', *Water Resources Publication*, pp. 809–846.

Riahi, K. *et al.* (2017) 'The Shared Socioeconomic Pathways and their energy, land use, and greenhouse gas emissions implications: An overview', *Global Environmental Change*, 42, pp. 153–168. doi:10.1016/j.gloenvcha.2016.05.009.

Rinaldo, A., Marani, A. and Rigon, R. (1991) 'Geomorphological dispersion', *Water Resources Research*, 27(4), pp. 513–525. doi:10.1029/90WR02501.

Rinaldo, A. and Rodriguez-Iturbe, I. (1996) 'Geomorphological theory of the hydrological response', *Hydrological Processes*, 10(6), pp. 803–829. doi:10.1002/(SICI)1099-1085(199606)10:6<803::AID-HYP373>3.0.CO;2-N.

Ritchie, P.D.L. *et al.* (2019) 'Large changes in Great Britain's vegetation and agricultural land-use predicted under unmitigated climate change', *Environmental Research Letters*, 14(11), p. 114012. doi:10.1088/1748-9326/ab492b.

Roberts, J. and Rosier, P. (2005) 'The impact of broadleaved woodland on water resources in lowland UK: I. Soil water changes below beech woodland and grass on chalk sites in Hampshire', *Hydrology and Earth System Sciences*, 9(6), pp. 596–606. doi:10.5194/hess-9-596-2005.

Robinson, A. *et al.* (2021) 'Increasing heat and rainfall extremes now far outside the historical climate', *npj Climate and Atmospheric Science*, 4(1), pp. 3–6. doi:10.1038/s41612-021-00202-w.

Robinson, E.L., Blyth, E.M., Clark, D.B., Comyn-Platt, E., *et al.* (2017) 'Climate hydrology and ecology research support system meteorology dataset for Great Britain (1961-2015) [CHESS-met] v1.2. NERC Environmental Information Data Centre. (Dataset).' NERC Environmental Information Data Centre. doi:https://doi.org/10.5285/b745e7b1-626c-4ccc-ac27-56582e77b900.

Robinson, E.L., Blyth, E.M., Clark, D.B., Finch, J., *et al.* (2017) 'Trends in atmospheric evaporative demand in Great Britain using high-resolution meteorological data', *Hydrology and Earth System Sciences*, 21(2), pp. 1189–1224. doi:10.5194/hess-21-1189-2017.

Robinson, E.L. *et al.* (2022) *CHESS-SCAPE: Future projections of meteorological variables at 1 km resolution for the United Kingdom 1980-2080 derived from UK Climate Projections 2018*, *NERC EDS Centre for Environmental Data Analysis*. doi:: http://dx.doi.org/10.5285/8194b416cbee482b89e0dfbe17c5786c.

Robinson, M. and Dupeyrat, A. (2005) 'Effects of commercial timber harvesting on streamflow regimes in the Plynlimon catchments, mid-Wales', *Hydrological Processes*, 19(6), pp. 1213–1226. doi:10.1002/hyp.5561.

Robinson, M., Gannon, B. and Schuch, M. (1991) 'A comparison of the hydrology of moorland

under natural conditions, agricultural use and forestry', *Hydrological Sciences Journal*, 36(6), pp. 565–577. doi:10.1080/02626669109492544.

Robinson, M., Rodda, J.C. and Sutcliffe, J. V. (2013) 'Long-term environmental monitoring in the UK: Origins and achievements of the Plynlimon catchment study', *Transactions of the Institute of British Geographers*, 38(3), pp. 451–463. doi:10.1111/j.1475-5661.2012.00534.x.

Roebroek, C. *et al.* (2020) 'Global distribution of hydrologic controls on forest growth', *Hydrology and Earth System Sciences Discussions*, (2016), pp. 1–22. doi:10.5194/hess-2020-32.

Rogger, M. *et al.* (2017) 'Land use change impacts on floods at the catchment scale: Challenges and opportunities for future research', *Water Resources Research*, 53(7), pp. 5209–5219. doi:10.1002/2017WR020723.

RStudio Team (2021) 'RStudio: Integrated Development Environment for R'. Boston, MA. Available at: http://www.rstudio.com/.

Samaniego, L. *et al.* (2017) 'Toward seamless hydrologic predictions across spatial scales', *Hydrology and Earth System Sciences*, 21(9), pp. 4323–4346. doi:10.5194/hess-21-4323-2017.

Sankarasubramanian, A., Vogel, R.M. and Limbrunner, J.F. (2001) 'Climate elasticity of streamflow in the United States', *Water Resources Research*, 37(6), pp. 1771–1781. doi:10.1029/2000WR900330.

Sawicz, K. *et al.* (2011) 'Catchment classification: Empirical analysis of hydrologic similarity based on catchment function in the eastern USA', *Hydrology and Earth System Sciences*, 15(9), pp. 2895–2911. doi:10.5194/hess-15-2895-2011.

Scaife, C.I. *et al.* (2020) 'Non-linear quickflow response as indicators of runoff generation mechanisms', *Hydrological Processes*, 34(13), pp. 2949–2964. doi:10.1002/hyp.13780.

Schillereff, D.N. *et al.* (2019) 'Convergent human and climate forcing of late-Holocene flooding in Northwest England', *Global and Planetary Change*, 182. doi:10.1016/j.gloplacha.2019.102998.

Schilling, K.E. *et al.* (2014) 'The potential for agricultural land use change to reduce flood risk in a large watershed', *Hydrological Processes*, 28(8), pp. 3314–3325. doi:10.1002/hyp.9865.

Schwaab, J. *et al.* (2020) 'Increasing the broad-leaved tree fraction in European forests mitigates hot temperature extremes', *Scientific Reports*, 10(1), pp. 1–9. doi:10.1038/s41598-020-71055-1.

Seddon, N. *et al.* (2020) 'Understanding the value and limits of nature-based solutions to climate change and other global challenges', *Philosophical Transactions of the Royal Society B: Biological Sciences*, 375(1794), p. 20190120. doi:10.1098/rstb.2019.0120.

Seddon, N. *et al.* (2021) 'Getting the message right on nature-based solutions to climate change', *Global Change Biology*, 27(8), pp. 1518–1546. doi:10.1111/gcb.15513.

Sellar, A.A. *et al.* (2019) 'UKESM1: Description and Evaluation of the U.K. Earth System Model', *Journal of Advances in Modeling Earth Systems*, 11(12), pp. 4513–4558. doi:10.1029/2019MS001739.

Sellers, P.J. (1985) 'Canopy reflectance, photosynthesis and transpiration', *International Journal of Remote Sensing*, 6(8), pp. 1335–1372. doi:10.1080/01431168508948283.

Sellers, P.J. *et al.* (1996) 'Comparison of Radiative and Physiological Effects of Doubled Atmospheric CO2 on Climate', *Science*, 271(5254), pp. 1402–1406. doi:10.1126/science.271.5254.1402.

Sen, P.K. (1968) 'Estimates of the Regression Coefficient Based on Kendall's Tau', *Journal of the American Statistical Association*, 63(324), pp. 1379–1389. doi:10.1080/01621459.1968.10480934.

Seyfried, M.S. and Wilcox, B.P. (1995) 'Scale and the Nature of Spatial Variability: Field Examples Having Implications for Hydrologic Modeling', *Water Resources Research*, 31(1), pp. 173–184. doi:10.1029/94WR02025.

Shapiro, S.S. and Wilk, M.B. (1965) 'An Analysis of Variance Test for Normality (Complete Samples)', *Biometrika*, 52(3/4), p. 591. doi:10.2307/2333709.

Short, C. *et al.* (2019) 'Capturing the multiple benefits associated with nature-based solutions: Lessons from a natural flood management project in the Cotswolds, UK', *Land Degradation and Development*, 30(3), pp. 241–252. doi:10.1002/ldr.3205.

Shreve, R.L. (1966) 'Statistical Law of Stream Numbers', *The Journal of Geology*, 74(1), pp. 17–37. doi:10.1086/627137.

Shuttleworth, E.L. *et al.* (2019) 'Restoration of blanket peat moorland delays stormflow from hillslopes and reduces peak discharge', *Journal of Hydrology X*, 2, p. 100006. doi:10.1016/j.hydroa.2018.100006.

Simmons, C.T. *et al.* (2020) 'Commemorating the 50th anniversary of the Freeze and Harlan (1969) Blueprint for a physically-based, digitally-simulated hydrologic response model',

Journal of Hydrology, 584(November 2019), p. 124309. doi:10.1016/j.jhydrol.2019.124309.

Sing, L. *et al.* (2018) 'A review of the effects of forest management intensity on ecosystem services for northern European temperate forests with a focus on the UK', *Forestry*, 91(2), pp. 151–164. doi:10.1093/forestry/cpx042.

Sing, L. and Aitkenhead, M. (2020) *Analysis of land suitability for woodland expansion in Scotland: update 2020*. doi:http://dx.doi.org/10.7488/era/494.

Slater, L.J. *et al.* (2019) 'Using R in hydrology: a review of recent developments and future directions', *Hydrology and Earth System Sciences Discussions*, 23(7), pp. 2939–2963. doi:10.5194/hess-23-2939-2019.

Slater, L.J., Villarini, G., *et al.* (2021) 'Global Changes in 20-Year, 50-Year, and 100-Year River Floods', *Geophysical Research Letters*, 48(6), pp. 1–10. doi:10.1029/2020GL091824.

Slater, L.J., Anderson, B., *et al.* (2021) 'Nonstationary weather and water extremes: a review of methods for their detection, attribution, and management', *Hydrology and Earth System Sciences*, 25(7), pp. 3897–3935. doi:10.5194/hess-25-3897-2021.

Slater, L.J. and Wilby, R.L. (2017) 'Measuring the changing pulse of rivers', *Science*, 357(6351), pp. 552–552. doi:10.1126/science.aao2441.

Slevin, D., Tett, S.F.B. and Williams, M. (2015) 'Multi-site evaluation of the JULES land surface model using global and local data', *Geoscientific Model Development*, 8(2), pp. 295–316. doi:10.5194/gmd-8-295-2015.

Smith, H.G. *et al.* (2018) 'Simulating a century of soil erosion for agricultural catchment management', *Earth Surface Processes and Landforms*, 43(10), pp. 2089–2105. doi:10.1002/esp.4375.

de Sosa, L.L. *et al.* (2018) 'Delineating and mapping riparian areas for ecosystem service assessment', *Ecohydrology*, 11(2), pp. 1–16. doi:10.1002/eco.1928.

Soulsby, C. *et al.* (2017) 'Taming the flood—How far can we go with trees?', *Hydrological Processes*, 31(17), pp. 3122–3126. doi:10.1002/hyp.11226.

Speich, M.J.R., Zappa, M. and Lischke, H. (2018) 'Sensitivity of forest water balance and physiological drought predictions to soil and vegetation parameters – A model-based study', *Environmental Modelling and Software*, 102, pp. 213–232. doi:10.1016/j.envsoft.2018.01.016.

Spracklen, D. V., Arnold, S.R. and Taylor, C.M. (2012) 'Observations of increased tropical rainfall preceded by air passage over forests', *Nature*, 489(7415), pp. 282–285.

doi:10.1038/nature11390.

Staal, A. *et al.* (2020) 'Feedback between drought and deforestation in the Amazon', *Environmental Research Letters*, 15(4), p. 44024. doi:10.1088/1748-9326/ab738e.

Strahler, A.N. (1957) 'Quantitative analysis of watershed geomorphology', *Eos, Transactions American Geophysical Union*, 38(6), pp. 913–920. doi:10.1029/TR038i006p00913.

Stratford, C. *et al.* (2017) *Do Trees in the UK-Relevant River Catchments Influence Fluvial Flood Peaks?* Available at: https://nora.nerc.ac.uk/id/eprint/517804/.

Sutherland, L.-A. and Huttunen, S. (2018) 'Linking practices of multifunctional forestry to policy objectives: Case studies in Finland and the UK', *Forest Policy and Economics*, 86(November 2017), pp. 35–44. doi:10.1016/j.forpol.2017.10.019.

Tang, Y., Lean, H.W. and Bornemann, J. (2013) 'The benefits of the Met Office variable resolution NWP model for forecasting convection', *Meteorological Applications*, 20(4), pp. 417–426. doi:10.1002/met.1300.

Tarasova, L. *et al.* (2023) 'Shifts in flood generation processes exacerbate regional flood anomalies in Europe', *Communications Earth & Environment*, 4(1), p. 49. doi:10.1038/s43247-023-00714-8.

Tellman, B. *et al.* (2021) 'Satellite imaging reveals increased proportion of population exposed to floods', *Nature*, 596(7870), pp. 80–86. doi:10.1038/s41586-021-03695-w.

Telteu, C.E. *et al.* (2021) 'Understanding each other's models An introduction and a standard representation of 16 global water models to support intercomparison, improvement, and communication', *Geoscientific Model Development*, 14(6), pp. 3843–3878. doi:10.5194/gmd-14-3843-2021.

Teuling, A.J. *et al.* (2009) 'Parameter Sensitivity in LSMs: An Analysis Using Stochastic Soil Moisture Models and ELDAS Soil Parameters', *Journal of Hydrometeorology*, 10(3), pp. 751–765. doi:10.1175/2008JHM1033.1.

Teuling, A.J. *et al.* (2010) 'Contrasting response of European forest and grassland energy exchange to heatwaves', *Nature Geoscience*, 3(10), pp. 722–727. doi:10.1038/ngeo950.

Teuling, A.J. *et al.* (2017) 'Observational evidence for cloud cover enhancement over western European forests', *Nature Communications*, 8(1), p. 14065. doi:10.1038/ncomms14065.

Teuling, A.J. *et al.* (2019) 'Climate change, reforestation/afforestation, and urbanization impacts on evapotranspiration and streamflow in Europe', *Hydrology and Earth System*

Sciences, 23(9), pp. 3631–3652. doi:10.5194/hess-23-3631-2019.

Theil, H. (1992) 'A Rank-Invariant Method of Linear and Polynomial Regression Analysis', in *Indagationes mathematicae*, pp. 345–381. doi:10.1007/978-94-011-2546-8_20.

Thomas, A. *et al.* (2020) 'Fragmentation and thresholds in hydrological flow-based ecosystem services', *Ecological Applications*, 30(2), p. eap.2046. doi:10.1002/eap.2046.

Thomas, H. and Nisbet, T.R. (2007) 'An assessment of the impact of floodplain woodland on flood flows', *Water and Environment Journal*, 21(2), pp. 114–126. doi:10.1111/j.1747-6593.2006.00056.x.

Thompson, V. *et al.* (2017) 'High risk of unprecedented UK rainfall in the current climate', *Nature Communications*, 8(1). doi:10.1038/s41467-017-00275-3.

Thomson, A. *et al.* (2018) *Quantifying the impact of future land use scenarios to 2050 and beyond, Final Report for the Committee on Climate Change*. Centre for Ecology & Hydrology. Available at: https://www.theccc.org.uk/wp-content/uploads/2018/11/Quantifying-the-impact-of-future-land-use-scenarios-to-2050-and-beyond-Full-Report.pdf.

Torres-Rojas, L. *et al.* (2022) 'Towards an Optimal Representation of Sub-Grid Heterogeneity in Land Surface Models', *Water Resources Research*, 58(12). doi:10.1029/2022WR032233.

Trabucco, A. *et al.* (2008) 'Climate change mitigation through afforestation / reforestation : A global analysis of hydrologic impacts with four case studies', 126, pp. 81–97. doi:10.1016/j.agee.2008.01.015.

Trenberth, K.E. *et al.* (2007) 'Estimates of the Global Water Budget and Its Annual Cycle Using Observational and Model Data', *Journal of Hydrometeorology*, 8(4), pp. 758–769. doi:10.1175/JHM600.1.

Trenberth, K.E. (2011) 'Changes in precipitation with climate change', *Climate Research*, 47(1–2), pp. 123–138. doi:10.3354/cr00953.

Tyralis, H. *et al.* (2021) 'Explanation and probabilistic prediction of hydrological signatures with statistical boosting algorithms', *Remote Sensing*, 13(3), pp. 1–23. doi:10.3390/rs13030333.

Vanderborght, J. *et al.* (2021) 'From hydraulic root architecture models to macroscopic representations of root hydraulics in soil water flow and land surface models', *Hydrology and Earth System Sciences*, 25(9), pp. 4835–4860. doi:10.5194/hess-25-4835-2021.

Vereecken, H. *et al.* (2010) 'Using Pedotransfer Functions to Estimate the van Genuchten-

Mualem Soil Hydraulic Properties: A Review', *Vadose Zone Journal*, 9(4), pp. 795–820. doi:10.2136/vzj2010.0045.

Vereecken, H. *et al.* (2022) 'Soil hydrology in the Earth system', *Nature Reviews Earth and Environment*, 3(9), pp. 573–587. doi:10.1038/s43017-022-00324-6.

Vertessy, R.A., Zhang, L. and Dawes, W.R. (2003) 'Plantations, river flows and river salinity', *Australian Forestry*, 66(1), pp. 55–61. doi:10.1080/00049158.2003.10674890.

Villarini, G. and Wasko, C. (2021) 'Humans, climate and streamflow', *Nature Climate Change*, 11(9), pp. 725–726. doi:10.1038/s41558-021-01137-z.

Le Vine, N. *et al.* (2016) 'Diagnosing hydrological limitations of a land surface model: Application of JULES to a deep-groundwater chalk basin', *Hydrology and Earth System Sciences*, 20(1), pp. 143–159. doi:10.5194/hess-20-143-2016.

Vitolo, C., Fry, M. and Buytaert, W. (2016) 'Rnrfa: An r package to retrieve, filter and visualize data from the uk national river flow archive', *R Journal*, 8(2), pp. 102–116. doi:10.32614/rj-2016-036.

Wagener, T. *et al.* (2021) 'On doing hydrology with dragons: Realizing the value of perceptual models and knowledge accumulation', *Wiley Interdisciplinary Reviews: Water*, 8(6), pp. 1–17. doi:10.1002/wat2.1550.

Wainwright, J. and Mulligan, M. (2013) *Environmental modelling: finding simplicity in complexity*. John Wiley \& Sons.

Wang-Erlandsson, L. *et al.* (2018) 'Remote land use impacts on river flows through atmospheric teleconnections', *Hydrology and Earth System Sciences*, 22(8), pp. 4311–4328. doi:10.5194/hess-22-4311-2018.

Wang, K. *et al.* (2022) 'Regional and seasonal partitioning of water and temperature controls on global land carbon uptake variability', *Nature Communications*, 13(1), pp. 1–11. doi:10.1038/s41467-022-31175-w.

Warner, E. *et al.* (2021) 'Does restoring native forest restore ecosystem functioning? Evidence from a large-scale reforestation project in the Scottish Highlands', *Restoration Ecology*, 30(3), pp. 1–10. doi:10.1111/rec.13530.

Wasko, C., Nathan, R., *et al.* (2021) 'Evidence of shorter more extreme rainfalls and increased flood variability under climate change', *Journal of Hydrology*, 603, p. 126994. doi:10.1016/j.jhydrol.2021.126994.

Wasko, C., Westra, S., *et al.* (2021) 'Incorporating climate change in flood estimation guidance', *Philosophical Transactions of the Royal Society A: Mathematical, Physical and Engineering Sciences*, 379(2195), p. 20190548. doi:10.1098/rsta.2019.0548.

Wasko, C. (2021) 'Review: Can temperature be used to inform changes to flood extremes with global warming?', *Philosophical Transactions of the Royal Society A: Mathematical, Physical and Engineering Sciences*, 379(2195). doi:10.1098/rsta.2019.0551.

Wasko, C., Sharma, A. and Lettenmaier, D.P. (2019) 'Increases in temperature do not translate to increased flooding', *Nature Communications*, 10(1), pp. 4–6. doi:10.1038/s41467-019-13612-5.

Weedon, G.P. *et al.* (2023) 'Geological controls of discharge variability in the Thames Basin, UK from cross-spectral analyses: Observations versus modelling', *Journal of Hydrology*, 625(PB), p. 130104. doi:10.1016/j.jhydrol.2023.130104.

Weiler, M. and Beven, K. (2015) 'Do we need a Community Hydrological Model?', *Water Resources Research*, 51(9), pp. 7777–7784. doi:10.1002/2014WR016731.

Welsh Government (2021) *Woodland Opportunity Map 2021 | DataMapWales*, *DataMapWales*. Available at: https://datamap.gov.wales/maps/woodland-opportunity-map-2021/ (Accessed: 4 August 2022).

Westra, S. *et al.* (2014) 'Future changes to the intensity and frequency of short-duration extreme rainfall', *Reviews of Geophysics*, 52(3), pp. 522–555. doi:10.1002/2014RG000464.

Wieder, W.R. *et al.* (2014) *Regridded harmonized world soil database v1. 2*, *ORNL DAAC*. doi:http://dx.doi.org/10.3334/ORNLDAAC/1247.

Wilby, R.L. and Quinn, N.W. (2013) 'Reconstructing multi-decadal variations in fluvial flood risk using atmospheric circulation patterns', *Journal of Hydrology*, 487, pp. 109–121. doi:10.1016/j.jhydrol.2013.02.038.

Wilkes, M.A. *et al.* (2020) 'Making way for trees? Changes in land-use, habitats and protected areas in Great Britain under "Global tree restoration potential"', *Sustainability (Switzerland)*, 12(14). doi:10.3390/su12145845.

Williams, K.E. *et al.* (2019) 'How can the First ISLSCP Field Experiment contribute to present-day efforts to evaluate water stress in JULESv5.0?', *Geoscientific Model Development*, 12(7), pp. 3207–3240. doi:10.5194/gmd-12-3207-2019.

Wiltshire, A.J. *et al.* (2020) 'JULES-GL7: The Global Land configuration of the Joint UK Land

Environment Simulator version 7.0 and 7.2', *Geoscientific Model Development*, 13(2), pp. 483–505. doi:10.5194/gmd-13-483-2020.

Winsemius, H.C. *et al.* (2016) 'Global drivers of future river flood risk', *Nature Climate Change*, 6(4), pp. 381–385. doi:10.1038/nclimate2893.

Wood, E.F. *et al.* (2011) 'Hyperresolution global land surface modeling: Meeting a grand challenge for monitoring Earth's terrestrial water', *Water Resources Research*, 47(5), pp. 1–10. doi:10.1029/2010WR010090.

Woodland Expansion Advisory Group (2012) *Report of the Woodland Expansion Advisory Group to the cabinet secretary for rural affairs and environment*. Available at: http://scotland.forestry.gov.uk/supporting/management/annual-review/woodland-expansion (Accessed: 4 August 2022).

Xu, C. *et al.* (2023) 'The Benefits of Using State-Of-The-Art Digital Soil Properties Maps to Improve the Modeling of Soil Moisture in Land Surface Models', *Water Resources Research*, 59(4), pp. 1–21. doi:10.1029/2022WR032336.

Xu, R. *et al.* (2022) 'Contrasting impacts of forests on cloud cover based on satellite observations', *Nature Communications*, 13(1), p. 670. doi:10.1038/s41467-022-28161-7.

Yadav, M., Wagener, T. and Gupta, H. (2007) 'Regionalization of constraints on expected watershed response behavior for improved predictions in ungauged basins', *Advances in Water Resources*, 30(8), pp. 1756–1774. doi:10.1016/j.advwatres.2007.01.005.

Young, P.J. *et al.* (2021) 'The Montreal Protocol protects the terrestrial carbon sink', *Nature*, 596(7872), pp. 384–388. doi:10.1038/s41586-021-03737-3.

Yu, Z. *et al.* (2022) 'Natural forest growth and human induced ecosystem disturbance influence water yield in forests', *Communications Earth and Environment*, 3(1), pp. 1–8. doi:10.1038/s43247-022-00483-w.

Zhang, M. *et al.* (2017) 'A global review on hydrological responses to forest change across multiple spatial scales: Importance of scale, climate, forest type and hydrological regime', *Journal of Hydrology*, 546, pp. 44–59. doi:10.1016/j.jhydrol.2016.12.040.

Zhang, X. *et al.* (2022) 'The Compensatory CO2 Fertilization and Stomatal Closure Effects on Runoff Projection From 2016–2099 in the Western United States', *Water Resources Research*, 58(1). doi:10.1029/2021wr030046.

Zhao, M. *et al.* (2022) 'Evapotranspiration frequently increases during droughts', *Nature*

Climate Change, 12(11), pp. 1024–1030. doi:10.1038/s41558-022-01505-3.

Zhou, G. *et al.* (2015) 'Global pattern for the effect of climate and land cover on water yield', *Nature Communications*, 6, pp. 1–9. doi:10.1038/ncomms6918.

Zhou, S. *et al.* (2023) 'Projected increase in global runoff dominated by land surface changes', *Nature Climate Change*, 13(5), pp. 442–449. doi:10.1038/s41558-023-01659-8.

473 Citations